AN ABSTRACT OF THE DISSERTATION OF

Ward Shalash for the degree of Doctor of Philosophy in Bioengineering presented on June 10, 2022.

Title: Engineering an Ex-Vivo System to Study Transport Phenomena in the Human Intervertebral Disc.

Abstract approved: _____

Morgan B. Giers

Back pain is the leading cause of disability worldwide, entailing a significant socioeconomic impact. A primary source of back pain can be attributed to intervertebral disc (IVD) degeneration allowing nerve ingrowth, facet joint arthritis, disc bulging, and osteophyte formations that press on nearby nerve roots or the spinal cord. While several methods like conservative therapy, discectomy, IVD replacement, and spinal fusion exist to alleviate back pain, no solution has been found to eliminate the pain and return the IVD to its full function.

Stem cell injections administered in the IVD have emerged as an attractive option to treat back pain compared to the conventional invasive methods. These injections can retain tissue hydration, improve the IVD's height, and alleviate pain. However, the IVD is prone to dehydration and calcification that inhibit nutrient transport and metabolite removal. Limitations in solute transport can thus render the IVD's microenvironment inhospitable to the injected cells.

This dissertation first introduces the solute transport conundrum in the literature, including conventional knowledge and methods to study transport. We then discuss the utilization of a whole organ bioreactor in the study of transport. The bioreactor provides a way to define the IVD's microenvironment, mimicking *in vivo* conditions in humans. In addition, the dissertation includes three manuscripts on the effects of culture conditions on IVD cells, cryopreservation of the IVD, and finite element modeling of solute transport. All of this work ties into the theme of

engineering a platform for the *ex vivo* study of nutrient transport in human intervertebral discs.

Manuscript one in Chapter 3 discusses the impact of cell culture conditions on phenotypic changes in IVD cells, activation of different metabolic pathways, and remodeling of the extracellular matrix (ECM). Current culture conditions fail to represent the IVD's *in vivo* microenvironment and lacks standardization. Cells in the IVD's outer annulus fibrosus (AF) and cartilaginous endplate (CEP) exist in well-oxygenated and nourished conditions compared to the inner AF and nucleus pulposus (NP). I discovered that the modulation of glucose levels every three days induced oxidative stress leading to senescence in AF but not in NP cells. Culture conditions also influenced the metabolic pathways in each cell type in which steady levels of glucose increased AF metabolic activity and remodeling of the ECM compared to NP cells. This study highlights the importance of the *in vivo* quasi-steady state nutrient transport conditions in IVD cell and tissue cultures experiments.

In manuscript two (Chapter 4), I describe a novel method to cryopreserve IVDs at -80°C while maintaining high cell viability. This will allow us to ship and store fresh human cadaveric IVDs until we have bioreactor space and experimental demand. The bioreactor system was utilized to compress bovine IVDs enhancing transport of the cryoprotectant (CPA) transport, reducing CPA cytotoxic effects, and increasing CPA penetration in the inner AF and NP. Our results showed a 95% improvement in the penetration of the CPA in the IVD's soft tissue. Improving the CPA's penetration resulted in cell viability equivalent to the fresh control, averaging 80%. This novel cryopreservation technique aims to improve the logistics of obtaining and storing human IVDs for research and clinical purposes. Specifically, this method enables convenient and flexible use of a whole human IVD bioreactor.

Next, manuscript four in Chapter 5 examines the development of a patient-specific model of IVD nutrient transport to select appropriate patients and determine optimal cell dose for stem cell therapy. This model is intended to be validated using the bioreactor system. The model used Magnetic Resonance Imaging (MRI) data to generate patient-specific solute transport models, factoring in the exact IVD geometry, water content, and diffusion coefficients, thus providing a realistic

representation of solute transport in the human IVD. This model provides a better alternative to study transport phenomena in the human IVD compared to animal models and can be used to infer factors that impact transport. The model will be validated and improved in conjunction with bioreactor experiments.

I conclude the dissertation with two proposals to improve this work. One is related to the creation of an intact IVD organ bank, and the second discussed the development of a clinically viable finite-element model to deduce transport information in patient IVDs. The second topic will show how all of the work presented in this dissertation feeds into an engineered *ex-vivo* platform for studying transport phenomena in human IVDs.

Engineering an Ex-Vivo System to Study Transport Phenomena in the Human
Intervertebral Disc

by
Ward Shalash

A DISSERTATION

submitted to

Oregon State University

in partial fulfillment of
the requirements for the
degree of

Doctor of Philosophy

Presented June 10, 2022
Commencement June 2023

Doctor of Philosophy dissertation of <u>Ward Shalash</u> presented on <u>June 10, 2022</u>

APPROVED:

_____

Major Professor, representing Bioengineering

_____

Head of the School of Chemical, Biological & Environmental Engineering

_____

Dean of the Graduate School

I understand that my dissertation will become part of the permanent collection of Oregon State University libraries. My signature below authorizes release of my dissertation to any reader upon request.

_____

Ward Shalash, Author

ACKNOWLEDGEMENTS

CONTRIBUTION OF AUTHORS

Dr. Morgan B. Giers was involved in the design, writing, and revision of all manuscripts.

Dr. Adam Higgins was involved in the design of manuscript two in chapter four (A Novel Method to Cryopreserve the Intact Intervertebral Disc).

Dr. Liudmila A. Bardonova was involved in the experiment design, and revision of manuscript three in chapter five (Patient-Specific Apparent Diffusion Maps Used to Model Nutrient Availability in Degenerated Intervertebral Discs).

Dr. Vadim A. Byvaltsev contributed the patient data set used in manuscript three in chapter 5 (Patient-Specific Apparent Diffusion Maps Used to Model Nutrient Availability in Degenerated Intervertebral Discs).

Lindsay G. Benage contributed to the NMR metabolite data analysis of manuscript one in chapter three (Effects of Glucose Modulation on AF and NP Synthesis of Glycosaminoglycans and Metabolomics).

Rees A. Rosene was involved in conducting the alginate bead experiments of manuscript one in chapter three (Effects of Glucose Modulation on AF and NP Synthesis of Glycosaminoglycans and Metabolomics).

Ryan Forcier contributed to experiment design and the writing of manuscript two in chapter four (A Novel Method to Cryopreserve the Intact Intervertebral Disc)

Sonia R. Ahrens contributed to the design, writing and revision of manuscript three in chapter five (Patient-Specific Apparent Diffusion Maps Used to Model Nutrient Availability in Degenerated Intervertebral Discs).

TABLE OF CONTENTS

TABLE OF CONTENTS (Continued)

TABLE OF CONTENTS (Continued)

LIST OF FIGURES

LIST OF FIGURES (Continued)

LIST OF FIGURES (Continued)

LIST OF TABLES

LIST OF APPENDICES

LIST OF APPENDIX TABLES

Chapter 1 – General Introduction and Literature Review

1.1 General introduction

Low back pain is a leading cause of disability and missed workdays worldwide, and it has been associated with the degeneration of the intervertebral disc (IVD) (Andersson 1999). While several methods exist to mitigate low back pain, no solution has been found to eliminate pain and restore IVD function. Stem cell injections administered in the IVD have emerged as an attractive alternative to conventional therapies for IVD regeneration.

Animal and human studies have shown that cell injections could restore IVD height, increase tissue hydration, and alleviate pain. However, the literature does not provide sufficient information on which IVD morphology and physiological conditions are appropriate to support stem cell injections. Current methods of stem cell administration are arbitrary where the injection dose size and location in the IVD are not predetermined before the procedure (Noriega et al. 2017; Orozco et al. 2011; Meisel et al. 2006b; Hohaus et al. 2008; Coric et al. 2013; Yoshikawa et al. 2010; Centeno et al. 2017; Tschugg et al. 2017; Tschugg et al. 2016; Sakai and Schol 2017; Smith et al. 2018).

Transport phenomena limitations in patient IVDs can become obstacles to successful cell-based treatments in patients. This work elucidates the need to consider limitations in patient IVD transport phenomena when developing cell injection treatments for back pain.

1.2 The intervertebral disc

1.2.1 Intervertebral disc anatomy

The IVD is the largest avascular structure in the human body, and it functions as a cushion between the vertebral bodies (Figure 1.1) (Urban, Smith, and Fairbank 2004; Vergroesen et al. 2015). This structure gives flexibility to the spine and a wide range of motion, including bending, twisting and rotation (Urban, Smith, and Fairbank 2004; Vergroesen et al. 2015). The IVD is about 7-10 mm in thickness and 4 cm in diameter (Urban, Smith, and Fairbank 2004; Vergroesen et al. 2015). Composed of three main types of tissues, the IVD contains: (1) two thin layers of hyaline cartilage on the superior and inferior sides of the IVD that transfer loads between the vertebrae in the spinal column, (2) a thick outer ring that is made up of type I collagen, and elastin, and (3) a

soft gelatinous core constituted by type II collagen and proteoglycans (PGs) (Urban, Smith, and Fairbank 2004; Vergroesen et al. 2015).

In adults, the IVD is avascular. Blood vessels penetrate through the bony vertebrae and end at the CEP. Nutrients, glucose, and oxygen that are important to sustain cell activity in the IVD must diffuse through the CEP to the center of the IVD. Conversely, cellular byproducts such as lactate, which is more concentrated at the center of the IVD, will have to diffuse outward to the blood vessels. The IVD's structure is held together by the ECM in the NP and AF. The NP center contains a random matrix of aggrecan, proteoglycan and type II collagen fibers that maintain a well hydrated core. The AF section of the disc is made up of 15-25 concentric rings of well-organized type I collagen fibers. Elastin fibers in the AF connect the concentric rings and maintain elastic attributes of the IVD's outer ring.

Various factors including limited nutrient availability, overload, injury, and aging can lead to deterioration of the IVD's tissue, causing loss of water content and height.
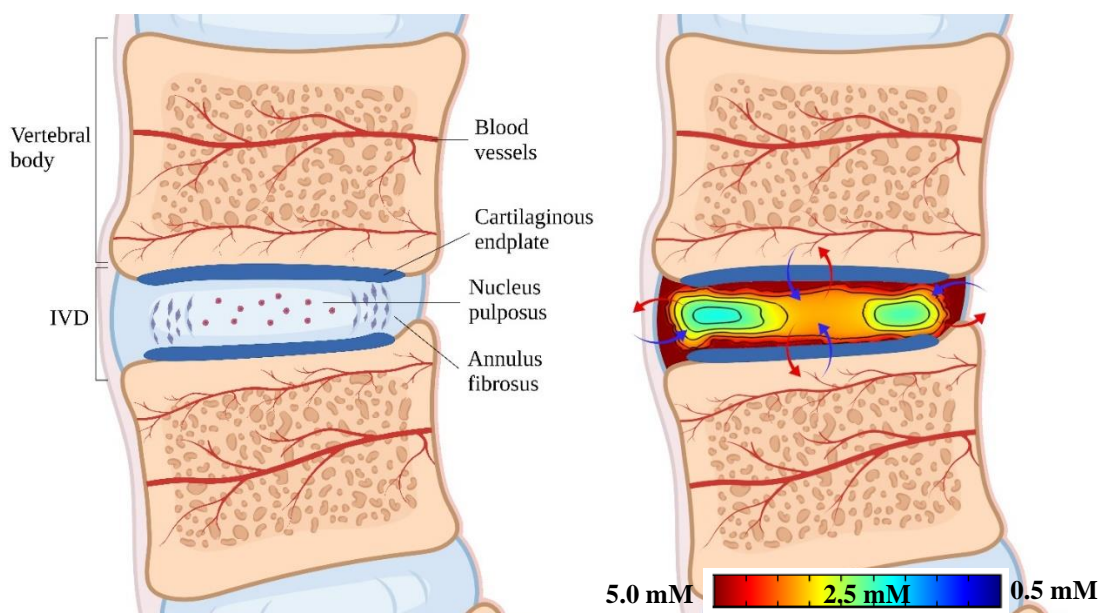
Figure 1.1. Solute transport in the intervertebral disc (left). The IVD is an avascular structure comprised of three types of tissues: the annulus fibrosus (AF), the cartilaginous endplates (CEP), and the nucleus pulposus (NP). Nearby vessels penetrating through the CEP provide the IVD with most nutrient supply. Concentration profile of solutes in the IVD (right). Solute transport in the IVD is dominated by diffusion through the CEP and outer AF creating solute gradients, where the IVD's boundaries have low nutrient levels and high metabolites (red area), and the inner AF has low nutrients and high metabolites (blue area). The scale bar indicates approximate glucose concentrations.

1.2.2 Intervertebral disc degeneration

IVD degeneration leads to changes in the extracellular matrix (ECM) which becomes more fragmented, and it loses most of its mechanical properties, shock absorption and elasticity (Urban, 2007). As the ECM deteriorates, the demarcation between the AF and NP slowly disappears, dehydration increases, and the cells present abnormal phenotypes like senescent and apoptotic (Urban, 2003).

The specific causes and mechanisms behind degeneration is not clearly known (Jeon et al. 2017; Wang et al. 2016b; Zhou et al. 2016; Iatridis and ap Gwynn 2004). However, studies point to several factors that can initiate degeneration:

- *Mechanical stressors*

  The IVD is constantly under various types of loads such as compression and torsion (Iatridis and ap Gwynn 2004). In some cases when the IVD is overloaded, the AF undergoes tears and lesions, propagating a negative chain of events including fiber failure and ECM cracking (Iatridis and ap Gwynn 2004). Accumulation of damage to the tissue can lead to mechanical failure of the IVD and a herniation (Iatridis and ap Gwynn 2004).

- *Aging*

  Several changes happen to the IVD as it ages contributing to its degeneration (Wang et al. 2016a). Studies report a shift in cellular phenotype, increasing the number of senescent and apoptotic cells (Vinatier et al. 2018; Wang et al. 2016b; Cisewski et al. 2018). Such cells can be burdensome on the starved microenvironment because they consume nutrients but fail to remodel the ECM. Thus, the ECM breaks down leading to dehydration of the IVD (Vinatier et al. 2018; Wang et al. 2016b; Cisewski et al. 2018). The aging IVD cells has also been shown to initiate inflammation, another cause for IVD degeneration.

- *Inflammation*

  Inflammation has long been associated with IVD degeneration (Molinos et al. 2015). When the IVD undergoes a traumatic event, it initiates an inflammatory response that activates and recruits immune cells to the injury site (Molinos et al. 2015). The NP is considered by the body as "non-self"; therefore, mechanical failure of the AF that exposes the NP can also initiate inflammatory positive feedback (Molinos et al. 2015). The recruited

cells secrete catabolic factors that contribute to ECM loss and cellular phenotypic changes (Molinos et al. 2015).

- *Limited nutrient transport*

    The adult IVD is known to lose its vasculature and deposit calcium in the CEP limiting solute transport (Nachemson et al. 1970; Shutkin 1952; Andersson 1999; Huang, Urban, and Luk 2014; Hassler 1969; Boos et al. 2002). It is reported that a drop in microenvironment glucose and pH level to 0.5 mM and 6.5, respectively, leads to cell death (Shirazi-Adl, Taheri, and Urban 2010; Bibby and Urban 2004; Jackson et al. 2009). Loss of viable cells in the IVD leads to the deterioration of the ECM, including loss in proteoglycans which are important to retain water molecules and facilitate solute transport (Bibby and Urban 2004).

- *Genetic causes*

    It is established that genetic factors play a significant role in initiating IVD degeneration (Oichi et al. 2020). In fact, three-quarters of IVD degeneration cases could be traced to genetic alterations in the IVD. Polymorphism and genetic variation of IVD proteins (e.g., collagen and aggrecan), enzymes, (including matrix metalloproteinases (MMPs)), and proinflammatory cytokines (such as interleukin-1 (IL-1) and IL-6) lead to impaired tissue homeostasis (Oichi et al. 2020). The accumulation of these changes eventually compromises the IVD's physiology and mechanical properties.

It is also worth mentioning other factors including smoking, diabetes and disc injury that lead to IVD degeneration (Molinos et al. 2015). These factors have been shown to induce catabolic pathways in the IVD. As a results, cells begin to lose their normal phenotype initiating the deterioration of the ECM and IVD degeneration.

1.2.3 The extracellular matrix

NP and AF cells in the IVD secrete extracellular matrix (ECM) to build and maintain a microenvironment that promotes cell survival. The ECM is composed of a network of collagens, fibers, and proteoglycans (PG) (Weidenbaum et al. 1992; Iatridis et al. 2007; Lyons, Eisenstein, and Sweet 1981). Studies have shown the important role that the ECM plays in IVD cell differentiation, proliferation and cell signaling (Weidenbaum et al. 1992; Iatridis et al. 2007;

Lyons, Eisenstein, and Sweet 1981). Additionally, the ECM influences the rate of diffusion for biomolecules inside the IVD. A recent study done by Kihara et al. at Osaka University, Japan used fibroblast mediated collagen gel to investigate biomolecular diffusion through the ECM (Kihara, Ito, and Miyake 2013). The study found a strong correlation between collagen fiber arrangement and diffusion of biomolecules- molecules with a diameter less than 10 nm (i.e., ions) diffused through the ECM as if they were diffusing through a Newtonian viscous fluid (Kihara, Ito, and Miyake 2013). On the contrary, GAG content in the ECM showed an ability to hinder diffusion of anionic molecules into the ECM due to their negative charge (Kihara, Ito, and Miyake 2013). The work of Dr. Stylianopoulos on diffusion of particles in the ECM also support the idea that ECM integrity is important for molecular diffusion (Stylianopoulos et al. 2010). His research shows that GAG content significantly determines the ability of charged molecules to diffuse in the ECM (Stylianopoulos et al. 2010). There are additional benefits to the ECM: (1) the ECM improves cell migration by assisting in cell adhesion; (2) Collagen in the ECM provides tensile strength and regulates cell adhesion; (3) GAGs form hydrophilic hydrogel like substance that withstands compressive forces in the disc; and (4) small leucine-rich proteoglycans (SLRPs) have been show to activate growth factor pathways in NP and AF tissues (Merline, Schaefer, and Schaefer 2009).

1.3 The intervertebral disc microenvironment

The avascular IVD receives its nutrient supply from the nearby vessels penetrating the outer regions of the AF and CEP (Urban, Smith, and Fairbank 2004). Solutes diffuse from the nearby vessels through the pores and channels of the CEP in order to reach the inner AF and NP (Urban, Smith, and Fairbank 2004). Diffusion of solutes creates gradients across the tissue in which the outer regions have physiological levels of glucose and oxygen estimated to be 5.0 mM and 5.1 kPa, respectively (Bibby and Urban 2004). In contrast, the NP and inner AF exist in hypoxic and acidic conditions with glucose and oxygen levels estimated to be 2.0 mM and 0.43 kPa (Bibby et al. 2005; Liebscher et al. 2011; Urban, Smith, and Fairbank 2004).

pH is another important factor of the IVD's environment that ranges between 6.7 to 7.4 (Mokhbi Soukane, Shirazi-Adl, and Urban 2009). It is well established that low pH levels decrease cellular proliferation, hinder ECM remodeling, and propagate senescent and apoptotic cell phenotypes (Guerrero et al. 2021). NP cells cultured under pH levels of 6.5 or lower showed a dramatic drop in viable cells and DNA expression (Gilbert et al. 2016). The study also reported

an increase in secreted proinflammatory cytokines and pain-related factors such as interleukin-1β (IL-1β) and IL-6. The activation of proinflammatory responses in the IVD initiates secretion of catabolic factors, like MMP-3 and ADAMTS-4, and the downregulation of collagen, aggrecan, and proteoglycans, leading to ECM deterioration (Gilbert et al. 2016).

Last, the IVD's microenvironment is very dynamic. As the IVD compresses structural changes take place in which the fibers in the ECM become denser, the pores get smaller, and charge density increases (Guerrero et al. 2021). In addition, compression of the IVD exposes the cells to various shear stresses and osmotic pressures. Compression of the IVD forces water out of the tissue, changing solute concentrations and thus modulating the osmotic pressure. The osmolarity in the NP can range between 300 mOsm/L (hypoosmotic) to 496 mOsm/L (hyperosmotic) depending on the applied load (Guerrero et al. 2021). The wide range in osmolarity that the NP experiences induces water "movement" through the tissue that also modulates solute levels (Guerrero et al. 2021). Degeneration of the IVD has been reported to include fragmentation of the ECM leading to floating charged fragments increasing osmolarity in the tissue (Guerrero et al. 2021). Considering the physiological environment of the IVD, NP cells are constantly exposed to changes in water content and shear stress through the natural compression of the IVD which also leads to fluctuations in the nutrient levels (Wang, Yang, and Hsieh 2011; Jackson et al. 2011).

1.4 Intervertebral disc culture microenvironments

It is crucial when studying the IVD to accurately reflect either the healthy or degenerated microenvironment discussed above. Unfortunately, there are still many challenges in recreating those environments. Scaffold-based cultures in alginate, cellulose, gelatin, polystyrene, or silk, are typical alternatives to monolayer cultures, providing the cells with a more physiological environment (Knight and Przyborski 2015; Mahmoudifar and Doran 2010; Kwon and Peng 2002). In monolayer cultures, cells are intended to adhere to the bottom of the vessel, flattening the cell's geometry and changing gene expression (Knight and Przyborski 2015). On the other hand, scaffolds provide the cells with a complex environment, similar to the IVD's ECM, in which the cells can attain their natural shape, elongated or round (Bruehlmann et al. 2002; Pattappa et al. 2012; Knight and Przyborski 2015; Kwon and Peng 2002). The scaffold's complex matrix also enhances cell signaling, proliferation, and resistance to therapeutic agents,

increasing the value of the collected data for researchers (Knight and Przyborski 2015; Bibby et al. 2005; Mahmoudifar and Doran 2010). Another advantage of using scaffolds is the ability to immobilize cells in bioreactors, enabling the design of experiments with defined nutritional conditions, which is essential when investigating the effects of therapeutics and microenvironmental factors on cell viability, phenotype, metabolism, and gene expression (Martin, Wendt, and Heberer 2004). Bioreactors can also address limitations associated with mass transport in three-dimensional cultures by modulating flow rates increasing cellular metabolism and expression of the ECM (Martin, Wendt, and Heberer 2004).

Currently, it is not common to apply hypoxic conditions to IVD cell and tissue cultures, raising questions about outcome relevance compared to *in vivo*. Furthermore, high glucose media with a cyclical feeding schedule is common among research groups despite some evidence showing induced oxidative stress due to elevated glucose concentrations in cell cultures (Park et al. 2014; Shan et al. 2019; Cheng et al. 2016). Monolayer cultures, inaccurate nutrient concentrations, and fluctuations in media conditions are factors that can induce altered cellular responses, inaccurately reflecting *in vivo* conditions.

1.5 Cryopreservation

Access to cells and tissues can also be a barrier in recreating accurate representations of deceased or healthy disc environments. Human cells can be collected during surgical procedures where portions of the IVD are normally removed. Intact human IVDs must be collected from cadavers within hours of the person's death. The cells or whole IVDs must then be processed to a state where they can be cultured. For instance, cells must be extracted from the tissue and whole IVDs must be detached from the vertebrae and cleaned. Cells or tissues are then either cultured immediately or need to be cryopreserved from long term storage. Cryopreservation has been increasingly used to preserve cells, tissues, organelles, and intact organs for research and medical applications (Lam et al. 2011). This process has revolutionized allograft clinical research by overcoming the increasing supply-demand imbalance for viable specimens (Aijaz et al. 2018; Bradley, Bolton, and Pedersen 2002). The cell's vital functions slow down significantly at low temperatures, making it viable to store cells long-term (Lam et al. 2011). However, freeze-thaw cycles damage the cells due to formation of ice crystals that lead to osmotic shock, membrane damage, and cell death (Lam et al. 2011). As the cells begin to freeze water transitions from its

liquid phase to ice leading to changes in the intra- and extracellular solute concentrations (Jang et al. 2017b). These changes are thought to induce various stressors including osmotic shock and mechanical damage to the cell's cytoskeleton and ECM (Jang et al. 2017b). Therefore, there has been an increasing need in the IVD research community to optimize cryopreservation techniques that protect the fine structure of the cells in intact IVDs during long-term storage.

Researchers have developed various strategies to prevent cryoinjury in mammalian cells including (1) slow freezing, (2) vitrification, and (3) subzero nonfreezing storage(Jang et al. 2017a). The major steps in each type of cryopreservation includes the addition of a cryoprotectant (CPA), cooling the tissue at a constant rate, long-term storage of the samples, bringing the the sample to a functioning temperature (usually 37°C), and removal of the CPA (Jang et al. 2017a). The addition of the CPA is essential in controlling ice crystal formation, freezing rate of water, and the rate of solute and solvent transport across the cellular membranes (Jang et al. 2017a). There are two types of CPA used in cryopreservation applications, including intracellular and extracellular CPAs(Jang et al. 2017a). Intracellular CPAs, such as dimethyl sulfoxide (DMSO) and glycerol, permeate through the cell's membrane and impede ice crystal formation (Jang et al. 2017a). Extracellular CPAs, including saccharides like trehalose, limit the interactions between cells and the extracellular ice crystals and prevent mechanical damage to the ECM (Lam et al. 2011).

Despite the breakthroughs that have been accomplished in tissue cryopreservation, there are limitations to this application. It would be ideal to completely saturate the tissue and cells with the CPA (e.g., DMSO) to achieve perfect cryopreservation. However, DMSO is toxic to the cells, and it has been shown to shift the gene expression leading to tumor development in some instances. Next, cryopreservation of large intact tissue has been challenging due to limitations in mass and heat transport. Failure to ensure complete saturation of large tissues with the CPA hinders the cryoprotective properties leading to areas within the tissue with poor cell viability. Current methods for whole IVD cryopreservation also fall victim to transport phenomena limitations, with the CPA taking up to 72 hours to penetrate the IVD, but cytotoxicity occurring within 6 hrs.

1.6 Literature review on transport phenomena

Transport phenomena is known to be limited in the IVD not only for CPAs, but for nutrients as well. Most information known about IVD transport phenomena is from studies of nutrient

transport in the IVD, so I will outline the collective knowledge of IVD transport phenomena in this context. The availability of nutrients for IVD cells depends on the balance of transport and consumption rates. This balance is disrupted as the IVD degenerates and undergoes complex structural changes leading to diminished transport. This includes (1) loss of proteoglycans (PG), (2) tissue dehydration, (3) disruption of the lamellae in the annulus fibrosus (AF), (4) and calcification of the cartilaginous endplates (CEP) (Andersson 1999; Huang, Urban, and Luk 2014; Willems et al. 2016). As a result, the IVD's tissue becomes starved of glucose and oxygen, preventing the cells from carrying out their normal cellular functions, maintaining homeostasis, and remodeling the tissue leading to an endless cycle of degeneration (Le Maitre, Freemont, and Hoyland 2007; Risbud et al. 2015; Payne and Spillane 1957; Baber and Erdek 2016; Turner 1959; King 1959; Maroudas et al. 1975; Hassler 1969; Shirazi-Adl, Taheri, and Urban 2010; Bibby and Urban 2004).

This section reviews our accumulated knowledge in the field of IVD nutrient transport and the various factors that affect it including biochemistry, biomechanics, and cellularity. We also review the latest knowledge on modeling transport, experimental validation of transport in the disc, and methods to improve nutrient status of the IVD. Below is a list of important terms that are used throughout the chapter to discuss solute transport. Each term is briefly explained within the context of transport phenomena in the IVD and provided with an elementary equation.

1. Convection. This method of solute transport relies on the movement of bulk flow due to hydraulic and osmotic pressure gradients (Adams and Hutton 1986). In the IVD, bulk flow movement is facilitated by postural variation motion of the spine (Adams and Hutton 1986).

Equation 1.1

$$N_A = k_c \nabla c_A$$

Molar flux of solute A is represented by N_A with a mass transfer coefficient of k_c, which combines properties of the system including, geometry, velocity, and fluid properties. The driving force for mass transfer is represented by the concentration gradient ∇c_A (Pathak and Basu 2013).

2. Diffusion. Diffusion describes the process of solute movement from a high to a low concentration region through means of random Brownian motion (Torzilli P.A. 1990).

Diffusion of solutes can be modeled using Fick's first law (Equation 1.2) (Travascio, Valladares-Prieto, and Jackson 2020; Torzilli P.A. 1990).

Equation 1.2

$$J = -D\nabla c_A$$

Where J is solute flux per cross-sectional area, D is the solute's diffusion coefficient (i.e., diffusivity), which depends on the temperature, viscosity, and molecular size, and ∇c_A describes concentration gradient as the driving force for diffusion (Travascio, Valladares-Prieto, and Jackson 2020). Fick's first law can describe most diffusion processes in the IVD; however, it has its limitations when other factors such as pore size and solute-matrix interactions are present (Travascio, Valladares-Prieto, and Jackson 2020).

3. Permeability. This property characterizes the tissue's capacity to enable fluid flow through the extracellular matrix (ECM). It is described by the permeability coefficient (m^4/Ns) derived from Darcy's law (Equation 1.3) (Gu et al. 1999).

Equation 1.3

$$k = \frac{\frac{Q}{\Delta P}}{\frac{h}{A}}$$

Where Q describes the volumetric flow, ΔP is the pressure difference across the sample, A is the sample's cross sectional area available for fluid permeation, and h describes the sample's thickness.

4. Porosity. The amount of space within a solid that is occupied by a fluid describes porosity (φ) (Gu et al. 2004). In the IVD, porosity varies based on location and mechanical load (Malandrino et al. 2014). The value for porosity in the IVD can be measured by taking the ratio of wet and dry tissue multiplied by the ratio of solute density to solvent density (Equation 1.4) (Gu et al. 2004).

Equation 1.4

$$\varphi^w = \frac{W_{wet} - W_{dry}}{W_{wet} - W_{sol}} \cdot \frac{\rho_{sol}}{\rho_w}$$

In this equation, φ^w denotes the volume fraction of water, $W_{wet} - W_{dry}$ is water content in the tissue, $W_{wet} - W_{sol}$ describes the tissue's buoyancy force, ρ_{sol} describes bathing solution density, and ρ_w represents the density of water.

1.6.1 Nutrient supply in the intervertebral disc

Two sets of capillaries supply the IVD with its nutrients (Figure 1.1): one set is adjacent to the CEP and supplies the IVD with most of its nutritional demands (Nachemson et al. 1970; Naylor, Happey, and Macrae 1955; King 1959); the other set penetrates several millimeters into the AF and supplies the surrounding AF tissue primarily (Sakai and Schol 2017; Urban et al. 1977; Maroudas et al. 1975; Nachemson et al. 1970). IVD developmental studies highlight hyper-vascularized tissue in early childhood, with significant devascularization occurring during maturation (Nachemson et al. 1970; Shutkin 1952). Decreased vessel density in the boney endplate correlates with diminished nutrient supply in the IVD (Hassler 1969; Boos et al. 2002). Due to the avascular nature of the IVD, the nutrients and metabolites rely on two transport mechanisms: diffusion and convection.

1.6.1.1 Diffusion

Loss in the vasculature led early researchers including Bohmig, Schmorl, and Ubermuth to study molecular transport in the IVD and investigate the effects of disc degeneration on transport (Nachemson et al. 1970; Malcolmson 1935; Bush 1934; Albert 1942; Shutkin 1952). Their work can be summarized in three key points. (1) Solute transport in the IVD relies on molecular diffusion, (2) most solute diffusion takes place through the CEP, and (3) calcification of the IVD hinders molecular diffusion propagating the cycle of degeneration (Nachemson et al. 1970; Malcolmson 1935; Bush 1934; Albert 1942; Shutkin 1952).

Most solute diffusion occurs in the IVD through the large surface area shared by the CEP and NP. This interface has been termed a "gateway" for solute diffusion due to pores and channels that facilitate transport (Figure 1.2) (Naylor 1951; Yin et al. 2019; Naresh-Babu et al. 2016; Wong et al. 2019; Nachemson et al. 1970; Roberts, Menage, and Urban 1989; Ogata and Whiteside 1981; Nguyen-minh et al. 1998; Urban et al. 1977; Silverman 1954; Urban, Holm, and Maroudas 1978; Albert 1942; Naylor, Happey, and Macrae 1955; King 1959; Urban and Maroudas 1979). Solute transport through the CEP can be appreciated through experiments that look at diffusion patterns in IVDs (Ashinsky et al. 2020; Rajasekaran et al. 2004; Rajasekaran et al. 2008; Nguyen-minh et al. 1997; Muftuler et al. 2015). To mimic degenerated IVDs with mineralized CEPs and low vasculature, researchers blocked the CEPs with bone cement (Ashinsky et al. 2020; Rajasekaran et al. 2004; Rajasekaran et al. 2008; Nguyen-minh et al. 1997; Muftuler et al. 2015). These studies

support the notion that blocked IVDs suffer from diminished solute diffusion coefficients and disrupted solute gradients (Ashinsky et al. 2020; Rajasekaran et al. 2004; Rajasekaran et al. 2008; Nguyen-minh et al. 1997; Muftuler et al. 2015).

Once solutes cross the CEP, they travel several millimeters to reach the IVD's axial center (Bibby et al. 2001). This slow and gradual movement of solutes creates concentration gradients that decrease from physiological levels near the IVD's boundaries to critical levels at the IVD's center (Sakai and Grad 2015; Shirazi-Adl, Taheri, and Urban 2010; Bibby and Urban 2004; Jackson et al. 2009). Worthy to note that lactate and other metabolites have a reversed trend (Sakai and Grad 2015; Shirazi-Adl, Taheri, and Urban 2010; Bibby and Urban 2004; Jackson et al. 2009).
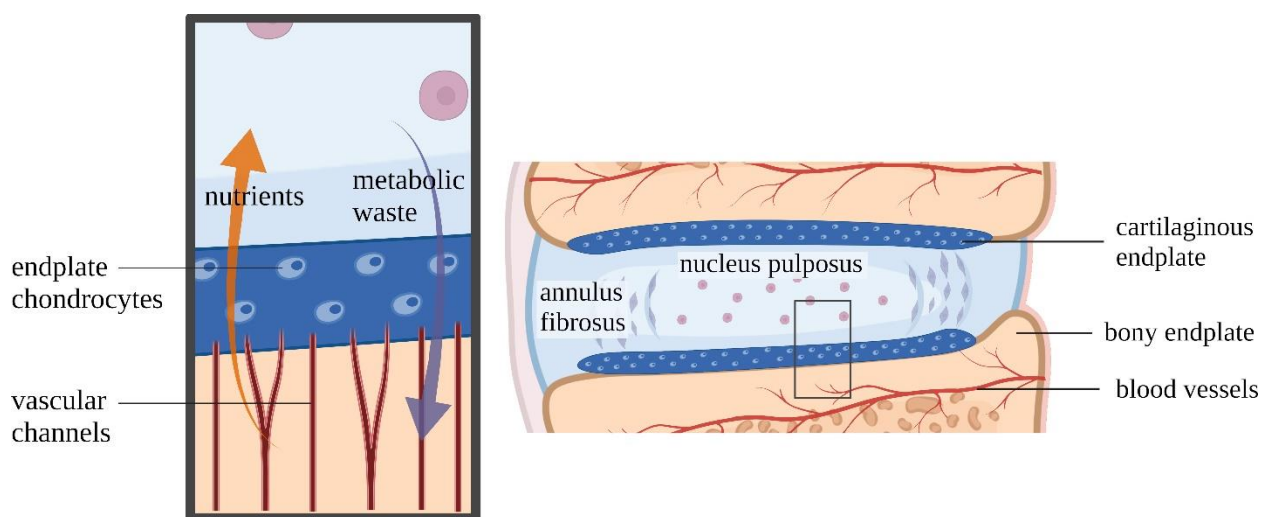
Figure 1.2. Most nutrient transport into the IVD occurs through the surface area shared between the NP and the CEP (left). At this interface, solute diffusion of nutrients and metabolic waste occurs readily through the large number of pores and vascular channels (right).

Molecular diffusion can also occur through the highly organized extracellular matrix of the AF (Urban et al. 1977; Naresh-Babu et al. 2016; Jackson et al. 2008; Hsu and Setton 1999). In a diffusion tensor imaging study, Stein et al. concluded that the outer AF could have an increasingly important role in the diffusion of nutrients as individuals age (Stein et al. 2021). They further stated that while the CEP pathway for nutrient diffusion becomes diminished due to aging, the highly ordered fibers of the outer AF could aid in the directional displacement of nutrients into the IVD (Stein et al. 2021). However, diffusion through the AF is believed to be insufficient in supporting the IVD's total nutritional demands. MRI tracking of contrast agents in the IVD show solutes in

the NP to depend on diffusion through the CEP, while diffusion through the AF only penetrated a few millimeters through the AF in adult IVDs (Naresh-Babu et al. 2016). It is fitting to note that the specific alignment of AF fibers increases the diffusion of solutes in the axial and circumferential aspects of healthy adult AF tissue (Jackson et al. 2008). Please refer to Table 1 for diffusion coefficient values of glucose, oxygen, and lactate in the IVD.

Table 1.1. Diffusion coefficients for glucose, lactate, and oxygen in the IVD.

Model	Tissue	Temperature [°C]	D_g [m²/s]	D_l [m²/s]	D_o [m²/s]	References
Human *ex vivo*	CEP	37	3.44E-11	5.52E-11	-	(Wu et al. 2016)
Human *in vitro*	AF	Room temperature	3.56E-11 - 8.71E-11	-	1.13E-10 - 1.85E-9	(Jackson et al. 2012)
Bovine *in vitro*	AF	Room temperature	-	2.73E-6	-	(Das et al. 2009)
	NP		-	5.12E-6	-	
FE model	CEP	37	9.17E-10	1.39E-09	3.00E-09	(Magnier et al. 2009)
Bovine *in vitro*	AF	Room temperature	1.38E-10 - 9.17E-11	-	1.43E-09	(Jackson et al. 2008)
FE model	CEP	-	2.11E-10	3.14E-10	7.81E-10	(Soukane, Shirazi-Adl, and Urban 2007)
	AF		2.85E-10	4.24E-10	1.05E-09	
	NP		3.78E-10	5.61E-10	1.39E-09	
FE model	AF	-	2.50E-10	4.86E-10	8.33E-10	(Sélard, Shirazi-Adl, and Urban 2003)
	NP		3.75E-10	6.11E-10	1.28E-09	
Canine *in vivo*	CEP	37	-	6.25E-10	1.28E-09	(Holm et al. 1981)
	NP		-	7.64E-10	1.39E-09	
Human *in vitro*	CEP	37	2.43E-10	-	-	(Maroudas et al. 1975)
	AF		2.50E-10	-	-	

1.6.1.2 Convection

Despite the profound evidence that diffusion is the main means of transport in the IVD, recent studies show conflicting results about the role of convection in molecular transport (Jackson et al. 2012; Das et al. 2009). Because of the IVD's large area and avascularity, it is thought that diffusion alone cannot be the only driving force for solute transport (Sylven 1951; Giers et al.

2017a). The transport of solutes via convection depends on the IVD's fluctuating water content due to spinal compression and traction throughout the day (Adams and Hutton 1983). MR scans have shown IVD water content in patients to vary throughout the day significantly (Ludescher et al. 2008; Malko, Hutton, and Fajman 1999). The IVD tends to have a higher water content after a long night sleep, and due to sustained loading during the day, the IVD loses some of its water content (Belavý et al. 2011; Malko, Hutton, and Fajman 2002). Changes in water content are believed to induce bulk flow by generating hydraulic and osmotic pressure gradients (Adams and Hutton 1986). Recent studies showed axial loading-induced convection enhancing the transport of small molecules into rabbit IVDs (Holm and Nachemson 1983; Adams and Hutton 1986; KRAEMER, KOLDITZ, and GOWIN 1985a; Gullbrand et al. 2015; Sampson, Sylvia, and Fields 2019). Convection in the IVD was reported to improve the transport of small and large molecules was improved by a factor of 1.85 and 4.97, respectively (Gullbrand et al. 2015; Sampson, Sylvia, and Fields 2019).

Research is still unclear on the importance of dynamic loading and convective transport in the IVD. Some studies suggest an insignificant effect of dynamic loading on small molecules, e.g., glucose, but a significant one on large molecules such as albumin proteins (O'Hara, Urban, and Maroudas 1990; URBAN et al. 1982; KATZ, HARGENS, and GARFIN 1986). Other studies show no improvement in the penetration of solutes into the IVD by means of dynamic loading (Giers et al. 2017a; Hughes et al. 1993). More studies are still needed to elucidate the importance of convection on solute transport in the IVD, providing clinical insight into tailoring IVD treatment regimens to fit the patient's lifestyle.

1.6.2 Intervertebral disc properties affecting transport

Solute transport in IVDs plays an essential role in maintaining the physiological microenvironment, contributing to cellular homeostasis, nutrient replenishment, and the removal of metabolites. The complex structure of the IVD's ECM, which is made of a mosaic of polysaccharides and glycoproteins, introduces several factors that can affect molecular transport, such as tissue biochemistry, charge density, permeability, and cellular metabolism.

1.6.2.1 Intervertebral disc biochemistry

The IVD's extracellular matrix (ECM) is a biochemical mosaic of different proteins and polysaccharides, the two most common compounds are proteoglycans (PGs), and glycosaminoglycans (GAGs) (Oegema 1993). PGs are a type of non-collagenous proteins (lecticans such as aggrecan) with a serine-rich core connecting sulfated GAGs, including sulfated chondroitin and keratan sulfate (Figure 1.3) (Eyre 1979). The negative charge of the sulfated GAGs attracts and retains water molecules within the tissue contributing to molecular transport, osmotic pressures, viscoelastic properties of the tissue, and the ability to withstand load (Sylven 1951; Vo et al. 2016; Risbud et al. 2015; Bezci et al. 2019).
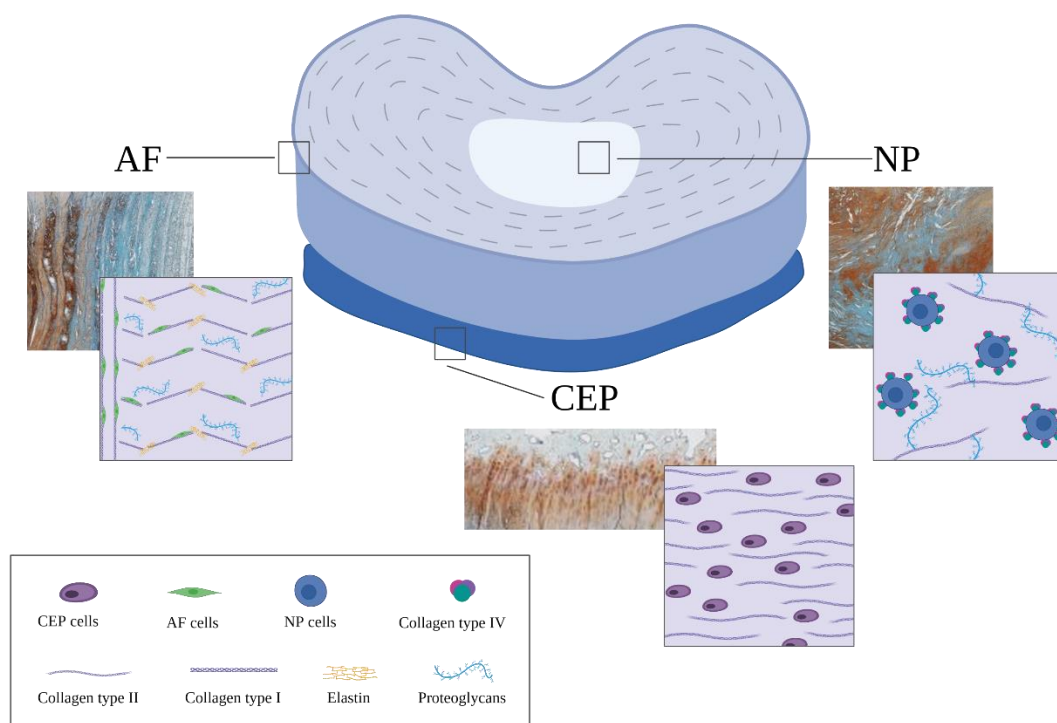
Figure 1.3. Biochemical composition of the IVD. The IVD consists of three different tissue types: the AF, CEP and NP. The AF is made of concentric lamella of type I collagen and PGs. Due to the AF's compact area and stiffness, it helps withstand torsional forces. At the center of the IVD exists the NP, which is made of disorganized type II collagen fiber and PGs. The NP is known to have the highest PG content retaining water molecules. This structure is responsible of withstanding compressive forces. The inferior and superior sides of the IVD are attached to the vertebral bodies through the CEPs. CEPs are thin, porous plates of cartilage that are made of organized type II collagen and hyaline.

Variation in the amount of chondroitin and keratan sulfates can alter the ECM's total charge density, total steric hindrance, and water content (Figure 1.4) (Antoniou et al. 2004; Vo et al. 2016). The average charge density in the NP is measured to be 317 mM compared to 48.1 mM in the AF (Cortes et al. 2014). Since most sulfated GAGs are located at the center of the NP and gradually drop moving outward to the outer AF, we can expect the hydraulic and osmotic pressures to follow the same profile since they are closely related to water content (Figure 1.4) (Iatridis et al. 2007; Adams and Hutton 1986). Iatridis et al. developed a linear correlation between GAG content and water percent based on measurements in human lumbar IVD (Equation 1.5) (Iatridis et al. 2007).

Equation 1.5

$$GAG = -1329 + 20.9 \times \%H2O$$

The total charge density of the IVD's ECM can also affect the diffusion pathways of administered antibiotics and drugs (Table 2) (Thomas Rde et al. 1995). Hence, negatively charged molecules face greater exclusion in the NP due to the high fixed charge density. Therefore, less negatively-charged molecules, about one third, diffuse into the NP compared to more positively charged molecules (Urban and Maroudas 1979). Sustained loading of the IVD is believed to compress the ECM and force the sulfated GAGs to pack closely, resulting in a localized high charge density which reduces the diffusion of both small and charged molecules (Gu et al. 2004). An MRI study observed a change in the diffusion coefficient of Gadoteridol, a nonionic contrast agent, due to prolonged cyclic loading of the IVD (Arun et al. 2009).

Table 1.2. Diffusion coefficients for several large and charged molecules in the IVD.

Compound	Charge	Molecular weight (g/mol)	Apparent diffusion coefficient in the AF (m²/s)	Reference
Dextran-3	0	3,000	2.47E-11	(Boubriak et al. 2000)
Dextran-10	0	1.71E-07	1.73E-11	(Boubriak et al. 2000)
Dextran-40	0	1.59E-07	1.64E-11	(Boubriak et al. 2000)
Dextran-70	0	1.61E-07	1.13E-11	(Boubriak et al. 2000)
Vancomycin	+1	1449	7.94E-12	(Jackson et al. 2018)
Oxacillin	-1	401	2.26E-10	(Jackson et al. 2018)
Fluorescein	-2	332	~1E-10	(Travascio and Gu 2007)

Degeneration of the IVD involves the loss of PGs and sulfated GAGs, reducing the total negative charge density in the ECM (Figure 1.4) (Martins et al. 2018; Pulickal et al. 2019). Once the IVD's total charge density becomes less negative, the tissue's ability to retain water decreases and becomes dehydrated (Figure 1.4) (Naylor, Happey, and Macrae 1955). Degeneration of the NP can lead to a 20-30% loss in water content and is thought to reduce nutrition transport to this compartment (Naylor 1951; Gruber and Hanley 1998). X-ray studies also show increased crystallization of the collagen in the NP which reduces its ability to absorb and hold water (Naylor 1962).
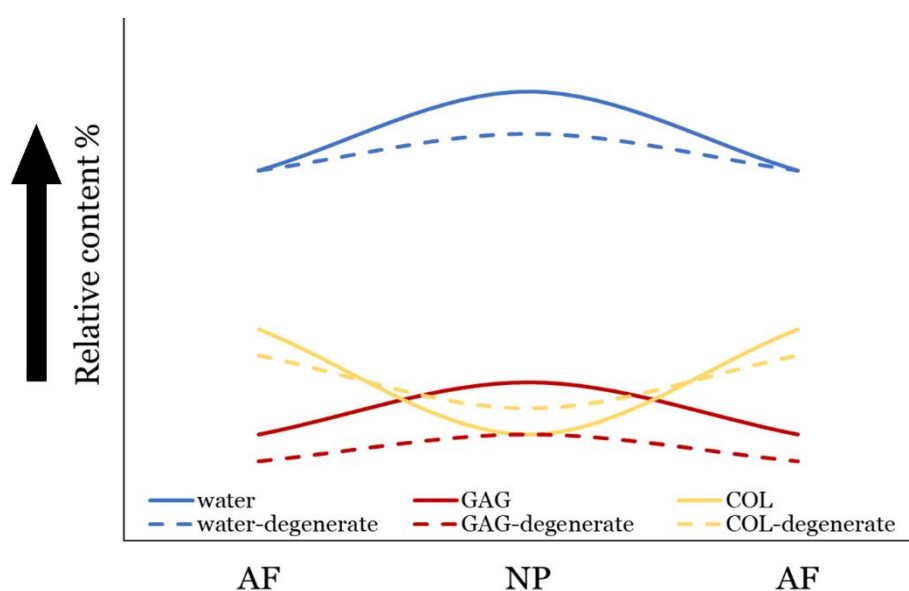
Figure 1.4. The profile of water, GAG, and collagen (COL) in a healthy IVD (continuous line), and a degenerate IVD (dashed line) (Weidenbaum et al. 1992; Iatridis et al. 2007; Lyons, Eisenstein, and Sweet 1981). The NP's high content of GAGs helps with the retainment of water which aids in withstanding compressive forces (Iatridis et al. 2007). The AF's high content of COL contributes to its rigidity so it can contain the NP, and withstand torsional forces (Iatridis et al. 2007). IVD degeneration leads to loss of GAG in the NP, and it also alters the phenotype of NP cells prompting them to deposit more COL, instead of GAG, leading to a drop in water content and loss of biomechanical function (Hartman et al. 2018).

Another problem associated with degeneration of the IVD includes high osmolarity and internal pressure due to free-floating molecules (Naylor 1962). Increased osmolarity in the AF can lead to a rise in water absorption and internal pressure leading to rupture of the AF (Naylor 1962). In conclusion, the biochemistry of the ECM is important in maintaining the flux of nutrients and

metabolites. Loss of PG and GAG due to degeneration can be very detrimental to the IVD's health leading to compromised nutrient transport, reduced IVD height, and abnormal biomechanical loading (Vo et al. 2016; Beattie, Morgan, and Peters 2008; Niinimäki et al. 2009; Kealey et al. 2005; Belykh et al. 2017; Adams and Hutton 1985; Bibby et al. 2002; Jackson et al. 2008; Kraemer, Kolditz, and Gowin 1985b; Yuan et al. 2009; Yang and O'Connell 2019; Sampson, Sylvia, and Fields 2019; Iatridis et al. 2007).

1.6.2.2 Permeability in the intervertebral disc

Permeability in the IVD refers to the tissue's capacity to permit fluid flow through its ECM and it relies on the pressure, area, and height of the tissue (Gu et al. 1999). The CEP and NP have a relatively low water permeability of $5.5 \cdot 10^{-16}$ (m^4/N·s) compared to the AF's of $64 \cdot 10^{-16}$ (m^4/N·s) (Maroudas et al. 1975; Cortes et al. 2014). The low permeability of both tissues (CEP and NP) is thought to restrict local water loss due to dynamic loading contributing to the tissue's resistance of compression (Cortes et al. 2014; Tourell et al. 2017; Adams and Hutton 1985; Bibby et al. 2002; Jackson et al. 2008; Kraemer, Kolditz, and Gowin 1985b; Yuan et al. 2009; Yang and O'Connell 2019; Sampson, Sylvia, and Fields 2019; Iatridis et al. 2007; McMillan, Garbutt, and Adams 1996). On the other hand, as the AF is compressed it loses 30% of its water content due to its high permeability values (Figure 1.5) (McMillan, Garbutt, and Adams 1996). Thus, permeability plays an important role in controlling water content in the tissue which facilitates solute transport and affects solute concentration gradients.
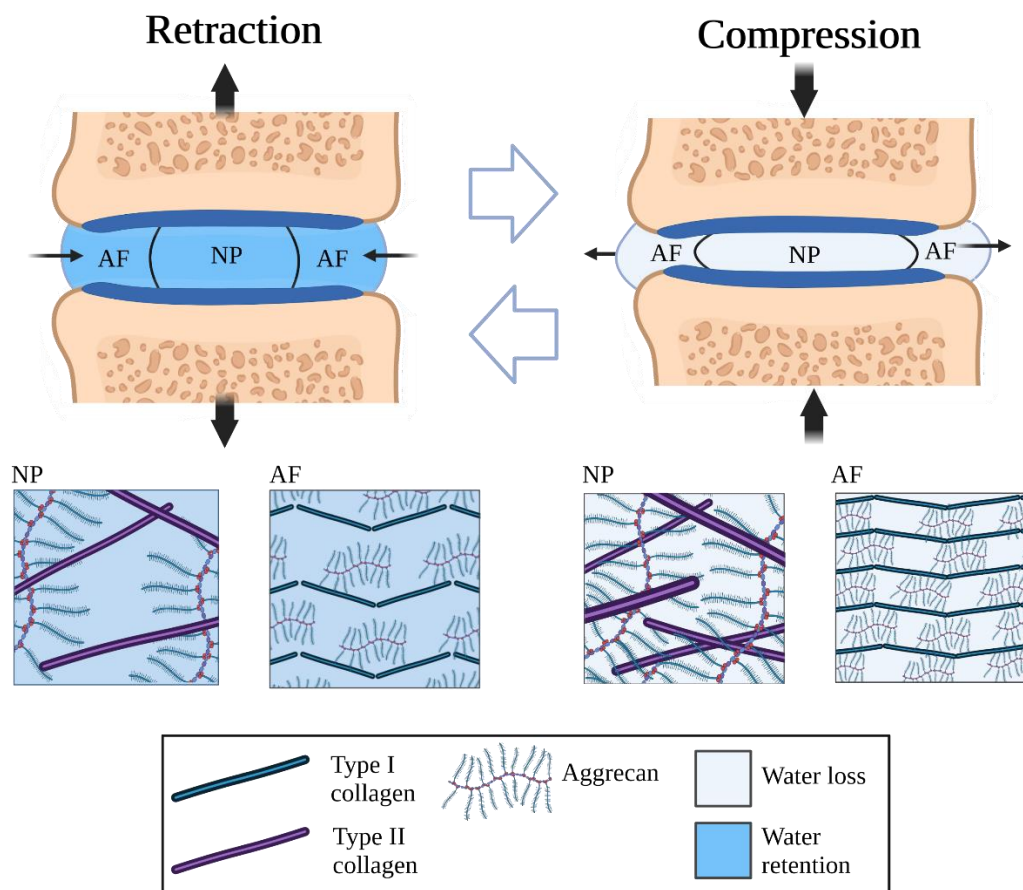
Figure 1.5. Retraction and compression of the IVD changes its water content and ECM density. As axial load compresses the IVD, pore size is reduced, and water is pushed out of the tissue. Type II collagen and aggrecan move closer together and become denser in the NP as the IVD is compressed. Likewise, type I collagen and aggrecan become denser in the AF.

Degeneration of the IVD has been shown to alter tissue properties leading to reduced permeability. For example, blood flow becomes restricted to the bony endplates increasing the deposition of calcium ions in the CEP which reduces permeability by 60-70% and restricts transport distance by 50% (Figure 1.6) (Törner and Holm 1985; Wong et al. 2019; Jones and Roberts 1933; Albert 1942; Silverman 1954; Gu et al. 1999; DeLucca et al. 2016; Fields et al. 2018; Giers et al. 2017a; Van Der Werf et al. 2007; Bibby and Urban 2004; Han et al. 2019; Liu et al. 2016).

Normal IVD · Degenerated IVD
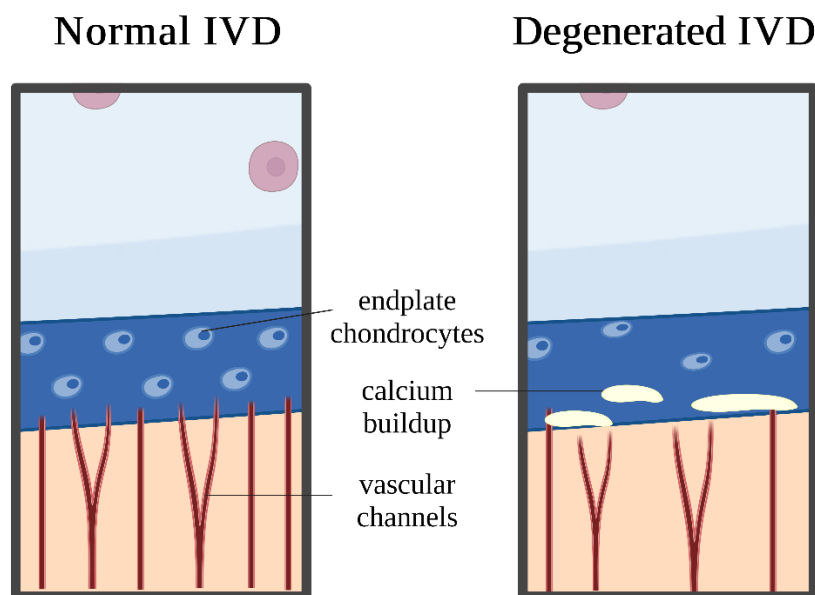
Figure 1.6. Comparison of the CEP between a normal and degenerated IVD. Degeneration leads to restricted blood flow to the bony endplates and increased deposition of calcium in the CEP.

Lower permeability levels in the tissue can thus be responsible for high accumulation of lactate and low levels of glucose contributing to cell death, low metabolic rates, and slow remodeling of the ECM (DeLucca et al. 2016; Brodin 1955; Naylor, Happey, and Macrae 1955; King 1959).

1.6.2.3 Cell metabolism and density

Despite low cell numbers in the IVD which make up ~1% of the tissue, having a healthy population of cells is crucial to maintaining matrix homeostasis and IVD biomechanical functions (Hohaus et al. 2008; Gruber et al. 2004). It is believed that the IVD's cell distribution follows that of nutrients (Maroudas et al. 1975). As mentioned previously, a steep gradient of nutrients exists from the outer to the inner regions of the IVD creating hypoxic and acidic microenvironments in the inner AF and NP (Holm et al. 1981; Holm and Selstam 1982; HOLM, SELSTAM, and NACHEMSON 1982; Naqvi and Buckley 2015). Oxygen drops from physiological levels near the outer parts of the IVD to about 0-1 kPa (Ejeskär and Holm 1979). As a result of nutrient and oxygen distributions, higher cell count is found in the outer regions of the IVD especially in the CEP (Bibby et al. 2002; Martins et al. 2018; Holm et al. 1981; Holm and Selstam 1982; HOLM, SELSTAM, and NACHEMSON 1982). In contrast, low cell count is found in the inner region of

the IVD such as the NP and inner AF (Huang, Urban, and Luk 2014; Holm et al. 1981; Holm and Selstam 1982; HOLM, SELSTAM, and NACHEMSON 1982; Martins et al. 2018).

IVD cells are known to have distinct microenvironments due to lack of vasculature. For example, NP cells are known to be under hypoxia which prompts their reliance on glycolysis for the generation of ATP resulting in high accumulation of lactate, and acidification of the tissue (Silagi et al. 2021). Whereas AF cells tend to be more oxygenated and thus rely on phosphorylation for their ATP production (Hartman et al. 2018). The high acidity experienced in the NP has been shown to affect the main metabolic pathways as cells in such environments upregulate the expression of glucose transporters and glycolytic enzymes (Agrawal et al. 2008; Risbud et al. 2006). Hypoxic conditions in the IVD are also thought to increase the production of intermediates in the glycolytic cycle such as glucose-6-phosphate and decrease ones in the tricarboxylic cycle (TCA) including aspartate, and glutamate (Risbud et al. 2006). Acidification of the NP tissue, and generally in the IVD, has been linked to degeneration of the IVD leading to lower ECM turnover, inflammation, and cell senescence (Gilbert et al. 2016). In addition, high acidity has shown to reduce the expression of collagen and GAGs expression in the ECM propagating IVD degeneration (Bibby and Urban 2004; Martins et al. 2018; Naqvi and Buckley 2015). Accordingly, it has been postulated that tackling the high lactate levels in the IVD would slow down IVD degeneration and alleviate pain (Gilbert et al. 2016). A recent study however showed that excess content of lactate in the tissue is not all that harmful since the more oxygenated cells of the AF consume it in oxidative phosphorylation to produce ATP (Wang et al. 2021).

In addition to changes in cellular metabolic pathways, the harsh microenvironment at the axial center of IVDs can lead to changes in cell viability, induce senescence, apoptosis, and autophagy (Horner and Urban 2001; Yurube et al. 2020; Silagi et al. 2020; Le Maitre et al. 2021). If pH levels in the IVD drop to 6.8 due to lactate accumulation, it can lead to a 40-65% loss in cell density (Bibby and Urban 2004; Martins et al. 2018). A shift in IVD cell phenotype is also expected because of degeneration and high acidity. For example, the membrane potential for the cells' mitochondria decreases harming the process of ATP production and compromising the tissue's response to various environmental stresses including nutrient deprivation, and inflammation (Hartman et al. 2018). The shift in cell phenotype drives aging NP cells to fibrosis and increased expression of collagen instead of PG (Hartman et al. 2018; Byvaltsev et al. 2018). As a result, the NP compartment becomes dehydrated and loses its ability to withstand compression (Ishihara and

Urban 1999; Hartman et al. 2018). Changes in the phenotype of CEP cells have shown increased deposition of minerals like calcium into the ECM leading to a 50-60% decrease in permeability (Ishihara and Urban 1999; Hartman et al. 2018; Giers et al. 2017a; Van Der Werf et al. 2007; Bibby and Urban 2004; Han et al. 2019; Liu et al. 2016). In addition, the number of senescent cells triple further increasing the demand for nutrients by 3-5 times compared to healthy IVD cells (Cisewski et al. 2018).

Understanding how the nutrient status of the IVD affects cell viability and metabolism is important to develop studies that aim to improve the overall health of the IVD. Several studies have incorporated cell density and metabolic data to create finite element models to further investigate the effects of limited transport on nutrient availability and IVD degeneration (Holm et al. 1981; Holm and Selstam 1982; HOLM, SELSTAM, and NACHEMSON 1982; Bibby et al. 2005).

1.6.3 Modeling transport

Researchers have pivoted toward developing advanced mathematical modeling techniques to study transport phenomena in the human IVD to overcome challenges in obtaining appropriate specimens that represent human discs. Studies have been relying on animal IVDs because of shared properties to human discs including geometry (O'Connell, Vresilovic, and Elliott 2007; O'Connell, Vresilovic, and Elliott 2007). However, animal IVDs have profound differences including cell population, tissue composition, degeneration mechanisms, and mechanical properties making it challenging to draw conclusions on human IVDs and thus are incompatible for translatable studies (Alini et al. 2008).

Studies have been successful in using finite element (FE) modeling to study transport of glucose, oxygen, and lactate in human IVDs. These models compartmentalized the IVD into three areas, the AF, CEP, and NP, and assigned each compartment with different experimentally measured transport properties, including diffusion coefficients for glucose, oxygen, and lactate, water content, cell density, and rate of glycolysis (Urban, Smith, and Fairbank 2004; Sélard, Shirazi-Adl, and Urban 2003; Bibby et al. 2005; Ferguson, Ito, and Nolte 2004; Jackson et al. 2009; Soukane, Shirazi-Adl, and Urban 2007). These models investigated the effects of various factors on transport in the IVD, e.g., cell metabolism, cell density, degeneration, calcification, vasculature density, and biomechanical loading (refer to Table 1 of Appendix A1).

Finite element modeling of solutes has the potential to provide patient-specific results leading the way for clinically viable tools to assess the nutrient status of human IVDs. One possible application for patient-specific models of human IVDs we believe, can be used in determining the appropriate dose and location of stem cells in patients who seek cell-based therapies to regenerate the IVD (Shalash et al. 2021). The authors of this paper have explained in a previous publication the advantages of developing a patient-specific platform to study molecular transport. We also demonstrated the importance of generating specific models that incorporate patient-specific parameters that play an essential role in molecular diffusion including IVD geometry, diffusion coefficients, and reaction rates (Shalash et al. 2021).

1.6.4 Validation of transport

Imaging techniques that have been widely used to assess tissue properties in the human body were also adapted to study transport phenomena in the IVD. For imaging techniques to be successful they are required to have the following four requirements: (1) reproducibility in which the techniques are able to reproduce the same results in subsequent measurements; (2) the ability to differentiate patients, in which the technique can produce significant differences in measured values between patients with different stages of degeneration and those who are healthy; (3) monitoring of therapy and prediction of risk of disease; (4) validation requires the imaging technique to measure what is supposed to be measuring with high accuracy and precision (Link, Neumann, and Li 2017). A summary of common imaging techniques to assess molecular transport is provided including MRI, CT, etc. (Table 1.3).

Table 1.3. A list of various imaging techniques used to study transport in the IVD

Imaging technique	Application	Reference
Magnetic Resonance (MR)	• Diffusion properties • Dynamic information • Fiber alignment • Functional information • Water content	(Tourell et al. 2017; Naresh-Babu et al. 2016; Haughton 2004, 2006)

Table 1.3. A list of various imaging techniques used to study transport in the IVD. (Continued)

Imaging technique	Application	Reference
Dynamic Contrast Enhanced (DCE)-MRI	• ECM integrity • Pathology • Solute transport	(Arpinar et al. 2015; Rajasekaran et al. 2010)
T2	• Classification of degeneration • Functional information • IVD structure • Morphology and pathology • Neurography • Water content	(Chiu et al. 2001; Haughton 2004, 2006; Xiong et al. 2018)
T1-w	• Functional information • IVD biochemistry • IVD structure • Water content	(Chiu et al. 2001; Xiong et al. 2018; Giers et al. 2013)
Diffusion Tensor Imaging (DTI)	• Diffusion properties • Fiber integrity	(Haughton 2004)
DWI	• Functional information • Pathology • Tissue consistency • Water diffusion	(Xiong et al. 2018)
ADC	• Classification of degeneration • Diffusion properties • ECM integrity • Pathology • Water content	(Zhang et al. 2014; Beattie, Morgan, and Peters 2008; Niinimäki et al. 2009; Kealey et al. 2005; Belykh et al. 2017)
Chemical Exchange Saturation Transfer (CEST)	• Classification of degeneration • IVD biochemistry	(Xiong et al. 2018)
Computed Tomography (CT)	• Dynamic imaging • Movement of spine • Structural integrity	(Haughton 2004)

1.3.5 Improvement of the intervertebral disc's nutrient status

Solute transport is important in maintaining balanced levels of nutrients and metabolites in the IVD to facilitate normal cellular functions and prevent hypoxic and acidic conditions from forming. Evidence suggests that restricted diffusion can be a driving factor for painful IVD degeneration and thus enhancing transport might be one way to maintain IVD health by preventing, slowing, or reversing degeneration (citation). Studies have suggested ways to improve transport including pharmacological and mechanical ones (Table 1.4).

Table 1.4. Summary of experiments that enhanced solute transport in the IVD.

Method used to enhance transport	Conclusions	References
• **Pharmacological**	• Nimodipine increased vasculature in the CEP	(Turgut et al. 2003)
• **Pharmacological**	• Recombinant-human Growth Differentiation Factor-5 (rhGDF-5) increased PG and water content	(Chujo et al. 2006)
• **Pharmacological**	• Osteogenic protein-1 increased PG and collagen contents	(Miyamoto et al. 2006)
• **Pharmacological**	• Nimodipine improved diffusion in patient lumbar IVDs	(Rajasekaran et al. 2008)
• **Pharmacological**	• Nimodipine (calcium channel antagonist) enhanced vessel size increasing diffusion in the IVD • Changing vessel density is not sufficient to improve diffusion	(Gullbrand et al. 2014)
• **Mechanical**	• Low-rate loading, 0.5 Hz at 0-200N, enhanced transport of nutrients and metabolites in rabbit IVDs	(Gullbrand et al. 2015)
Method used to enhance transport	Conclusions	References
• **Mechanical**	• Traction increased solute transport	(Giers et al. 2017b)
• **Implant**	• Polyurethane implantation increased nutrient transport and energy production	(Wang et al. 2017)
• **Pharmacological**	• MMP-8 reduced matrix density in the CEP enhancing the transport of small molecules	(Dolor et al. 2019)
• **Pharmacological**	• o-Vanillin and RG-7112 increased PG and water content	(Cherif et al. 2020)
• **Mechanical**	• Low-tension traction improved IVD's microenvironment and increased ECM synthesis	(Guo et al. 2020)

1.7 Conclusion

Restricted molecular transport is thought to be an initiator for intervertebral disc (IVD) degeneration leading to lower back pain. This review covers the latest understanding of transport in the IVD including the main transport mechanisms, common ways to validate transport theory, and breakthrough-methods aimed to improve molecular transport. The review also sheds light on the complexity of the nutrient transport problem in the IVD which motivated researchers to develop finite element models to better predict transport phenomena in the IVD. Transport phenomena limitations in patient IVDs can become an obstacle to guaranteed successful cell-based treatments. Therefore, future efforts to improve stem cell therapy outcomes should include improving the nutrient status in the IVD. This involves developing a platform that incorporates finite element modeling and the various factors affecting transport phenomena such as IVD pathology state, tissue diffusivity, ECM composition, and vessel density.

In the next chapter, I present the bioreactor system which was applied in this work to innovate a method to cryopreserve the IVD. Whole organ bioreactors are emerging as a preferred cultivation method compared to current protocols. For instance, bioreactors offer controlled and adaptable microenvironments that could mimic various *in vivo* scenarios overcoming a limitation in common culture systems, including two- and three-dimensional.

1.8 Acknowledgement

I would like to acknowledge Rylee A. Ramsey for her assistance with the figures.

1.9 References

Adams, M. A., and W. C. Hutton. 1983. 'The effect of posture on the fluid content of lumbar intervertebral discs', *Spine (Phila Pa 1976)*, 8: 665-71.

———. 1985. 'The effect of posture on the lumbar spine', *J Bone Joint Surg Br*, 67: 625-9.

———. 1986. 'The effect of posture on diffusion into lumbar intervertebral discs', *Journal of Anatomy*, 147: 121-34.

Agrawal, A., S. Gajghate, H. Smith, D. G. Anderson, T. J. Albert, I. M. Shapiro, and M. V. Risbud. 2008. 'Cited2 modulates hypoxia-inducible factor-dependent expression of vascular endothelial growth factor in nucleus pulposus cells of the rat intervertebral disc', *Arthritis Rheum*, 58: 3798-808.

Aijaz, A., M. Li, D. Smith, D. Khong, C. LeBlon, O. S. Fenton, R. M. Olabisi, S. Libutti, J. Tischfield, M. V. Maus, R. Deans, R. N. Barcia, D. G. Anderson, J. Ritz, R. Preti, and B. Parekkadan. 2018. 'Biomanufacturing for clinically advanced cell therapies', *Nat Biomed Eng*, 2: 362-76.

Albert, M. 1942. 'Calcification of the Intervertebral Disks', *Br Med J*, 1: 666-8.

Alini, Mauro, Stephen M. Eisenstein, Keita Ito, Christopher Little, A. Annette Kettler, Koichi Masuda, James Melrose, Jim Ralphs, Ian Stokes, and Hans Joachim Wilke. 2008. 'Are animal models useful for studying human disc disorders/degeneration?', *European Spine Journal*, 17: 2-19.

Andersson, G. B. 1999. 'Epidemiological features of chronic low-back pain', *Lancet*, 354: 581-5.

Antoniou, John, Caroline N. Demers, Gilles Beaudoin, Tapas Goswami, Fackson Mwale, Max Aebi, and Mauro Alini. 2004. 'Apparent diffusion coefficient of intervertebral discs related to matrix composition and integrity', *Magnetic Resonance Imaging*, 22: 963-72.

Arpinar, Volkan Emre, Scott D. Rand, Andrew P. Klein, Dennis J. Maiman, and L. Tugan Muftuler. 2015. 'Changes in perfusion and diffusion in the endplate regions of degenerating intervertebral discs: a DCE-MRI study', *European Spine Journal*, 24: 2458-67.

Arun, Ranganathan, Brian J. C. Freeman, Brigitte E. Scammell, Donal S. McNally, Eleanor Cox, and Penny Gowland. 2009. '2009 ISSLS Prize Winner: What Influence Does Sustained Mechanical Load Have on Diffusion in the Human Intervertebral Disc?: An In Vivo

Study Using Serial Postcontrast Magnetic Resonance Imaging', *Spine (Phila Pa 1976)*, 34: 2324-37.

Ashinsky, B. G., E. D. Bonnevie, S. A. Mandalapu, S. Pickup, C. Wang, L. Han, R. L. Mauck, H. E. Smith, and S. E. Gullbrand. 2020. 'Intervertebral Disc Degeneration Is Associated With Aberrant Endplate Remodeling and Reduced Small Molecule Transport', *J Bone Miner Res*, 35: 1572-81.

Baber, Z., and M. A. Erdek. 2016. 'Failed back surgery syndrome: current perspectives', *J Pain Res*, 9: 979-87.

Beattie, Paul F., Paul S. Morgan, and Denise Peters. 2008. 'Diffusion-Weighted Magnetic Resonance Imaging of Normal and Degenerative Lumbar Intervertebral Discs: A New Method to Potentially Quantify the Physiologic Effect of Physical Therapy Intervention', *Journal of Orthopaedic & Sports Physical Therapy*, 38: 42-49.

Belavý, Daniel L., Gabriele Armbrecht, Carolyn A. Richardson, Dieter Felsenberg, and Julie A. Hides. 2011. 'Muscle Atrophy and Changes in Spinal Morphology: Is the Lumbar Spine Vulnerable After Prolonged Bed-Rest?', *Spine (Phila Pa 1976)*, 36: 137-45.

Belykh, Evgenii, Andrey A. Kalinin, Arpan A. Patel, Eric J. Miller, Michael A. Bohl, Ivan A. Stepanov, Liudmila A. Bardonova, Talgat Kerimbaev, Anton O. Asantsev, Morgan B. Giers, Mark C. Preul, and Vadim A. Byvaltsev. 2017. 'Apparent diffusion coefficient maps in the assessment of surgical patients with lumbar spine degeneration', *PLOS ONE*, 12: e0183697.

Bezci, Semih E., Benjamin Werbner, Minhao Zhou, Katerina G. Malollari, Gabriel Dorlhiac, Carlo Carraro, Aaron Streets, and Grace D. O'Connell. 2019. 'Radial variation in biochemical composition of the bovine caudal intervertebral disc', *JOR SPINE*, 2: e1065.

Bibby, S. R., J. C. Fairbank, M. R. Urban, and J. P. Urban. 2002. 'Cell viability in scoliotic discs in relation to disc deformity and nutrient levels', *Spine (Phila Pa 1976)*, 27: 2220-8; discussion 27-8.

Bibby, S. R., D. A. Jones, R. M. Ripley, and J. P. Urban. 2005. 'Metabolism of the intervertebral disc: effects of low levels of oxygen, glucose, and pH on rates of energy metabolism of bovine nucleus pulposus cells', *Spine (Phila Pa 1976)*, 30: 487-96.

Bibby, S. R., and J. P. Urban. 2004. 'Effect of nutrient deprivation on the viability of intervertebral disc cells', *Eur Spine J*, 13: 695-701.

Bibby, Susan R. S., Deborah A. Jones, Robert B. Lee, Jing Yu, and Jill P. G. Urban. 2001. 'The pathophysiology of the intervertebral disc', *Joint Bone Spine*, 68: 537-42.

Boos, N., S. Weissbach, H. Rohrbach, C. Weiler, K. F. Spratt, and A. G. Nerlich. 2002. 'Classification of age-related changes in lumbar intervertebral discs: 2002 Volvo Award in basic science', *Spine (Phila Pa 1976)*, 27: 2631-44.

Boubriak, O. A., J. P. G. Urban, S. Akhtar, K. M. Meek, and A. J. Bron. 2000. 'The Effect of Hydration and Matrix Composition on Solute Diffusion in Rabbit Sclera', *Experimental Eye Research*, 71: 503-14.

Bradley, J. A., E. M. Bolton, and R. A. Pedersen. 2002. 'Stem cell medicine encounters the immune system', *Nat Rev Immunol*, 2: 859-71.

Brodin, H. 1955. 'Paths of nutrition in articular cartilage and intervertebral discs', *Acta Orthop Scand*, 24: 177-83.

Bruehlmann, S. B., J. B. Rattner, J. R. Matyas, and N. A. Duncan. 2002. 'Regional variations in the cellular matrix of the annulus fibrosus of the intervertebral disc', *J Anat*, 201: 159-71.

Bush, G. B. 1934. 'The Clinical Importance of the Intervertebral Discs, with Special Reference to Nuclear Prolapses', *Bristol Med Chir J (1883)*, 51: 173-82.

Byvaltsev, V. A., S. I. Kolesnikov, L. A. Bardonova, E. G. Belykh, L. I. Korytov, M. B. Giers, and M. C. Preul. 2018. 'Assessment of Lactate Production and Proteoglycans Synthesis by the Intact and Degenerated Intervertebral Disc Cells under the Influence of Activated Macrophages: an In Vitro Study', *Bulletin of Experimental Biology and Medicine*, 166: 170-73.

Centeno, C., J. Markle, E. Dodson, I. Stemper, C. J. Williams, M. Hyzy, T. Ichim, and M. Freeman. 2017. 'Treatment of lumbar degenerative disc disease-associated radicular pain with culture-expanded autologous mesenchymal stem cells: a pilot study on safety and efficacy', *J Transl Med*, 15: 197.

Cherif, Hosni, Daniel G. Bisson, Matthew Mannarino, Oded Rabau, Jean A. Ouellet, and Lisbet Haglund. 2020. 'Senotherapeutic drugs for human intervertebral disc degeneration and low back pain', *eLife*, 9: e54693.

Chiu, Elaine J., David C. Newitt, Mark R. Segal, Serena S. Hu, Jeffrey C. Lotz, and Sharmila Majumdar. 2001. 'Magnetic Resonance Imaging Measurement of Relaxation and Water

Diffusion in the Human Lumbar Intervertebral Disc Under Compression In Vitro', *Spine (Phila Pa 1976)*, 26.

Chujo, Takehide, Howard S. An, Koji Akeda, Kei Miyamoto, Carol Muehleman, Mohamed Attawia, Gunnar Andersson, and Koichi Masuda. 2006. 'Effects of Growth Differentiation Factor-5 on the Intervertebral Disc−In Vitro Bovine Study and In Vivo Rabbit Disc Degeneration Model Study', *Spine (Phila Pa 1976)*, 31.

Cisewski, S. E., Y. Wu, B. J. Damon, B. L. Sachs, M. J. Kern, and H. Yao. 2018. 'Comparison of Oxygen Consumption Rates of Nondegenerate and Degenerate Human Intervertebral Disc Cells', *Spine (Phila Pa 1976)*, 43: E60-E67.

Coric, D., K. Pettine, A. Sumich, and M. O. Boltes. 2013. 'Prospective study of disc repair with allogeneic chondrocytes presented at the 2012 Joint Spine Section Meeting', *J Neurosurg Spine*, 18: 85-95.

Cortes, Daniel H., Nathan T. Jacobs, John F. DeLucca, and Dawn M. Elliott. 2014. 'Elastic, permeability and swelling properties of human intervertebral disc tissues: A benchmark for tissue engineering', *Journal of Biomechanics*, 47: 2088-94.

Crevensten, G., A. J. Walsh, D. Ananthakrishnan, P. Page, G. M. Wahba, J. C. Lotz, and S. Berven. 2004. 'Intervertebral disc cell therapy for regeneration: mesenchymal stem cell implantation in rat intervertebral discs', *Ann Biomed Eng*, 32: 430-4.

Das, D. B., A. Welling, J. P. Urban, and O. A. Boubriak. 2009. 'Solute transport in intervertebral disc: experiments and finite element modeling', *Ann N Y Acad Sci*, 1161: 44-61.

DeLucca, J. F., D. H. Cortes, N. T. Jacobs, E. J. Vresilovic, R. L. Duncan, and D. M. Elliott. 2016. 'Human cartilage endplate permeability varies with degeneration and intervertebral disc site', *J Biomech*, 49: 550-7.

Dolor, Aaron, Sara L. Sampson, Ann A. Lazar, Jeffrey C. Lotz, Francis C. Szoka, and Aaron J. Fields. 2019. 'Matrix modification for enhancing the transport properties of the human cartilage endplate to improve disc nutrition', *PLOS ONE*, 14: e0215218.

Ejeskär, Arvid, and Sten Holm. 1979. 'Oxygen Tension Measurements in the Intervertebral Disc', *Upsala Journal of Medical Sciences*, 84: 83-93.

Eyre, David R. 1979. 'Biochemistry of the Intervertebral Disc.' in David A. Hall and D. S. Jackson (eds.), *International Review of Connective Tissue Research* (Elsevier).

Ferguson, S. J., K. Ito, and L. P. Nolte. 2004. 'Fluid flow and convective transport of solutes within the intervertebral disc', *J Biomech*, 37: 213-21.

Fields, Aaron J., Alexander Ballatori, Ellen C. Liebenberg, and Jeffrey C. Lotz. 2018. 'Contribution of the Endplates to Disc Degeneration', *Current Molecular Biology Reports*, 4: 151-60.

Giers, M. B., B. T. Munter, K. J. Eyster, G. D. Ide, Agus Newcomb, J. N. Lehrman, E. Belykh, V. A. Byvaltsev, B. P. Kelly, M. C. Preul, and N. Theodore. 2017a. 'Biomechanical and Endplate Effects on Nutrient Transport in the Intervertebral Disc', *World Neurosurg*, 99: 395-402.

Giers, Morgan B., Alex C. McLaren, Jonathan D. Plasencia, David Frakes, Ryan McLemore, and Michael R. Caplan. 2013. 'Spatiotemporal Quantification of Local Drug Delivery Using MRI', *Computational and Mathematical Methods in Medicine*, 2013: 149608.

Giers, Morgan B., Bryce T. Munter, Kyle J. Eyster, George D. Ide, Anna G. U. S. Newcomb, Jennifer N. Lehrman, Evgenii Belykh, Vadim A. Byvaltsev, Brian P. Kelly, Mark C. Preul, and Nicholas Theodore. 2017b. 'Biomechanical and Endplate Effects on Nutrient Transport in the Intervertebral Disc', *World Neurosurg*, 99: 395-402.

Gilbert, H. T., N. Hodson, P. Baird, S. M. Richardson, and J. A. Hoyland. 2016. 'Acidic pH promotes intervertebral disc degeneration: Acid-sensing ion channel -3 as a potential therapeutic target', *Sci Rep*, 6: 37360.

Gruber, H. E., K. Leslie, J. Ingram, G. Hoelscher, H. J. Norton, and E. N. Hanley, Jr. 2004. 'Colony formation and matrix production by human anulus cells: modulation in three-dimensional culture', *Spine (Phila Pa 1976)*, 29: E267-74.

Gruber, Helen E., and Edward N. Jr. Hanley. 1998. 'Analysis of Aging and Degeneration of the Human Intervertebral Disc: Comparison of Surgical Specimens With Normal Controls', *Spine (Phila Pa 1976)*, 23: 751-57.

Gu, W. Y., X. G. Mao, R. J. Foster, M. Weidenbaum, V. C. Mow, and B. A. Rawlins. 1999. 'The Anisotropic Hydraulic Permeability of Human Lumbar Anulus Fibrosus: Influence of Age, Degeneration, Direction, and Water Content', *Spine (Phila Pa 1976)*, 24: 2449.

Gu, W. Y., H. Yao, A. L. Vega, and D. Flagler. 2004. 'Diffusivity of ions in agarose gels and intervertebral disc: effect of porosity', *Ann Biomed Eng*, 32: 1710-7.

Guerrero, J., S. Häckel, A. S. Croft, S. Hoppe, C. E. Albers, and B. Gantenbein. 2021. 'The nucleus pulposus microenvironment in the intervertebral disc: the fountain of youth?', *Eur Cell Mater*, 41: 707-38.

Gullbrand, S. E., J. Peterson, R. Mastropolo, T. T. Roberts, J. P. Lawrence, J. C. Glennon, D. J. DiRisio, and E. H. Ledet. 2015. 'Low rate loading-induced convection enhances net transport into the intervertebral disc in vivo', *Spine J*, 15: 1028-33.

Gullbrand, Sarah E., Joshua Peterson, Rosemarie Mastropolo, James P. Lawrence, Luciana Lopes, Jeffrey Lotz, and Eric H. Ledet. 2014. 'Drug-induced changes to the vertebral endplate vasculature affect transport into the intervertebral disc in vivo', *Journal of Orthopaedic Research*, 32: 1694-700.

Guo, Jiang-Bo, Yan-Jun Che, Jun-Jun Hou, Ting Liang, Wen Zhang, Yan Lu, Hui-Lin Yang, and Zong-Ping Luo. 2020. 'Stable mechanical environments created by a low-tension traction device is beneficial for the regeneration and repair of degenerated intervertebral discs', *The Spine Journal*, 20: 1503-16.

Han, Y., X. Li, M. Yan, M. Yang, S. Wang, J. Pan, L. Li, and J. Tan. 2019. 'Oxidative damage induces apoptosis and promotes calcification in disc cartilage endplate cell through ROS/MAPK/NF-kappaB pathway: Implications for disc degeneration', *Biochem Biophys Res Commun*, 516: 1026-32.

Hartman, R., P. Patil, R. Tisherman, C. St Croix, L. J. Niedernhofer, P. D. Robbins, F. Ambrosio, B. Van Houten, G. Sowa, and N. Vo. 2018. 'Age-dependent changes in intervertebral disc cell mitochondria and bioenergetics', *Eur Cell Mater*, 36: 171-83.

Hassler, O. 1969. 'The human intervertebral disc. A micro-angiographical study on its vascular supply at various ages', *Acta Orthop Scand*, 40: 765-72.

Haufe, S. M., and A. R. Mork. 2006. 'Intradiscal injection of hematopoietic stem cells in an attempt to rejuvenate the intervertebral discs', *Stem Cells Dev*, 15: 136-7.

Haughton, Victor. 2004. 'Medical Imaging of Intervertebral Disc Degeneration: Current Status of Imaging', *Spine (Phila Pa 1976)*, 29.

———. 2006. 'Imaging Intervertebral Disc Degeneration', *JBJS*, 88: 15-20.

Hohaus, C., T. M. Ganey, Y. Minkus, and H. J. Meisel. 2008. 'Cell transplantation in lumbar spine disc degeneration disease', *Eur Spine J*, 17 Suppl 4: 492-503.

Holm, S., A. Maroudas, J. P. G. Urban, G. Selstam, and A. Nachemson. 1981. 'Nutrition of the Intervertebral Disc: Solute Transport and Metabolism', *Connective Tissue Research*, 8: 101-19.

Holm, S., and A. Nachemson. 1983. 'Variations in the nutrition of the canine intervertebral disc induced by motion', *Spine (Phila Pa 1976)*, 8: 866-74.

Holm, Sten, and Gunnar Selstam. 1982. 'Oxygen Tension Alterations in the Intervertebral Disc as a Response to Changes in the Arterial Blood', *Upsala Journal of Medical Sciences*, 87: 163-74.

HOLM, STEN, GUNNAR SELSTAM, and ALF NACHEMSON. 1982. 'Carbohydrate metabolism and concentration profiles of solutes in the canine lumbar intervertebral disc', *Acta Physiologica Scandinavica*, 115: 147-56.

Horner, Heather A., and Jill P. G. Urban. 2001. '2001 Volvo Award Winner in Basic Science Studies: Effect of Nutrient Supply on the Viability of Cells From the Nucleus Pulposus of the Intervertebral Disc', *Spine (Phila Pa 1976)*, 26.

Hsu, Edward W., and Lori A. Setton. 1999. 'Diffusion tensor microscopy of the intervertebral disc anulus fibrosus', *Magnetic Resonance in Medicine*, 41: 992-99.

Huang, Y. C., J. P. Urban, and K. D. Luk. 2014. 'Intervertebral disc regeneration: do nutrients lead the way?', *Nat Rev Rheumatol*, 10: 561-6.

Hughes, S. P. F., A. L. Wallace, I. D. McCarthy, R. H. Fleming, and B. C. Wyatt. 1993. 'Measurement of blood flow to the vertebral bone and disc', *European Spine Journal*, 2: 96-98.

Iatridis, J. C., J. J. MacLean, M. O'Brien, and I. A. Stokes. 2007. 'Measurements of proteoglycan and water content distribution in human lumbar intervertebral discs', *Spine (Phila Pa 1976)*, 32: 1493-7.

Iatridis, James C., and Iolo ap Gwynn. 2004. 'Mechanisms for mechanical damage in the intervertebral disc annulus fibrosus', *Journal of Biomechanics*, 37: 1165-75.

Ishihara, H., and J. P. Urban. 1999. 'Effects of low oxygen concentrations and metabolic inhibitors on proteoglycan and protein synthesis rates in the intervertebral disc', *J Orthop Res*, 17: 829-35.

Jackson, A. R., T. Y. Yuan, C. Y. Huang, and W. Y. Gu. 2009. 'A conductivity approach to measuring fixed charge density in intervertebral disc tissue', *Ann Biomed Eng*, 37: 2566-73.

Jackson, A. R., T. Y. Yuan, C. Y. Huang, F. Travascio, and W. Yong Gu. 2008. 'Effect of compression and anisotropy on the diffusion of glucose in annulus fibrosus', *Spine (Phila Pa 1976)*, 33: 1-7.

Jackson, Alicia R., Adam Eismont, Lu Yu, Na Li, Weiyong Gu, Frank Eismont, and Mark D. Brown. 2018. 'Diffusion of antibiotics in intervertebral disc', *Journal of Biomechanics*, 76: 259-62.

Jackson, Alicia R., Chun-Yuh C. Huang, Mark D. Brown, and Wei Yong Gu. 2011. '3D Finite Element Analysis of Nutrient Distributions and Cell Viability in the Intervertebral Disc: Effects of Deformation and Degeneration', *Journal of Biomechanical Engineering*, 133.

Jackson, Alicia R., Tai-Yi Yuan, Chun-Yuh Huang, Mark D. Brown, and Wei Yong Gu. 2012. 'Nutrient Transport in Human Annulus Fibrosus is Affected by Compressive Strain and Anisotropy', *Annals of Biomedical Engineering*, 40: 2551-58.

Jang, T. H., S. C. Park, J. H. Yang, J. Y. Kim, J. H. Seok, U. S. Park, C. W. Choi, S. R. Lee, and J. Han. 2017a. 'Cryopreservation and its clinical applications', *Integr Med Res*, 6: 12-18.

Jang, Tae Hoon, Sung Choel Park, Ji Hyun Yang, Jung Yoon Kim, Jae Hong Seok, Ui Seo Park, Chang Won Choi, Sung Ryul Lee, and Jin Han. 2017b. 'Cryopreservation and its clinical applications', *Integrative Medicine Research*, 6: 12-18.

Jeon, O. H., C. Kim, R. M. Laberge, M. Demaria, S. Rathod, A. P. Vasserot, J. W. Chung, D. H. Kim, Y. Poon, N. David, D. J. Baker, J. M. van Deursen, J. Campisi, and J. H. Elisseeff. 2017. 'Local clearance of senescent cells attenuates the development of post-traumatic osteoarthritis and creates a pro-regenerative environment', *Nat Med*, 23: 775-81.

Jones, W., and R. E. Roberts. 1933. 'Pathological Calcification and Ossification in Relation to Leriche and Policard's Theory', *Proc R Soc Med*, 26: 853-9.

KATZ, MICHAEL M., ALAN R. HARGENS, and STEVEN R. GARFIN. 1986. 'Intervertebral Disc Nutrition: Diffusion Versus Convection', *Clinical Orthopaedics and Related Research®*, 210: 243-45.

Kealey, Susan M., Todd Aho, David Delong, Daniel P. Barboriak, James M. Provenzale, and James D. Eastwood. 2005. 'Assessment of Apparent Diffusion Coefficient in Normal and Degenerated Intervertebral Lumbar Disks: Initial Experience', *Radiology*, 235: 569-74.

Kihara, Takanori, Junri Ito, and Jun Miyake. 2013. 'Measurement of Biomolecular Diffusion in Extracellular Matrix Condensed by Fibroblasts Using Fluorescence Correlation Spectroscopy', *PLOS ONE*, 8: e82382.

King, T. 1959. 'Another look at the problem of lumbo-sacral pain and sciatica', *Med J Aust*, 46: 8-12.

Knight, Eleanor, and Stefan Przyborski. 2015. 'Advances in 3D cell culture technologies enabling tissue-like structures to be created in vitro', *Journal of Anatomy*, 227: 746-56.

KRAEMER, J, D KOLDITZ, and R GOWIN. 1985a. 'Water and Electrolyte Content of Human Intervertebral Discs Under Variable Load', *Spine (Phila Pa 1976)*, 10: 69-71.

Kraemer, J., D. Kolditz, and R. Gowin. 1985b. 'Water and electrolyte content of human intervertebral discs under variable load', *Spine (Phila Pa 1976)*, 10: 69-71.

Kwon, Young Jik, and Ching-An Peng. 2002. 'Calcium-Alginate Gel Bead Cross-Linked with Gelatin as Microcarrier for Anchorage-Dependent Cell Culture', *BioTechniques*, 33: 212-18.

Lam, S. K., S. C. Chan, V. Y. Leung, W. W. Lu, K. M. Cheung, and K. D. Luk. 2011. 'The role of cryopreservation in the biomechanical properties of the intervertebral disc', *Eur Cell Mater*, 22: 393-402.

Le Maitre, Christine L., Chitra L. Dahia, Morgan Giers, Svenja Illien-Junger, Claudia Cicione, Dino Samartzis, Gianluca Vadala, Aaron Fields, and Jeffrey Lotz. 2021. 'Development of a standardized histopathology scoring system for human intervertebral disc degeneration: an Orthopaedic Research Society Spine Section Initiative', *JOR SPINE*, 4: e1167.

Le Maitre, Christine Lyn, Anthony John Freemont, and Judith Alison Hoyland. 2007. 'Accelerated cellular senescence in degenerate intervertebral discs: a possible role in the pathogenesis of intervertebral disc degeneration', *Arthritis Research & Therapy*, 9: R45.

Liebscher, T., M. Haefeli, K. Wuertz, A. G. Nerlich, and N. Boos. 2011. 'Age-related variation in cell density of human lumbar intervertebral disc', *Spine (Phila Pa 1976)*, 36: 153-9.

Link, T. M., J. Neumann, and X. Li. 2017. 'Prestructural cartilage assessment using MRI', *J Magn Reson Imaging*, 45: 949-65.

Liu, M. H., C. Sun, Y. Yao, X. Fan, H. Liu, Y. H. Cui, X. W. Bian, B. Huang, and Y. Zhou. 2016. 'Matrix stiffness promotes cartilage endplate chondrocyte calcification in disc degeneration via miR-20a targeting ANKH expression', *Sci Rep*, 6: 25401.

Ludescher, Burkhard, Julia Effelsberg, Petros Martirosian, Günter Steidle, Bernd Markert, Claus Claussen, and Fritz Schick. 2008. 'T2- and diffusion-maps reveal diurnal changes of intervertebral disc composition: An in vivo MRI study at 1.5 Tesla', *Journal of Magnetic Resonance Imaging*, 28: 252-57.

Lyons, Gillian, S. M. Eisenstein, and M. B. E. Sweet. 1981. 'Biochemical changes in intervertebral disc degeneration', *Biochimica et Biophysica Acta (BBA) - General Subjects*, 673: 443-53.

Magnier, Carole, Olivier Boiron, Sylvie Wendling-Mansuy, Patrick Chabrand, and Valérie Deplano. 2009. 'Nutrient distribution and metabolism in the intervertebral disc in the unloaded state: A parametric study', *Journal of Biomechanics*, 42: 100-08.

Mahmoudifar, Nastaran, and Pauline M. Doran. 2010. 'Chondrogenic differentiation of human adipose-derived stem cells in polyglycolic acid mesh scaffolds under dynamic culture conditions', *Biomaterials*, 31: 3858-67.

Malandrino, A., D. Lacroix, C. Hellmich, K. Ito, S. J. Ferguson, and J. Noailly. 2014. 'The role of endplate poromechanical properties on the nutrient availability in the intervertebral disc', *Osteoarthritis Cartilage*, 22: 1053-60.

Malcolmson, P. H. 1935. 'Radiologic Study of the Development of the Spine and Pathologic Changes of the Intervertebral Disc', *Radiology*, 25: 98-104.

Malko, John A., William C. Hutton, and William A. Fajman. 1999. 'An In Vivo Magnetic Resonance Imaging Study of Changes in the Volume (and Fluid Content) of the Lumbar Intervertebral Discs During a Simulated Diurnal Load Cycle', *Spine (Phila Pa 1976)*, 24: 1015-22.

———. 2002. 'An In Vivo MRI Study of the Changes in Volume (and Fluid Content) of the Lumbar Intervertebral Disc After Overnight Bed Rest and During an 8-Hour Walking Protocol', *Clinical Spine Surgery*, 15: 157-63.

Maroudas, A., R. A. Stockwell, A. Nachemson, and J. Urban. 1975. 'Factors involved in the nutrition of the human lumbar intervertebral disc: cellularity and diffusion of glucose in vitro', *J Anat*, 120: 113-30.

Martin, I., D. Wendt, and M. Heberer. 2004. 'The role of bioreactors in tissue engineering', *Trends Biotechnol*, 22: 80-6.

Martins, Delio Eulalio, Valquiria Pereira de Medeiros, Marcelo Wajchenberg, Edgar Julian Paredes-Gamero, Marcelo Lima, Rejane Daniele Reginato, Helena Bonciani Nader, Eduardo Barros Puertas, and Flavio Faloppa. 2018. 'Changes in human intervertebral disc biochemical composition and bony end plates between middle and old age', *PLOS ONE*, 13: e0203932.

McMillan, D. W., G. Garbutt, and M. A. Adams. 1996. 'Effect of sustained loading on the water content of intervertebral discs: implications for disc metabolism', *Annals of the rheumatic diseases*, 55: 880-87.

Meisel, H. J., T. Ganey, W. C. Hutton, J. Libera, Y. Minkus, and O. Alasevic. 2006a. 'Clinical experience in cell-based therapeutics: intervention and outcome', *Eur Spine J*, 15 Suppl 3: S397-405.

Meisel, H. J., V. Siodla, T. Ganey, Y. Minkus, W. C. Hutton, and O. J. Alasevic. 2007. 'Clinical experience in cell-based therapeutics: disc chondrocyte transplantation A treatment for degenerated or damaged intervertebral disc', *Biomol Eng*, 24: 5-21.

Meisel, Hans Joerg, Timothy Ganey, William C. Hutton, Jeanette Libera, Yvonne Minkus, and Olivera Alasevic. 2006b. 'Clinical experience in cell-based therapeutics: intervention and outcome', *European spine journal : official publication of the European Spine Society, the European Spinal Deformity Society, and the European Section of the Cervical Spine Research Society*, 15 Suppl 3: S397-S405.

Merline, Rosetta, Roland M. Schaefer, and Liliana Schaefer. 2009. 'The matricellular functions of small leucine-rich proteoglycans (SLRPs)', *Journal of Cell Communication and Signaling*, 3: 323-35.

Miyamoto, Kei, Koichi Masuda, Jesse G. Kim, Nozomu Inoue, Koji Akeda, Gunnar B. J. Andersson, and Howard S. An. 2006. 'Intradiscal injections of osteogenic protein-1 restore the viscoelastic properties of degenerated intervertebral discs', *The Spine Journal*, 6: 692-703.

Mokhbi Soukane, D., A. Shirazi-Adl, and J. P. Urban. 2009. 'Investigation of solute concentrations in a 3D model of intervertebral disc', *Eur Spine J*, 18: 254-62.

Molinos, Maria, Catarina R. Almeida, Joana Caldeira, Carla Cunha, Raquel M. Gonçalves, and Mário A. Barbosa. 2015. 'Inflammation in intervertebral disc degeneration and regeneration', *Journal of The Royal Society Interface*, 12: 20141191.

Muftuler, L. Tugan, Joshua P. Jarman, Hon J. Yu, Vance O. Gardner, Dennis J. Maiman, and Volkan Emre Arpinar. 2015. 'Association between intervertebral disc degeneration and endplate perfusion studied by DCE-MRI', *European Spine Journal*, 24: 679-85.

Murrell, W., E. Sanford, L. Anderberg, B. Cavanagh, and A. Mackay-Sim. 2009. 'Olfactory stem cells can be induced to express chondrogenic phenotype in a rat intervertebral disc injury model', *Spine J*, 9: 585-94.

Nachemson, A., T. Lewin, A. Maroudas, and M. A. Freeman. 1970. 'In vitro diffusion of dye through the end-plates and the annulus fibrosus of human lumbar inter-vertebral discs', *Acta Orthop Scand*, 41: 589-607.

Naqvi, S. M., and C. T. Buckley. 2015. 'Extracellular matrix production by nucleus pulposus and bone marrow stem cells in response to altered oxygen and glucose microenvironments', *J Anat*, 227: 757-66.

Naresh-Babu, J., G. Neelima, S. Reshma Begum, and V. Siva-Leela. 2016. 'Diffusion characteristics of human annulus fibrosus-a study documenting the dependence of annulus fibrosus on end plate for diffusion', *Spine J*, 16: 1007-14.

Naylor, A. 1951. 'Brachial neuritis, with particular reference to lesions of the cervical intervertebral discs', *Ann R Coll Surg Engl*, 9: 158-88.

———. 1962. 'The biophysical and biochemical aspects of intervertebral disc herniation and degeneration', *Ann R Coll Surg Engl*, 31: 91-114.

Naylor, A., F. Happey, and T. Macrae. 1955. 'Changes in the human intervertebral disc with age: a biophysical study', *J Am Geriatr Soc*, 3: 964-73.

Nguyen-minh, C, V M Haughton, R A Papke, H An, and S C Censky. 1998. 'Measuring diffusion of solutes into intervertebral disks with MR imaging and paramagnetic contrast medium', *American Journal of Neuroradiology*, 19: 1781-84.

Nguyen-minh, C, L Riley, K C Ho, R Xu, H An, and V M Haughton. 1997. 'Effect of degeneration of the intervertebral disk on the process of diffusion', *American Journal of Neuroradiology*, 18: 435-42.

Niinimäki, Jaakko, Arto Korkiakoski, Outi Ojala, Jaro Karppinen, Jyrki Ruohonen, Marianne Haapea, Raija Korpelainen, Antero Natri, and Osmo Tervonen. 2009. 'Association between visual degeneration of intervertebral discs and the apparent diffusion coefficient', *Magnetic Resonance Imaging*, 27: 641-47.

Noriega, D. C., F. Ardura, R. Hernandez-Ramajo, M. A. Martin-Ferrero, I. Sanchez-Lite, B. Toribio, M. Alberca, V. Garcia, J. M. Moraleda, A. Sanchez, and J. Garcia-Sancho. 2017. 'Intervertebral Disc Repair by Allogeneic Mesenchymal Bone Marrow Cells: A Randomized Controlled Trial', *Transplantation*, 101: 1945-51.

O'Connell, G. D., E. J. Vresilovic, and D. M. Elliott. 2007. 'Comparison of animals used in disc research to human lumbar disc geometry', *Spine (Phila Pa 1976)*, 32: 328-33.

O'Hara, B. P., J. P. Urban, and A. Maroudas. 1990. 'Influence of cyclic loading on the nutrition of articular cartilage', *Annals of the rheumatic diseases*, 49: 536-39.

O'Connell, Grace D., Edward J. Vresilovic, and Dawn M. Elliott. 2007. 'Comparison of Animals Used in Disc Research to Human Lumbar Disc Geometry', *Spine (Phila Pa 1976)*, 32.

Oegema, Theodore R. 1993. 'Biochemistry of the Intervertebral Disc', *Clinics in Sports Medicine*, 12: 419-38.

Ogata, K., and L. A. Whiteside. 1981. '1980 Volvo award winner in basic science. Nutritional pathways of the intervertebral disc. An experimental study using hydrogen washout technique', *Spine (Phila Pa 1976)*, 6: 211-16.

Oichi, Takeshi, Yuki Taniguchi, Yasushi Oshima, Sakae Tanaka, and Taku Saito. 2020. 'Pathomechanism of intervertebral disc degeneration', *JOR SPINE*, 3: e1076.

Orozco, L., R. Soler, C. Morera, M. Alberca, A. Sanchez, and J. Garcia-Sancho. 2011. 'Intervertebral disc repair by autologous mesenchymal bone marrow cells: a pilot study', *Transplantation*, 92: 822-8.

Pathak, Ranoo, and Suddhasatwa Basu. 2013. 'Mathematical modeling and experimental verification of direct glucose anion exchange membrane fuel cell', *Electrochimica Acta*, 113: 42-53.

Pattappa, G., Z. Li, M. Peroglio, N. Wismer, M. Alini, and S. Grad. 2012. 'Diversity of intervertebral disc cells: phenotype and function', *J Anat*, 221: 480-96.

Payne, E. E., and J. D. Spillane. 1957. 'The cervical spine; an anatomico-pathological study of 70 specimens (using a special technique) with particular reference to the problem of cervical spondylosis', *Brain*, 80: 571-96.

Pulickal, Tina, Johannes Boos, Markus Konieczny, Lino Morris Sawicki, Anja Müller-Lutz, Bernd Bittersohl, Joachim Gerß, Markus Eichner, Hans-Jörg Wittsack, Gerald Antoch, and Christoph Schleich. 2019. 'MRI identifies biochemical alterations of intervertebral discs in patients with low back pain and radiculopathy', *European Radiology*, 29: 6443-46.

Rajasekaran, S., J. N. Babu, R. Arun, B. R. Armstrong, A. P. Shetty, and S. Murugan. 2004. 'ISSLS prize winner: A study of diffusion in human lumbar discs: a serial magnetic resonance imaging study documenting the influence of the endplate on diffusion in normal and degenerate discs', *Spine (Phila Pa 1976)*, 29: 2654-67.

Rajasekaran, S., K. Venkatadass, J. Naresh Babu, K. Ganesh, and A. P. Shetty. 2008. 'Pharmacological enhancement of disc diffusion and differentiation of healthy, ageing and degenerated discs', *European Spine Journal*, 17: 626-43.

Rajasekaran, S., S. Vidyadhara, M. Subbiah, V. Kamath, R. Karunanithi, A. P. Shetty, K. Venkateswaran, M. Babu, and J. Meenakshi. 2010. 'ISSLS prize winner: a study of effects of in vivo mechanical forces on human lumbar discs with scoliotic disc as a biological model: results from serial postcontrast diffusion studies, histopathology and biochemical analysis of twenty-one human lumbar scoliotic discs', *Spine (Phila Pa 1976)*, 35: 1930-43.

Richardson, S. M., G. Kalamegam, P. N. Pushparaj, C. Matta, A. Memic, A. Khademhosseini, R. Mobasheri, F. L. Poletti, J. A. Hoyland, and A. Mobasheri. 2016. 'Mesenchymal stem cells in regenerative medicine: Focus on articular cartilage and intervertebral disc regeneration', *Methods*, 99: 69-80.

Risbud, M. V., A. Guttapalli, D. G. Stokes, D. Hawkins, K. G. Danielson, T. P. Schaer, T. J. Albert, and I. M. Shapiro. 2006. 'Nucleus pulposus cells express HIF-1 alpha under normoxic culture conditions: a metabolic adaptation to the intervertebral disc microenvironment', *J Cell Biochem*, 98: 152-9.

Risbud, Makarand V., Zachary R. Schoepflin, Fackson Mwale, Rita A. Kandel, Sibylle Grad, James C. Iatridis, Daisuke Sakai, and Judith A. Hoyland. 2015. 'Defining the phenotype

of young healthy nucleus pulposus cells: Recommendations of the Spine Research Interest Group at the 2014 annual ORS meeting', *Journal of Orthopaedic Research*, 33: 283-93.

Roberts, S., J. Menage, and J. P. Urban. 1989. 'Biochemical and structural properties of the cartilage end-plate and its relation to the intervertebral disc', *Spine (Phila Pa 1976)*, 14: 166-74.

Sakai, D., and G. B. Andersson. 2015. 'Stem cell therapy for intervertebral disc regeneration: obstacles and solutions', *Nat Rev Rheumatol*, 11: 243-56.

Sakai, D., and S. Grad. 2015. 'Advancing the cellular and molecular therapy for intervertebral disc disease', *Adv Drug Deliv Rev*, 84: 159-71.

Sakai, D., and J. Schol. 2017. 'Cell therapy for intervertebral disc repair: Clinical perspective', *J Orthop Translat*, 9: 8-18.

Sampson, S. L., M. Sylvia, and A. J. Fields. 2019. 'Effects of dynamic loading on solute transport through the human cartilage endplate', *J Biomech*, 83: 273-79.

Sélard, E., A. Shirazi-Adl, and J. P. Urban. 2003. 'Finite element study of nutrient diffusion in the human intervertebral disc', *Spine (Phila Pa 1976)*, 28: 1945-53; discussion 53.

Shalash, Ward, Sonia R. Ahrens, Liudmila A. Bardonova, Vadim A. Byvaltsev, and Morgan B. Giers. 2021. 'Patient-specific apparent diffusion maps used to model nutrient availability in degenerated intervertebral discs', *JOR SPINE*, 4: e1179.

Shirazi-Adl, A., M. Taheri, and J. P. Urban. 2010. 'Analysis of cell viability in intervertebral disc: Effect of endplate permeability on cell population', *J Biomech*, 43: 1330-6.

Shutkin, N. M. 1952. 'Syndrome of the degenerated intervertebral disc', *Am J Surg*, 84: 162-71.

Silagi, Elizabeth S., Emanuel J. Novais, Sara Bisetto, Aristeidis G. Telonis, Joseph Snuggs, Christine L. Le Maitre, Yunping Qiu, Irwin J. Kurland, Irving M. Shapiro, Nancy J. Philp, and Makarand V. Risbud. 2020. 'Lactate Efflux From Intervertebral Disc Cells Is Required for Maintenance of Spine Health', *Journal of Bone and Mineral Research*, 35: 550-70.

Silagi, Elizabeth S., Ernestina Schipani, Irving M. Shapiro, and Makarand V. Risbud. 2021. 'The role of HIF proteins in maintaining the metabolic health of the intervertebral disc', *Nature Reviews Rheumatology*, 17: 426-39.

Silverman, F. N. 1954. 'Calcification of the intervertebral disks in childhood', *Radiology*, 62: 801-16.

Smith, L. J., L. Silverman, D. Sakai, C. L. Le Maitre, R. L. Mauck, N. R. Malhotra, J. C. Lotz, and C. T. Buckley. 2018. 'Advancing cell therapies for intervertebral disc regeneration from the lab to the clinic: Recommendations of the ORS spine section', *JOR Spine*, 1: e1036.

Soukane, D. M., A. Shirazi-Adl, and J. P. Urban. 2007. 'Computation of coupled diffusion of oxygen, glucose and lactic acid in an intervertebral disc', *J Biomech*, 40: 2645-54.

Stein, Dan, Yaniv Assaf, Gali Dar, Haim Cohen, Viviane Slon, Einat Kedar, Bahaa Medlej, Janan Abbas, Ori Hay, Daniel Barazany, and Israel Hershkovitz. 2021. '3D virtual reconstruction and quantitative assessment of the human intervertebral disc's annulus fibrosus: a DTI tractography study', *Scientific Reports*, 11: 6815.

Stylianopoulos, Triantafyllos, Ming-Zher Poh, Numpon Insin, Moungi G. Bawendi, Dai Fukumura, Lance L Munn, and Rakesh K. Jain. 2010. 'Diffusion of Particles in the Extracellular Matrix: The Effect of Repulsive Electrostatic Interactions', *Biophysical Journal*, 99: 1342-49.

Sylven, B. 1951. 'On the biology of nucleus pulposus', *Acta Orthop Scand*, 20: 275-9.

Tam, V., I. Rogers, D. Chan, V. Y. Leung, and K. M. Cheung. 2014. 'A comparison of intravenous and intradiscal delivery of multipotential stem cells on the healing of injured intervertebral disk', *J Orthop Res*, 32: 819-25.

Thomas Rde, W., J. J. Batten, S. Want, I. D. McCarthy, M. Brown, and S. P. Hughes. 1995. 'A new in-vitro model to investigate antibiotic penetration of the intervertebral disc', *J Bone Joint Surg Br*, 77: 967-70.

Törner, Marianne, and Sten Holm. 1985. 'Studies of the Lumbar Vertebral End-plate Region in the Pig', *Upsala Journal of Medical Sciences*, 90: 243-58.

Torzilli P.A., Askari E., Jenkins J.T. 1990. *Water Content and Solute Diffusion Properties in Articular Cartilage* (Springer: New York, NY).

Tourell, M. C., M. Kirkwood, M. J. Pearcy, K. I. Momot, and J. P. Little. 2017. 'Load-induced changes in the diffusion tensor of ovine anulus fibrosus: A pilot MRI study', *J Magn Reson Imaging*, 45: 1723-35.

Travascio, Francesco, and Wei Yong Gu. 2007. 'Anisotropic Diffusive Transport in Annulus Fibrosus: Experimental Determination of the Diffusion Tensor by FRAP Technique', *Annals of Biomedical Engineering*, 35: 1739-48.

Travascio, Francesco, Sabrina Valladares-Prieto, and Alicia R. Jackson. 2020. 'Effects of solute size and tissue composition on molecular and macromolecular diffusivity in human knee cartilage', *Osteoarthritis and Cartilage Open*, 2: 100087.

Tschugg, A., F. Michnacs, M. Strowitzki, H. J. Meisel, and C. Thome. 2016. 'A prospective multicenter phase I/II clinical trial to evaluate safety and efficacy of NOVOCART Disc plus autologous disc chondrocyte transplantation in the treatment of nucleotomized and degenerative lumbar disc to avoid secondary disease: study protocol for a randomized controlled trial', *Trials*, 17: 108.

Tschugg, Anja, Michael Diepers, Steinert Simone, Felix Michnacs, Sebastian Quirbach, Martin Strowitzki, Hans Jörg Meisel, and Claudius Thomé. 2017. 'A prospective randomized multicenter phase I/II clinical trial to evaluate safety and efficacy of NOVOCART disk plus autologous disk chondrocyte transplantation in the treatment of nucleotomized and degenerative lumbar disks to avoid secondary disease: safety results of Phase I—a short report', *Neurosurgical Review*, 40: 155-62.

Turgut, M., A. Uysal, S. Uslu, N. Tavus, and M. E. Yurtseven. 2003. 'The effects of calcium channel antagonist nimodipine on end-plate vascularity of the degenerated intervertebral disc in rats', *J Clin Neurosci*, 10: 219-23.

Turner, V. 1959. 'The rationale of the non-operative management of lesions of the lumbar intervertebral disc', *Q Bull Northwest Univ Med Sch*, 33: 279-81.

URBAN, J. P. G., S. HOLM, A. MAROUDAS, and A. NACHEMSON. 1982. 'Nutrition of the Intervertebral Disc: Effect of Fluid Flow on Solute Transport', *Clinical Orthopaedics and Related Research®*, 170: 296-302.

Urban, J. P. G., and A. Maroudas. 1979. 'The measurement of fixed charged density in the intervertebral disc', *Biochimica et Biophysica Acta (BBA) - General Subjects*, 586: 166-78.

Urban, J. P., S. Holm, and A. Maroudas. 1978. 'Diffusion of small solutes into the intervertebral disc: as in vivo study', *Biorheology*, 15: 203-21.

Urban, J. P., S. Holm, A. Maroudas, and A. Nachemson. 1977. 'Nutrition of the intervertebral disk. An in vivo study of solute transport', *Clinical orthopaedics and related research*: 101-14.

Urban, J. P., S. Smith, and J. C. Fairbank. 2004. 'Nutrition of the intervertebral disc', *Spine (Phila Pa 1976)*, 29: 2700-9.

Van Der Werf, Marije, Patrick Lezuo, Otto Maissen, Corrinus C. Van Donkelaar, and Keita Ito. 2007. 'Inhibition of vertebral endplate perfusion results in decreased intervertebral disc intranuclear diffusive transport', *Journal of Anatomy*, 211: 769-74.

Vergroesen, P. P. A., I. Kingma, K. S. Emanuel, R. J. W. Hoogendoorn, T. J. Welting, B. J. van Royen, J. H. van Dieën, and T. H. Smit. 2015. 'Mechanics and biology in intervertebral disc degeneration: a vicious circle', *Osteoarthritis and Cartilage*, 23: 1057-70.

Vinatier, C., E. Dominguez, J. Guicheux, and B. Carames. 2018. 'Role of the Inflammation-Autophagy-Senescence Integrative Network in Osteoarthritis', *Front Physiol*, 9: 706.

Vo, N. V., R. A. Hartman, P. R. Patil, M. V. Risbud, D. Kletsas, J. C. Iatridis, J. A. Hoyland, C. L. Le Maitre, G. A. Sowa, and J. D. Kang. 2016. 'Molecular mechanisms of biological aging in intervertebral discs', *J Orthop Res*, 34: 1289-306.

Wang, Dong, Robert Hartman, Chao Han, Chao-Ming Zhou, Brandon Couch, Matias Malkamaki, Vera Roginskaya, Bennett Van Houten, Steven J. Mullett, Stacy G. Wendell, Michael J. Jurczak, James Kang, Joon Lee, Gwendolyn Sowa, and Nam Vo. 2021. 'Lactate oxidative phosphorylation by annulus fibrosus cells: evidence for lactate-dependent metabolic symbiosis in intervertebral discs', *Arthritis Research & Therapy*, 23: 145-45.

Wang, F., F. Cai, R. Shi, X. H. Wang, and X. T. Wu. 2016a. 'Aging and age related stresses: a senescence mechanism of intervertebral disc degeneration', *Osteoarthritis and Cartilage*, 24: 398-408.

———. 2016b. 'Aging and age related stresses: a senescence mechanism of intervertebral disc degeneration', *Osteoarthritis Cartilage*, 24: 398-408.

Wang, Ping, Li Yang, and Adam H. Hsieh. 2011. 'Nucleus Pulposus Cell Response to Confined and Unconfined Compression Implicates Mechanoregulation by Fluid Shear Stress', *Annals of Biomedical Engineering*, 39: 1101-11.

Wang, Yu-Fu, Howard B. Levene, Weiyong Gu, and C. Y. Charles Huang. 2017. 'Enhancement of Energy Production of the Intervertebral Disc by the Implantation of Polyurethane Mass Transfer Devices', *Annals of Biomedical Engineering*, 45: 2098-108.

Weidenbaum, M., R. J. Foster, B. A. Best, F. Saed-Nejad, E. Nickoloff, J. Newhouse, A. Ratcliffe, and V. C. Mow. 1992. 'Correlating magnetic resonance imaging with the biochemical content of the normal human intervertebral disc', *Journal of Orthopaedic Research*, 10: 552-61.

Willems, Nicole, Anna R. Tellegen, Niklas Bergknut, Laura B. Creemers, Jeannette Wolfswinkel, Christian Freudigmann, Karin Benz, Guy C. M. Grinwis, Marianna A. Tryfonidou, and Björn P. Meij. 2016. 'Inflammatory profiles in canine intervertebral disc degeneration', *BMC Veterinary Research*, 12: 10.

Wong, J., S. L. Sampson, H. Bell-Briones, A. Ouyang, A. A. Lazar, J. C. Lotz, and A. J. Fields. 2019. 'Nutrient supply and nucleus pulposus cell function: effects of the transport properties of the cartilage endplate and potential implications for intradiscal biologic therapy', *Osteoarthritis Cartilage*, 27: 956-64.

Wu, Y., S. E. Cisewski, N. Wegner, S. Zhao, V. D. Pellegrini, Jr., E. H. Slate, and H. Yao. 2016. 'Region and strain-dependent diffusivities of glucose and lactate in healthy human cartilage endplate', *J Biomech*, 49: 2756-62.

Xiong, Xuanqi, Zhengwei Zhou, Matteo Figini, Junjie Shangguan, Zhuoli Zhang, and Wei Chen. 2018. 'Multi-parameter evaluation of lumbar intervertebral disc degeneration using quantitative magnetic resonance imaging techniques', *American journal of translational research*, 10: 444-54.

Yang, B., and G. D. O'Connell. 2019. 'GAG content, fiber stiffness, and fiber angle affect swelling-based residual stress in the intact annulus fibrosus', *Biomech Model Mechanobiol*, 18: 617-30.

Yin, Si, Heng Du, Weigong Zhao, Shaohui Ma, Ming Zhang, Min Guan, and Miao Liu. 2019. 'Inhibition of both endplate nutritional pathways results in intervertebral disc degeneration in a goat model', *Journal of Orthopaedic Surgery and Research*, 14: 138.

Yoshikawa, T., Y. Ueda, K. Miyazaki, M. Koizumi, and Y. Takakura. 2010. 'Disc regeneration therapy using marrow mesenchymal cell transplantation: a report of two case studies', *Spine (Phila Pa 1976)*, 35: E475-80.

Yuan, T. Y., A. R. Jackson, C. Y. Huang, and W. Y. Gu. 2009. 'Strain-dependent oxygen diffusivity in bovine annulus fibrosus', *J Biomech Eng*, 131: 074503.

Yurube, Takashi, Masaaki Ito, Yuji Kakiuchi, Ryosuke Kuroda, and Kenichiro Kakutani. 2020. 'Autophagy and mTOR signaling during intervertebral disc aging and degeneration', *JOR SPINE*, 3: e1082.

Zhang, Wei, Xiaohui Ma, Yan Wang, Jian Zhao, Xujing Zhang, Yu Gao, and Shiling Li. 2014. 'Assessment of apparent diffusion coefficient in lumbar intervertebral disc degeneration', *European Spine Journal*, 23: 1830-36.

Zhou, N., X. Lin, W. Dong, W. Huang, W. Jiang, L. Lin, Q. Qiu, X. Zhang, J. Shen, Z. Song, X. Liang, J. Hao, D. Wang, and Z. Hu. 2016. 'SIRT1 alleviates senescence of degenerative human intervertebral disc cartilage endo-plate cells via the p53/p21 pathway', *Sci Rep*, 6: 22628.

Chapter 2 – Intact Intervertebral Disc Bioreactor

2.1 Introduction

Back pain is one of the major causes of disability in the world. It has been reported to have devastating effects on the workers' productivity, costing the economy over $85 billion annually (Baber and Erdek 2016). One of the leading causes of back pain is degeneration of the intervertebral disc (IVD) (Baber and Erdek 2016; Andersson 1999). Various factors can contribute to IVD degeneration, including transport limitations, trauma, inflammation, and aging (Baber and Erdek 2016). As the IVD undergoes degeneration, calcium and other minerals start to accumulate in the cartilaginous endplates (CEP), restricting solute transport (Cheung et al. 2009; Wang, Videman, and Battié 2012; Teraguchi et al. 2014; Boubriak et al. 2013; Urban and Roberts 2003; Urban, Smith, and Fairbank 2004). In addition, cellular phenotypes become more apoptotic, necrotic, and senescent leading to catabolic reactions in the extracellular matrix (ECM) (Cheung et al. 2009; Wang, Videman, and Battié 2012; Teraguchi et al. 2014; Boubriak et al. 2013; Urban and Roberts 2003; Urban, Smith, and Fairbank 2004).

Researchers have been interested in developing models that mimic the *in vivo* environment to test various IVD regeneration regimens (Pfannkuche et al. 2020). The IVD is known to have distinct microenvironments where the outer AF and CEP have high nutrient levels compared to the inner AF and NP (Pfannkuche et al. 2020; Urban, Smith, and Fairbank 2004). In addition, the IVD exists under mechanical load, which was reported to regulate cellular functions, including gene expression and ECM remodeling (Neidlinger-Wilke et al. 2012). Therefore, it is essential to study the impact of regenerative therapies on IVDs in their natural environment to prevent phenotypic changes (Urban, Smith, and Fairbank 2004; Pfannkuche et al. 2020; Knight and Przyborski 2015).

Studies have used animal IVDs to conduct studies on transport phenomena, including lumbar discs from porcine, ovine, rabbit, rat, mouse, and bovine tails. Some animal models share common properties with human IVDs (Daly et al. 2016). For example, goat and sheep models lose notochordal cells in early adulthood like human IVDs (Daly et al. 2016). They also have a similar size and mechanical loading to human IVDs, making them ideal for studying transport phenomena (Daly et al. 2016; Beckstein et al. 2008; Showalter et al. 2012)**.** Animal models,

however, might possess properties that differ from humans, such as the ECM's composition, so researchers are careful about expanding their conclusions to patients (Daly et al. 2016).

Novel bioreactors have been created to improve culture conditions and address various limitations of *in vitro* cultures, including control over the nutritional microenvironment, improvement of solute transport in the IVD, and the application of mechanical loading (Lisbet Haglund et al. 2011). Researchers have reported the successful cultivation of intact IVDs for weeks maintaining cellular function and phenotype in the AF, CEP, and NP (Lisbet Haglund et al. 2011; Hartman et al. 2012; Chan et al. 2015).

These systems are designed to cultivate intact IVDs in a chamber, maintaining a sterile controlled environment. The IVD is usually situated between two platens that distribute culture medium into the CEP (Lisbet Haglund et al. 2011). Many of these bioreactor systems come equipped with pistons to apply a mechanical load mimicking various loading schemes such as walking, standing, or lying supine (Lisbet Haglund et al. 2011; Pfannkuche et al. 2020; Hartman et al. 2012).

Our research laboratory collaborated with Drs. Lisbet Haglund and Thomas Steffen's teams to develop an axially loaded bioreactor system that could facilitate performing experiments on intervertebral discs (IVD) in a sterile and controlled environment (Lisbet Haglund et al. 2011).

2.2 Materials and Methods

The bioreactor comprises three independent chambers to support one IVD each under controlled conditions, including temperature, CO_2 and O_2 environment, circulation of nutrients, and dynamic or static loading. An important feature of this bioreactor includes the chamber's MRI-compatible material to avoid artifacts when imaging the IVDs mid-experiment.

2.2.1 Bioreactor parts

2.2.1.1 Chambers

In this bioreactor, there are three chambers. Each chamber comprises a borosilicate glass tube sealed with silicone O-rings. The IVD is immersed in media inside the glass tube (Figure 2.1). The media is circulated through upper and lower porous platens, which are in contact with the endplates of the IVD. The upper platen is connected to a plunger, sealed by a neoprene

bellow to the upper-end cap (Figure 2.1). Additional features of the chambers include incorporating MRI-compatible materials and adding three titanium screws to fasten the plunger. Fastening the plunger is essential when removing the chamber to perform various tests, including acquiring MRI scans. This improved design of the chambers allows the study of transport phenomena using various imaging modalities.

2.3.1.2 Pneumatic pistons

The pneumatic piston, shown in figure 2.2, puts a load on the cultivated IVDs by pushing down on the collar and onto the chamber. This load is controlled by a MATLAB® (R2022a, Natick, MA) software package which determines the voltage input sent to the pressure control. Each piston used in this system includes a displacement sensor that continuously measures IVD height changes.

Figure 2.1. Intervertebral disc chamber. A blue piece of Styrofoam represents the IVD in this picture.

2.3.1.3 Pressure control

A proportional pressure controller (PPC) supplies air pressure to the pneumatic piston in response to a 0-10 VDC signal (Figure 2.3). The air pressure supplied to the pneumatic piston applies a load to the cultivated IVD via the plunger. The MATLAB® (R2022a, Natick, MA) software package controls the programmed load.

2.3.1.4 Load cell

Each chamber sits atop a strain-gauge <u>load cell</u> that measures the actual load applied to the specimen.

2.3.1.5 Air supply

In-house pressurized air at 120 psi is used to push the pistons and provide mechanical loading.

Figure 2.2. Pneumatic piston.

2.3.1.6 Data acquisition

   This bioreactor is controlled via the Labjack U6 DAQ unit fitted with an expansion board (CB37). The DAQ is fitted with analog output modules (LJTick-DAC) and amplifier modules (LJTick-InAmp) to capture the load cell signals.

Figure 2.3. Pressure controller.

2.2.2 Intervertebral disc software

   A software package was developed in MATLAB® (R2022a, Natick, MA) to provide seamless bioreactor control (Figure 2.4). The software features control panels for the three chambers and a status sidebar shown in the figure. A calibration feature is added to each chamber to reset the displacement and load sensors. Each main panel is comprised of five sub-panels that provide information on (1) experiment progress, (2) experiment parameters, (3) load parameters, and (4) live plots of load and displacement data. The status sidebar indicates an estimated finish time and live readings of load and displacement.
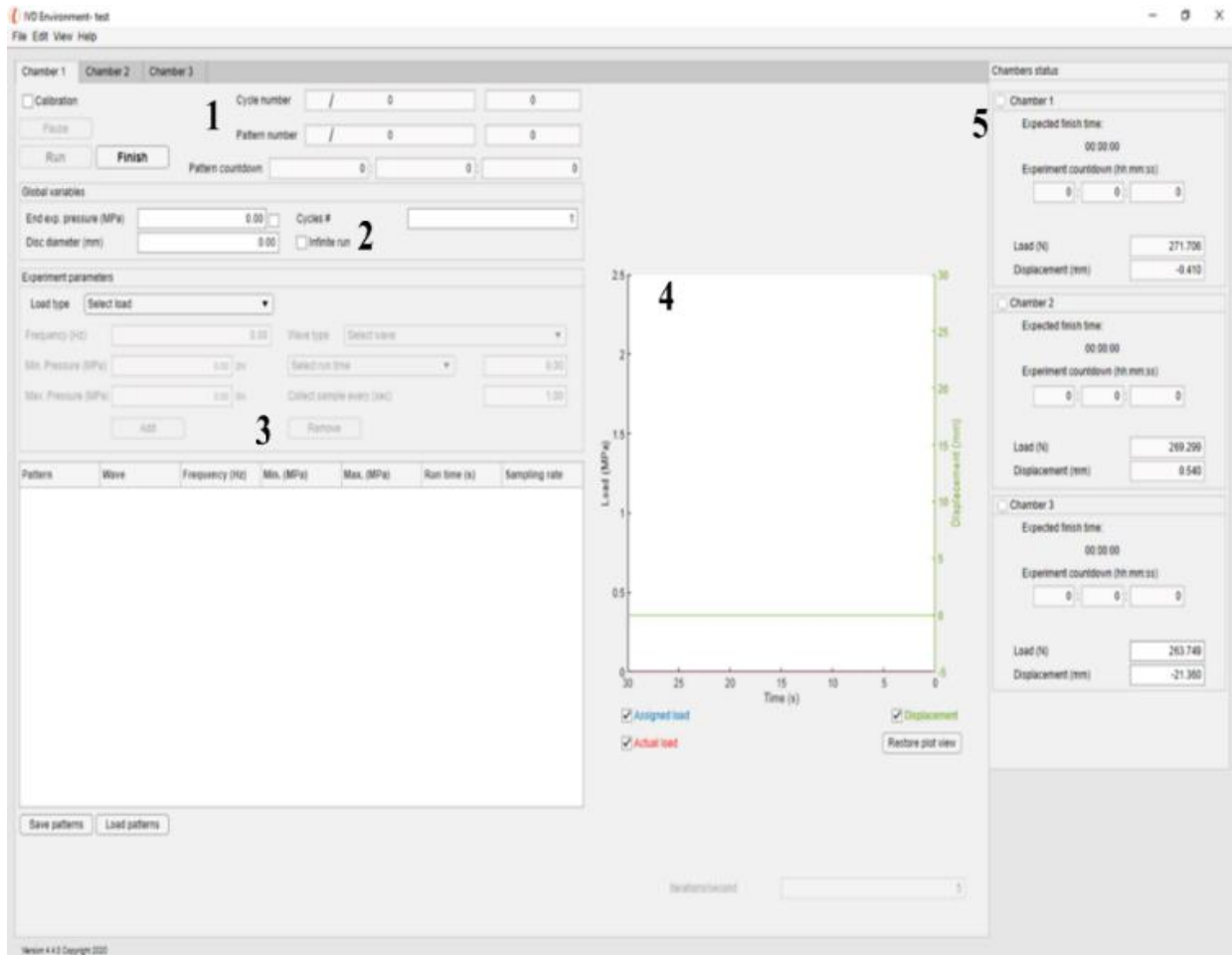
Figure 2.4. User interface of the bioreactor. The image shows the control panel for chamber 1 including 5 sub-panels, (1) experiment progress, (2) experiment input parameters, (3) load parameters, (4) live data plot, and (5) experiment status sidebar.

2.2.3 Operational procedure

The operation of the bioreactor starts by calibrating the displacement sensor and the load cell. The user can initiate the calibration window from the software package in each chamber panel. The chambers are calibrated to 0 MPa accounting for the weight of the chamber, media, and IVD without load. The upper plunger is lowered to touch the IVD before calibrating the displacement sensor.

Once the IVD has been placed in the chamber, connected to media lines, and chambers calibrated, the user is ready to enter the experiment parameters. In the main panel for the chamber, the user is presented with an option to choose between dynamic and static load

schemes. The user can also indicate the run time for each loading cycle. To start an experiment, the user would push the button start. There are options to pause and end the experiment.

Upon experiment termination, the software will send a message to the user indicating that the experiment has ended with a reading of the applied load.

2.3 Results

The bioreactor was used to cultivate IVDs over two weeks at 37°C and 5% CO_2 under various loading schemes. An example of a loading scheme is presented in figure 2.5.
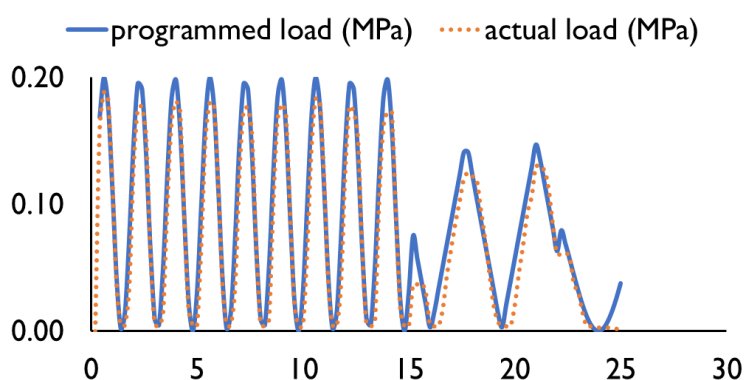
Figure 2.5. Plot of load data collected by the software. The plot shows two loading schemes (1) a high activity period between 0 and 15 seconds and (2) a resting period with low loading frequency between 15 and 25 seconds.

We also used the bioreactor to develop a novel method to cryopreserve the IVD described in Chapter 5. Bovine IVDs were compressed to enhance convective cryoprotectant (CPA) transport through the tissue. Compression increased the saturation of the CPA and improved its protective properties in the tissue.

2.4 Discussion and conclusion

Bioreactor systems have emerged as an attractive method for studying transport phenomena. These systems allow researchers to cultivate IVDs under controlled microenvironments, apply defined mechanical stresses, and maintain *in vivo* cell phenotypes(Lisbet Haglund et al. 2011). The bioreactor system presented in this work facilitates the research process by ensuring that the chambers' materials are autoclavable. In addition, the

MRI-compatible materials, which is an added feature, prevent imaging artifacts. This bioreactor will be used in performing experiments on solute transport phenomena in the human IVD to validate the finite element model discussed in Chapter 5. Cultivated IVDs will be scanned using an MRI at specific time intervals (e.g., every two days) to infer changes in local solute distributions, including glucose, oxygen, and lactate. Therefore, it was essential to design the chambers with MRI-compatible materials to prevent image artifacts that can distort the data. In addition, we added a set of three fastening screws, as shown in figure 2.1 to secure the plunger in place, maintaining a constant load during the transportation of the chamber to the MRI facilities. Keeping the load on the IVD to prevent it from free-swelling and altering internal solute distributions is essential.

The bioreactor presented in this chapter has some design limitations that could affect the cultivation of IVDs. For example, the bioreactor applies axial load only, which is not representative of the forces *in vivo*. The IVD is under various mechanical stresses, including axial, torsional, and complex (Yang and O'Connell 2017; Hirsch 1955). Cells in the IVD use external stimuli to modulate their processes and communicate to nearby cells; therefore, we might expect the absence of torsional load in this design to affect cellular functions in the IVD. In one study, IVD cells responded to complex loading (compression and torsion), inducing degenerative pathways compared to simple loading (Chan et al. 2013). Despite this limitation, the bioreactor provides a great tool to mimic *in vivo* conditions, including the nutrient environment and mechanical load, and prevent cell phenotypic changes.

In the following chapter I discuss the impact of the microenvironment in cultivation cultures on the AF and NP cells. In general, cells are sensitive to their environment, and they interact with it by communicating the various stressors, often in the form of proinflammatory cytokines. In this work, I established how steady glucose levels in the culture could affect IVD cells differently. We discovered that steady glucose levels increase metabolic rates in the AF while increase anaerobic glycolysis in NP cells. This work further elucidates the importance of considering the *in vitro* microenvironment when designing studies.

2.5 References

Andersson, G. B. 1999. 'Epidemiological features of chronic low-back pain', *Lancet*, 354: 581-5.

Baber, Zafeer, and Michael A. Erdek. 2016. 'Failed back surgery syndrome: current perspectives', *Journal of pain research*, 9: 979-87.

Beckstein, Jesse C., Sounok Sen, Thomas P. Schaer, Edward J. Vresilovic, and Dawn M. Elliott. 2008. 'Comparison of Animal Discs Used in Disc Research to Human Lumbar Disc: Axial Compression Mechanics and Glycosaminoglycan Content', *Spine*, 33.

Boubriak, Olga. A., Natasha Watson, Sarit. S. Sivan, Naomi Stubbens, and Jill P. G. Urban. 2013. 'Factors regulating viable cell density in the intervertebral disc: blood supply in relation to disc height', *Journal of Anatomy*, 222: 341-48.

Chan, S. C., J. Walser, S. J. Ferguson, and B. Gantenbein. 2015. 'Duration-dependent influence of dynamic torsion on the intervertebral disc: an intact disc organ culture study', *Eur Spine J*, 24: 2402-10.

Chan, Samantha C. W., Jochen Walser, Patrick Käppeli, Mohammad Javad Shamsollahi, Stephen J. Ferguson, and Benjamin Gantenbein-Ritter. 2013. 'Region Specific Response of Intervertebral Disc Cells to Complex Dynamic Loading: An Organ Culture Study Using a Dynamic Torsion-Compression Bioreactor', *PLOS ONE*, 8: e72489.

Cheung, Kenneth M. C., Jaro Karppinen, Danny Chan, Daniel W. H. Ho, You-Qiang Song, Pak Sham, Kathryn S. E. Cheah, John C. Y. Leong, and Keith D. K. Luk. 2009. 'Prevalence and Pattern of Lumbar Magnetic Resonance Imaging Changes in a Population Study of One Thousand Forty-Three Individuals', *Spine (Phila Pa 1976)*, 34: 934-40.

Daly, Chris, Peter Ghosh, Graham Jenkin, David Oehme, and Tony Goldschlager. 2016. 'A Review of Animal Models of Intervertebral Disc Degeneration: Pathophysiology, Regeneration, and Translation to the Clinic', *BioMed Research International*, 2016: 5952165.

Hartman, Robert A., Kevin M. Bell, Richard E. Debski, James D. Kang, and Gwendolyn A. Sowa. 2012. 'Novel ex-vivo mechanobiological intervertebral disc culture system', *Journal of Biomechanics*, 45: 382-85.

Hirsch, Carl. 1955. 'THE REACTION OF INTERVERTEBRAL DISCS TO COMPRESSION FORCES', *JBJS*, 37.

Knight, Eleanor, and Stefan Przyborski. 2015. 'Advances in 3D cell culture technologies enabling tissue-like structures to be created in vitro', *Journal of Anatomy*, 227: 746-56.

Lisbet Haglund, Janet Moir, Lorne Beckman , Kyle R. Mulligan , Bernice Jim , Jean A. Ouellet , Peter Roughley , and and Thomas Steffen 2011. 'Development of a Bioreactor for Axially Loaded Intervertebral Disc Organ Culture', *Tissue Engineering Part C: Methods*, 17: 1011-19.

Neidlinger-Wilke, Cornelia, Antje Mietsch, Christina Rinkler, Hans-Joachim Wilke, Anita Ignatius, and Jill Urban. 2012. 'Interactions of environmental conditions and mechanical loads have influence on matrix turnover by nucleus pulposus cells', *Journal of Orthopaedic Research*, 30: 112-21.

Pfannkuche, Judith-Johanna, Wei Guo, Shangbin Cui, Junxuan Ma, Gernot Lang, Marianna Peroglio, R. Geoff Richards, Mauro Alini, Sibylle Grad, and Zhen Li. 2020. 'Intervertebral disc organ culture for the investigation of disc pathology and regeneration – benefits, limitations, and future directions of bioreactors', *Connective Tissue Research*, 61: 304-21.

Showalter, Brent L., Jesse C. Beckstein, John T. Martin, Elizabeth E. Beattie, Alejandro A. Espinoza Orías, Thomas P. Schaer, Edward J. Vresilovic, and Dawn M. Elliott. 2012. 'Comparison of animal discs used in disc research to human lumbar disc: torsion mechanics and collagen content', *Spine*, 37: E900-E07.

Teraguchi, M., N. Yoshimura, H. Hashizume, S. Muraki, H. Yamada, A. Minamide, H. Oka, Y. Ishimoto, K. Nagata, R. Kagotani, N. Takiguchi, T. Akune, H. Kawaguchi, K. Nakamura, and M. Yoshida. 2014. 'Prevalence and distribution of intervertebral disc degeneration over the entire spine in a population-based cohort: the Wakayama Spine Study', *Osteoarthritis and Cartilage*, 22: 104-10.

Urban, J. P., S. Smith, and J. C. Fairbank. 2004. 'Nutrition of the intervertebral disc', *Spine (Phila Pa 1976)*, 29: 2700-9.

Urban, Jill P. G., and Sally Roberts. 2003. 'Degeneration of the intervertebral disc', *Arthritis Res Ther*, 5: 120.

Wang, Yue, Tapio Videman, and Michele C. Battié. 2012. 'ISSLS Prize Winner: Lumbar Vertebral Endplate Lesions: Associations With Disc Degeneration and Back Pain History', *Spine (Phila Pa 1976)*, 37: 1490-96.

Yang, Bo, and Grace D. O'Connell. 2017. 'Effect of collagen fibre orientation on intervertebral disc torsion mechanics', *Biomechanics and Modeling in Mechanobiology*, 16: 2005-15.

Chapter 3 – Effects of Glucose Modulation on AF and NP Synthesis of Glycosaminoglycans and Metabolomics

Ward Shalash, Lindsay G. Benage, Rees A. Rosene, Morgan B. Giers[*]

School of Chemical, Biological and Environmental Engineering, Oregon State University, Corvallis, OR 97331

3.1 Abstract

In this study, we cultured AF And NP cells in alginate beads to infer the effects of glucose level modulation in cell culture on (1) cell senescence, (2) synthesis of sulfated glycosaminoglycans (GAGs), and (3) the levels of intracellular metabolites. Cell culture conditions used in IVD research lack standardization among research groups and deviate from the IVD's in vivo microenvironment. This discrepancy causes variations in the cell phenotypes and cellular functions, leading to inconsistent results. Studies have shown a strong correlation between culture conditions, including cell phenotype, extracellular (ECM) composition, and cellular metabolism.

Therefore, there is a need to investigate the effects of culture conditions on IVD cells and establish standard culture conditions. Encapsulated AF and NP cells were cultured under unsteady- and steady-state glucose in a well plate and a fluidized bed for ten days. Culture media in the unsteady-state group was replaced every three days, while under the steady-state condition, the media was replaced three times every day. In the bioreactor cultures, cells under unsteady-state had their media replaced manually once every three times. The media for cells under steady-state was replaced continuously using a pump at a 0.139 mL/hour flow rate. Cells were harvested after ten days of culture and further processed to elucidate senescence, GAG content, and intracellular metabolite levels. This work highlighted the differential phenotypic responses between NP and AF cells, supporting our hypothesis that cell culture conditions affected cell phenotypes. For example, NP cells cultured in the well-plate acquired twice as many senescent phenotypes when exposed to steady glucose compared to unsteady glucose.

Nonetheless, AF cells showed a reversed trend in which more cells in the bioreactor culture acquired senescence when exposed to unsteady glucose levels compared to steady glucose levels. In addition, NP cells under unsteady glucose were observed to synthesize more sulfated GAGs (5-fold) compared to the steady-state. AF cells showed a reversed trend in which higher levels of GAGs were measured in the steady-state compared to the unsteady state. In addition, more senescent NP cells were observed in steady-state conditions, while AF cells acquired senescence when experiencing unsteady glucose levels. Our results strongly support the hypothesis that culture conditions impact vital cellular functions and phenotypes. Although we did not expect AF and NP to respond differently to the same environmental stimuli, it emphasized the need to control culture conditions mimicking the in vivo microenvironment.

3.2 Introduction

Culture conditions used in intervertebral disc (IVD) degeneration research are reported to vary widely between research groups, which may affect research outcomes and the development of efficient treatments (Mizuno, Allemann, and Glowacki 2001; Liu et al. 2020; Martin, Wendt, and Heberer 2004; Gruber, Stasky, and Hanley 1997).

Degenerative disc disease (DDD) is a prevalent medical condition that occurs in more than 90% of individuals over the age of 50, often leading to nerve compression and chronic back pain (Andersson 1999). Although pharmacological and psychotherapeutic treatments have been demonstrated to alleviate early and minor symptoms caused by the disease, invasive surgery is necessary for more than 500,000 patients throughout the U.S. every year (Brodke and Ritter 2005; Rajaee et al. 2012). Studies hypothesize that DDD occurs due to mechanical failure of the intervertebral disc (IVD) and slow regeneration of the worn tissue (Cheung et al. 2009; Wang, Videman, and Battié 2012; Teraguchi et al. 2014; Boubriak et al. 2013; Urban and Roberts 2003; Urban, Smith, and Fairbank 2004). Trauma, aging, and limitations in the nutrient supply are propagate cell death leading to IVD degeneration (Cheung et al. 2009; Wang, Videman, and Battié 2012; Teraguchi et al. 2014; Boubriak et al. 2013; Urban and Roberts 2003; Urban, Smith, and Fairbank 2004).

The IVD is an avascular joint that is comprised of three major tissue types including the annulus fibrosus (AF), the cartilaginous endplates (CEP), and the nucleus pulposus (NP) (Vergroesen et al. 2015). Inseparably, they assist in absorbing mechanical stresses and provide flexibility in the spine (Vergroesen et al. 2015). Due to the IVD's avascularity and anatomy, the cells in each tissue are exposed to distinct microenvironments (Urban, Smith, and Fairbank 2004). Most nourished and oxygenated cells are located in the CEP and outer AF due to nearby blood vessels (Urban, Smith, and Fairbank 2004). While inner AF and NP cells exist under elevated hypoxia and acidity (Table 3.1) (Bibby et al. 2005; Liebscher et al. 2011; Urban, Smith, and Fairbank 2004). Cells in degenerated IVDs experience hypoxic and acidic conditions in which glucose and pH levels can drop to 0.5 mol/m^3 and 6.7, respectively (Shirazi-Adl, Taheri, and Urban 2010; Bibby and Urban 2004; Jackson et al. 2009; Bibby et al. 2005; Urban, Smith, and Fairbank 2004).

Table 3.1. Values for cell density, glucose, lactate, and oxygen in the intervertebral disc[1].

Tissue	Cell density (10^3 cells per mm^3)	Glucose concentration (mM)	Lactate concentration (mM)	Oxygen tension (kPa)
AF	2.1 ± 0.73[*#]	5.0-2.0	0.90-4.0	5.8-0.43
NP	2.5 ± 0.65[*]	2.0	4.0	0.43
CEP	11 ± 3.7[*#]	5.0	0.90	5.1

[1](Liebscher et al. 2011) (Holm et al. 1981; Urban, Smith, and Fairbank 2004) (Holm et al. 1981)
[*]Average of age groups 16-29 and 30-60
[#]Values are averaged across all tissue regions

Culture conditions used in IVD research vary widely between research groups and can deviate from the IVD's *in vivo* microenvironment. This discrepancy is hypothesized to cause inconsistencies in research data due to the strong correlation between culture conditions and cell phenotype, ECM composition, and cellular metabolism (Martin, Wendt, and Heberer 2004; Gruber, Stasky, and Hanley 1997). Biomarkers for anaerobic glycolysis in IVD cells, such as lactate levels, can drop to 75% in acidic environments compared to non-acidic ones (Bibby et al. 2005). High acidity has also been reported to decrease glucose consumption, reducing ECM remodeling and affecting its composition, demonstrating the need to standardize IVD cell cultures (Bibby et al. 2005).

Scaffold-based cultures in alginate, cellulose, gelatin, polystyrene, or silk, are emerging as an alternative to monolayer cultures, providing the cells with a more physiological 3D environment (Knight and Przyborski 2015; Mahmoudifar and Doran 2010; Kwon and Peng 2002). In monolayer cultures, cells are intended to adhere to the bottom of the vessel, flattening the cell's geometry and changing gene expression (Knight and Przyborski 2015). On the other hand, scaffolds provide the cells with a complex environment, similar to the IVD's ECM, in which the cells can attain their natural shape, elongated or round (Bruehlmann et al. 2002; Pattappa et al. 2012; Knight and Przyborski 2015; Kwon and Peng 2002). The scaffold's complex matrix also enhances cell signaling, proliferation, and resistance to therapeutic agents, increasing the value of the collected data for researchers (Knight and Przyborski 2015; Bibby et al. 2005; Mahmoudifar and Doran 2010). Another advantage of using scaffolds is the ability to immobilize cells in bioreactors,

enabling the design of experiments with defined nutritional conditions, which is essential when investigating the effects of therapeutics and microenvironmental factors on cell viability, phenotype, metabolism, and gene expression (Martin, Wendt, and Heberer 2004). Bioreactors can also address limitations associated with mass transport in three-dimensional cultures by modulating flow rates increasing cellular metabolism and expression of the ECM (Martin, Wendt, and Heberer 2004).

The strong correlation between culture conditions, such as nutrients, metabolites, and acidity, raises the need to establish standardized protocols to culture IVD cells (Martin, Wendt, and Heberer 2004; Mizuno, Allemann, and Glowacki 2001). In this study, we encapsulated bovine AF and NP cells in alginate beads to investigate the effects of modulating glucose levels on cell senescence, glycosaminoglycan (GAG) content, and metabolic processes. We hypothesized that constant glucose levels would reduce cell senescence, increase GAG deposition in the ECM, and upregulate the metabolic pathways involved in ECM production. We also hypothesized that culturing cells in a bioreactor with continuous fluid flow conditions would enhance nutrient availability in the alginate beads and thus enhance metabolic processes and ECM remodeling. The findings of this study would demonstrate the need to standardize cell culture conditions for DDD research and encourage the consistent production of results among various research groups.

3.3 Materials and Methods

3.3.1 Isolation of AF and NP cells

AF and NP cells for monolayer cell culture were isolated by an enzymatic reaction from Black Angus IVDs (Wiseman et al. 2005). Two freshly skinned tails were obtained from a local abattoir within 24 hours of slaughter and kept on ice for three hours. The tails were disinfected in a 1% betadine (RC3955, VWR International, PA) solution with tap water for five minutes and then allowed to dry in a sterile environment. Muscle and fat tissue were removed from each tail, exposing the IVDs. The most proximal three IVDs (caudal levels two to four) were separated due to their large size using a butcher saw. Isolated IVDs were wrapped with a sterile gauze soaked in 0.9% sodium chloride (IC102892.5, VWR International, PA) and 55 mM sodium citrate (BDH9288, VWR International, PA). AF and NP tissue were removed from each IVD using a surgical blade size 10. Each tissue fragment was chopped into smaller pieces to speed up the enzymatic digestion process, which was conducted in a cell culture incubator at 37°C and 5% CO_2.

Digestion of each tissue required incubation in 0.2% Pronase **E** (97062-916, VWR International, PA) for 1hr, centrifugation of digestion solution at $300 \times$ g for five minutes to remove the supernatant, incubation in 0.025% Collagenase (103701-190, VWR International, PA) for 18hr, an additional centrifugation step to pellet cells, and incubation in cell culture media comprised of 89% low glucose Dulbecco's Modified Eagle's Medium (DMEM**)** - (D6046, Sigma, MO), 10% Fetal Bovine Serum (F0926, Sigma, MO), and 1% Antibiotic-Antimycotic (A5955, Sigma, MO). Monolayer cultures were passaged three times prior to alginate encapsulation.

3.3.2 Alginate encapsulation

AF and NP cell encapsulation in 2% low-viscosity alginate (A0682, Sigma, MO) was adapted from a protocol by Le Maitre et al. (Le Maitre, Freemont, and Hoyland 2005). Cell concentration in alginate was adjusted to 1 million cells per mL and verified by running a Trypan Blue assay using Countess FL II (Thermo Fisher, MA). For each cell type, AF, and NP, ten batches of alginate beads with a total volume of 10 mL per batch were made. The beads were formed in 200 mM $CaCl_2$ (C4901, Sigma, MO) using a 16-gauge needle and placed on a rocker for 15 minutes until the alginate was crosslinked. The beads were washed twice with 150 mM NaCl (IC102892.5, VWR International, PA) before being placed in the fluidized -bed bioreactor.

3.3.3 Bioreactor setup

The fluidized-bed bioreactor for the alginate beads was adapted and modified from Park and Stephanopoulos (Park and Stephanopoulos 1993). The beads were held in a 50 mL conical tube connected to a peristaltic pump establishing continuous flow by circulating the media at a rate of 4mL/min. Two peristaltic pumps were connected to a second 50 mL conical tube, acting as a holding vessel, at a constant rate of 0.139 mL/hour to replace glucose in the holding vessel (Figure 3.1).

3.3.4 Experimental groups

Out of the ten alginate-bead batches, two were incubated in a fluidized-bed bioreactor to maintain steady glucose levels using a media pump (Figure 3.1A). An additional two batches of beads were incubated in a batch reactor with manual modulation of glucose levels every three days (Figure 3.1B).
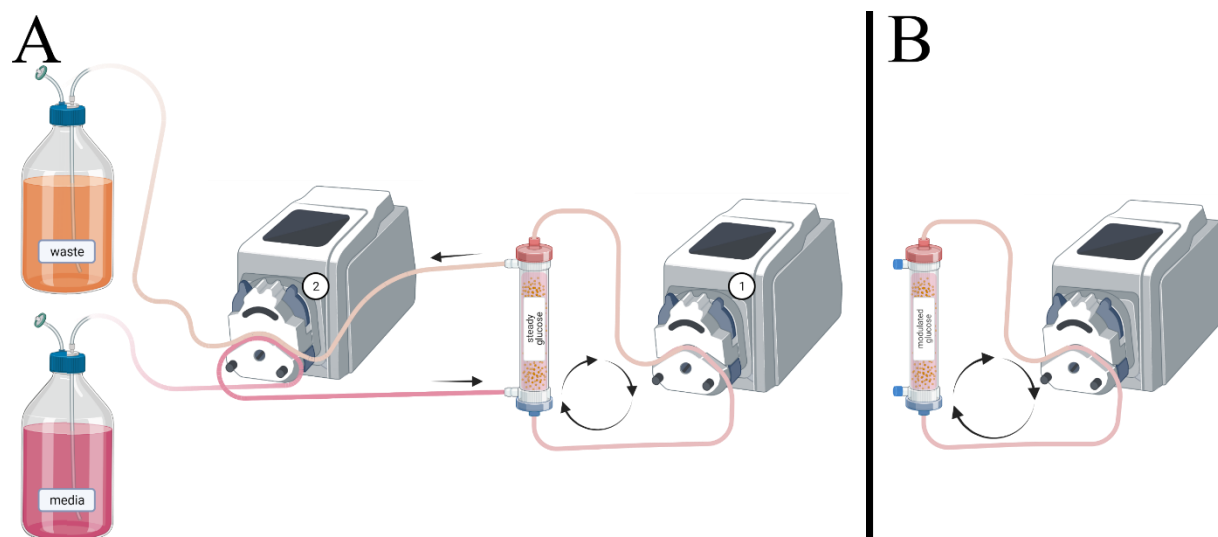
Figure 3.1. Schematic of the bioreactor showing the two setups for steady-state (A), And unsteady-state (B) glucose levels. In (A), pump one circulated the media at a constant rate of 4mL/min to achieve well-mixing conditions in the bioreactor. Pump 2 was used to replace 10 mL of media over a 3-day period. In (B), only one peristaltic pump was used to maintain constant mixing in the bioreactor at a flow rate of 4mL/min. Cell culture media was replaced once every three days over ten days.

The remaining six batches were incubated in a 6-well plate and randomly assigned to manual modulation of glucose levels at 8-hour intervals or three days (n=3) (Figure 3.2).
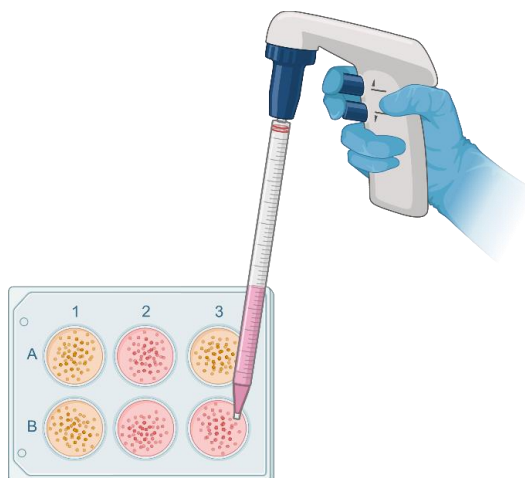
Figure 3.2. Schematic of culturing encapsulated AF and NP cells in a well-plate. Six batches of AF and NP cells were cultured in well-plates under steady-state glucose, changing the media three times per day, and under unsteady-state glucose, replacing culture media once every three days.

3.3.5 Cell extraction from alginate beads

Alginate beads were collected and washed with NaCl (IC102892.5, VWR International, PA) twice for 10 minutes. AF and NP cells were extracted from the alginate beads by gentle pipetting in a dissolving buffer of pH 7.4 containing 55 mM sodium citrate (BDH9288, VWR International, PA), 30 mM EDTA (BDH9232, VWR International, PA), and 150 mM NaCl (IC102892.5, VWR International, PA) in distilled water. The solution was immediately incubated at 37°C with agitation for 10 minutes prior to pelleting the cells at $300 \times g$ for five minutes. The cell pellet was reconstituted in 5 mL 1X PBS and used to measure cell viability, cell senescence, and metabolomics. The supernatant was collected to measure GAG content in the beads using dimethyl-methylene blue (DMMB).

3.3.6 Glucose measurements

Glucose levels in cell media were measured daily using ReliOn blood glucose meter (Novo Nordisk, Denmark). A volume of 10 μL was sufficient to provide a reading. Glucose readings were converted from mg/dL to mM and reported in this study.

3.3.7 AF and NP cell viability

Cells in alginate were pelleted and then reconstituted in 1X PBS as described previously. Cell viability was measured in each sample by mixing 10 µL of cells with trypan blue (15250061, ThermoFisher, MA) at a 1:1 ratio and analyzed with Countess FL II (ThermoFisher, MA).

3.3.8 SA-β-Gal cell senescence assay

A cellular senescence assay was performed on 1 million cells using a senescence kit (KAA002, ThermoFisher, MA). The cells were washed twice in 1X PBS, pelleted at $300 \times g$ for five minutes, and aspirated the supernatant in-between washes. The cells were then fixed in 1X fixation solution at room temperature for 15 minutes, centrifuged at $300 \times g$, and washed with 2 mL 1X PBS aspirating the supernatant each time. The cells were pelleted and gently mixed with 2 mL pre-made 1X SA-β-Gal detection solution as per the kit's protocol. The cells were incubated at 37°C for 4 hours, washed twice with 1X PBS, and reconstituted in 1 mL 1X PBS prior to counting the cells using Countess FL II (ThermoFisher, MA).

3.3.9 (HR-MAS) NMR metabolomics

The protocol for NMR metabolite process and data acquisition was adapted from Long et al (Long et al. 2020). Cells obtained from the extraction step were pelleted at $300 \times g$ for five minutes, quenched with 300 µL pre-chilled HPLC grade methanol at-20°C (BDH2018, VWR International, PA), vortexed briefly, mixed well with equal amounts of 300 µL distilled water and chloroform (25666, Sigma, MO), and chilled on ice for 10 minutes. Liquid phase extraction was used to separate cell metabolites. Each sample was centrifuged for 10 minutes at $16,000 \times g$ and 4°C. The top aqueous layer containing cell metabolites was transferred to a 2.0 mL tube and stored at -80°C. A speed-vacuum was used to remove methanol from the samples prior to elucidating organic compound contents via proton high resolution magic angle spinning (HR-MAS) NMR (Oregon State University, OR). Briefly, the dried metabolite samples were resuspended in 200 µL 50 mM sodium citrate (pH 7.0 with 10% D_2O and 0.456 mM DSS), loaded into 3 mm NMR tubes (Bruker, Billerica, MA), and stored at 5°C prior to NMR analysis. Metabolite profile analysis was performed at Oregon State University using an 800 MHz Bruker Avance III HD NMR spectrometer equipped with 5 mm cryogenic triple resonance (TCI) probe. The NMR data were collected at room temperature using a presat-NOESY pulse sequence with 512 scans, 4s

acquisition time per scan, 1s recycle delay, and a 12 ppm spectral window. Data was processed, apodised, phased, and spline baseline corrected using the Chenomx software suite (Edmonton, Alberta, Canada). Metabolite profiling was performed using Chenomx NMR Suite 9.0 (Chenomx, Edmonton, Canada).

3.3.10 Glycosaminoglycan (GAG) content in alginate beads

Deposited GAG in the alginate was measured using a protocol adapted and modified from Coulson-Thomas, V. J. and Gesteira, T. F. and Zheng et al. (Coulson-Thomas and Gesteira 2014; Zheng and Levenston 2015). Briefly, the supernatant from the cell extraction step was collected, centrifuged at 16,000 × g, and reconstituted in 1 mL 1X PBS. A DMMB detection solution (pH 3.0) was prepared by dissolving the following in 500 mL distilled water:16 mg DMMB (341088, Sigma, MO), 1.52 g glycine, 0.8 NaCl (IC102892.5, VWR International, PA), and 47.5 mL of 100 mM acetic acid (AA10994, VWR International, PA). In a 96-well plate, 20 µL from each sample was mixed with 200 µL DMMB and scanned immediately at 525 and 595 nm (Coulson-Thomas and Gesteira 2014; Zheng and Levenston 2015). The GAG content was calculated by taking the absorbance difference between both wavelengths and compared to a standard curve ranging from 0 to 10 µg/mL (Zheng and Levenston 2015).

3.3.11 Statistical analysis

This study investigated the impact of steady glucose levels and fluid flow in cell culture media on alginate-encapsulated AF and NP cells. We used the following metrics to assess the impact of the culture technique: cell viability, senescence, GAG content, and cellular metabolites.

Six batches of AF and NP cells were cultured in 6 well-plates under two glucose conditions: steady-state glucose, changing the media three times per day (n=3), and unsteady-state glucose, replacing culture media once every three days (n=3). Four batches of AF and NP cells were cultured in a fluidized-bed bioreactor with continuous fluid flow at 4 mL/min. The cultures were under two glucose conditions: steady-state glucose, replacing culture media with a pump at a rate of 0.139 mL per hour, and unsteady-state glucose, replacing culture media once every three days (n=2).

Factorial analysis of variance (factorial ANOVA) followed by a Tukey HSD test were performed in TIBCO Statistica v13.5 (Palo Alto, CA, USA) to determine significant difference in the means across treatment groups with alpha = 0.05.

3.4 Results

3.4.1 Glucose levels

In AF and NP cell cultures, glucose levels were measured over 10-12 days in triplicates using a blood glucose meter (Figure 3.3). Glucose in the unsteady-state cultures fluctuated between 2 mM and 6 mM, with the peaks indicating the addition of fresh media to the cell culture. In steady-state cultures, glucose levels stabilized after three days at an average of 2 mM to 3 mM (Figure 3.3. A-C). NP cell in the bioreactor steady-state treatment group had a higher mean glucose concentration of 5.3 mM compared to the other groups (Figure 3.3D). Starting glucose concentrations on day 0 were different between the groups due to the separate processing of each bead-group in NaCl which diluted the glucose in the well-plates; additional variance may be attributed to the glucose meter.

AF cell culture

well-plate (static flow)   bioreactor (dynamic flow)

NP cell culture

well-plate (static flow)   bioreactor (dynamic flow)
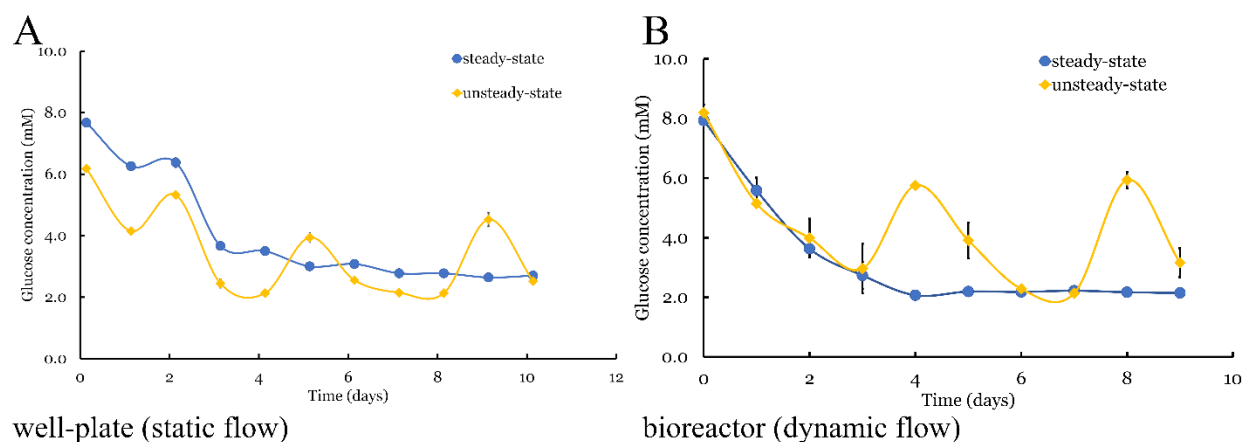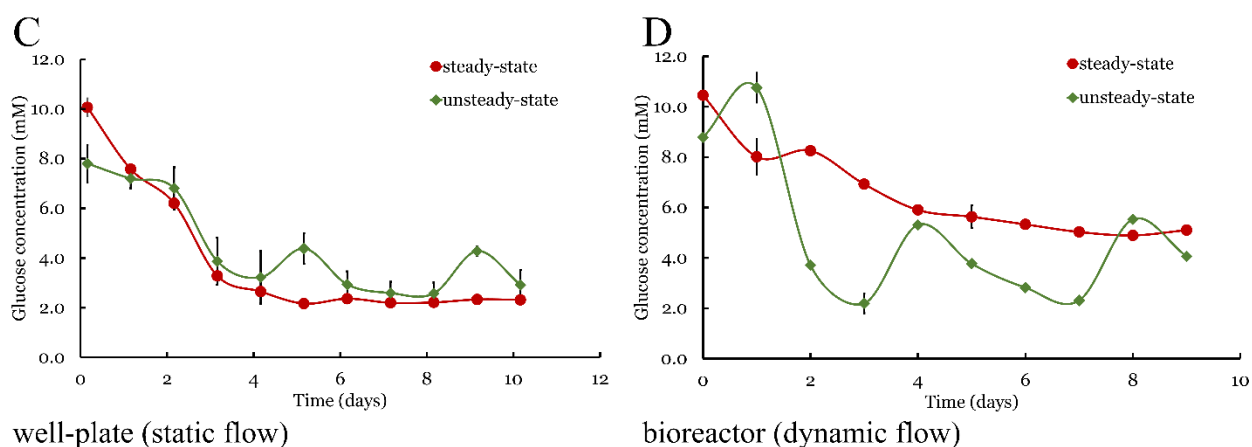
Figure 3.3. Average glucose concentrations (mM) in AF (A-B) and NP (C-D) cell cultures a well-plate n=3 (A-C) and in a bioreactor n=2 (B-D). Under unsteady-state conditions, glucose fluctuated between 2 mM and 6 mM. Glucose levels in steady-state conditions were maintained between 2 mM and 3 mM, except in D, where glucose levels stabilized at an average of 5.3 mM.

3.4.2 Cell senescence

Cell senescence was measured to investigate the impact of culture conditions on cellular phenotype (Figure 3.4). We compared the results against the steady-state treatment group in the well-plate and bioreactor set-ups. There was no difference in AF senescence in the bioreactor groups (factorial ANOVA, $p = 0.95$). Whereas more senescent AF cells were observed in the well-plates under steady-state conditions compared to unsteady-state (factorial ANOVA, $p = 0.01$) (Figure 3.4). NP cells in the bioreactor group showed more senescence under steady-state

conditions when compared to unsteady-state (factorial ANOVA, p = 0.03) (Figure 3.4). However, no change in senescence was observed in the well-plate group when comparing unsteady-state with steady-state conditions (factorial ANOVA, p = 0.14) (Figure 3.4).
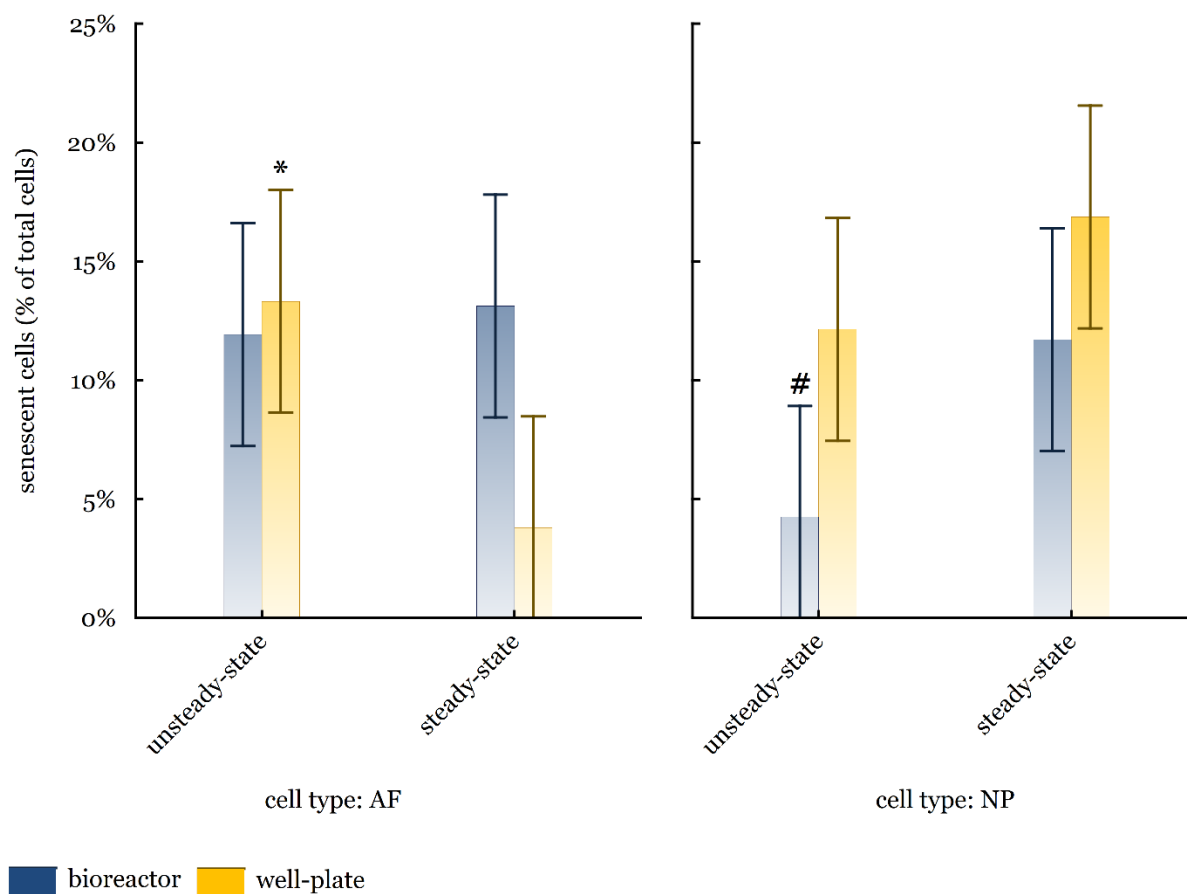
Figure 3.4. Cell senescence of AF and NP cells cultured in a bioreactor and well-plate under two glucose conditions, steady-state and unsteady-state. AF cells showed higher senescence when cultured in the well-plates under unsteady-state glucose compared with steady-state (p = 0.01), indicated with *. But no difference in mean senescent AF cells was observed in the bioreactor culture when comparing unsteady-state glucose with steady-state glucose (p = 0.95). NP cells in the well-plates showed no difference in mean cell senescence when comparing steady-state and unsteady-state glucose (p = 0.14). However, when NP cells were cultured in the bioreactor, we observed higher senescence when under unsteady-state compared to steady-state (factorial ANOVA, p = 0.03), indicated with #.

3.4.3 (HR-MAS) NMR metabolomics

To elucidate the effects of unsteady glucose levels in cell culture on the metabolic pathways in AF and NP cells, we performed an NMR metabolomics analysis after harvesting the cells from the alginate beads. We considered steady-state as the baseline to calculate the percent difference of metabolite concentrations in the unsteady-state cell cultures. To infer significance, we applied a repeated measures ANOVA with $p < 0.05$ and marked the significant changes in metabolites by a * in Figure 3.5.

NMR data showed a differential metabolic response between AF and NP cells cultured in the well-plate and the bioreactor. Although not significant, AF cells in the well-plate showed an increase in the utilization of amino acids under unsteady-state conditions, which was indicated by concentration ratios less than 100%. AF cells cultured in the bioreactor showed a reversed trend where cells under unsteady-state utilized more amino acids, including alanine, leucine, tyrosine, and valine. In addition, the TCA substrates like glucose were utilized more under unsteady state conditions leading to increased levels of lactate compared to steady conditions ($p<0.05$) (Figure 3.5).

Interestingly, NP cells showed a reversed trend compared to AF cell cultures. In the well-plate culture, NP cells showed increased utilization of amino acids under steady-state conditions indicated by % ratios higher than 100%. We also observed an increase in lactate accumulation in the unsteady-state, indicating an increase in TCA cycle activation. NP cells acquired a different metabolite profile in the bioreactor cultures with a dramatic increase in methionine. In addition, the utilization of all amino acids and most TCA cycle intermediates decreased in unsteady-state conditions compared to steady-state (Figure 3.5).

Intracellular glutamate levels, which are utilized in the production of GAGs in IVD cells, increased under steady-state conditions for AF cells compared to unsteady conditions. We observed an opposite trend in NP cells, where glutamate levels increased under unsteady-state conditions. We observed a reversed trend in the bioreactor culture where AF cells under unsteady-state accumulated glutamate levels compared to steady-state. NP cells in the bioreactor showed increased glutamate levels under steady-state compared to unsteady-state (Figure 3.5).
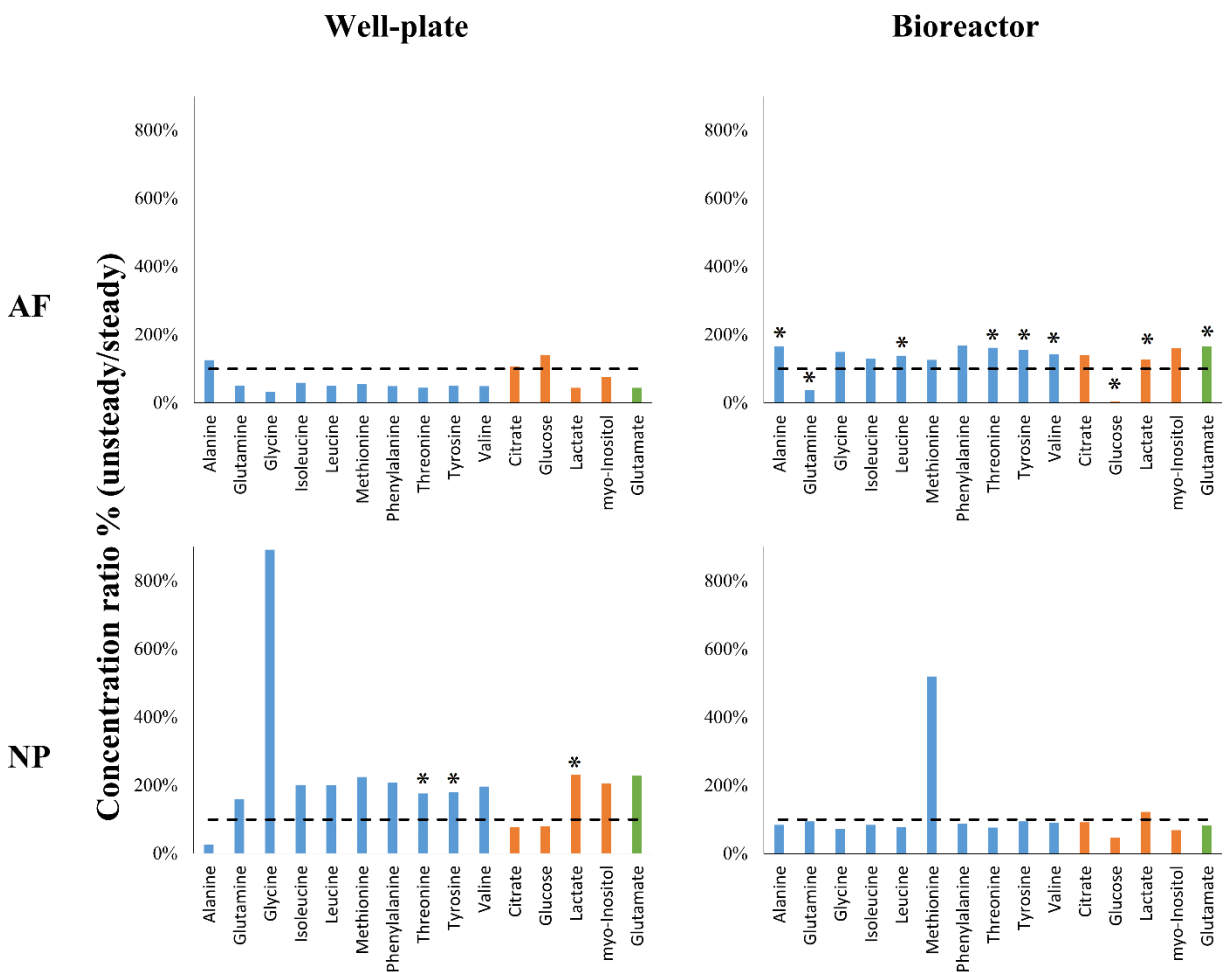
Figure 3.5. Results of (HR-MAS) NMR metabolomics of AF and NP cells cultured in the well-plate and bioreactor. Amino acids are shown in blue, TCA cycle intermediates are shown in orange, and glutamate is shown in green. The dashed line indicates a 100% ratio, indicating no change in metabolite concentration between unsteady and steady conditions. A repeated measures ANOVA with $p = 0.05$ was performed to infer significance between unsteady and steady conditions indicated with *.

3.4.4 GAG content in alginate beads

  The amount of deposited GAG into the alginate beads was measured using a DMMB assay elucidating the rate of ECM remodeling by AF and NP cells. When cultured under steady- and unsteady-state conditions, AF cells deposited the same amount of GAG into their ECM (Figure 3.6). NP cells with a feeding schedule of 3-time per day (steady-state conditions) produced, on average, about 30% GAG compared to NP cells with a feeding schedule of 3-days (unsteady-state).
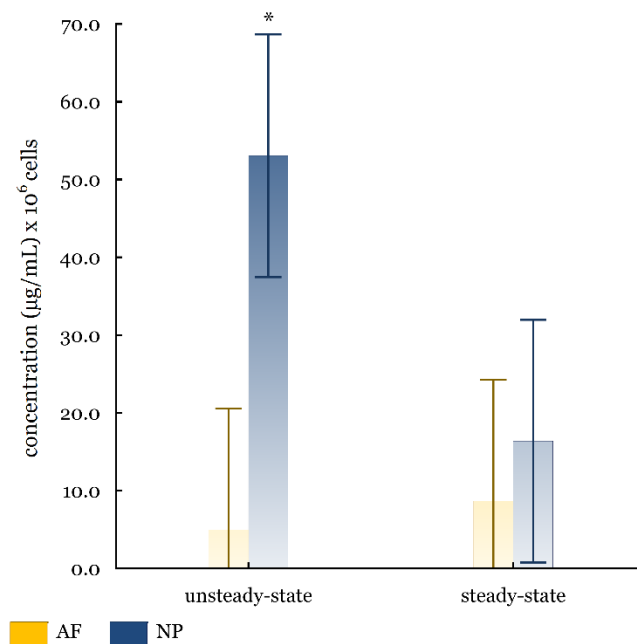
Figure 3.6. The figure shows averaged glycosaminoglycan (GAG) content in the ECM of AF and NP cells cultured in a well-plate. GAG content was normalized to 1 million cells. Significance is indicated by *, comparing unsteady with steady-state (ANOVA, $p < 0.05$).

GAG content was similar for the bioreactor cell culture, in which AF cells under unsteady and steady glucose levels secreted the same amount of sulfated GAG into the ECM, averaging 7.5 µg/mL. NP cells under unsteady glucose produced 50% more GAG compared to steady glucose (Figure 3.7).
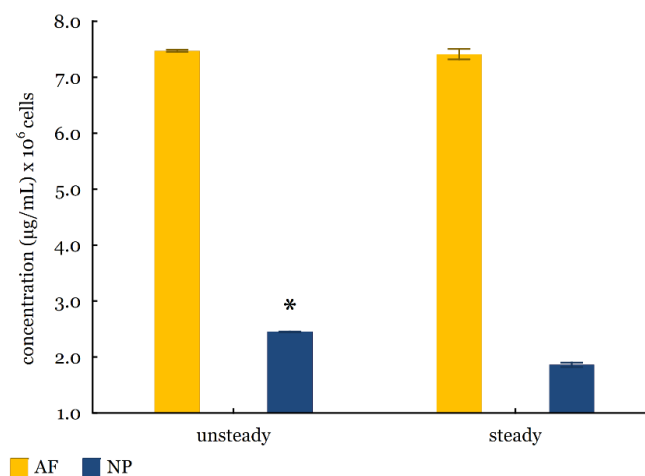
Figure 3.7. The figure shows averaged sulfated glycosaminoglycan (GAG) content (n = 2) in the ECM of AF and NP cells cultured in the bioreactor. GAG content was normalized to 1 million cells. Significance is indicated by *, comparing unsteady with steady-state (ANOVA, $p < 0.05$).

3.5 Discussion

To our knowledge, this was the first study that determined effects of fluctuating glucose levels in cell culture media on AF and NP cells. DDD is a common cause of low back pain in adulthood (Andersson 1999). Various research groups have been studying the mechanisms for IVD degeneration, providing an understanding of potential strategies to alleviate back pain.

However, studies performed on IVD cells lacked standardization in culture conditions, leading to inconsistent data regarding cell phenotype, ECM composition, and cellular metabolism (Mizuno, Allemann, and Glowacki 2001; Liu et al. 2020; Martin, Wendt, and Heberer 2004). Studies reported using various glucose sources, including Low-Glucose DMEM, High-Glucose DMEM, Opti-MEM, α-MEM, Ham's F-12, or a mixture of each (Sato et al. 2003; Chen et al. 2016; Hegewald et al. 2011; Schubert et al. 2018; Preradovic et al. 2005; Dimozi et al. 2015; Xiao et al. 2017). In addition, there is inconsistency in cell culture supplements, including various concentrations of fetal bovine serum and different antibiotics and antimycotics, e.g., penicillin, streptomycin, and fungizone (Sato et al. 2003; Chen et al. 2016; Hegewald et al. 2011; Schubert et al. 2018; Preradovic et al. 2005; Dimozi et al. 2015; Xiao et al. 2017). Currently utilized culture conditions do not only fail to mimic the IVD's *in vivo* microenvironment, which is hypoxic and acidic, but it can also be a source of conflicting results.

This study demonstrated the importance of standardizing cell culture conditions by showing the effects of culture media modulation on cell senescence, GAG expression, and metabolic processes.

3.5.1 Cell senescence

When IVD cells detect degenerative stimuli such as high acidity and inflammation, they undergo an irreversible process of cell cycle arrest known as senescence, changing their morphology, gene expression, and ECM secretion rates (Ogrodnik 2021; Feng et al. 2016; Shan et al. 2019). In this study, AF senescence in the well-plate increased by ~10% under unsteady-state conditions compared to steady-state, averaging 16% (Figure 3.4). NP cells in the bioreactor experienced lower senescence (~10% decrease) when cultured under unsteady-state glucose compared to steady-state (Figure 3.4). Thus, this work highlighted the differential phenotypic responses between NP and AF cells further supporting our hypothesis that cell culture conditions affected cell phenotypes. Elevated glucose levels were postulated to induce apoptosis and senescence, impeding proliferation and tissue repair rates (Liu et al. 2020). In one study investigating the effects of diabetic blood glucose levels on IVD cell senescence, researchers found that elevated levels of glucose induced oxidative stress leading to senescence and apoptosis (Park et al. 2014; Shan et al. 2019; Cheng et al. 2016).

Glucose values implemented in our study were lower than those used in Park et al. (Park et al. 2014); however, they were close to diabetic blood glucose levels of 7.7 mM, which has also been shown to initiate senescence in IVD cells (Jouven et al. 2005; Jiang et al. 2013). Our results demonstrated a possible interaction between fluid flow, glucose modulation, and cell type that could induce senescence. Senescent cells secrete proinflammatory factors like chemokines and cytokines, which may accumulate in the cells' environment when under static fluid conditions, i.e. in the well-plate, amplifying senescence (Zhang et al. 2020). It is possible that continuous fluid flow in the bioreactor prevented the accumulation of senescent factors in the NP beads. While the data shows NP cells benefiting from fluid flow, AF cells seemed to acquire more senescent phenotypes under the same conditions. There is increasing evidence that fluid flow in cell cultures is important in regulating ECM homeostasis and cellular functions (Chen et al. 2020; Ye et al. 2018). Considering the physiological environment of the IVD, NP cells are constantly exposed to changes in water content and shear stress through the natural compression of the IVD which also

lead to fluctuations in the nutrient levels (Chen et al. 2020; Wang, Yang, and Hsieh 2011; Jackson et al. 2011). In contrast, AF cells existing on the periphery of the IVD experience less modulations in water content and shear stress as it transfers from the NP (Jackson et al. 2012; Chen et al. 2020). However, the direct effect of shear stress *in vitro* is necessary to elucidate the mechanism of cellular senescence in this culture system.

In this experiment, we used the increased activity of β-galactosidase in AF and NP cells to measure senescence, yet it is important to consider the limitations of this assay. Studies reported unreliable results associated with the β-galactosidase marker used for senescence due to increased activity in dormant (quiescent) cells, starved cells, and cells treated with H_2O_2 (Yang and Hu 2005). Additional studies would require controlling for these confounding factors.

Due to the β-galactosidase assay's low specificity for senescence in IVD cells, it would be useful to consider more robust markers. Cells that undergo senescence are known to have incomplete DNA replication due to telomere shortening and dysfunction, which can be detected by the increased activation of the p53-p21-pRB pathway in aging IVD cells (Kim et al. 2009). Increased expression of cytokines like interleukin-6 (IL-6), interleukin-1 (IL-1), and matrix metalloproteinases (MMPS) can also be used to infer senescence levels in IVD cells (Loeser 2009).

This study shows that the cell culture environment impacts cell senescence. NP cells have adapted to exist in microenvironments with variations in nutrient levels and shear stress (Chen et al. 2020; Ye et al. 2018; Jackson et al. 2011). Meanwhile, AF cells have adapted to thrive under steady levels of nutrients and little shear stress (Chen et al. 2020; Wang, Yang, and Hsieh 2011).

3.5.2 (HR-MAS) NMR metabolomics

Proton high-resolution magic angle spinning (HR-MAS) NMR is a non-destructive technique that can profile various metabolites in cells, providing invaluable information on the regulation of metabolic processes (Keshari, Lotz, et al. 2005; Keshari, Zektzer, et al. 2005; Keshari et al. 2008). This method has been used to quantify metabolic changes associated with IVD degeneration (Keshari, Lotz, et al. 2005; Keshari, Zektzer, et al. 2005; Keshari et al. 2008).

In this study, distinct metabolic profiles for both the AF and NP cell population under similar culturing conditions were illustrated, further supporting the notion that different cell types require individual culture environments.

In the AF cells, metabolite concentrations involved in the TCA cycle, anaplerotic flux (amino acids), and glycolysis (glucose and lactate) all increased under steady glucose levels in the well-plate (Figure 3.5). Increased levels of metabolites may be attributed to the increased availability of nutrients associated with the steady-state. Since cells were cultured in normoxic conditions, we expected the recruitment of other metabolic pathways to generate energy, such as fatty acid metabolism, explaining the increase in choline and O-phosphocholine (data not shown) (Pacholczyk-Sienicka et al. 2015). AF cells in the bioreactor utilized more amino acids compared to the unsteady-state which could be attributed to increased availability of these metabolites. Additionally, fluid flow in the bioreactor improves solute transport, prompting the utilization of amino acids in various anabolic pathways compared to the well-plate culture. Another effect of normoxic conditions was increased oxidative stress, which could be elucidated by the upregulation of methionine, an essential compound in antioxidant function (Pacholczyk-Sienicka et al. 2015; Feng et al. 2017). We also observed increased levels of myo-inositol, a chemical that facilitates the regulation of cellular osmotic pressure between the intra- and extracellular environments (Pacholczyk-Sienicka et al. 2015).

Similar to AF cells, most metabolite concentrations either increased in unsteady-state conditions or did not change compared to the steady-state. Interestingly, NP cells under unsteady-state conditions had a decrease in glucose concentrations with an associated increase in lactate levels (Figure 3.5). This suggests that unsteady-state conditions upregulated anaerobic glycolysis despite having greater glucose availability (Bibby et al. 2005). Yet further analysis is necessary to confirm these findings with either lactate dehydrogenase activity or other glycolytic rates assays. In addition, increases in alanine may be associated with increased glycolysis and amino acid synthesis. Intermediates of the TCA cycle, such as citrate, and anaplerotic flux contributors, such as glutamate and methionine, were also upregulated, though not significantly (Pacholczyk-Sienicka et al. 2015; Madhu et al. 2020). However, it was unclear if these were shifts towards the upregulation of the TCA cycle or towards amino acid synthesis and thus require further analysis. Compared to AF cells, there was no drastic increase in fatty acid or amino acid metabolism, indicating the difference in the metabolite profile for AF and NP cells. In addition, we expected steady glucose levels to increase fatty acid and amino acid metabolism due to the constant supply of nutrients. Interestingly, we did not observe NP cells upregulating their antioxidant mechanisms significantly despite being in normoxic conditions.

Our results suggested that the metabolite profile can vary due to cell type and different cell culture conditions, further supporting the need to standardize cell culture protocols.

<u>3.5.3 Glycosaminoglycan content</u>

Glycosaminoglycans (GAGs) are essential in the AF and NP ECM. While the NP has higher GAG content than the AF, estimated to be 11% compared to 8%, sulfated GAGs facilitate the swelling of both tissue types, retaining water levels that are important in maintaining homeostasis in the IVD (Yang and O'Connell 2019).

In this study, we measured the content of secreted GAGs into the matrix of the alginate beads to assess changes in cell phenotype and cellular processes. The expression of GAG has been used as a biomarker for DDD (Nguyen et al. 2008; Sato, Kikuchi, and Yonezawa 1999; Adams and Roughley 2006; Antoniou et al. 1996). We reported decreased GAG content produced by NP cells under steady glucose levels and no change in AF GAG content (Figures 3.5). The drop in NP GAG content could be attributed to the accumulation of senescence. The drop in GAG content in NP cells correlated with a 10% drop in glutamine which is important in the production of GAGs in mammalian cells (Figure 3.5 and Figure 3.6) (Handley et al. 1980; Speight, Handley, and Lowther 1978). Observing decreased GAG content in NP cells under steady glucose levels provides further evidence that supports developing protocols which mimic the NP's *in vivo* microenvironment.

The main limitation of this work includes culturing cells under normoxic conditions. In the IVD, cells exist under low oxygen levels, affecting glycolysis and ECM synthesis rates (Bibby et al. 2005). However, one study suggests that no change in GAG synthesis was observed in AF and NP cells due to changing oxygen levels from 1% to 21% (Mwale et al. 2011). One study further suggests that IVD cells have developed mechanisms to survive under low oxygen levels, preventing impaired cellular functions (Mwale et al. 2011). In addition, cell samples under unsteady-state were exposed to a narrow range of glucose concentrations, ranging between 2 mM and 6 mM, compared to cell culture protocols using high glucose concentrations of 15 mM. Such concentrations could change the metabolites profile for both AF and NP cells and lead to increased senescence (Park et al. 2014).

3.6 Conclusion

This study shows a strong correlation between cell culture conditions, including glucose and fluid flow on cell phenotype. Our results suggest that lack of standardization in the IVD research can lead to inconsistent results. Steady glucose levels were shown to increase senescence in NP cells. AF cells showed increased senescence when exposed to shear stress through fluid flow. Steady glucose levels also affected the metabolite profile of each cell type differently by upregulating amino acid and fatty acid synthesis in AF cells and the TCA cycle in NP cells. Therefore, developing a standardized protocol to culture AF and NP cells under physiological conditions would be essential in the study of IVD degeneration.

3.7 Acknowledgments

3.8 References

Adams, Michael A., and Peter J. Roughley. 2006. 'What is Intervertebral Disc Degeneration, and What Causes It?', *Spine (Phila Pa 1976)*, 31: 2151-61.

Andersson, G. B. 1999. 'Epidemiological features of chronic low-back pain', *Lancet*, 354: 581-5.

Antoniou, J., T. Steffen, F. Nelson, N. Winterbottom, A. P. Hollander, R. A. Poole, M. Aebi, and M. Alini. 1996. 'The human lumbar intervertebral disc: evidence for changes in the biosynthesis and denaturation of the extracellular matrix with growth, maturation, ageing, and degeneration', *J Clin Invest*, 98: 996-1003.

Bibby, S. R., D. A. Jones, R. M. Ripley, and J. P. Urban. 2005. 'Metabolism of the intervertebral disc: effects of low levels of oxygen, glucose, and pH on rates of energy metabolism of bovine nucleus pulposus cells', *Spine (Phila Pa 1976)*, 30: 487-96.

Bibby, S. R., and J. P. Urban. 2004. 'Effect of nutrient deprivation on the viability of intervertebral disc cells', *Eur Spine J*, 13: 695-701.

Boubriak, Olga. A., Natasha Watson, Sarit. S. Sivan, Naomi Stubbens, and Jill P. G. Urban. 2013. 'Factors regulating viable cell density in the intervertebral disc: blood supply in relation to disc height', *Journal of Anatomy*, 222: 341-48.

Brodke, D. S., and S. M. Ritter. 2005. 'Nonsurgical management of low back pain and lumbar disk degeneration', *Instr Course Lect*, 54: 279-86.

Bruehlmann, S. B., J. B. Rattner, J. R. Matyas, and N. A. Duncan. 2002. 'Regional variations in the cellular matrix of the annulus fibrosus of the intervertebral disc', *J Anat*, 201: 159-71.

Chen, Deheng, Dongdong Xia, Zongyou Pan, Daoliang Xu, Yifei Zhou, Yaosen Wu, Ningyu Cai, Qian Tang, Chenggui Wang, Meijun Yan, Jing Jie Zhang, Kailiang Zhou, Quan Wang, Yongzeng Feng, Xiangyang Wang, Huazi Xu, Xiaolei Zhang, and Naifeng Tian. 2016. 'Metformin protects against apoptosis and senescence in nucleus pulposus cells and ameliorates disc degeneration in vivo', *Cell Death & Disease*, 7: e2441-e41.

Chen, Sheng, Lei Qin, Xiaohao Wu, Xuekun Fu, Sixiong Lin, Di Chen, Guozhi Xiao, Zengwu Shao, and Huiling Cao. 2020. 'Moderate Fluid Shear Stress Regulates Heme Oxygenase-1 Expression to Promote Autophagy and ECM Homeostasis in the Nucleus Pulposus Cells', *Frontiers in Cell and Developmental Biology*, 8.

Cheng, Xiaofei, Bin Ni, Feng Zhang, Ying Hu, and Jie Zhao. 2016. 'High Glucose-Induced Oxidative Stress Mediates Apoptosis and Extracellular Matrix Metabolic Imbalances Possibly via p38 MAPK Activation in Rat Nucleus Pulposus Cells', *Journal of Diabetes Research*, 2016: 3765173.

Cheung, Kenneth M. C., Jaro Karppinen, Danny Chan, Daniel W. H. Ho, You-Qiang Song, Pak Sham, Kathryn S. E. Cheah, John C. Y. Leong, and Keith D. K. Luk. 2009. 'Prevalence and Pattern of Lumbar Magnetic Resonance Imaging Changes in a Population Study of One Thousand Forty-Three Individuals', *Spine (Phila Pa 1976)*, 34: 934-40.

Coulson-Thomas, Vivien Jane, and Tarsis Ferreira Gesteira. 2014. 'Dimethylmethylene Blue Assay (DMMB)', *Bio-protocol*, 4: e1236.

Dimozi, A., E. Mavrogonatou, A. Sklirou, and D. Kletsas. 2015. 'Oxidative stress inhibits the proliferation, induces premature senescence and promotes a catabolic phenotype in human nucleus pulposus intervertebral disc cells', *Eur Cell Mater*, 30: 89-102; discussion 03.

Feng, Chencheng, Huan Liu, Minghui Yang, Yang Zhang, Bo Huang, and Yue Zhou. 2016. 'Disc cell senescence in intervertebral disc degeneration: Causes and molecular pathways', *Cell Cycle*, 15: 1674-84.

Feng, Chencheng, Minghui Yang, Minghong Lan, Chang Liu, Yang Zhang, Bo Huang, Huan Liu, and Yue Zhou. 2017. 'ROS: Crucial Intermediators in the Pathogenesis of Intervertebral Disc Degeneration', *Oxidative Medicine and Cellular Longevity*, 2017: 5601593.

Gruber, Helen E., Audrey A. Stasky, and Edward N. Hanley. 1997. 'Characterization and phenotypic stability of human disc cells in Vitro', *Matrix Biology*, 16: 285-88.

Handley, C. J., G. Speight, K. M. Leyden, and D. A. Lowther. 1980. 'Extracellular matrix metabolism by chondrocytes 7. Evidence that L-glutamine is an essential amino acid for chondrocytes and other connective tissue cells', *Biochimica et Biophysica Acta (BBA) - General Subjects*, 627: 324-31.

Hegewald, Aldemar A., Michaela Endres, Alexander Abbushi, Mario Cabraja, Christian Woiciechowsky, Kirsten Schmieder, Christian Kaps, and Claudius Thomé. 2011. 'Adequacy of herniated disc tissue as a cell source for nucleus pulposus regeneration: Laboratory investigation', *Journal of Neurosurgery: Spine SPI*, 14: 273-80.

Holm, S., A. Maroudas, J. P. Urban, G. Selstam, and A. Nachemson. 1981. 'Nutrition of the intervertebral disc: solute transport and metabolism', *Connect Tissue Res*, 8: 101-19.

Jackson, A. R., T. Y. Yuan, C. Y. Huang, and W. Y. Gu. 2009. 'A conductivity approach to measuring fixed charge density in intervertebral disc tissue', *Ann Biomed Eng*, 37: 2566-73.

Jackson, Alicia R., Chun-Yuh C. Huang, Mark D. Brown, and Wei Yong Gu. 2011. '3D Finite Element Analysis of Nutrient Distributions and Cell Viability in the Intervertebral Disc: Effects of Deformation and Degeneration', *Journal of Biomechanical Engineering*, 133.

Jackson, Alicia R., Tai-Yi Yuan, Chun-Yuh Huang, Mark D. Brown, and Wei Yong Gu. 2012. 'Nutrient Transport in Human Annulus Fibrosus is Affected by Compressive Strain and Anisotropy', *Annals of Biomedical Engineering*, 40: 2551-58.

Jiang, Libo, Xiaolei Zhang, Xuhao Zheng, Ao Ru, Xiao Ni, Yaosen Wu, Naifeng Tian, Yixing Huang, Enxing Xue, Xiangyang Wang, and Huazi Xu. 2013. 'Apoptosis, senescence, and autophagy in rat nucleus pulposus cells: Implications for diabetic intervertebral disc degeneration', *Journal of Orthopaedic Research*, 31: 692-702.

Jouven, Xavier, Rozenn N. Lemaître, Thomas D. Rea, Nona Sotoodehnia, Jean-Philippe Empana, and David S. Siscovick. 2005. 'Diabetes, glucose level, and risk of sudden cardiac death', *European Heart Journal*, 26: 2142-47.

Keshari, K. R., J. C. Lotz, J. Kurhanewicz, and S. Majumdar. 2005. 'Correlation of HR-MAS spectroscopy derived metabolite concentrations with collagen and proteoglycan levels and Thompson grade in the degenerative disc', *Spine (Phila Pa 1976)*, 30: 2683-8.

Keshari, K. R., J. C. Lotz, T. M. Link, S. Hu, S. Majumdar, and J. Kurhanewicz. 2008. 'Lactic acid and proteoglycans as metabolic markers for discogenic back pain', *Spine (Phila Pa 1976)*, 33: 312-7.

Keshari, K. R., A. S. Zektzer, M. G. Swanson, S. Majumdar, J. C. Lotz, and J. Kurhanewicz. 2005. 'Characterization of intervertebral disc degeneration by high-resolution magic angle spinning (HR-MAS) spectroscopy', *Magn Reson Med*, 53: 519-27.

Kim, Ki-Won, Ha-Na Chung, Kee-Yong Ha, Jun-Seok Lee, and Young-Yul Kim. 2009. 'Senescence mechanisms of nucleus pulposus chondrocytes in human intervertebral discs', *The Spine Journal*, 9: 658-66.

Knight, Eleanor, and Stefan Przyborski. 2015. 'Advances in 3D cell culture technologies enabling tissue-like structures to be created in vitro', *Journal of Anatomy*, 227: 746-56.

Kwon, Young Jik, and Ching-An Peng. 2002. 'Calcium-Alginate Gel Bead Cross-Linked with Gelatin as Microcarrier for Anchorage-Dependent Cell Culture', *BioTechniques*, 33: 212-18.

Le Maitre, Christine Lyn, Anthony J. Freemont, and Judith Alison Hoyland. 2005. 'The role of interleukin-1 in the pathogenesis of human Intervertebral disc degeneration', *Arthritis Research & Therapy*, 7: R732.

Liebscher, T., M. Haefeli, K. Wuertz, A. G. Nerlich, and N. Boos. 2011. 'Age-related variation in cell density of human lumbar intervertebral disc', *Spine (Phila Pa 1976)*, 36: 153-9.

Liu, Y., Y. Li, L. P. Nan, F. Wang, S. F. Zhou, J. C. Wang, X. M. Feng, and L. Zhang. 2020. 'The effect of high glucose on the biological characteristics of nucleus pulposus-derived mesenchymal stem cells', *Cell Biochem Funct*, 38: 130-40.

Loeser, R. F. 2009. 'Aging and osteoarthritis: the role of chondrocyte senescence and aging changes in the cartilage matrix', *Osteoarthritis and Cartilage*, 17: 971-79.

Long, Dani M., Ariel K. Frame, Patrick N. Reardon, Robert C. Cumming, David A. Hendrix, Doris Kretzschmar, and Jadwiga M. Giebultowicz. 2020. 'Lactate dehydrogenase expression modulates longevity and neurodegeneration in Drosophila melanogaster', *Aging*, 12: 10041-58.

Madhu, Vedavathi, Paige K Boneski, Elizabeth Silagi, Yunping Qiu, Irwin Kurland, Anyonya R Guntur, Irving M Shapiro, and Makarand V Risbud. 2020. 'Hypoxic Regulation of Mitochondrial Metabolism and Mitophagy in Nucleus Pulposus Cells Is Dependent on HIF-1α–BNIP3 Axis', *Journal of Bone and Mineral Research*, 35: 1504-24.

Mahmoudifar, Nastaran, and Pauline M. Doran. 2010. 'Chondrogenic differentiation of human adipose-derived stem cells in polyglycolic acid mesh scaffolds under dynamic culture conditions', *Biomaterials*, 31: 3858-67.

Martin, I., D. Wendt, and M. Heberer. 2004. 'The role of bioreactors in tissue engineering', *Trends Biotechnol*, 22: 80-6.

Mizuno, S., F. Allemann, and J. Glowacki. 2001. 'Effects of medium perfusion on matrix production by bovine chondrocytes in three-dimensional collagen sponges', *J Biomed Mater Res*, 56: 368-75.

Mwale, Fackson, Ioana Ciobanu, Demetri Giannitsios, Peter Roughley, Thomas Steffen, and John Antoniou. 2011. 'Effect of Oxygen Levels on Proteoglycan Synthesis by Intervertebral Disc Cells', *Spine (Phila Pa 1976)*, 36: E131-E38.

Nguyen, An M., Wade Johannessen, Jonathon H. Yoder, Andrew J. Wheaton, Edward J. Vresilovic, Arijitt Borthakur, and Dawn M. Elliott. 2008. 'Noninvasive quantification of human nucleus pulposus pressure with use of T1rho-weighted magnetic resonance imaging', *The Journal of bone and joint surgery. American volume*, 90: 796-802.

Ogrodnik, Mikolaj. 2021. 'Cellular aging beyond cellular senescence: Markers of senescence prior to cell cycle arrest in vitro and in vivo', *Aging Cell*, 20: e13338.

Pacholczyk-Sienicka, Barbara, Maciej Radek, Andrzej Radek, and Stefan Jankowski. 2015. 'Characterization of metabolites determined by means of 1H HR MAS NMR in intervertebral disc degeneration', *Magnetic Resonance Materials in Physics, Biology and Medicine*, 28: 173-83.

Park, Jong-Soo, Jong-Beom Park, In-Joo Park, and Eun-Young Park. 2014. 'Accelerated premature stress-induced senescence of young annulus fibrosus cells of rats by high glucose-induced oxidative stress', *International Orthopaedics*, 38: 1311-20.

Park, S., and G. Stephanopoulos. 1993. 'Packed bed bioreactor with porous ceramic beads for animal cell culture', *Biotechnol Bioeng*, 41: 25-34.

Pattappa, G., Z. Li, M. Peroglio, N. Wismer, M. Alini, and S. Grad. 2012. 'Diversity of intervertebral disc cells: phenotype and function', *J Anat*, 221: 480-96.

Preradovic, Adrijana, Guenther Kleinpeter, Hans Feichtinger, Ernest Balaun, and Walter Krugluger. 2005. 'Quantitation of collagen I, collagen II and aggrecan mRNA and expression of the corresponding proteins in human nucleus pulposus cells in monolayer cultures', *Cell and Tissue Research*, 321: 459-64.

Rajaee, Sean S., Hyun W. Bae, Linda E. A. Kanim, and Rick B. Delamarter. 2012. 'Spinal fusion in the United States: analysis of trends from 1998 to 2008', *Spine (Phila Pa 1976)*, 37: 67-76.

Sato, Katsuhiko, Shinichi Kikuchi, and Takumi Yonezawa. 1999. 'In Vivo Intradiscal Pressure Measurement in Healthy Individuals and in Patients With Ongoing Back Problems', *Spine (Phila Pa 1976)*, 24: 2468.

Sato, Masato, Takashi Asazuma, Masayuki Ishihara, Toshiyuki Kikuchi, Kazunori Masuoka, Shoichi Ichimura, Makoto Kikuchi, Akira Kurita, and Kyosuke Fujikawa. 2003. 'An atelocollagen honeycomb-shaped scaffold with a membrane seal (ACHMS-scaffold) for the culture of annulus fibrosus cells from an intervertebral disc', *Journal of Biomedical Materials Research Part A*, 64A: 248-56.

Schubert, Ann-Kathrin, Jeske J. Smink, Matthias Pumberger, Michael Putzier, Michael Sittinger, and Jochen Ringe. 2018. 'Standardisation of basal medium for reproducible culture of human annulus fibrosus and nucleus pulposus cells', *Journal of Orthopaedic Surgery and Research*, 13: 209.

Shan, Lizhen, Di Yang, Danjie Zhu, Fabo Feng, and Xiaolin Li. 2019. 'High glucose promotes annulus fibrosus cell apoptosis through activating the JNK and p38 MAPK pathways', *Bioscience Reports*, 39.

Shirazi-Adl, A., M. Taheri, and J. P. Urban. 2010. 'Analysis of cell viability in intervertebral disc: Effect of endplate permeability on cell population', *J Biomech*, 43: 1330-6.

Speight, G., C. J. Handley, and D. A. Lowther. 1978. 'Extracellular matrix metabolism by chondrocytes 4. Role of glutamine in glycosaminoglycan synthesis in vitro by chondrocytes', *Biochimica et Biophysica Acta (BBA) - General Subjects*, 540: 238-45.

Teraguchi, M., N. Yoshimura, H. Hashizume, S. Muraki, H. Yamada, A. Minamide, H. Oka, Y. Ishimoto, K. Nagata, R. Kagotani, N. Takiguchi, T. Akune, H. Kawaguchi, K. Nakamura, and M. Yoshida. 2014. 'Prevalence and distribution of intervertebral disc degeneration over the entire spine in a population-based cohort: the Wakayama Spine Study', *Osteoarthritis and Cartilage*, 22: 104-10.

Urban, J. P., S. Smith, and J. C. Fairbank. 2004. 'Nutrition of the intervertebral disc', *Spine (Phila Pa 1976)*, 29: 2700-9.

Urban, Jill P. G., and Sally Roberts. 2003. 'Degeneration of the intervertebral disc', *Arthritis Res Ther*, 5: 120.

Vergroesen, P. P. A., I. Kingma, K. S. Emanuel, R. J. W. Hoogendoorn, T. J. Welting, B. J. van Royen, J. H. van Dieën, and T. H. Smit. 2015. 'Mechanics and biology in intervertebral disc degeneration: a vicious circle', *Osteoarthritis and Cartilage*, 23: 1057-70.

Wang, Ping, Li Yang, and Adam H. Hsieh. 2011. 'Nucleus Pulposus Cell Response to Confined and Unconfined Compression Implicates Mechanoregulation by Fluid Shear Stress', *Annals of Biomedical Engineering*, 39: 1101-11.

Wang, Yue, Tapio Videman, and Michele C. Battié. 2012. 'ISSLS Prize Winner: Lumbar Vertebral Endplate Lesions: Associations With Disc Degeneration and Back Pain History', *Spine (Phila Pa 1976)*, 37: 1490-96.

Wiseman, M. A., H. L. Birch, M. Akmal, and A. E. Goodship. 2005. 'Segmental variation in the in vitro cell metabolism of nucleus pulposus cells isolated from a series of bovine caudal intervertebral discs', *Spine (Phila Pa 1976)*, 30: 505-11.

Xiao, Li, Mengmeng Ding, Osama Saadoon, Eric Vess, Andrew Fernandez, Ping Zhao, Li Jin, and Xudong Li. 2017. 'A novel culture platform for fast proliferation of human annulus fibrosus cells', *Cell and Tissue Research*, 367: 339-50.

Yang, Bo, and Grace D. O'Connell. 2019. 'Intervertebral disc swelling maintains strain homeostasis throughout the annulus fibrosus: A finite element analysis of healthy and degenerated discs', *Acta Biomaterialia*, 100: 61-74.

Yang, N. C., and M. L. Hu. 2005. 'The limitations and validities of senescence associated-beta-galactosidase activity as an aging marker for human foreskin fibroblast Hs68 cells', *Exp Gerontol*, 40: 813-9.

Ye, Dongping, Weiguo Liang, Libing Dai, and Yicun Yao. 2018. 'Moderate Fluid Shear Stress Could Regulate the Cytoskeleton of Nucleus Pulposus and Surrounding Inflammatory Mediators by Activating the FAK-MEK5-ERK5-cFos-AP1 Signaling Pathway', *Disease Markers*, 2018: 9405738.

Zhang, Yuang, Biao Yang, Jingkai Wang, Feng Cheng, Kesi Shi, Liwei Ying, Chenggui Wang, Kaishun Xia, Xianpeng Huang, Zhe Gong, Chao Yu, Fangcai Li, Chengzhen Liang, and Qixin Chen. 2020. 'Cell Senescence: A Nonnegligible Cell State under Survival Stress in Pathology of Intervertebral Disc Degeneration', *Oxidative Medicine and Cellular Longevity*, 2020: 9503562.

Zheng, C. H., and M. E. Levenston. 2015. 'Fact versus artifact: avoiding erroneous estimates of sulfated glycosaminoglycan content using the dimethylmethylene blue colorimetric assay for tissue-engineered constructs', *Eur Cell Mater*, 29: 224-36; discussion 36.

Chapter 4 – A Novel Method to Cryopreserve the Intact Intervertebral Disc

Ward Shalash, Ryan Forcier, Adam Z. Higgins, Morgan B. Giers[*]

School of Chemical, Biological and Environmental Engineering, Oregon State University,

Corvallis, OR 97331

4.1 Abstract

Low back pain is a leading cause of disability and missed workdays worldwide, and it has been associated with degeneration of the intervertebral disc (IVD). *Ex vivo* human IVD models have emerged as an attractive way to study different regeneration strategies. However, there are many logistical challenges to acquiring and working with whole fresh IVDs. Establishing a tissue bank to cryopreserve IVDs for long periods, maintain high cellular viability, and preserve mechanical integrity would lower the barriers to working with *ex vivo* human IVDs. It would also enable whole IVD allograft transplantations to treat IVD degeneration in patients. Current IVD cryopreservation protocols report poor cell viability due to limitations in the transport of cryoprotectants (CPAs). In this study, we incorporated a low-cytotoxicity CPA mixture and compression to improve the transport of the CPA and prevent cryoinjury to cells. Our results showed that 80-85% of cells in the outer AF, inner AF, and NP were viable after one week of storage at -80°C and not significantly different from fresh, unfrozen controls. IVDs that were cryopreserved without compression had poor cell viability compared to the fresh IVDs. This study aims to lead the way in solving a major roadblock in storing IVDs for long periods improving the logistics of experiments and clinical trials. We demonstrated how incorporating convective transport and a low-cytotoxic CPA mixture was crucial in preventing cryoinjury to IVD cells, leading to better optimization of IVD cryopreservation.

4.2 Introduction

Back pain is a leading cause of disability worldwide, with devastating effects on the well-being of affected individuals. This condition can be attributed to degeneration of the intervertebral disc (IVD), often leading to nerve compression and chronic back pain (Andersson 1999). Studies hypothesize that degeneration of the IVD happens due to the ongoing mechanical failure of the IVD and slow regeneration of the worn tissue (Cheung et al. 2009; Wang, Videman, and Battié 2012; Teraguchi et al. 2014; Boubriak et al. 2013; Urban and Roberts 2003; Urban, Smith, and Fairbank 2004). Trauma, aging, and limitations in the nutrient supply are additional factors that have been shown to propagate the cycle of degeneration (Cheung et al. 2009; Wang, Videman, and Battié 2012; Teraguchi et al. 2014; Boubriak et al. 2013; Urban and Roberts 2003; Urban, Smith, and Fairbank 2004).

It is estimated that every year over 500,000 Americans undergo invasive surgery, such as spinal fusion, to alleviate early and minor symptoms caused by IVD degeneration (Brodke and Ritter 2005; Rajaee et al. 2012). Although spinal fusions have been rising, this procedure fails to treat degeneration. The procedure can also lead to further health complications, limiting the spine's range of motion and the patient's mobility (Biswas, Rana, et al. 2022). The failing spinal fusion outcomes can be attributed to the deficient guidelines outlining the best strategies to treat IVD degeneration (Reisener et al. 2020a; Lam et al. 2011; Reisener et al. 2020b). These strategies are left to the surgeon's discretion, considering personal preference, skill level, procedure complexity, and the patient's condition (Reisener et al. 2020a; Lam et al. 2011; Reisener et al. 2020b).

Artificial IVDs made of various metals and polymers have emerged as an attractive alternative to treat IVD degeneration, maintaining the spine's range of motion and mobility (Biswas, Rana, et al. 2022; Biswas, Malas, et al. 2022; Yang et al. 2022; Harmon et al. 2020). Moreover, these implants have been shown to limit degeneration at nearby IVDs compared to spinal fusion (Biswas, Rana, et al. 2022; Biswas, Malas, et al. 2022). However, one of the concerns associated with IVD implants is the deterioration of the material, limiting its lifetime, and requiring a replacement surgery (BHATTACHARYA et al. 2019).

Implants of IVD allografts can thus provide an alternative to surgical strategies and implants in treating degeneration and restoring spinal function (Lam et al. 2011). However, IVD allograft accessibility for research and clinical studies is limited due to challenges in long-term storage, compromising the viability of these specimens (Lam et al. 2011). One suggestion to overcome this challenge is to establish a bank of cryopreserved IVDs, which would enable IVD size matching between donors and recipients (Lam et al. 2011). A cryopreservation bank would also improve the logistics of clinical trials and IVD research by decreasing experiment costs and accommodating experimentation schedules (Lam et al. 2011). Cryopreservation provides a solution to the long-term storage of cells and tissues by lowering the specimen's temperature to -80°C or -196°C, where cellular functions are limited and preserved (Lam et al. 2011; Jang et al. 2017). It controls exchange of ions between the intracellular and extracellular environments of the cell, controlling the rate of cell shrinkage and ion exchange. This way, cryopreservation can prevent damage to cells caused by the growth of intracellular ice crystals, the formation of extracellular ice, and changes in solute and osmotic levels (McGann, Yang, and Walterson 1988; Toner et al. 1993; Jang et al. 2017; Chang and Zhao 2021). This process has revolutionized

allograft clinical research by overcoming the increasing supply-demand imbalance for viable specimens (Aijaz et al. 2018; Bradley, Bolton, and Pedersen 2002). Multiple strategies have been optimized to manage the formation of ice crystals, including chemical techniques that rely on cryoprotectants (CPAs) (McGann, Yang, and Walterson 1988; Toner et al. 1993; Jang et al. 2017). CPAs can be divided into two categories: cell-permeable CPAs, including dimethyl sulfide (DMSO) and glycerol, preventing intracellular crystal formation (Jang et al. 2017; Bakhach 2009); cell-impermeable CPAs, including polymers and starches that protect the tissue from extracellular damage (Jang et al. 2017; Bakhach 2009).

Several cryopreservation protocols for the IVD have been developed using various CPAs and incubation times ranging from 2 to 20 hours to improve cell viability (Chan, Lam, et al. 2010; Chan, Gantenbein-Ritter, et al. 2010; Katsuura and Hukuda 1994; Xin; et al. 2013; Ishihara, Matsuzaki, and Wakabayashi 1996). To our knowledge, this is the first study to provide a novel cryopreservation method that can preserve up to 80% of the cells in the outer AF, inner AF, and NP. We developed this technique by capitalizing on the viscoelastic properties of the IVD and convective transport, speeding up CPA delivery and limiting its cytotoxic impact on the cells. We hypothesized that the compression of IVDs would decrease the transport time of the CPA, limiting toxic CPA exposure to the cells and thus increasing the number of viable cells. The methods demonstrated here should provide the research community with another tool to cryopreserve IVDs as well as other cartilage tissues with limited transport, improving experimental logistics.

4.3 Materials and methods

4.3.1 Intervertebral disc harvest and cell isolation

NP cells were isolated following a protocol adapted and modified from Wiseman et al., 2005 (Wiseman et al. 2005). Two freshly skinned skeletally mature bovine tails were obtained from a local abattoir, disinfected for five minutes in a 1% Betadine solution (RC3955, VWR International, PA), and allowed to dry in a sterile environment for ten minutes. Muscle and fat tissue were removed from each tail, exposing the IVDs. The isolated IVDs were wrapped with a sterile gauze soaked in 0.9% sodium chloride (IC102892.5, VWR International, PA) and 55 mM sodium citrate (BDH9288, VWR International, PA) while awaiting dissection.

NP tissue was removed with a scalpel, cut into ~4 mm^2 pieces, and digested in a humidified cell incubator at 37°C and 5% CO2. Digestion involved a one-hour incubation period in DMEM

(D6046, Sigma) with 0.2% Pronase E (97062-916, VWR International, PA), centrifugation at 400 RCF for 10 minutes to remove the supernatant, and incubation in Dulbecco Modified Eagle Medium (DMEM) (D6046, Sigma, MO) with 0.025% Collagenase (103701-190, VWR International, PA) for 18 hours. Digested NP tissue was filtered using a 70-µm cell strainer (CLS431751, Sigma, MO) and washed twice with 1X PBS. Cells in the filtrate were also washed twice with 1X PBS, resuspended in cell culture media solution (89% DMEM (D6046, Sigma, MO), 10% FBS (F0926, Sigma, MO), and 1% antibiotic/antimycotic solution (A5955, Sigma, MO), and seeded in monolayer cultures at their appropriate seeding density. Cells were passaged three times prior to performing cell viability assays.

4.3.2 Cell encapsulation in alginate beads

Confluent NP cells were detached from the flasks using a 0.25% trypsin solution (82003-688, VWR International). Cells were centrifuged at 400 RCF for 10 minutes then resuspended in 2% low-viscosity alginate (A0682, Sigma, MO) in 0.15M NaCl (IC102892.5, VWR International, PA) to a final density of 300,000 cells/mL. The alginate cell solution was slowly dropped into 0.15M CaCl$_2$ (C4901, Sigma, MO) using a 16G needle, incubated for 15 minutes on a rocker, washed twice with 0.15M NaCl, and incubated in cell culture media for 24 hours at 5% CO$_2$ at 37°C before performing cryopreservation toxicity test.

4.3.3 Effect of CPA mixture 1 on NP cells

NP cells were cultured in 6 well-plates to elucidate the cytotoxicity of CPA mixture 1 composed of 80% DMEM (D6046, Sigma), 10% DMSO (IC0219605590, VWR International, PA), and %10 propylene glycol (PG) (P4347, Sigma, MO). The wells were assigned randomly to incubation times of 2, 6, 12, 18, or 24 hours (n = 3) at 4°C. Cells were stained with a fluorescent LIVE/DEAD™ assay (L3224, ThermoFisher, MA) and scanned using Keyence BZ-X700 fluorescence microscope (Oregon State University, OR). The captured scans were processed on ImageJ 1.53i to estimate cell viability(Schneider, Rasband, and Eliceiri 2012).

4.3.4 Optimization of CPA mixture type

We assessed the interaction between the CPA type (CPA mixture 1 and CPA mixture 2) and incubation time on cell viability at 4°C. CPA mixture 2 included 80% DMEM (D6046, Sigma),

10% DMSO (IC0219605590, VWR International, PA), and %10 ethylene glycol (EG) (324558, Sigma, MO). Five encapsulated beads were assigned randomly to a CPA mixture type and an incubation time of 0, 2, 4, 8, or 48 hours. Cells were stained using the LIVE/DEAD™ assay (L3224, ThermoFisher, MA) and scanned with Keyence BZ-X700 (Oregon State University, OR). The captured scans were processed on ImageJ 1.53i to estimate cell viability (Schneider, Rasband, and Eliceiri 2012).

4.3.5 CPA transport in the IVD

We assessed the transport of DMSO in IVDs without compression. Three skeletally mature Black Angus bovine IVDs were incubated in 10% DMSO for three days and CT-scanned at 0, 24, 56, and 72 hours. DMSO penetration was tracked using a Toshiba Aquilion 64-slice Computed Tomography (CT) unit provided by the Carlson College of Veterinary Medicine (Oregon State University, OR). Acquisition parameters were set to 120 kVp, 240 FoV, 0.6 pitch, and 250 mA. Materialize Mimics® 21.0 was used to segment the IVD's soft tissue (AF and NP). A code was developed in MATLAB® 9.9 to perform a Gaussian curve-fitting analysis of the segmented scans, estimating the mean signal intensity (Figure 4.1).
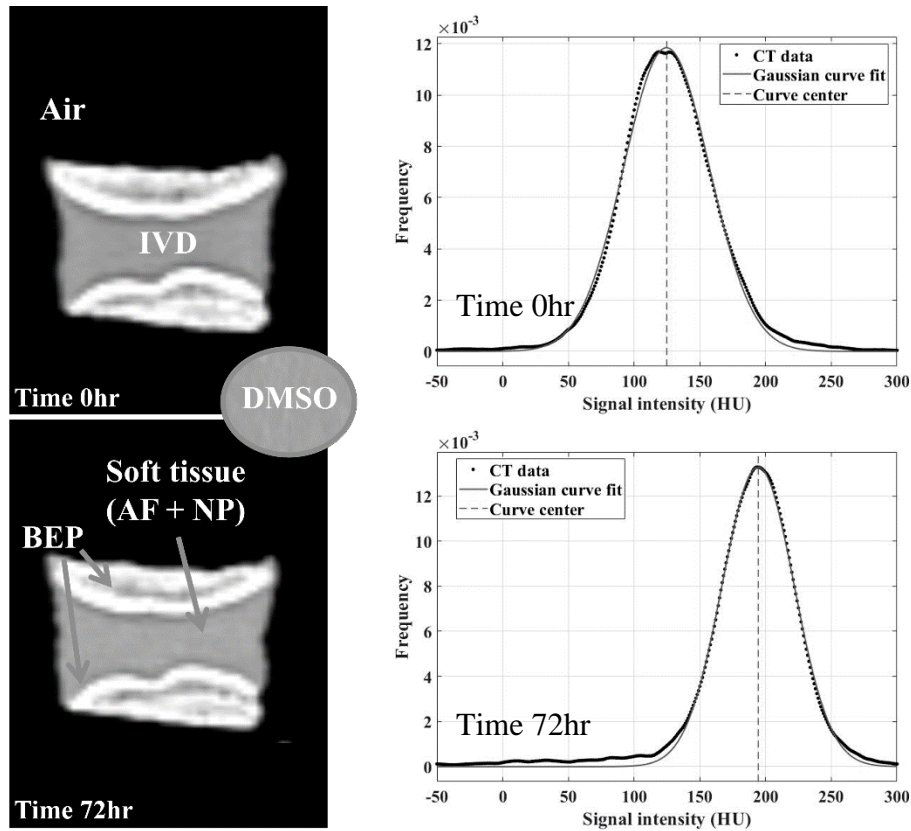
Figure 4.1. The mean signal intensity of the IVD's soft tissue increased due to the penetration of DMSO. CT scans of IVDs were segmented in Materialize Mimics® 21.0 (left), and a Gaussian curve was fitted in MATLAB® 9.9 (right) to find the mean signal intensity in the tissue.

To relate mean signal intensity to penetration % we developed the correlation in equation 4.1, in which we normalized the mean signal intensity for the sample of interest (IVD_n) to the intensities of both a fresh IVD (IVD_0) and a fully-saturated IVD (IVD_F)*.

Equation 4.2

$$\frac{IVD_n}{IVD_F} - \frac{IVD_0}{IVD_0}$$

* IVD_F was soaked in 10% DMSO for a week- CT scan showed to further increase in DMSO penetration after a week – data not shown).

We also assessed the effectiveness of PrimeGrowth™ (n = 3) and compression (n = 3) in improving the transport of DMSO and decreasing cell CPA exposure time. PrimeGrowth™ is designed to clear blood clots in the CEP, improving transport through its pores and channels (Grant

et al. 2016). Axial compression could enhance the convection transport of fluids in the IVD. IVDs treated with PrimeGrowth™ were incubated in a 30 mL Isolation Medium for one hour and rinsed in an equal volume of Neutralization Medium for two minutes (Grant et al. 2016). In a separate protocol, bovine IVDs were compressed in a custom-built bioreactor for four hours under a sine-wave load (0 MPa to 2.5 MPa at 0.1 Hz) and soaked in 10% DMSO. DMSO penetration in IVDs was tracked via CT scans compared to a control group (n = 3) soaking in 10% DMSO. CT scans were acquired at 0, 5, 8, 24, and 36 hours.

4.3.6 IVD cryopreservation

IVDs were cryopreserved using our optimized method comprised of compressing the IVDs and then allowing them to free-swell in CPA mixture 2. A total of 16 IVDs were isolated from freshly harvested bovine tails and assigned randomly to four groups: fresh, no C.C. (IVDs were frozen without CPA mixture 2 or compression), CPA (IVDs free-soaked in CPA mixture 2 without compression prior to cryopreservation), and C.C. (IVDs were compressed then free-soaked in CPA mixture 2 for 4 hours prior to cryopreservation). The IVDs were cryopreserved at -80°C with a freezing rate of -1°C/minute measured using a thermocouple. After one week of storage at -80°C, the IVDs were thawed in a warm water bath and the CPA was removed through a step-wise dilution process using compression and free-swelling. The IVDs were compressed for 4 hours in 1X PBS to achieve minimum IVD height, and then allowed to soak under no load for 3-4 hours to recover IVD height. This process was repeated until DMSO levels were not considered toxic. To ensure the dilution of DMSO (1% of initial value), we tracked osmolarity in the solution with a micro-osmometer (Advanced® Model 3320, Advanced Instruments, MA). Once the DMSO was removed, all IVDs were cultured in DMEM for12 hours, then cut in the sagittal plane to estimate cell viability.

4.3.7 Cell viability

A cross section of thickness 2 mm was acquired using a surgical blade at the sagittal center of the IVD to perform a fluorescent LIVE/DEAD™ assay (L3224, ThermoFisher, MA). The manufacturer's protocol recommended incubating tissue in the stain for 45 minutes at room temperature and rinsing the tissue with 1X PBS prior to scanning. Next, the slices were scanned

using Keyence BZ-X700 fluorescence microscope (Itasc, IL) and processed on ImageJ 1.53i to estimate cell viability in the outer AF, inner AF, and NP (Schneider, Rasband, and Eliceiri 2012).

4.4 Results

Conventional protocols for cryopreservation of IVD demonstrated the need for optimization of CPA transport to improve cell viability. The viability of NP cells decreased when exposed to CPA mixture 1 by about 95% at six hours of incubation (Figure 4.2).
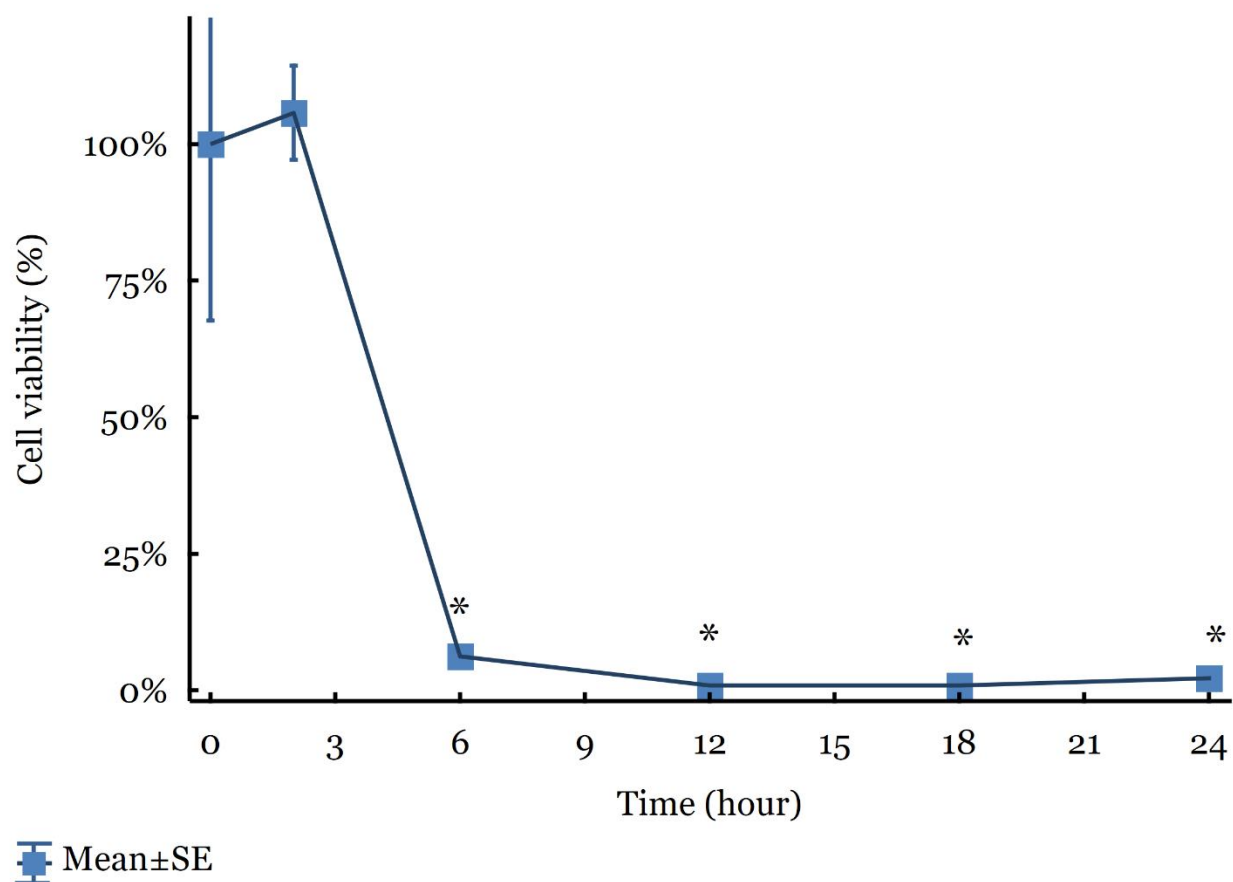
Figure 4.2. Cell viability of an NP cells in a monolayer culture exposed to CPA mixture 1 at 4°C for 24 hours (n = 3). A one-way ANOVA analysis (p < 0.01) indicated significant difference in mean cell viability % between time 0 and all times greater than or equal to 6 hours. No significant difference was observed in mean cell viability % between time 0 and 3 hours.

DMSO attenuates CT beam intensity and thus can be used to track its penetration through the IVD's soft tissue. It was observed in a free swelling IVD without compression that DMSO

achieved a 50% saturation level after 24 hours increasing to 75% by 72 hours of incubation. The observed rate of DMSO penetration would lead to total cell death in the IVD before reaching a 100% saturation state (Figure 4.3).
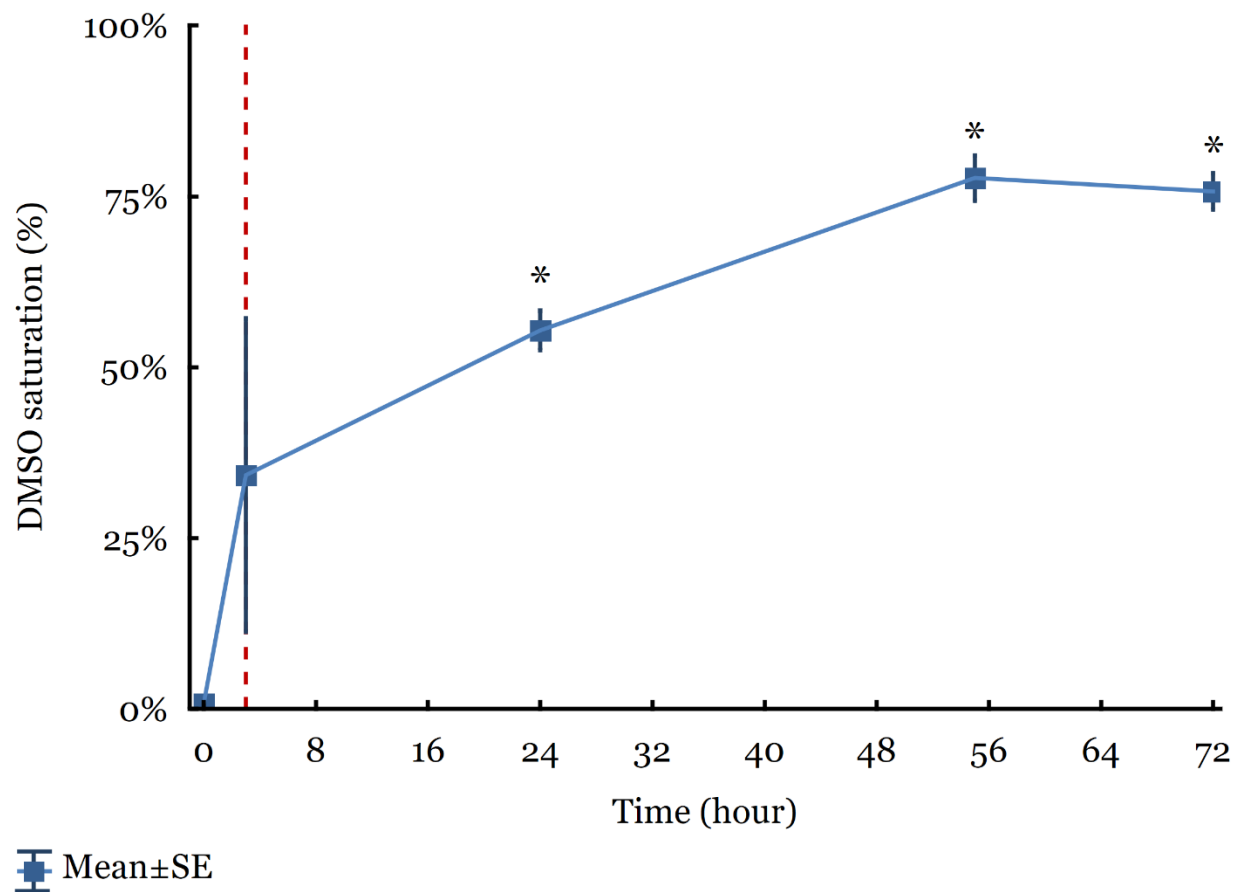
Figure 4.3. Average DMSO penetration % in free-swelling IVDs (n = 3). Mean DMSO penetration % in the IVD's soft tissue was significantly different after 24 hours of incubation compared to time 0 (one-way ANOVA, $p < 0.05$). The data was normalized to IVDs that had soaked in 10% DMSO for one week. The dashed line shows the time at which significant cell death was observed in the cell culture cytotoxicity experiment (Figure 4.2).

Optimization of CPA type required finding a CPA with lower cytotoxic effects compared to PG, which was observed to be devastating for cell viability in a monolayer cell culture (Figure 4.2). CPA mixture 2, which replaced PG with EG, showed to decrease the CPA mixture's cytotoxicity and improve overall cell viability for 8 hours (Figure 4.4)
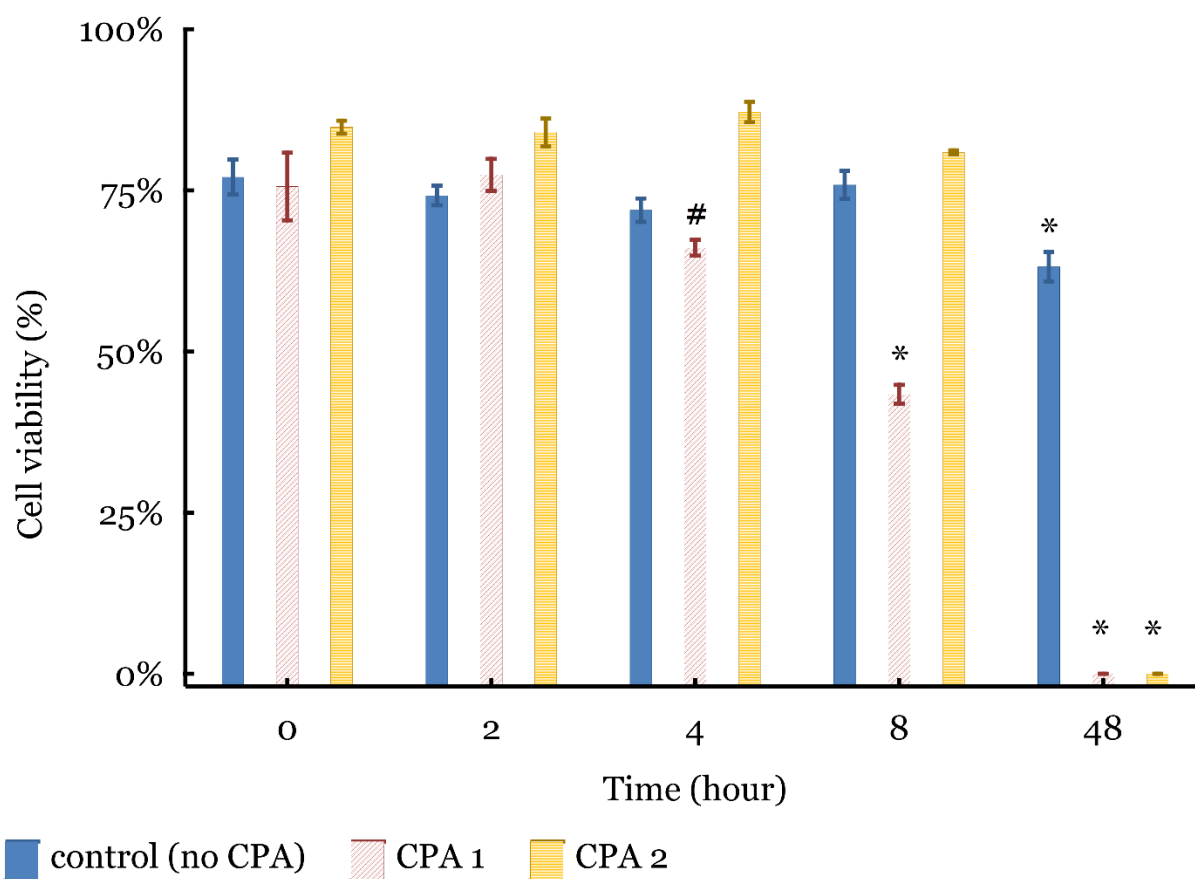
Figure 4.4. The effect of CPA type and incubation time on the average NP viability encapsulated in alginate. Cells exposed to CPA mixture 1 observed a decreasing viability at 4 hours compared to the control at time 0. CPA mixture 2 was not observed to affect cell viability at 8 hours of incubation. At 48 hours, cell viability was estimated to be 0% for both CPA groups. Significance was estimated by comparing the samples with the control at time 0 with # indicating $p < 0.05$ and * indicating $p < 0.001$ (Factorial ANOVA).

Next, the rate at which DMSO penetrated through the IVD was still slow when compared to the rate at which cell viability was lost. It required 72 hours for DMSO to reach a 75% level of penetration, while most cells stayed viable only until 8 hours of incubation time. Compression and PrimeGrowth™ were hypothesized to decrease the overall time it required DMSO to fully saturate the IVD's tissue. The results demonstrated compression to be superior to PrimeGrowth™, decreasing the time it required DMSO to fully saturate the disc to 3 hours, a 96% improvement (Figure 4.5). In contrast, PrimeGrowth™ showed no detectable improvement to DMSO transport (Figure 4.5).
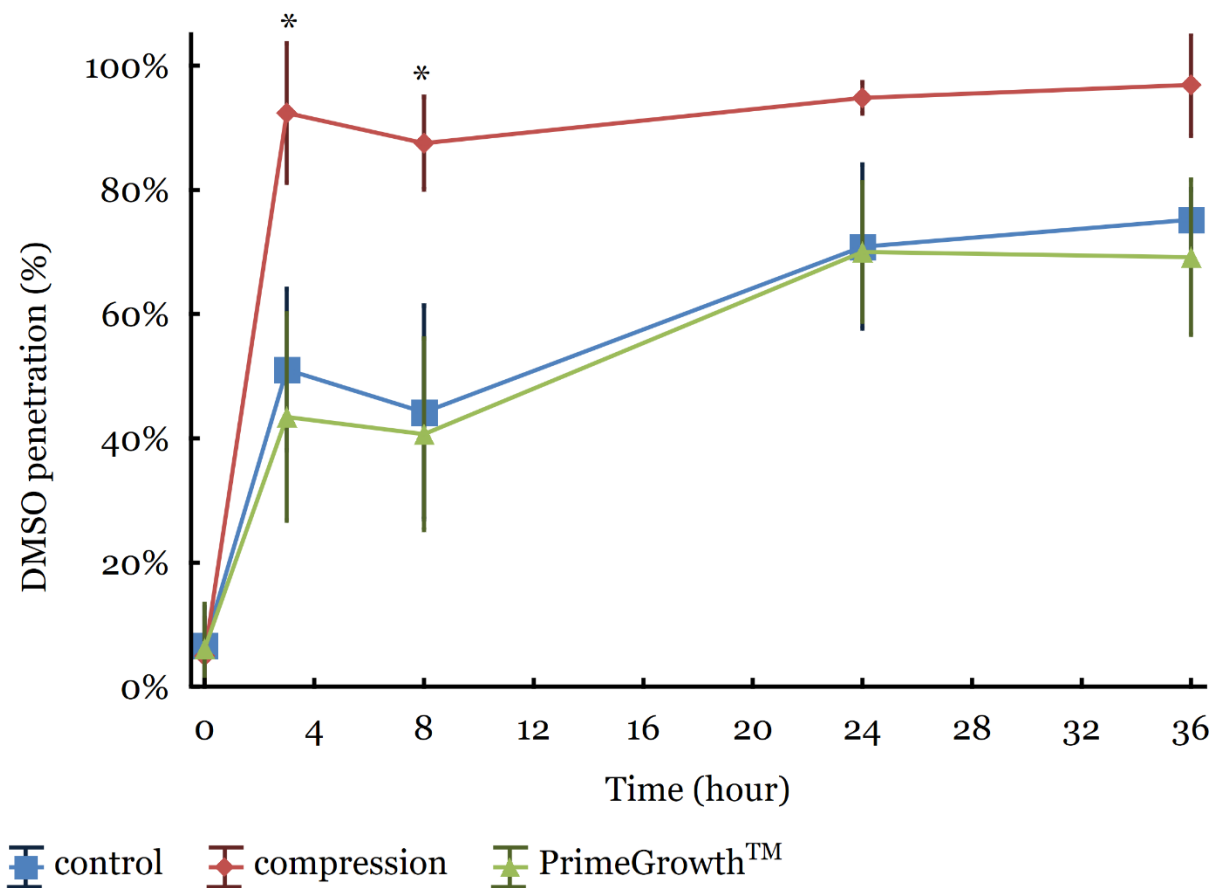
Figure 4.5. Optimization of DMSO penetration % in IVDs (n = 3). Compression increased DMSO penetration to 97% compared to the control at 3 hours. IVDs treated with PrimeGrowth™ did not observe improved transport when compared to the control at each time point (Factorial ANOVA, $p < 0.05$). DMSO penetration % was normalized to three fully equilibrated IVDs.

Scans of LIVE/DEAD™ assay from frozen compressed IVDs in CPA mixture 2 showed a significant difference in the number of viable cells and their distribution in the tissue. We also observed cell death in the areas that were sliced by the scalpel (Figure 4.6).
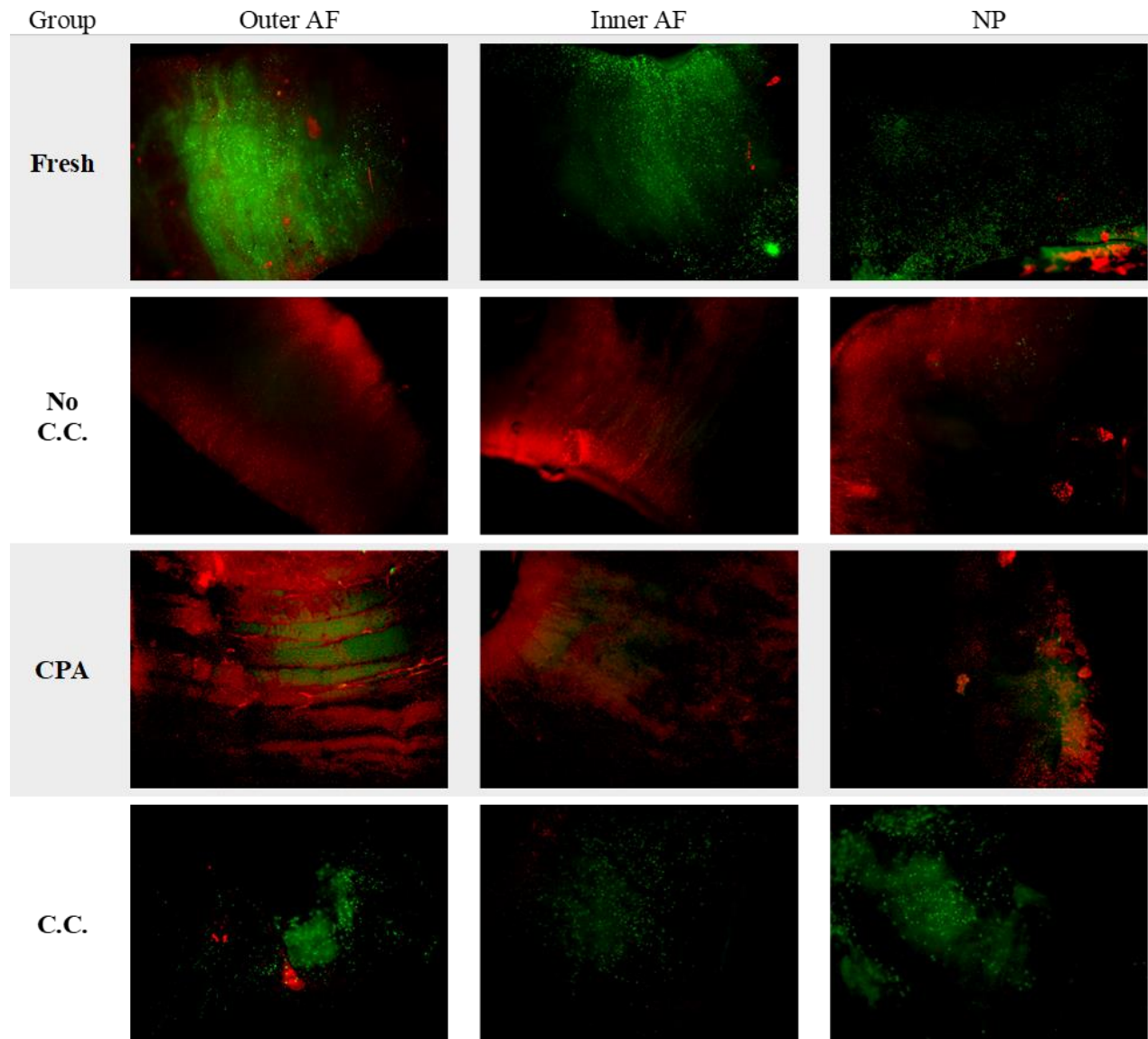
Figure 4.6. A representative sample of cell viability fluorescent scans.

Cell viability was measured in the sagittal plane for al cryopreserved IVDs and compared with a fresh sample. IVDs in treatment groups no C.C. and CPA only showed a ~5% mean viable cells. IVDs in C.C. group, which were compressed in a custom-built bioreactor to improve transport of CPA mixture 2, had an average of 80-85% viable cells (Figure 4.7), which was not significantly different from the fresh unfrozen controls.
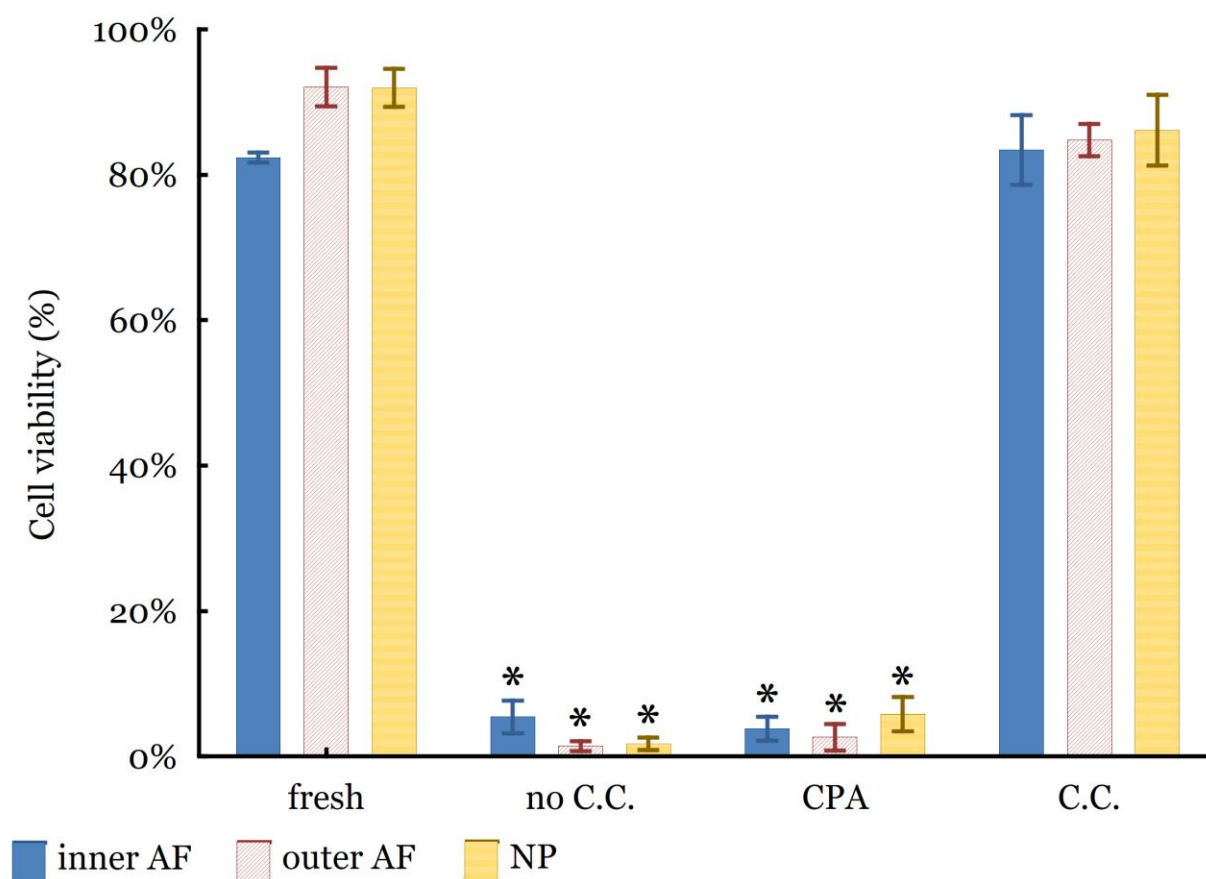
Figure 4.7. Mean cell viability in cryopreserved samples (n = 4) was improved with compression optimizing transport of DMSO into the IVD. Prior to cryopreservation, IVDs were treated with no compression or CPA mixture 2 (no C.C.), with CPA mixture 2 only (CPA), and with compression and CPA mixture 2 (C.C.). Mean cell viability was estimated from sagittal slices and compared against the slices taken from the fresh samples. Significance was denoted by an * comparing treatment groups with the fresh control (factorial ANOVA, $p < 0.05$).

4.5 Discussion

In this study, we innovated a new method to cryopreserve intact bovine IVDs maintaining up to 80% cell viability in all tissue compartments: the outer AF, inner AF, and NP (Figure 4.7). Previous cryopreservation protocols failed to maintain cell viability due to limitations in CPA cytotoxicity and IVD transport.

The first limitation constituted long exposure times to the cytotoxic CPA, leading to DNA damage and apoptosis (Sugishita et al. 2021). IVD cells are vulnerable to CPA-induced osmotic changes instigating apoptotic pathways, accumulating DNA damage, and compromising the

membrane's integrity (Gao et al. 1993; Xu et al. 2010; Sugishita et al. 2021). Our results demonstrated complete cell death after six hours in the monolayer culture and poor cell viability in the alginate beads at eight hours, reflecting results obtained by other researchers (Chan, Gantenbein-Ritter, et al. 2010). We compared literature cytotoxicity values for various CPA cocktails, including DMSO, ethylene glycol (EG), glycerol, and propylene glycol (PG). Interestingly, DMSO alone is highly toxic at low concentrations of 0.5 to 8.0%, upregulating interleukin-6 and increasing reactive oxygen species (Awan et al. 2020). However, it is thought that mixing DMSO with other CPAs could reduce its concentration in the solution, and thus decease its devastating effects on the cells (Awan et al. 2020; Jomha et al. 2010). This study reported better cell viability numbers when DMSO was mixed with EG compared to PG (Figure 4.4).

It was essential to optimize the transport of the CPA to improve cryopreservation of the IVD (Bernemann et al. 2010). X-ray computer tomography (CT) was adopted to track DMSO permeation in the IVD (Bernemann et al. 2010). Unsurprisingly, we observed a slow permeation rate reaching an equilibrium with the surrounding solution after 72 hours (Figure 4.3). These results suggested that commonly practiced incubation times ranging between 2 to 20 hours were insufficient for CPA to fully penetrate the disc and prevent cryoinjury (Chan, Lam, et al. 2010; Chan, Gantenbein-Ritter, et al. 2010; Katsuura and Hukuda 1994; Xin; et al. 2013; Ishihara, Matsuzaki, and Wakabayashi 1996; Lawson, Ahmad, and Sambanis 2011).

We compared two methods to improve transport in the IVD by (1) clearing transport pathways in the CEPs using PrimeGrowth™ and (2) capitalizing on convective transport through compression. PrimeGrowth™ is a proprietary solution that dissolves blood clots in the porous CEP post IVD harvest, improving solute transport (Grant et al. 2016). Our results showed that the PrimeGrowth™ treatment failed to improve DMSO permeation (Figure 4.5). Due to the protected nature of the product, we were unable to infer the factors behind our negative results. Compressing the IVD provided superior outcomes decreasing the required transport time by 95% on average to achieve full penetration (Figure 4.5). With this technique, we capitalized on the viscoelastic properties of the IVD. Compression works by decreasing the IVD's height, pushing out the water and other solutes, and decreasing the internal pressure (Bezci and O'Connell 2018). When the IVD free-swells, it retracts, forcing the dissolved DMSO to flow into the tissue at a faster rate. With

this method, we accomplished ~90% DMSO penetration in 3-4 hours, preventing cytotoxic and cryogenic injury (Figure 4.6).

IVD transport has been of interest to many research groups looking to enhance its nutrient status. Many of these studies reported limited transport in the IVD due to its geometry, creating a solute gradient (Nachemson et al. 1970; Malcolmson 1935; Bush 1934; Albert 1942; Shutkin 1952; Shalash et al. 2021). It is possible that in our study, a DMSO gradient existed but was not captured with our limited x-ray capabilities, loading the outer AF with higher DMSO % compared to the inner AF and NP. This gradient could expose the outer AF to increased osmotic pressure leading to cell injury. In contrast, it could also be possible that the NP was the first compartment to be thoroughly permeated because it shares a larger surface area with the CEP, where most molecular transport takes place through the thin, porous layers of the CEP (Naylor 1951; Yin et al. 2019; Naresh-Babu et al. 2016; Wong et al. 2019; Nachemson et al. 1970; Roberts, Menage, and Urban 1989; Ogata and Whiteside 1981; Nguyen-minh et al. 1998; Urban et al. 1977; Silverman 1954; Urban, Holm, and Maroudas 1978; Albert 1942; Naylor, Happey, and Macrae 1955; King 1959; Urban and Maroudas 1979). Our previously published finite element model study on molecular transport in the IVD demonstrated the importance of the CEP in facilitating transport, showing high solute flux going through the NP and inner AF compared to the outer AF (Shalash et al. 2021). Therefore, it is advantageous to elucidate the main pathways for transport, including the first compartments to equilibrate with the IVD's environment to accomplish homogeneous DMSO permeation and better manage cryoinjury (Lawson, Ahmad, and Sambanis 2011).

Despite the rewarding results of this study, it comes with its limitations. First, it is essential to study the factors affecting CPA transport in the IVD to understand better how the time required to load and remove the CPA would change from one species to another. Factors such as IVD size, extracellular matrix composition, and bone density have varied between species and affect transport (Shalash et al. 2021; Aerssens et al. 1998; Alini et al. 2008; Showalter et al. 2012). In addition, this study lacked critical analyses on cell phenotype, morphology, gene expression, and protein levels which can be impacted due to cryopreservation (Gao et al. 1993; Xu et al. 2010; Sugishita et al. 2021). Last, we suggest conducting a long-term experiment on human specimens to investigate the effects of cryopreservation on its mechanical properties.

Despite the limitations of this study, we successfully improved cell viability in cryopreserved bovine IVDs. An important application of our results is creating an intact human

IVD tissue bank that will improve access to viable specimens. This method will allow research groups to obtain any number of IVDs, improve experimental schedules, reduce materials costs, and provide an alternative to animal models. An IVD tissue bank would also improve the logistics of clinical trials by providing physicians with ample time to match donor IVDs with the proper recipients (Lam et al. 2011). We anticipate that this method will change how we do cryopreservation leading to further breakthroughs in IVD research.

4.6 Conclusion

In this study we described an innovative method to improve IVD cryopreservation through compression. Bovine IVDs were cryopreserved in a 10% DMSO-10% ethylene glycol over one week. Cell viability was measured in the sagittal plane averaging 80%-85% in the outer AF, inner AF, and NP. We demonstrated how incorporating convective transport and a low-cytotoxic CPA was important in preventing cryoinjury to IVD cell, leading the way to better optimization of IVD cryopreservation to improve clinical research.

4.7 acknowledgements

4.7 References

Aerssens, Jeroen, Steven Boonen, Geert Lowet, and Jan Dequeker. 1998. 'Interspecies Differences in Bone Composition, Density, and Quality: Potential Implications for in Vivo Bone Research*', *Endocrinology*, 139: 663-70.

Aijaz, A., M. Li, D. Smith, D. Khong, C. LeBlon, O. S. Fenton, R. M. Olabisi, S. Libutti, J. Tischfield, M. V. Maus, R. Deans, R. N. Barcia, D. G. Anderson, J. Ritz, R. Preti, and B. Parekkadan. 2018. 'Biomanufacturing for clinically advanced cell therapies', *Nat Biomed Eng*, 2: 362-76.

Albert, M. 1942. 'Calcification of the Intervertebral Disks', *Br Med J*, 1: 666-8.

Alini, Mauro, Stephen M. Eisenstein, Keita Ito, Christopher Little, A. Annette Kettler, Koichi Masuda, James Melrose, Jim Ralphs, Ian Stokes, and Hans Joachim Wilke. 2008. 'Are animal models useful for studying human disc disorders/degeneration?', *European Spine Journal*, 17: 2-19.

Andersson, G. B. 1999. 'Epidemiological features of chronic low-back pain', *Lancet*, 354: 581-5.

Awan, Maooz, Iryna Buriak, Roland Fleck, Barry Fuller, Anatoliy Goltsev, Julie Kerby, Mark Lowdell, Pavel Mericka, Alexander Petrenko, Yuri Petrenko, Olena Rogulska, Alexandra Stolzing, and Glyn N Stacey. 2020. 'Dimethyl sulfoxide: a central player since the dawn of cryobiology, is efficacy balanced by toxicity?', *Regenerative Medicine*, 15: 1463-91.

Bakhach, Joseph. 2009. 'The cryopreservation of composite tissues', *Organogenesis*, 5: 119-26.

Bernemann, I., N. Manuchehrabadi, R. Spindler, J. Choi, W. F. Wolkers, J. C. Bischof, and B. Glasmacher. 2010. 'Diffusion of dimethyl sulfoxide in tissue engineered collagen scaffolds visualized by computer tomography', *Cryo Letters*, 31: 493-503.

Bezci, Semih E., and Grace D. O'Connell. 2018. 'Osmotic Pressure Alters Time-dependent Recovery Behavior of the Intervertebral Disc', *Spine*, 43: E334-E40.

BHATTACHARYA, SHAMBO, SANDIPAN ROY, MASUD RANA, SREERUP BANERJEE, SANTANU KUMAR KARMAKAR, and JAYANTA KUMAR BISWAS. 2019. 'BIOMECHANICAL PERFORMANCE OF A MODIFIED DESIGN OF DYNAMIC CERVICAL IMPLANT COMPARED TO CONVENTIONAL BALL AND SOCKET DESIGN OF AN ARTIFICIAL INTERVERTEBRAL DISC IMPLANT: A FINITE ELEMENT STUDY', *Journal of Mechanics in Medicine and Biology*, 19: 1950017.

Biswas, Jayanta Kumar, Anindya Malas, Sourav Majumdar, and Masud Rana. 2022. 'A comparative finite element analysis of artificial intervertebral disc replacement and pedicle screw fixation of the lumbar spine', *Computer Methods in Biomechanics and Biomedical Engineering*: 1-9.

Biswas, Jayanta Kumar, Masud Rana, Anindya Malas, Sandipan Roy, Subhomoy Chatterjee, and Sandeep Choudhury. 2022. 'Effect of single and multilevel artificial inter-vertebral disc replacement in lumbar spine: A finite element study', *The International Journal of Artificial Organs*, 45: 193-99.

Boubriak, Olga. A., Natasha Watson, Sarit. S. Sivan, Naomi Stubbens, and Jill P. G. Urban. 2013. 'Factors regulating viable cell density in the intervertebral disc: blood supply in relation to disc height', *Journal of Anatomy*, 222: 341-48.

Bradley, J. A., E. M. Bolton, and R. A. Pedersen. 2002. 'Stem cell medicine encounters the immune system', *Nat Rev Immunol*, 2: 859-71.

Brodke, D. S., and S. M. Ritter. 2005. 'Nonsurgical management of low back pain and lumbar disk degeneration', *Instr Course Lect*, 54: 279-86.

Bush, G. B. 1934. 'The Clinical Importance of the Intervertebral Discs, with Special Reference to Nuclear Prolapses', *Bristol Med Chir J (1883)*, 51: 173-82.

Chan, S. C., S. Lam, V. Y. Leung, D. Chan, K. D. Luk, and K. M. Cheung. 2010. 'Minimizing cryopreservation-induced loss of disc cell activity for storage of whole intervertebral discs', *Eur Cell Mater*, 19: 273-83.

Chan, Samantha C. W., Benjamin Gantenbein-Ritter, Victor Y. L. Leung, Danny Chan, Kenneth M. C. Cheung, and Keita Ito. 2010. 'Cryopreserved intervertebral disc with injected bone marrow–derived stromal cells: a feasibility study using organ culture', *The Spine Journal*, 10: 486-96.

Chang, Tie, and Gang Zhao. 2021. 'Ice Inhibition for Cryopreservation: Materials, Strategies, and Challenges', *Advanced Science*, 8: 2002425.

Cheung, Kenneth M. C., Jaro Karppinen, Danny Chan, Daniel W. H. Ho, You-Qiang Song, Pak Sham, Kathryn S. E. Cheah, John C. Y. Leong, and Keith D. K. Luk. 2009. 'Prevalence and Pattern of Lumbar Magnetic Resonance Imaging Changes in a Population Study of One Thousand Forty-Three Individuals', *Spine*, 34: 934-40.

Gao, D. Y., E. Ashworth, P. F. Watson, F. W. Kleinhans, P. Mazur, and J. K. Critser. 1993. 'Hyperosmotic Tolerance of Human Spermatozoa: Separate Effects of Glycerol, Sodium Chloride, and Sucrose on Spermolysis1', *Biology of Reproduction*, 49: 112-23.

Grant, Michael, Laura Epure, Omar Salem, Motaz Alaqeel, John Antoniou, and Fackson Mwale. 2016. 'Development of a Whole Bovine Long-term Organ Culture System that Retains Vertebral Bone for Intervertebral Disc Repair and Biomechanical Studies using PrimeGrowth Media', *Global Spine Journal*, 6: s-0036-1582897-s-0036-97.

Harmon, M. D., D. M. Ramos, D. Nithyadevi, R. Bordett, S. Rudraiah, S. P. Nukavarapu, I. L. Moss, and S. G. Kumbar. 2020. 'Growing a backbone - functional biomaterials and structures for intervertebral disc (IVD) repair and regeneration: challenges, innovations, and future directions', *Biomater Sci*, 8: 1216-39.

Ishihara, Kazuhiro, Hiromi Matsuzaki, and Ken Wakabayashi. 1996. 'Cryopreserved intervertebral disc allografts in dogs: Chronological changes in 3-year period after transplantation', *Journal of Orthopaedic Science*, 1: 259-67.

Jang, T. H., S. C. Park, J. H. Yang, J. Y. Kim, J. H. Seok, U. S. Park, C. W. Choi, S. R. Lee, and J. Han. 2017. 'Cryopreservation and its clinical applications', *Integr Med Res*, 6: 12-18.

Jomha, Nadr M., Andrew D. H. Weiss, J. Fraser Forbes, Garson K. Law, Janet A. W. Elliott, and Locksley E. McGann. 2010. 'Cryoprotectant agent toxicity in porcine articular chondrocytes', *Cryobiology*, 61: 297-302.

Katsuura, A., and S. Hukuda. 1994. 'Experimental study of intervertebral disc allografting in the dog', *Spine*, 19: 2426-32.

King, T. 1959. 'Another look at the problem of lumbo-sacral pain and sciatica', *Med J Aust*, 46: 8-12.

Lam, S. K., S. C. Chan, V. Y. Leung, W. W. Lu, K. M. Cheung, and K. D. Luk. 2011. 'The role of cryopreservation in the biomechanical properties of the intervertebral disc', *Eur Cell Mater*, 22: 393-402.

Lawson, A., H. Ahmad, and A. Sambanis. 2011. 'Cytotoxicity effects of cryoprotectants as single-component and cocktail vitrification solutions', *Cryobiology*, 62: 115-22.

Malcolmson, P. H. 1935. 'Radiologic Study of the Development of the Spine and Pathologic Changes of the Intervertebral Disc', *Radiology*, 25: 98-104.

McGann, L. E., H. Y. Yang, and M. Walterson. 1988. 'Manifestations of cell damage after freezing and thawing', *Cryobiology*, 25: 178-85.

Nachemson, A., T. Lewin, A. Maroudas, and M. A. Freeman. 1970. 'In vitro diffusion of dye through the end-plates and the annulus fibrosus of human lumbar inter-vertebral discs', *Acta Orthop Scand*, 41: 589-607.

Naresh-Babu, J., G. Neelima, S. Reshma Begum, and V. Siva-Leela. 2016. 'Diffusion characteristics of human annulus fibrosus-a study documenting the dependence of annulus fibrosus on end plate for diffusion', *Spine J*, 16: 1007-14.

Naylor, A. 1951. 'Brachial neuritis, with particular reference to lesions of the cervical intervertebral discs', *Ann R Coll Surg Engl*, 9: 158-88.

Naylor, A., F. Happey, and T. Macrae. 1955. 'Changes in the human intervertebral disc with age: a biophysical study', *J Am Geriatr Soc*, 3: 964-73.

Nguyen-minh, C, V M Haughton, R A Papke, H An, and S C Censky. 1998. 'Measuring diffusion of solutes into intervertebral disks with MR imaging and paramagnetic contrast medium', *American Journal of Neuroradiology*, 19: 1781-84.

Ogata, K., and L. A. Whiteside. 1981. '1980 Volvo award winner in basic science. Nutritional pathways of the intervertebral disc. An experimental study using hydrogen washout technique', *Spine*, 6: 211-16.

Rajaee, Sean S., Hyun W. Bae, Linda E. A. Kanim, and Rick B. Delamarter. 2012. 'Spinal fusion in the United States: analysis of trends from 1998 to 2008', *Spine*, 37: 67-76.

Reisener, Marie-Jacqueline, Matthias Pumberger, Jennifer Shue, Federico P. Girardi, and Alexander P. Hughes. 2020a. 'Trends in lumbar spinal fusion-a literature review', *Journal of spine surgery (Hong Kong)*, 6: 752-61.

Reisener, Marie-Jacqueline;, Matthias; Pumberger, Jennifer; Shue, Federico P.; Girardi, and Alexander P.; Hughes. 2020b. 'Trends in lumbar spinal fusion—a literature review', *Journal of Spine Surgery*, 6: 752-61.

Roberts, S., J. Menage, and J. P. Urban. 1989. 'Biochemical and structural properties of the cartilage end-plate and its relation to the intervertebral disc', *Spine*, 14: 166-74.

Schneider, Caroline A., Wayne S. Rasband, and Kevin W. Eliceiri. 2012. 'NIH Image to ImageJ: 25 years of image analysis', *Nature Methods*, 9: 671-75.

Shalash, Ward, Sonia R. Ahrens, Liudmila A. Bardonova, Vadim A. Byvaltsev, and Morgan B. Giers. 2021. 'Patient-specific apparent diffusion maps used to model nutrient availability in degenerated intervertebral discs', *JOR spine*, 4: e1179-e79.

Showalter, Brent L., Jesse C. Beckstein, John T. Martin, Elizabeth E. Beattie, Alejandro A. Espinoza Orías, Thomas P. Schaer, Edward J. Vresilovic, and Dawn M. Elliott. 2012. 'Comparison of animal discs used in disc research to human lumbar disc: torsion mechanics and collagen content', *Spine*, 37: E900-E07.

Shutkin, N. M. 1952. 'Syndrome of the degenerated intervertebral disc', *Am J Surg*, 84: 162-71.

Silverman, F. N. 1954. 'Calcification of the intervertebral disks in childhood', *Radiology*, 62: 801-16.

Sugishita, Yodo, Lingbo Meng, Yuki Suzuki-Takahashi, Sandy Nishimura, Sayako Furuyama, Atsushi Uekawa, Akiko Tozawa-Ono, Junko Migitaka-Igarashi, Tomoe Koizumi, Hibiki Seino, Yasunori Natsuki, Manabu Kubota, Junki Koike, Keisuke Edashige, and Nao Suzuki. 2021. 'Quantification of residual cryoprotectants and cytotoxicity in thawed bovine ovarian tissues after slow freezing or vitrification', *Human Reproduction*, 37: 522-33.

Teraguchi, M., N. Yoshimura, H. Hashizume, S. Muraki, H. Yamada, A. Minamide, H. Oka, Y. Ishimoto, K. Nagata, R. Kagotani, N. Takiguchi, T. Akune, H. Kawaguchi, K. Nakamura, and M. Yoshida. 2014. 'Prevalence and distribution of intervertebral disc degeneration over the entire spine in a population-based cohort: the Wakayama Spine Study', *Osteoarthritis and Cartilage*, 22: 104-10.

Toner, M., E. G. Cravalho, J. Stachecki, T. Fitzgerald, R. G. Tompkins, M. L. Yarmush, and D. R. Armant. 1993. 'Nonequilibrium freezing of one-cell mouse embryos. Membrane integrity and developmental potential', *Biophys J*, 64: 1908-21.

Urban, J. P. G., and A. Maroudas. 1979. 'The measurement of fixed charged density in the intervertebral disc', *Biochimica et Biophysica Acta (BBA) - General Subjects*, 586: 166-78.

Urban, J. P., S. Holm, and A. Maroudas. 1978. 'Diffusion of small solutes into the intervertebral disc: as in vivo study', *Biorheology*, 15: 203-21.

Urban, J. P., S. Holm, A. Maroudas, and A. Nachemson. 1977. 'Nutrition of the intervertebral disk. An in vivo study of solute transport', *Clinical orthopaedics and related research*: 101-14.

Urban, J. P., S. Smith, and J. C. Fairbank. 2004. 'Nutrition of the intervertebral disc', *Spine*, 29: 2700-9.

Urban, Jill P. G., and Sally Roberts. 2003. 'Degeneration of the intervertebral disc', *Arthritis Res Ther*, 5: 120.

Wang, Yue, Tapio Videman, and Michele C. Battié. 2012. 'ISSLS Prize Winner: Lumbar Vertebral Endplate Lesions: Associations With Disc Degeneration and Back Pain History', *Spine*, 37: 1490-96.

Wiseman, M. A., H. L. Birch, M. Akmal, and A. E. Goodship. 2005. 'Segmental variation in the in vitro cell metabolism of nucleus pulposus cells isolated from a series of bovine caudal intervertebral discs', *Spine*, 30: 505-11.

Wong, J., S. L. Sampson, H. Bell-Briones, A. Ouyang, A. A. Lazar, J. C. Lotz, and A. J. Fields. 2019. 'Nutrient supply and nucleus pulposus cell function: effects of the transport properties of the cartilage endplate and potential implications for intradiscal biologic therapy', *Osteoarthritis Cartilage*, 27: 956-64.

Xin;, Hongkui, Chao Zhang;, Zhiyuan Shi; Deli Wang, Chaofeng Wang; Tao Gu, Jianhong Wu;, Yan Zhang;, Qing He;, and Dike Ruan;. 2013. 'Tissue-Engineered Allograft Intervertebral Disc Transplantation for the Treatment of Degenerative Disc Disease: Experimental Study in a Beagle Model', *Tissue Engineering Part A*, 19: 143-51.

Xu, X., J. P. G. Urban, U. K. Tirlapur, and Z. Cui. 2010. 'Osmolarity effects on bovine articular chondrocytes during three-dimensional culture in alginate beads', *Osteoarthritis and Cartilage*, 18: 433-39.

Yang, Mengying, Dingding Xiang, Yuru Chen, Yangyang Cui, Song Wang, and Weiqiang Liu. 2022. 'An Artificial PVA-BC Composite That Mimics the Biomechanical Properties and Structure of a Natural Intervertebral Disc', *Materials*, 15: 1481.

Yin, Si, Heng Du, Weigong Zhao, Shaohui Ma, Ming Zhang, Min Guan, and Miao Liu. 2019. 'Inhibition of both endplate nutritional pathways results in intervertebral disc degeneration in a goat model', *Journal of Orthopaedic Surgery and Research*, 14: 138.

Chapter 5 – Patient-Specific Apparent Diffusion Maps Used to Model Nutrient Availability in Degenerated Intervertebral Discs

Ward Shalash[1], Sonia R. Ahrens[1], Liudmila A. Bardonova[1,2], Vadim A. Byvaltsev [2,3], Morgan B. Giers[1,*]

[1] School of Chemical, Biological and Environmental Engineering, Oregon State University

Corvallis, OR 97331

[2] Irkutsk State Medical University

Irkutsk, 664003, Russia

[3] Railway Clinical Hospital at the Irkutsk-Passazhirsky Station

Irkutsk, 664005, Russia

5.1 Abstract

In this study, magnetic resonance imaging data was used to (1) model IVD-specific gradients of glucose, oxygen, lactate, and pH; and (2) investigate possible effects of covariate factors (i.e., disc geometry, and mean apparent diffusion coefficient values) on the IVD's microenvironment. Mathematical modeling of the patient's specific IVD microenvironment could be important when selecting patients for stem cell therapy due to the increased nutrient demand created by that treatment. Disc geometry and water diffusion coefficients were extracted from MRIs of 37 patients using sagittal $T_{1\text{-weighted}}$ images, $T_{2\text{-weighted}}$ images, and ADC Maps. A 2-D steady state finite element mathematical model was developed in COMSOL Multiphysics® 5.4 to compute concentration maps of glucose, oxygen, lactate and pH. Concentration of nutrients (i.e., glucose, and oxygen) dropped with increasing distance from the cartilaginous endplates (CEP), whereas acidity levels increased. Most discs experienced poor nutrient levels along with high acidity values in the inner annulus fibrosus (AF). The disc's physiological microenvironment became more deficient as degeneration progressed. For example, minimum glucose concentration in grade 4 dropped by 31.1% compared to grade 3 ($p < 0.0001$). The model further suggested a strong effect of the following parameters: disc size, AF and CEP diffusivities, metabolic reactions, and cell density on solute concentrations in the disc ($p < 0.05$). The significance of this work implies that the individual morphology and physiological conditions of each disc, even among discs of the same Pfirrmann grade, should be evaluated when modeling IVD solute concentrations.

5.2 Introduction

Back pain is the leading cause of disability worldwide, causing a significant socioeconomic impact (Hoy et al. 2014). A source of back pain can be the degeneration of the intervertebral disc (IVD), allowing nerve ingrowth, facet joint arthritis, and disc bulging or osteophyte formations that press on nearby nerve roots or the spinal cord (Brinjikji et al. 2015; Ohtori et al. 2015). Animal and human studies have shown promising potential for cell injections to restore IVD health. In a pilot study performed on 14 patients, chondrocyte injections demonstrated the ability to maintain disc height and hydration level (Meisel et al. 2006a; Richardson et al. 2016). The results showed a significant reduction in the disability index in treated patients two years post discectomy (Meisel et al. 2006a; Richardson et al. 2016). Introducing disc cells into the annulus fibrosus (AF) and nucleus pulposus (NP) of animal models maintained the demarcation between the AF and the NP. They also delayed the degeneration process of the IVD by increasing the remodeling of the extracellular matrix (ECM) (Nomura et al. 2001; Okuma et al. 2000; Sato et al. 2003). Studies assessing the viability of transplanted cells showed good cellular viability and proliferation rates after treatment (Bertram et al. 2005; Sato et al. 2003). In rabbit models, transplanted human NP cells increased disc height, the expression of aggrecan, and type II collagen (Iwashina et al. 2006). The results of these studies implied good integration of injected cells into the disc's environment, which demonstrated the promising potential in using cell therapy to regenerate the disc (Nomura et al. 2001; Okuma et al. 2000; Sato et al. 2003; Watanabe et al. 2003; Bertram et al. 2005; Iwashina et al. 2006; Meisel et al. 2006a).

There are, however, limitations to relying on cell therapy to restore the IVD due to the morphological and biochemical changes attributed to IVD degeneration. First, degenerated IVDs suffer from a loss in their proteoglycan content, leading to IVD dehydration. Bulk water content is critical for IVD health as it contributes to molecular transport and the IVD's biomechanics (Andersson 1999; Huang, Urban, and Luk 2014). Second, structural changes of the AF and the cartilaginous endplates (CEP) limit molecular transport through the IVD (Andersson 1999; Huang, Urban, and Luk 2014). Lastly, degeneration of the IVD leads to changes in the NP's ECM that altered diffusion kinetics of solutes through the IVD (Gullbrand, Peterson, Ahlborn, et al. 2015; Kuo et al. 2014; Byvaltsev et al. 2017). As a result of the changes in IVD biology, diffusion rates decrease dramatically, leading to poor nutrition (i.e., glucose and oxygen), high acidity, and high cell death (Bibby and Urban 2004; Ishihara and Urban 1999; Junger et al. 2009; Giers et al. 2018;

Noriega et al. 2017; Orozco et al. 2011; Sakai and Andersson 2015; Shirazi-Adl, Taheri, and Urban 2010; Grunhagen et al. 2011; Ferguson, Ito, and Nolte 2004; Belykh et al. 2017; Sampson, Sylvia, and Fields 2019; Wong et al. 2019; Wu et al. 2016).

In addition, clinical stem cell studies reported widely varying cell doses being administered to treat IVD degeneration, ranging from 1 million to 40 million cells per patient as reviewed by Sakai and Schol (Noriega et al. 2017; Orozco et al. 2011; Meisel et al. 2006b; Hohaus et al. 2008; Coric et al. 2013; Yoshikawa et al. 2010; Centeno et al. 2017; Tschugg et al. 2017; Tschugg et al. 2016; Sakai and Schol 2017; Smith et al. 2018). Considering the lack of nutrient supply in the human IVD (Huang, Urban, and Luk 2014), we believed it was essential to model the patient-specific nutrient distributions before cell therapy and identify the appropriate dose of cell injections based on the nutritional capacity of the individual disc (Sakai and Schol 2017).

Mathematical models used experimentally measured transport properties, including diffusion coefficients for glucose, oxygen, and lactate (Bibby et al. 2005; Ferguson, Ito, and Nolte 2004; Gullbrand, Peterson, Ahlborn, et al. 2015; Jackson et al. 2009; Malandrino, Noailly, and Lacroix 2011; Soukane, Shirazi-Adl, and Urban 2007; Zhu, Jackson, and Gu 2012). In addition to IVD properties such as IVD water content, cell density, and the rate of cellular glycolysis as a function of oxygen content to simulate solute transport phenomena in the disc (Bibby et al. 2005; Ferguson, Ito, and Nolte 2004; Gullbrand, Peterson, Ahlborn, et al. 2015; Jackson et al. 2009; Malandrino, Noailly, and Lacroix 2011; Soukane, Shirazi-Adl, and Urban 2007; Zhu, Jackson, and Gu 2012).

These models predicted a high concentration of nutrients in the outer regions of the disc: closer to the endplates and the outer AF, compared to the mid-axial center of the disc and in the inner AF (Mokhbi Soukane, Shirazi-Adl, and Urban 2009; Jackson, Huang, and Gu 2011; Soukane, Shirazi-Adl, and Urban 2005). The results from said models agreed with experimentally measured solute concentrations in the disc. Oxygen concentration profiles measured during discography were high in the outer regions of the disc and gradually decreased towards the mid-axial center of the disc (Bartels et al. 1998). Lactate concentrations measured in the NP tissue taken by biopsy from patients and excised segments of the disc were low in the outer regions of the disc and higher in the mid-axial center of the disc (Diamant, Karlsson, and Nachemson 1968; Bartels et al. 1998). There was no literature data about actual glucose measurements in human IVDs. Since glucose is required to produce lactate, their concentrations are necessarily coupled (Soukane,

Shirazi-Adl, and Urban 2005). Therefore, glucose levels should decrease towards the mid-axial center of the disc (Maroudas et al. 1975). Lastly, studies measured pH values in the NP of patients with sciatica to range between 5.7-7.5 (Diamant, Karlsson, and Nachemson 1968; Nachemson 1969).

This study aimed to use data from magnetic resonance imaging (MRI) to model patient-specific IVD distributions of glucose, oxygen, and lactate and investigate factors affecting solute availability in the disc. Disc geometry was extracted from MR T1-weighted (T_{1w}) and T2-weighted images (T_{2w}). NP diffusion coefficients were calculated from apparent diffusion coefficient (ADC) maps. The first part of this study looked at significant differences in solute concentrations between the different degeneration grades. We hypothesized the following with increasing IVD degeneration: (1) average nutrient concentration in the entire disc would decrease, accompanied by an increase in lactate concentrations; (2) minimum concentration values of nutrients would decrease accompanied by an increase in maximum lactate concentrations (3) average solute concentrations in the disc would correlate with their extreme solute values (minimum/maximum) in the inner AF. Then we looked at the effect of disc area, disc height, and average apparent diffusion coefficient (ADC) on solute concentrations.

5.3 Materials and methods

5.3.1 Patient MR data

This study was approved by the Institutional Ethics Committee at the Irkutsk Scientific Center of Surgery and Traumatology, Irkutsk, Russia (identifier no. 15-15-30037). All patients voluntarily provided their written consent to take part in this study. A total of 37 IVDs were randomly chosen from a preexisting MR patient database (Belykh et al. 2017). Each Pfirrmann grade group (grades 2 to 4) had ten randomly selected MR scans of IVDs. Only 7 sets of IVD MR scans with degeneration grade 5 were available for modeling; therefore, randomization was not possible for this group. The IVDs included in this study represented disc levels between L3L4 and L5S1 due to the wrap-around artifacts that distorted higher levels, i.e., L1L2 and L2L3. No MR scans of grade 1 were available for modeling since they suffered from image artifacts. Patient characteristics were summarized in Table 5.1.

Table 5.1. Summary of patient characteristics. Ten IVDs from each degeneration grade were randomly chosen from the 21 patients. Randomization could not be applied for grade 5 because only 7 IVDs were available. IVDs included in this study represent levels between L3L4 and L5S1 due to image artifacts that distorted higher levels, i.e., L1L2 and L2L3. The table also consists of each patient's age and IVD pathology condition. ^p-values reported are from one-way ANOVA or Kruskal Wallis when data was parametric or nonparametric respectively.

Patient characteristic	Grade 2 (n=10)	Grade 3 (n=10)	Grade 4 (n=10)	Grade 5 (n=7)	p-Value^
Age	36.5 ± 7.0	36.6 ± 6.6	37.4 ± 7.5	48.4 ± 6.8	0.0014
BMI	142.2 ± 51	101.5 ± 37	92.8 ± 17	103 ± 29	0.4770
Height (cm)	116.8 ± 49	152 ± 47	175 ± 6.4	163 ± 45	0.2534
Sex (m:f)	9:1	9:1	10:0	7:0	0.6442
Disc pathology	-	-	-	-	1.82E-06
None	90.0%	80.0%	20.0%	0.0%	-
Herniation	0.0%	20.0%	70.0%	57.1%	-
Spondylosis	0.0%	0.0%	10.0%	28.6%	-
Stenosis	10.0%	0.0%	0.0%	14.3%	
Disc level	-	-	-	-	0.0241
L3L4	70.0%	30.0%	10.0%	0.0%	-
L4L5	10.0%	60.0%	40.0%	28.6%	-
L5S1	20.0%	10.0%	50.0%	71.4%	-

5.3.2 Magnetic resonance imaging

Briefly, Sagittal T1-weighted (T_{1w}), T2-weighted (T_{2w}), and diffusion weighted-imaging (DWI) scans of human lumbar discs were obtained using a 1.5T Siemens Magnetom Essenza scanner (Siemens Healthineers, Erlangen, Germany) (Belykh et al. 2017). Images had a 30×30 cm field of view. The following matrix sizes 320×320, 384×384 were used for T_{1w}, and T_{2w}, with pixel sizes 1.0438×1.0438 mm/px and 0.8698×0.8698 mm/px, respectively (Belykh et al. 2017). DWIs were collected at three different b-values (b= 50, 400, 800 s/mm^2) using a body coil with a TR of 3000 ms, TE of 93 ms, six averages, a matrix size of 156 x 192, and a pixel size of 1.7396×1.7396 mm/px (Belykh et al. 2017). The mid-sagittal slice of each MR imaging modality

was used to generate 2D models of the disc. Time of day when the scans were performed was not controlled for (Belykh et al. 2017).

5.3.3 Pfirrmann grading

Discs were evaluated for degeneration and assigned a Pfirrmann grade by 3 neurosurgeons specializing in spinal surgery with 5-15 years of experience (Belykh et al. 2017; Pfirrmann et al. 2001). Each surgeon graded all discs then collectively discussed and formed a consensus on any conflicting grades.

5.3.4 Segmentation of disc masks

Mask segmentation was performed in Materialize Mimics® 21.0 (Leuven, Belgium) (Figure 5.1). T_{1w} images were used to segment CEP masks by hand. Whole IVD and NP masks were segmented using histogram-based thresholding on T_{2w} images. AF masks were generated by subtracting NP and CEP masks from complete IVD masks. The masks were cropped in MATLAB® 9.5 (Natick, Massachusetts) to show the disc of interest. Further processing of masks, which included manual subtraction of masks from one another, was performed to prevent overlap between masks (in most cases, this last step was not needed).

Figure 5.1. Annulus fibrosus (AF), cartilaginous endplates (CEP), and nucleus pulposus (NP) masks (in white left to right) were segmented in Materialize Mimics 21.0 for each patient. AF, CEP, and NP masks from intervertebral disc #1 L3L4 were segmented then overlaid over a T2w scan in this figure

5.3.5 Generation of ADC map

Series of DWI scans were processed in MATLAB® 9.5 (Natick, Massachusetts) to generate apparent diffusion coefficient (ADC) maps for the NP using the mid-sagittal slice (Figure 5.2).
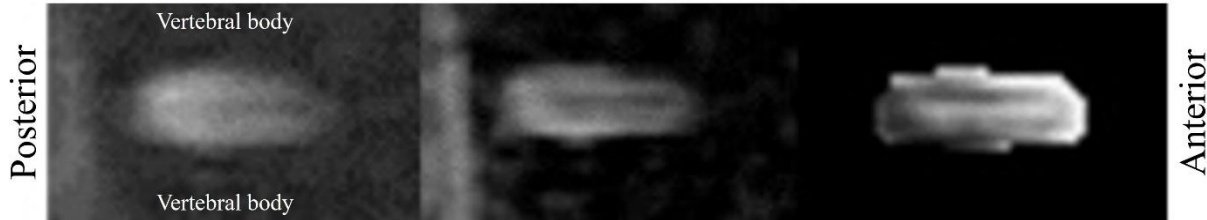
Figure 5.2. Diffusion weighted-imaging (left) for intervertebral disc #1, level L3L4, unprocessed apparent diffusion coefficient (ADC) map (middle), cropped ADC map (right)

ADC values were calculated using the Stejskal-Tanner equation as established by Le Bihan (Equation 5.1) (Le Bihan et al. 1986).

Equation 5.1

$$ADC = \ln\left(\frac{S_0}{S}\right) * \left(\frac{1}{b}\right)$$

Where, S_0 was the MR signal intensity at baseline, S the MR signal intensity after diffusion gradients had been applied, and b was the attenuation factor that depended on the gradient pulse. Raw ADC maps were further processed by replacing both negative and NAN (not a number) values with "0". Finally, ADC maps were cropped to match the dimensions of the corresponding NP mask. The cropped maps were used in the model to compute diffusion in the disc.

5.3.6 Model transport properties

A 2-Dimensional (2-D) steady-state mathematical model was developed in COMSOL Multiphysics® 5.4 (Stockholm, Sweden). The temperature was set to $37°C$ and diffusion throughout the disc was assumed to be isotropic. The simulated time in the model was 30 hours, and it converged with relative tolerance of 0.5%.

5.3.7 Model geometry

AF, CEP, and NP masks were overlaid on top of a square (45 mm × 45 mm) which represented a well-mixed container in which solute transport took place. Disc masks were scaled to their true size and always positioned at the center of the geometric shape. A physics-controlled mesh with extra fine element size (maximum element size 0.9 mm, minimum element size 0.00338 mm, curvature factor 0.25, maximum element growth rate 1.2) was implemented with Adaptive Mesh Refinement (Figure 5.3).
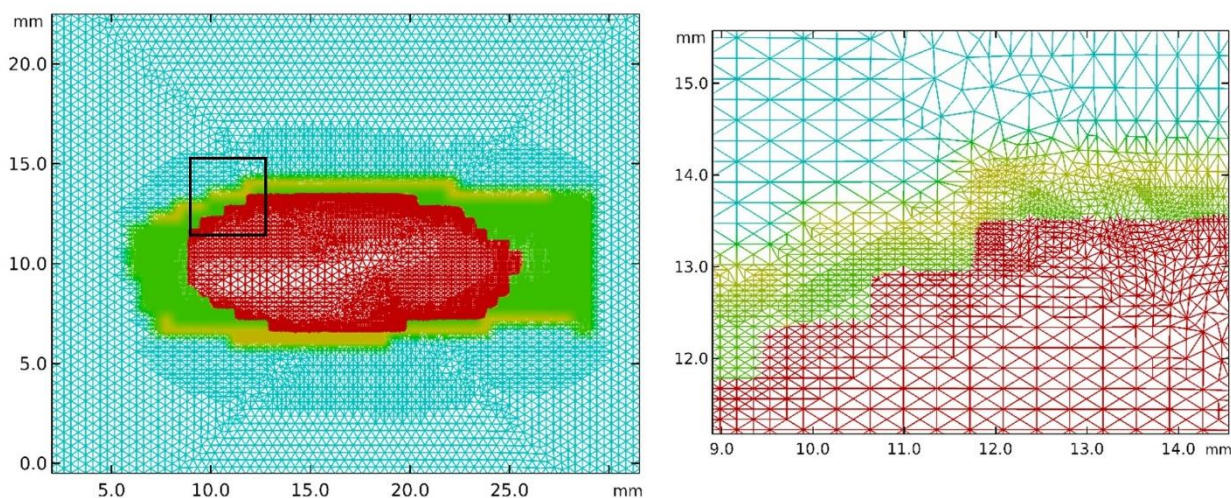
Figure 5.3. Adaptive mesh refinement for intervertebral disc #1, level L3L4. COMSOL Multiphysics had automatically inserted additional mesh elements to minimize error, increase accuracy. and decrease computational time (left). Zoomed view of mesh boundary layers (right) shows the areas around the IVD boundaries that contained additional smaller mesh elements.

5.3.8 Boundary and initial conditions

Boundary concentration values for glucose, oxygen, and lactate (5 mol/m^3, 0.06 kPa, and 0.9 mol/m^3, respectively) were chosen from previously published IVD finite element models (Bartels et al. 1998; Mokhbi Soukane, Shirazi-Adl, and Urban 2009; Soukane, Shirazi-Adl, and Urban 2007; Jackson, Huang, and Gu 2011). Boundary conditions were assigned to the sides of the geometric shape to simulate a disc suspended in a well-mixed solution. The assumption of a well-mixed solution was essential to eliminate variability in solute gradients outside the disc between different models (Figure 5.4). Physiological levels of glucose, oxygen, and lactate were assumed in the well-mixed solution (Soukane, Shirazi-Adl, and Urban 2005; Jackson, Huang, and

Gu 2011; Mokhbi Soukane, Shirazi-Adl, and Urban 2009). Initial conditions inside the disc for glucose, oxygen, and lactate were set to 1 mol/m^3 ,0.1 kPa, and 0 mol/m^3, respectively (Soukane, Shirazi-Adl, and Urban 2005; Jackson, Huang, and Gu 2011; Mokhbi Soukane, Shirazi-Adl, and Urban 2009).
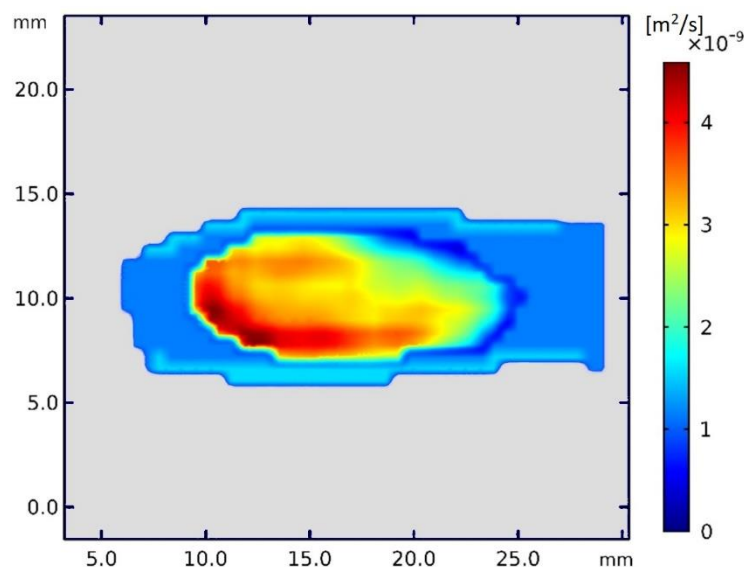
Figure 5.4. Glucose diffusion map of intervertebral disc #1, disc level L3L4. Incorporating apparent diffusion coefficient (ADC) maps to calculate diffusion in the nucleus pulposus reflected the local variation in diffusion coefficients. No gradient could be observed in the cartilaginous endplates and annulus fibrosus because ADC maps were not obtained at a resolution high enough to allow for extraction of diffusion coefficients

5.3.9 Constant parameters

Parameter maps for solute diffusion, water content, and cell density for each segment of the disc were generated in COMSOL Multiphysics® by multiplying the mask with the corresponding parameter value (Soukane, Shirazi-Adl, and Urban 2007) **(**Figure 5.4**).** Discs with degeneration grade of 2-3 were considered healthy, whereas 4-5 grade discs were considered degenerate (Table 5.2).

Table 5.2. The model's constant parameters. IVD parameters for water content, diffusion coefficients for glucose, oxygen, and lactate, and cell density were taken from other published models. These parameters were multiplied with each mask to create an IVD map of varying parameter values based on each anatomical part.

IVD region	Water content (%)		Diffusion coefficient (m^2/s)			Cell density (1/m^3)
-	Healthy disc	Degenerate disc	Glucose	Oxygen	Lactate	-
NP	83[1]	78[1]	*see "Diffusion coefficients in NP"*			4.0E+12[2]
AF*	69[3]	53[3]	2.85E-10[4]	1.1E-9[4]	4.24E-10[4]	9.0E+12[2]
CEP	60[5]	42[5]	2.11E-10[4]	7.81E-10[4]	3.14E-10[4]	1.5E+13[2]

[1](Lyons, Eisenstein, and Sweet 1981)
[2](Maroudas et al. 1975)
[3](Natarajan, Williams, and Andersson 2006)
[4](Soukane, Shirazi-Adl, and Urban 2007)
[5](Jackson, Huang, and Gu 2011)
* Indicates average values of inner and outer AF

5.3.10 Diffusion coefficients in NP

Solute diffusion coefficients in the NP were generated by converting water diffusion coefficients from ADC maps to the corresponding solute diffusion coefficient. Factors used to scale diffusion coefficients of water to glucose, oxygen, and lactate were 0.319, 1.02 and 0.478, respectively. These factors were generated by scaling the value of water diffusion in tissue to solute diffusion in tissue using hindered solute diffusion theory as developed by Renkin (Welty 2015). His equation describes the diffusion of a solute molecule (i.e., glucose, oxygen, lactate) through a tiny capillary pore filled with a liquid solvent (i.e., water). As the size of the solute increased, the diffusive transport through the solvent was hindered by the presence of the pore, specifically the pore wall (Renkin 1954; Welty 2015). Renkin's model was used to describe diffusion in the IVD because the ECM's pore diameter is 7 to 20 times the molecular diameter of glucose, oxygen, and lactate (Gillispie, Lee, and Yoo 2019).

Briefly, diffusion of molecules through porous material could be characterized using two controlling mechanisms, geometric tortuosity, and hindered diffusion. Geometric tortuosity represents the ratio between the average pathways and the straightest one taken by a specific molecule as it traverses from point A to B in a porous medium (Pardo-Alonso et al. 2014; Al-Raoush and Madhoun 2017; Elwinger, Pourmand, and Furó 2017). Hindered diffusion describes the molecular interactions with the pore's walls, which inhibit solute transport as described by Renkin's equation. In situations where the pore size is over 30-40 times the diameter of molecules,

diffusion is controlled by the geometric tortuosity theory (Elwinger, Pourmand, and Furó 2017). When the porous medium's pore size is ten times or less the molecule's diameter, then hindered diffusion is the dominating factor (Elwinger, Pourmand, and Furó 2017). This hindrance was modeled using Equation 5.2 (Welty 2015).

Equation 5.3

$$\frac{D_{Ae}}{D_{AB}^0} = F_1(\varphi)F_2(\varphi)$$

In this equation both correction factors, F_1 and F_2, are functions of the reduced pore diameter (φ), and are theoretically bounded by 0 and 1 as shown in Equation 5.3 (Welty 2015).

Equation 5.4

$$\varphi = \frac{d_s}{d_{pore}} = \frac{\text{solute molecular diameter}}{\text{pore diameter}}$$

$F_1(\varphi)$ is known as the stearic partition coefficient and is based on geometric arguments for stearic exclusion in Equation 5.4 (Welty 2015).

Equation 5.5

$$F_1(\varphi) = \frac{\text{flux area available to solute}}{\text{total flux area}} = \frac{\pi(d_{pore} - d_s)^2}{\pi d_{pore}^2} = (1 - \varphi)^2$$

The correction factor $F_2(\varphi)$ is known as the hydrodynamic hindrance factor. It is based on several hydrodynamic calculations, including the hindered Brownian motion of the solute within the solvent-filled pore (Welty 2015). Renkin developed the following relationship for $F_2(\varphi)$, assuming the solute is a rigid sphere diffusing through a straight cylindrical pore (Equation 5.5) (Welty 2015).

Equation 5.6

$$F_2(\varphi) = 1 - 2.104\varphi + 2.09\varphi^3 - 0.95\varphi^5$$

Based on this analysis, ADC values were scaled for a given solute based on a ratio of literature values for solute diffusion in water and the diffusion of water in water. It was assumed that all four solutes (glucose, oxygen, lactate, and water) were sufficiently small (on the scale of 300-900 pm) relative to the pore to approximate $F_1(\varphi)$ and $F_2(\varphi)$ as the same across all solutes.

The diffusion of water in tissue was modeled as hindered-self diffusion of water through a solvent-filled pore, in which diffusion constant parameters $F_1(\varphi)$ and $F_2(\varphi)$ were already accounted for in the ADC values. Based on this method, scaling factors were generated to relate

water diffusion in the tissue (extracted from ADC maps) to solute diffusion of glucose, oxygen, and lactate in the tissue.

A comparison of the diffusion coefficients used in this model and the reported values in the literature showed that this model's diffusion coefficients fell within the range of the reported values (Table 5.3).

Table 5.3. Comparison of this model's diffusion coefficients and literature values. Diffusion coefficients of glucose, oxygen, and lactate used in this model were compared with their corresponding values reported in the literature. This model's coefficients, which were extracted from ADC maps and multiplied by scaling factors, fell within the range of diffusion coefficients reported in the literature. The range of diffusion coefficients used in the NP for this model depicted the highest and lowest values obtained from the ADC maps.

IVD region	D_g (m^2/s)	D_l (m^2/s)	D_o (m^2/s)	References
CEP	6.73E-11	1.50E-10	7.96E-10	This model
AF	9.08E-11	2.02E-10	1.07E-09	This model
NP	1.22E-10 to 2.54E-10	1.83E-10 to 3.81E-10	3.90E-10 to 8.13E-10	This model
CEP	2.68E-11	4.52E-11	-	(Wu et al. 2016)
CEP	2.68E-11	4.52E-11	-	(Wu et al. 2016)
AF	3.56E-11 to 8.71E-11	-	1.13E-10 to 1.85E-9	(Jackson et al. 2012)
AF	-	-	1.56E-09	(Yuan et al. 2009)
AF	1.38E-10 to 9.17E-11	-	-	(Jackson et al. 2008)
CEP	9.17E-10	1.39E-09	3.00E-09	(Magnier et al. 2009)
CEP	2.11E-10	3.14E-10	7.81E-10	(Mokhbi Soukane, Shirazi-Adl, and Urban 2007)
AF	2.85E-10	4.24E-10	1.05E-09	
NP	3.78E-10	5.61E-10	1.39E-09	
CEP	2.43E-10	-	-	(Maroudas et al. 1975)
AF	2.50E-10	-	-	
AF	2.50E-10	4.86E-10	8.33E-10	(Sélard, Shirazi-Adl, and Urban 2003)
NP	3.75E-10	6.11E-10	1.28E-09	

5.3.11 Governing equations

    Diffusion of solutes (glucose, oxygen and lactate) was modeled by substituting Fick's first law for flux into the equation of mass conservation where C was solute concentration mol/m^3, t was time in seconds, D was solute diffusion coefficient m^2/s, $\dot{R}$ was the reaction term for either consumption or generation of solutes mol/(m$^3 \times$ s), and x was diffusion distance in meters (Equation 5.6) (McMurtrey 2016).

Equation 5.7

$$\frac{\partial C}{\partial t} = D\frac{\partial^2 C}{dx^2} - \dot{R}$$

    The reaction term in equation 6 was represented by nonlinear coupled equations for consumption of oxygen nmol/(million cells $\times$ hour) (Equation 5.7) and generation of lactate nmol/(million cells $\times$ hour) (Equation 5.8) (Bibby et al. 2005).

Equation 5.8

$$[\dot{O_2}] = \frac{7.28 \cdot [O_2] \cdot (pH - 4.95)}{1.46 + [O_2] + 4.03 \cdot (pH - 4.95)}$$

Equation 5.9

$$[\dot{L}] = e^{-2.74+0.93 \cdot pH+0.16 \cdot [O_2]-0.0058 \cdot [O_2]^2}$$

    Oxygen solubility in water was used to convert oxygen consumption levels to kPa via conversion factors (Equation 5.9) (Soukane, Shirazi-Adl, and Urban 2005).

Equation 5.10

$$s = 1.0268 \cdot 10^{-2} \; \mu mol/(kPa \times mL)$$

    pH values were correlated to lactate concentrations in the disc adapted from a study that investigated the correlation between lactate levels and pH in patient discs with lumbar sciatica (Equation 5.10) (Diamant, Karlsson, and Nachemson 1968).

Equation 5.11

$$pH = 8.05 - 0.10 \cdot [L]$$

    Glucose consumption was predicted based on lactate production. Bibby et al. estimated the ratio of lactic production to glucose consumption to 2.01 which was expected from glycolytic pathways (Equation 5.11) (Bibby et al. 2005).

Equation 5.12

$$[\dot{G}] = -0.5 \cdot [\dot{L}]$$

Reaction equations were multiplied by water content and cell density to arrive at a final reaction unit of mol/(m^3 × s).

Average operation function in COMSOL Multiphysics® (Equation 5.12) was used to calculate average solute concentration mol/(m^3 × s) within the boundaries of the disc.

Equation 5.13

$$aveop\#([solute] \times IVD(x,y))$$

Where, aveop# was the average operation function, and IVD(x,y) defined the boundaries of the disc.

5.3.12 Sensitivity analysis

A sensitivity analysis (SA) was performed on three randomly selected models of healthy IVDs to find the parameters with the most significant effect on nutrient distribution. The following model variables were changed by ±50% from baseline values: diffusivity of the AF, CEP, and NP, reaction rates for glucose, lactate, oxygen, disc size, and NP cell density. This SA was done to determine parameters that significantly affected both average concentrations in the IVD and minimum and maximum concentrations in the inner AF. A general regression model was performed on the % change in solute concentrations to find the effect size of model variables ($p < 0.05$).

5.3.13 Statistical analysis

For this study, ten discs were randomly selected to represent Pfirrmann degeneration grades 2 through 5 from a pre-existing patient MR database. Randomization could not be applied for degeneration grade 5 because only 7 IVD datasets were available. Discs included in this study represented levels between L3L4 and L5S1 due to the wrap-around artifacts that distorted higher levels, i.e., L1L2 and L2L3 (Table 5.1). Sample size in this study provided a statistical power of 95% for the mean difference of the following modeled parameters between different Pfirrmann grades: minimum glucose concentration, minimum oxygen concentration, maximum lactate concentration, average glucose concentration and average oxygen concentration. Average lactate concentration had a statistical power of 42% due to significant variance.

The homogeneity assumption of variance was verified using Levene's test ($p < 0.05$). Analysis of covariance (ANCOVA) was performed in TIBCO Statistica v13.5 (Palo Alto, CA,
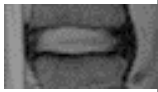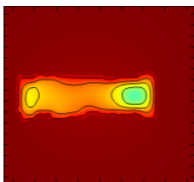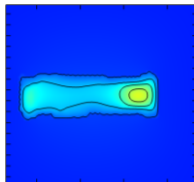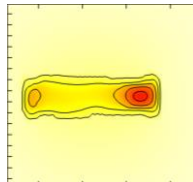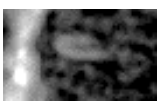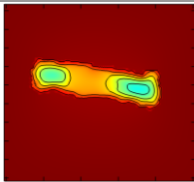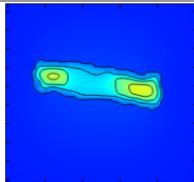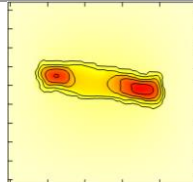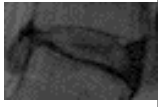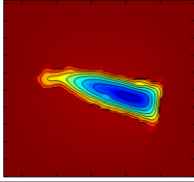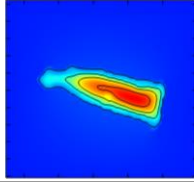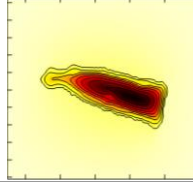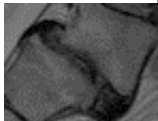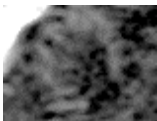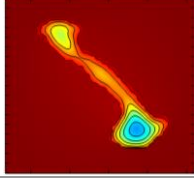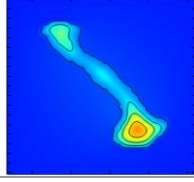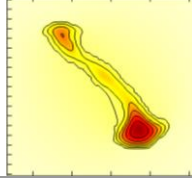
USA) to find a significant difference in mean solute concentrations and mean minimum and maximum solute concentrations between disc degeneration grades. ANCOVA was followed with a post-hoc Tukey honestly significant difference (HSD) test. Disc height, disc area, and ADC mean intensity were covariate factors. Outliers were measured using inclusive median quartile calculation. Partial correlations were performed between the estimated metrics (average solute concentrations in the disc as well as minimum and maximum solute concentrations in the inner AF) and disc properties (disc area, disc height, and average ADC intensity). Statistical analysis was performed on patient demographics using one-way ANOVA or Kruskal Wallis ($p < 0.05$) when data was parametric or nonparametric, respectively. Finally, one-way ANOVA followed by a post-hoc test was performed to investigate the possible effects of patient characteristics, i.e., sex, IVD pathology, and IVD level on solute concentrations.

5.4 Results

5.4.1 Nutrient distribution

For all degeneration grades, the concentration of nutrients (i.e., glucose and oxygen) dropped with distance from the CEP. In contrast, acidity levels increased especially towards the center of the disc (Table 5.4**).** Most discs experienced the lowest nutrient levels along with the highest lactate in the inner AF (Table 5.4). The model predicted minimum glucose concentrations to range between 0.393 mol/m^3 in most degenerated IVDs to 3.43 mol/m^3 in least degenerated IVDs. Minimum oxygen and pH values ranged from 4.67 kPa and 7.18 in least degenerated IVDs to 2.76 kPa and 6.96 in most degenerated IVDs.

Table 5.4. Examples of solute and pH distribution models of discs with different degeneration grades. All discs were presented with the posterior aspect on the left and the anterior side on the right. Each model was constructed in COMSOL Multiphysics® 5.4 using the middle sagittal slice of each patient's T_{2w}, T_{1w}, and DWI scans. pH distributions (linearly correlated to lactate levels) were not shown. The lowest levels of nutrients and the highest acidity levels appeared at the inner AF region in most discs (refer to Table 2 of Appendix A1 for the complete model results).

Patient	Grade level	T_{2w}	ADC	Glucose gradient (mM)	Lactate gradient (mM)	Oxygen gradient (kPa)
1	2					
4	3					
19	4					
10	5					

5.4.2 Between Pfirrmann grades

There was a significant difference in patient demographics, including age (p = 0.0014), IVD level (p = 0.0241), and IVD pathology (p = 1.82E-06), between the different grades (Table 5.1). The model demonstrated that the IVD's nutrient environment became harsh as degeneration progressed. For example, average glucose concentrations followed a decreasing trend that was more obvious in minimum glucose levels (Figure 5.5-A). Oxygen levels also decreased as the disc degenerated and showed a similar trend to glucose (Figure 5.5-C). The decrease in nutrient levels was accompanied by increased maximum lactate and acidity levels (Figure 5.5-B2).
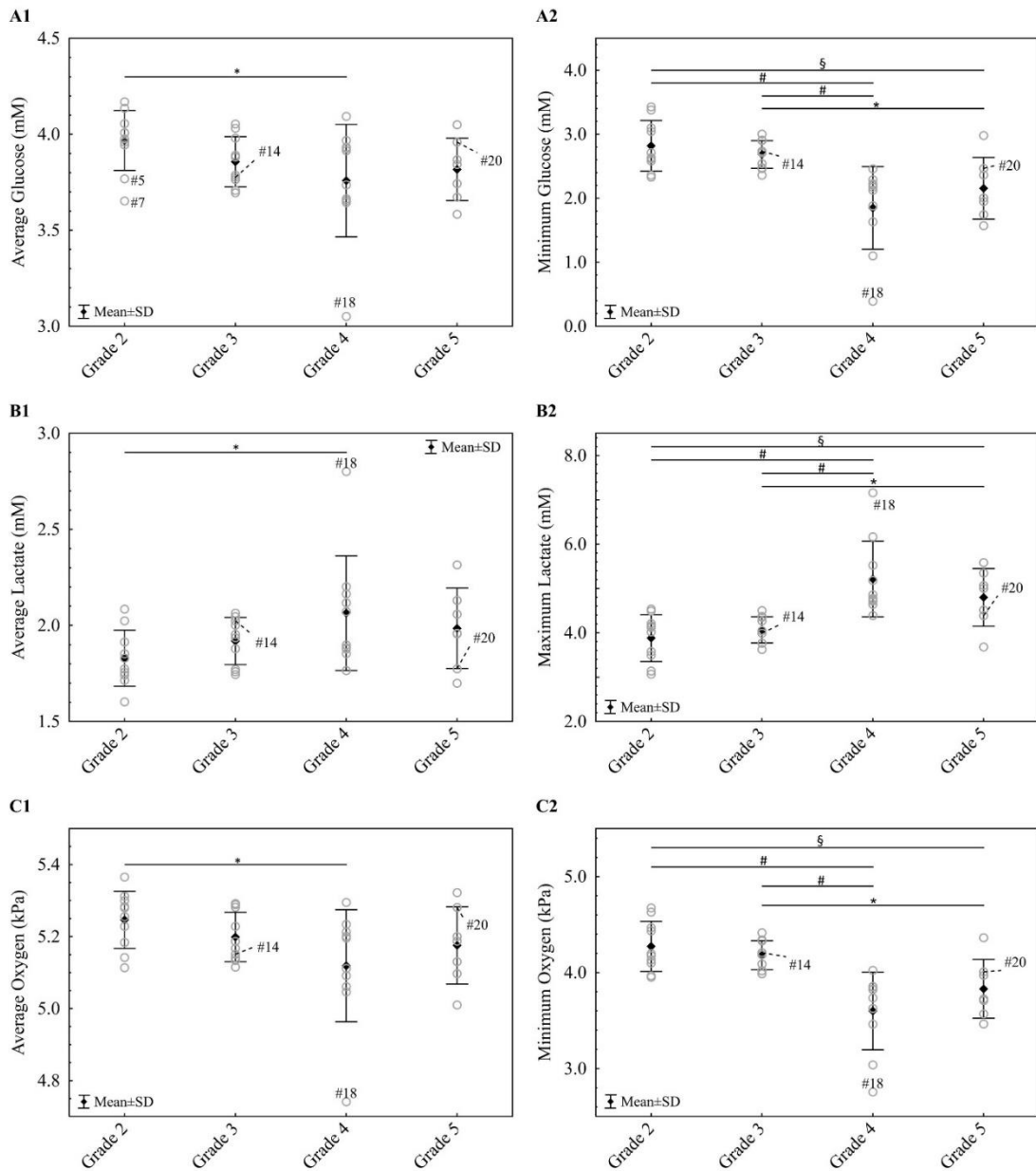
Figure 5.5. Estimation of concentration averages with SD in intervertebral discs (IVDs) of Pfirrmann grades 2–5. Average solute concentrations were calculated using COMSOL Multiphysics for (A1) glucose mM, (B1) lactate mM, (C1) oxygen kPa. COMSOL Multiphysics identified critical solute values in the inner AF for (A2) minimum glucose (B2), maximum lactate (C2) minimum oxygen (* = 0.05, § = 0.005, # = 0.0001). Patients #5, 7, and 18 were outliers. Patients #14 and 20 have larger and small IVD areas, respectively (Figure 5.7).

Quantitatively, the model showed a more substantial effect of degeneration on the minimum and maximum solutes compared to average solute concentrations in the IVD. For example, as the disc degenerated from grade 3 to 4, the average lactate concentration dropped by 7.59% (Table 5.5). In contrast, maximum lactate levels increased by 28.2%. In addition, minimum glucose and oxygen levels decreased with degeneration by 31.1% and 13.9% between grades 3 and 4; whereas average glucose and oxygen decreased by 2.54% and 1.53%, respectively (Table 5.5).

Table 5.5. Quantified changes in solute concentrations between different degeneration grades. COMSOL Multiphysics® 5.4 automatically identified minimum and maximum solute values in the IVD. However, all points fell within the inner AF (except for the following patients: #13, #15, and #18 in grade 4; and patient #20 in grade 5). (n=10 for grades 2, 3, 4 and n=7 for grade 5).

Degeneration progression	Glucose	Lactate	Oxygen
Grade 2 - Grade 3	-2.79%	4.84%	-0.91%
Grade 3 - Grade 4	-2.54%	7.59%	-1.53%
Grade 4 - Grade 5	1.55%	-3.81%	1.10%
Degeneration progression	Minimum glucose	Maximum lactate	Minimum oxygen
Grade 2 - Grade 3	-4.80%	4.79%	-2.17%
Grade 3 - Grade 4	-31.1%	28.2%	-13.9%
Grade 4 - Grade 5	16.5%	-8.00%	6.39%

5.4.3 Between patients

The effects of patient demographics, i.e., IVD level, IVD condition, and patient sex on solute concentrations were analyzed (Figure 5.6). Significant difference in average nutrient levels between IVD levels L3L4 and L4L5 (ANOVA, $p < 0.05$) (Figure 5.6-A1). There was also a significant difference between herniated and nonpathological IVDs (ANOVA, $p < 0.05$) (Figure 5.6-B2). Patient sex did not affect the mean solute concentrations, although only two IVDs from the same female patients were used in this study (Figure 5.6-C). Mean patient age of grade 5 was 13 years higher than the mean patient age in all other groups (ANOVA, $p < 0.005$) (Table 5.1).
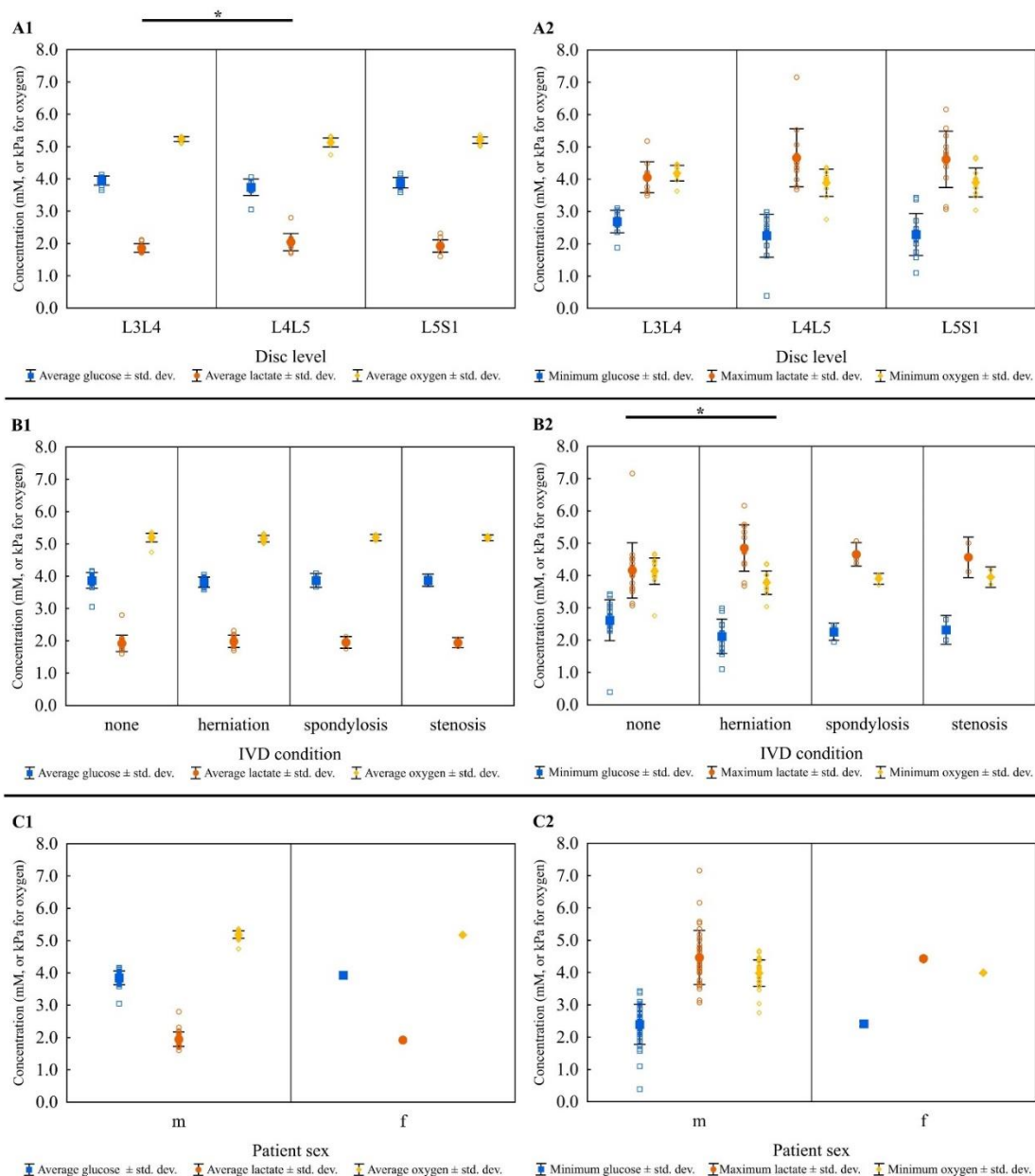
Figure 5.6. Estimation of solute concentration means for glucose mM, oxygen kPa, and lactate mM in the IVD vs patient characteristics. (A1, A2) disc level, (B1, B2) IVD pathology condition, and (C1, C2) patient sex. An * indicated significance with a P-value of .05.

There was no strong evidence to support the variation in mean patient BMI and mean patient height between degeneration grades (ANOVA, p = 0.4770, and p = 0.2534, respectively) (Table 5.1). No evidence was found to support a difference between patient sex between degeneration grades (Kruskal-Wallis, p = 0.6442) (Table 5.1). Lastly, grade 2 has significantly more L3L4 IVDs compared to all other degeneration groups (Kruskal-Wallis, p < 0.05) (Table

5.1). The model further suggested a strong effect (ANCOVA, p < 0.05) between solute concentrations in the disc and the following three covariate factors (which were made patient-specific), disc height, disc area, and mean NP ADC values (Table 5.6). Average concentrations of all solutes correlated with all minimum and maximum values (p < 0.05) (Table 6). Nutrient distributions varied significantly when visually compared model results in grades 3, 4, and 5 (Tables 5.4 and A.1).

Table 5.6. Partial correlations for different measured metrics in the disc. Reported numbers are Pearson R correlation values of fitted linear regression between groups. The sign indicates a positive or negative correlation. All correlations were considered significant with p < 0.05.

Variable	Min. glucose	Max. lactate	Min. oxygen	Ave. glucose	Ave. lactate	Ave. oxygen	Area	Height	Mean ADC intensity
Min. glucose	1.0	-1.0	0.99	0.79	-0.87	0.87	-0.60	-0.40	0.56
Max. lactate	-1.0	1.0	-0.99	-0.79	0.87	-0.86	0.60	0.41	-0.57
Min. oxygen	0.99	-0.99	1.0	0.77	-0.85	0.85	-0.61	-0.41	0.57
Ave. glucose	0.79	-0.77	0.77	1.0	-0.98	0.97	-0.67	-0.61	0.29
Ave. lactate	-0.87	0.87	-0.85	-0.98	1.0	-0.99	0.71	0.54	0.49
Ave. oxygen	0.87	-0.86	0.85	0.97	-0.99	1.0	-0.74	-0.61	-0.47

Examining the outliers in this study showed that IVDs with a large IVD area and a high Pfirrmann score (grades 4 or 5) were more likely to have very extreme levels of nutrients and lactate, as was the case for patient #18 (Figures 5.5 and 5.7, Table A.1.2). Patient #20 in grade 5 had a minimal IVD area due to a herniation, but solute levels fell within the expected values for that group (Figure 5.7, Table A.1.2). Large healthy discs did not seem to suffer from nutrient deprivation. For instance, patient #14 in grade 3 had a large disc area (33% larger than the mean

area for grade 3 discs), but the IVD's nutrient levels were within one standard deviation from that group's mean (Figures 5.5 and 5.7, Table A.1.2).
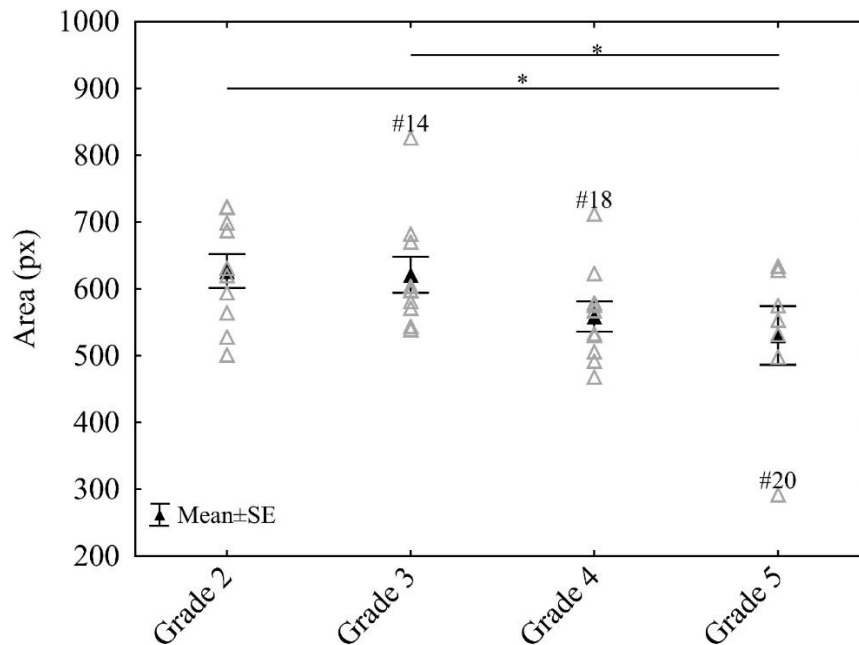
Figure 5.7. Average intervertebral disc area in pixels for each degeneration group. Outliers are marked with the corresponding patient number. An * indicated significance with a P-value of .05. Patients #14, 18, and 20 were outliers.

The sensitivity analysis (SA) for this model showed that modifications to the IVD size had the most notable effect on all solute concentrations (Figure 5.8). The results showed an increase in IVD size to correlate with poor nutrient availability, while a decrease in size led to an increase in nutrient levels. For example, increasing the IVD size by 50% decreased minimum glucose by 80%. In contrast, a 50% decrease in IVD size resulted in a 63% increase in glucose concentration. A decrease in AF and CEP diffusivities lowered minimum glucose levels in the disc by 43% and 17%, respectively, while increased lactate concentrations by 36% and 9%. The NP's diffusivity affected maximum lactate levels only (Figure 5.8-B). An increase in the consumption rates of glucose and oxygen showed a +10% drop in their minimum concentrations (Figure 3.8-A and C) while it did not affect lactate levels (Figure 5.8-B). Lactate production rates correlated with a +35% change in minimum glucose, and +30% change in maximum lactate concentrations (Figure 5.8-A and B). More factors affected minimum glucose by +40% compared to other solutes, including

disc size, glucose consumption rate, lactate production rate, AF, and CEP diffusivities (Figure 5.8-A). Changes to the IVD's cell density affected maximum lactate and oxygen concentrations (Figure 5.8-B and C).
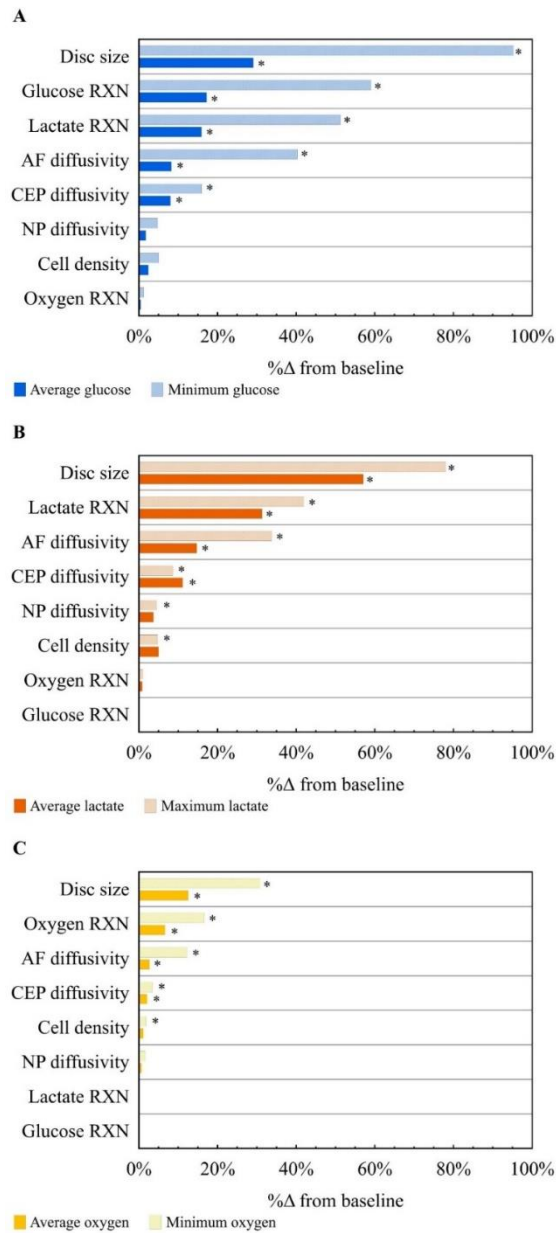
Figure 5.8. Sensitivity analysis on model variables including, diffusivity of the annulus fibrosus, cartilaginous endplates, and nucleus pulposus, reaction rates (RXN) of glucose, lactate, and oxygen, cell density, and disc size. Solute % change from baseline values are presented for (A) glucose, (B) lactate, and (C) oxygen. General linear model was performed to find significance indicated by * (P = .05)

5.5 Discussion

The main objective of this study was to create finite element models that incorporated patient-specific MRI data to model nutrient and metabolite distributions in IVDs of different Pfirrmann grades. The study also assessed the effects of disc area, disc height, and mean ADC on the IVD's nutrition (Table 5.6). The model estimated average glucose, oxygen, and lactate distributions in the disc, and minimum glucose, minimum oxygen, and maximum lactate concentrations. Taken together, these metrics identify potential low-nutrient regions in each disc, where cell growth is likely to be inferior.

5.5.1 Nutrient distribution

The model showed nutrient levels moving from physiological levels near the IVD's boundary to their minimums near the inner AF (Tables 5.4 and A.1). Critical solute levels were expected in this part of the IVD due to the long diffusion pathway that solutes need to take from the CEP (Figure 5.9).
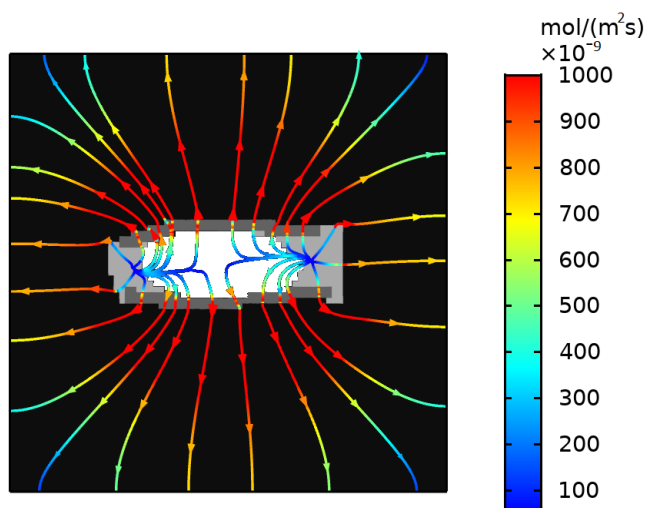
Figure 5.9. Streamlines show lactate flux through the different parts of the IVD (annulus fibrosus (AF): light gray, cartilaginous endplates (CEP): dark gray, nucleus pulposus (NP): white). The color scale reflects flux magnitude of lactate. High flux was observed near both CEPs, while the AF experienced low flux indicating better transport through the former. Long diffusion pathways extending from the inner AF through the CEP lead to low nutrient levels in the inner AF

Multiple studies have shown the dependency of nutrient availability on diffusion through the CEP, attributed to its porosity and low thickness (Naresh-Babu et al. 2016; Wong et al. 2019). The outer AF relies on molecular transport through its well-aligned collagen rings for nutrient supply (Naresh-Babu et al. 2016). Nonetheless, due to the AF's anisotropic properties and thicker layers, molecular transport was still less effective than through the CEP (Naresh-Babu et al. 2016). These IVD traits create regions that are vulnerable to nutrient deprivation and are believed to not support the cellular nutrient demand (Table 5.4). The amount of glucose that is consumed in each degeneration grade was equal to about half of the amount of lactate being produced, when comparing these values to the boundary conditions. For example, in grade 2, the amount of consumed glucose was 1 mM on average (Figure 5.5-A1) and the corresponding amount of lactate was about 1.8 mM on average (Figure 5.5-B1). When comparing the amount of lactate being produced in degenerated grades, one can notice that it is higher for grades 4 and 5 (about 2 mM) compared with healthy IVDs. This increase cannot be attributed to changes in metabolic rates or cell density because both variables were held constant. Instead, it is attributed to the disrupted balance between metabolic rates and diffusion rates of lactate. The decrease in the ADC values and diffusion coefficients for high Pfirrmann grade IVDs, reduces the disc's ability to clear lactate at an efficient rate. *In vivo* measurements and finite element models have already established these solute distribution characteristics in the disc. For example, oxygen levels in discs from patients with scoliosis were measured to be lower than plasma levels and progressively decrease towards the axial center of the disc, with minimums in the inner AF ranging between 0.67 kPa and 20 kPa (Bartels et al. 1998), which matches our model's predictions (Tables 5.4 and A.1, Figure 5.5-C). In addition, several finite element models have been used to illustrate glucose distribution in human IVDs where they predict glucose levels to decrease from plasma levels at the outer regions of the disc to mol/m^3 in the inner regions of the disc. As shown in Figure 5.5-A and Table A.1.2, the model's estimation for glucose levels reflected literature values and followed similar distribution patterns to that of oxygen (Table A.1.2) (Jackson, Huang, and Gu 2011; Soukane, Shirazi-Adl, and Urban 2007; Soukane, Shirazi-Adl, and Urban 2005; Zhu et al. 2016; Wu et al. 2013; Magnier et al. 2009). This model's prediction also agreed with measured lactate levels in human discs, which increased from 1 mol/m^3 (plasma level) to 6 mol/m^3 at the center of the disc (Figure 5.5-B) (Bartels et al. 1998). In this model, lactate was linearly correlated to pH, so regions with high lactate correspond to low pH values (Equation 5.10). Modeled pH levels fell within

literature values of 6.7-7.4 (Jackson, Huang, and Gu 2011; Mokhbi Soukane, Shirazi-Adl, and Urban 2009; Soukane, Shirazi-Adl, and Urban 2005). Furthermore, average glucose, oxygen, and lactate concentrations significantly correlated with their critical levels in the disc (Table 5.6).

Solute flux estimations reflected the critical role of the CEP in solute transport. Lactate flux density was greater in the CEP than the AF, indicating that the CEP was the path of least resistance in terms of molecular transport (Figure 5.9). In addition, predictions showed that solutes need to travel longer distances to reach or clear the inner AF (Figure 5.9). This circumstance may prevent nutrients from being replenished at an efficient rate; while lactate tends to accumulate and lead to high acidity (Andersson 1999; Wang et al. 2015; Urban and Roberts 2003; Urban and Winlove 2007; Kihara, Ito, and Miyake 2013; Yin et al. 2019; Grunhagen et al. 2011). Consequently, it is important to assess the ability of the inner AF to support cell injections, which cause a higher nutrient demand -and ultimately lead to low cellular viability (Bibby et al. 2002).

5.5.2 Between Pfirrmann grades

Model predictions demonstrated that the degeneration grade strongly correlated with average nutrient concentration and critical solute levels (i.e., glucose, oxygen, and lactate) (Figure 5.5). As the disc degenerates, it undergoes morphological and biochemical changes (Huang, Urban, and Luk 2014; Andersson 1999). IVD degeneration includes a significant loss in proteoglycans (PG), leading to disc dehydration, structural changes of the NP and AF, and calcification of the CEP (Andersson 1999; Huang, Urban, and Luk 2014). Those factors were shown to inhibit solute diffusion in the disc causing glucose and pH to drop to their critical levels of 0.5 mol/m^3 and 6.7, respectively, making the IVD's environment harsh for cells survival (Shirazi-Adl, Taheri, and Urban 2010; Bibby and Urban 2004; Jackson et al. 2009).

The model showed that healthier discs (grades 2 and 3), with sufficient water content and intact ECM, could facilitate better diffusion of nutrients into the disc and improve clearance of lactate (Figure 5.5-B and Table A.1.2). Although the model suggested an overall trend of increasing lactate content and acidity in the disc as it degenerated, this was not observed as the disc degenerated from grade 4 to 5 (Figure 5.5-B and Table 5.5). This may be attributed to the severe reduction in the height of grade 5 discs that possibly improved diffusion distance (Table 5.6) despite compromised solute diffusivity in the disc. Nonetheless, this observation does not

indicate that a grade 5 disc is suitable for cell injections because a large portion of the disc's ECM has already been compromised.

Last, a large overlap exists between the quartiles of the same solutes in different degeneration grades demonstrating the limitations of assessing IVD nutrient status solely based on degeneration grades. For example, average glucose and oxygen concentration means in grades 3 and 5 were similar (Figure 5.5-A1), but the distribution of said solutes was different such that the inner AF in grade 5 discs experienced deficient nutrient levels (Table A.1.2). In addition, there is an overlap in average lactate values between grades 2 and 4, indicating that grade 2 IVDs might share similar lactate levels to grade 4 discs (Figure 5.5-B1). This observation shows the importance of generating patient-specific nutrient distributions to accurately assess nutrient availability in the IVD.

5.5.3 Between patients

This study highlights the importance of making patient-specific model parameters such as disc size, metabolic rates, the diffusivity of the AF and CEP, and cell density. There was a significant correlation between increasing disc size to lower glucose and oxygen levels and higher lactate levels. For example, minimum glucose levels were 80% lower in a 50% larger IVD. This was expected since a larger IVD size means a longer diffusion pathway and vice versa (Grunhagen et al. 2006; Malandrino et al. 2015; Bibby et al. 2002). A decrease in nutrient availability has been reported during the first decade of human life as the IVD increases in size (Tomaszewski et al. 2015). Other factors such as surgery and degeneration can also alter the IVD's size leading to changes in nutritional status.

Model predictions show that degenerated discs with a relatively larger area exhibited deficient nutrients and high accumulation of lactate. For instance, IVD #18 in grade 4 has an area that is 27.5% larger than the group's average yet showcases minimum glucose levels below the critical concentrations at 0.39 mM. Maximum lactate levels in this IVD are also high at 7.3 mM. Despite this IVD not having any pathological conditions, its nutrient status cannot support normal cellular functions. In contrast, IVD #20 in grade 5 has a 45% smaller area than the group's mean, yet its minimum glucose levels are 2.5 mM, and maximum lactate is 4.39 mM, indicating nutrient conditions that can facilitate cellular functions. This improvement in IVD nutrient status may be attributed to the shorter diffusion pathway, which is also predicted in discs of varying sizes within

Pfirrmann grades 2 and 3 (Figure 5.5-B and Figure 5.7). In grade 2, IVD #2 and 8 have relatively small IVD areas compared to the group's mean and therefore have high nutrient concentrations. In contrast, patients #5 and 7 (grade 2) exhibited low average nutrient levels, yet their disc areas were not considered to be relatively large. In grade 3, only IVD #14 has a significantly large disc area, but surprisingly, it maintains a healthy nutrient status. Assessing the masks that were made for IVD #14 showed an artifact in the AF which did not enclose the NP completely which improved the nutrient status in this IVD. These observations point to the importance of tailoring the model's parameters to the specific IVD's geometry and size to more accurately assess nutrient status.

The sensitivity analysis (SA) shows glucose, lactate, and oxygen reaction rates significantly affect their corresponding concentrations in the IVD (Figure 5.8). Increasing the metabolic rates in the IVD leads to an increase in lactate levels and other by-products that are noxious to cells (Ito and Creemers 2013; Zhang et al. 2016). Aging and dehydration of the IVD, which can vary between patients, are two factors than can affect metabolic rates due to changes in cellularity and water content (Sakai and Grad 2015). Therefore, characterizing metabolic rates in patient IVDs with different degeneration grades may improve nutrient availability and solute transport modeling in the IVD. Different types of chemical exchange saturation transfer (CEST) MRI were developed to measure metabolism *in vivo.* CEST has also been optimized for human patients by significantly reducing the scan time to 5 minutes, rendering it viable to investigate metabolism in the IVD (Zhou et al. 2017).[31]P saturation transfer (ST) has been used to measure metabolic rates non-invasively in the human heart and brain (Du et al. 2007; Balaban, Kantor, and Ferretti 1983; Wang et al. 2016). This technique provides high spatial resolution and sensitivity in measuring energy metabolism in organs by assessing the conversion of phosphocreatine in creatine kinase reactions (Zhou et al. 2017; Du et al. 2007; Shoubridge, Briggs, and Radda 1982; Balaban, Kantor, and Ferretti 1983). Magnetic resonance spectroscopy (MRS) has been applied to complement MRI techniques by providing information on the chemical changes that occur within the disc as it degenerates. For example, MRS has been demonstrated to quantify metabolites, specifically lactate and PG as markers for pain in the disc (Mwale, Iatridis, and Antoniou 2008). In a 2019 study, researchers were able to optimize MRS to accurately assess the integrity of the extracellular matrix by analyzing contents of PG, carbohydrates, and acidity (alanine and lactate) (Zeng et al. 2019). Incorporating these techniques into the modeling of solute transport have the potential in generating more accurate nutrient distributions in patient IVDs.

We also found a significant effect of AF and CEP diffusivities on solute concentrations in the IVD and the inner AF (Figure 5.8). We expected the AF's diffusivity to play a substantial role in determining critical nutrient levels because they lie in the inner AF. The effect of CEP diffusivity on the IVD's nutrient status has been addressed by several studies (Nachemson et al. 1970; Malcolmson 1935; Bush 1934; Albert 1942; Shutkin 1952). The CEP has a large number of channels and shares the largest surface area with the NP, which allows for a larger solute flux (Urban et al. 1977; Naresh-Babu et al. 2016; Wong et al. 2019; Silverman 1954; Urban, Holm, and Maroudas 1978; Albert 1942; Nachemson et al. 1970; Naylor, Happey, and Macrae 1955; King 1959; Urban and Maroudas 1979; Malandrino et al. 2014). In addition, the CEP is relatively thin (~2 mm) and porous, which facilitates better transport of molecules (Malandrino et al. 2014). Due to the significant effects of AF and CEP diffusivities on solute concentrations in the inner AF and throughout the IVD, it is essential to include high-resolution ADC maps for both anatomical parts. Such maps have been generated to study variations in AF diffusivity in relation to degeneration grade and location within the AF (posterior, anterior, inner, and outer) (Antoniou et al. 2004; Dao et al. 2013; Li et al. 2018; Antoniou et al. 2013).

Interestingly, changes in NP diffusivity had a negligible impact on all measured metrics except for maximum lactate (Figure 5.8-B). The NP facilitates better diffusion due to its biochemical structure and large water content (Dao et al. 2013). Therefore, the chosen 50% change in NP diffusivity was not limiting to solute transport.

Cell density is shown to be a predictor for maximum lactate and average oxygen concentration (Figure 5.8-B and C). Interestingly, cell density was not considered a predictor for glucose levels despite the strong correlation between cell density and maximum lactate (Figure 5.8-B). We expected changes in cell density to substantially affect nutrient distributions in the IVD because it has been shown to alter metabolic rates (Magnier et al. 2009). It is suspected that the 150% dose of cells used in this model, which raises total NP cell density to 6,000 cells/mm^3, is too low to affect nutrient distribution compared to the highest dose used in some clinical trials which would increase total NP cell density to 11,000 cells/mm^3 (Figure 5.10) (Sakai and Andersson 2015; Sakai and Grad 2015). In addition, the study only assessed changes to the NP's cell density and overlooked any changes in the AF and CEP because cell injections often target the NP (Sakai and Andersson 2015; Sakai and Grad 2015; Tong et al. 2017; Schol and Sakai 2019). It is also possible that because healthy discs were used for the SA that changes in cell densities did not have a large

impact on IVD nutrient status. Further tests would need to be conducted to investigate the effects of changing cell density in the AF, and the CEP. Another untested but critical comparison is the effect of localized cell injection in the NP versus an increase in total NP cell density which could be useful in understanding the effects of cell delivery to various parts of the IVD.
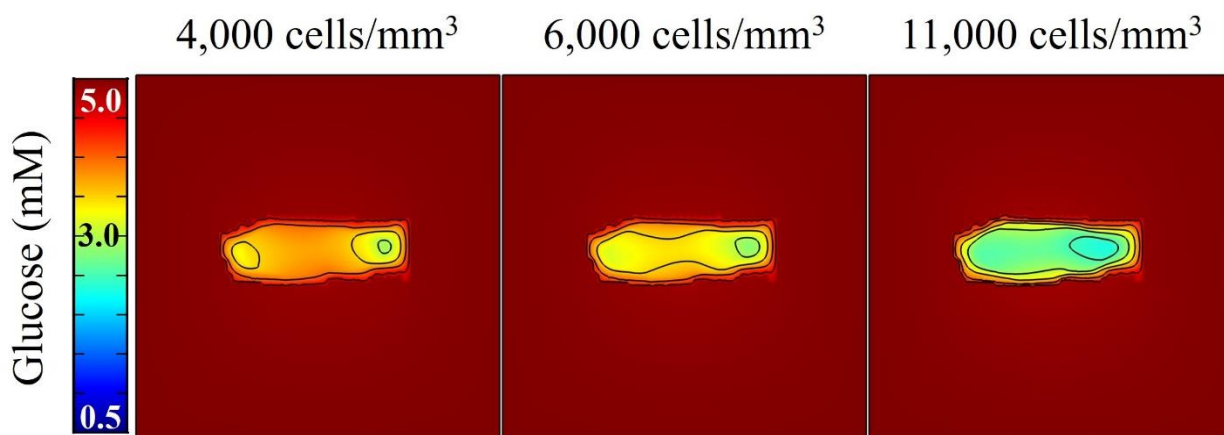
Figure 5.10. Comparison of increasing the nucleus pulposus cell density on glucose distribution mM in patient # 2, grade 3. Cell density of 4000 cells/mm^3 was used as a baseline value. 6000 cells/mm^3 represents a 150% increase. While 11 000 cells/mm^3 was the highest dose reported to be used by clinical trials.

Patient demographics showed IVD level to significantly vary between grade 2 and the remaining grades. However, disc level had no significant effect on minimum or maximum solute levels in the IVD (Kruskal Wallis, $p < 0.05$). The constant parameters chosen for this study, e.g., water content, cell density, etc., vary with IVD degeneration. Therefore, observed solute variation between groups could be attributed to degeneration grades. This makes sense given that healthier discs have shown to have better ADC values (Belykh et al. 2017). Lastly, nutrient distributions in patient outliers could not be predicted based on the degeneration level alone or IVD pathology, as was the case for patient #18. These IVDs had a specific disc shape and size, that led to specific nutrient distributions.

Last, the model predicted that modifications to disc size, metabolic rates, and the diffusivities of the AF and CEP greatly influenced the IVD's nutrient status (Figure 5.8). Therefore, future modeling techniques that aim to investigate the IVD's nutrient status should consider tailoring these parameters to the individual patient's IVD.

5.5.4 Model limitations

Some of the limitations to this model included possible artifacts in IVD masks. For example, IVD #14 in grade 3 did not exhibit abnormal levels of solutes in the disc due to a defect in the AF mask. This defect did not completely enclose the NP, and this significantly enhanced diffusion through the disc. This mask defect was a limitation of the model which inaccurately led to low levels of lactate and high levels of glucose and oxygen in discs with large areas.

Furthermore, the only model parameters made patient-specific were disc geometry and NP diffusion coefficients. There are many other parameters that could be expected to vary between patients that were not included in this model. A list of parameters and the basis of expected variation between patients was summarized in Table 5.7.

Table 5.7. Summary of current vs expected variations in solute transport parameters. The specificity of each model parameter is given as well as the expected source of variation for each parameter. Patient specific factors are highlighted in grey.

Parameter	Current Model Specificity	Expected Variation Between Patients
IVD Morphology	Patient specific	Expected to vary based on patient height, biochemical composition, gross defects, degeneration, mechanical loading, and level
AF solute diffusion coefficients	Pfirrmann specific	Expected to vary based on biochemical composition, location, mechanical loading, and gross defects
CEP solute diffusion coefficients	Pfirrmann specific	Expected to vary based on biochemical composition, location, mechanical loading, and gross defects
NP solute diffusion coefficients	Patient specific	Expected to vary based on biochemical composition, location, and gross defects
AF solute boundary conditions	Uniform	Expected to vary based on capillary density, and solute perfusion

Table 5.7. Summary of current vs expected variations in solute transport parameters. The specificity of each model parameter is given as well as the expected source of variation for each parameter. Patient specific factors are highlighted in grey. (Continued)

Parameter	Current Model Specificity	Expected Variation Between Patients
CEP solute boundary conditions	Uniform	Expected to vary based on thickness of the boney endplate, capillary density, number of marrow cavities and gross abnormalities
Solute initial condition	Uniform	Expected to vary based on IVD physiological conditions
AF diffusivity	Pfirrmann specific	Expected to vary based on spinal morphology, biochemical composition, location, mechanical loading, and pathophysiology
CEP diffusivity	Pfirrmann specific	Expected to vary based on spinal morphology, location, and endplate pathophysiology, including capillary density, lesions, and calcification
NP diffusivity	Pfirrmann specific	Expected to vary based on spinal morphology, location, biochemical composition, and pathophysiology
AF cell density	Uniform	Expected to vary based on glucose and oxygen availability, acidity, location, and patient age
CEP cell density	Uniform	Expected to vary based on glucose and oxygen availability, acidity, location, and patient age
NP cell density	Uniform	Expected to vary based on glucose and oxygen availability, acidity, location, and patient age
Cell Metabolism	Based on glucose/oxygen concentrations	Expected to vary more widely based on signaling factors, senescence, and patient age
Water Content	Pfirrmann specific	Expected to vary based on biochemical composition, location, mechanical loading, and pathophysiology

Such limitations include applying constant homogeneous cell density between the different degeneration grades. Liebscher et al. has shown that cell density varies even within the same anatomical part of the IVD; however, the same study suggested cell density in the AF, CEP, and NP does not correlate to disc degeneration caused by normal aging (Liebscher et al. 2011). Still, this limitation significantly altered model results, as demonstrated by the SA. Cell density is expected to decrease with increasing degeneration grade, which would lead to reduced metabolic rates. Studies reported changes in the IVD's metabolic rates to alter glycolysis rates and change

the levels of by-products including lactate that could lead to further degeneration of the IVD (Ito and Creemers 2013; Zhang et al. 2016; Sakai and Grad 2015).

This model also assumed constant water content in the AF and CEP. However, studies demonstrated variations in water content based on location within the same tissue, which affected local solute diffusion (Wu et al. 2016). Future models could eliminate this limitation by including a water content map for each part of the IVD. Antoniou et. al., used different MR modalities (i.e., T_1, T_2, $T_{1\rho}$, MTR and ADC) to calculate water content in the NP and AF (Mwale et al. 2008). Applying this method in future iterations of the model should provide more accurate and specific model results. It was also important to note that a variation exists in published values for water content % and cell density (Table 5.8), and thus utilizing MR scans to personalize some of these parameters, e.g., water content, could produce more accurate results. Also, the model did not consider other factors that can impact nutrient transport such as changes in load, charge density and varying cellular metabolic rates(Gullbrand, Peterson, Mastropolo, et al. 2015; Sampson, Sylvia, and Fields 2019; Tourell et al. 2017).

Table 5.8. Literature values of water content and cell density showing various values reported and used for IVD modeling. An * indicated the high value for the inner AF and the low value for the outer AF. A # indicated a high value for healthy young individuals, while the low value for older individuals.

	Water Content (%)			Cell Density $\times 10^3$ (1/mm^3)			References
Model	CEP	AF	NP	CEP	AF	NP	
3D model	-	70-85*	85	-	9	4	Zhu(Zhu et al. 2016)
3D model	60	66-73*	80	15	4-16	4	A.Shirazi(Shirazi-Adl, Taheri, and Urban 2010)
	-	66	86	-	-	-	Iatridis(Iatridis et al. 2007)
3D model	-	-	85	-	9	4	Soukane(Soukane, Shirazi-Adl, and Urban 2005)
Human *in vivo*	-	-	-	15	9	4	Bartels(Bartels et al. 1998)
Human *in vitro*	-	-	75-85*	-	-	-	Urban(Urban and McMullin 1988)
Human *in vivo*	-	73-80#	76-90#	-	-	-	Kraemer(Kraemer, Kolditz, and Gowin 1985)

This model also simplified factors affecting solute perfusion to include calcification of the CEP only, which was modeled by decreasing CEP water content by 18% (Jackson, Huang, and Gu 2011). It has been shown that disc degeneration alters the number of capillaries contacting the endplates (Benneker et al. 2005). Such changes in solute availability at the disc endplates could

invalidate our assumption of constant boundary conditions across different Pfirrmann grades. Future work would seek to evaluate endplate capillary densities *in vivo*.

Time of day when MR scans were acquired was not controlled. This limitation could considerably affect solute diffusion in the disc because different patient postures and activities during the day were shown to affect disc geometry and water content (Malko, Hutton, and Fajman 2002). For example, MR scans of IVDs taken in the morning showed higher water content and increased IVD height (Belavý et al. 2011; Malko, Hutton, and Fajman 2002) – two factors that were demonstrated by this model to significantly impact solute diffusion in the disc (Table 6). In addition, this model was created in 2D instead of 3D. This allowed for the collection of a large MRI data set, which would have been prohibitive with the longer scan time associated with more slices. Furthermore, it decreased model computation times. While the model showcased variations in solute distributions between patients and degeneration grades, the results were not validated experimentally. As with other models that have been developed, it was challenging to validate model results due to a knowledge gap regarding important parameters that were needed to model solute distribution in patients. The SA performed in this study had successfully identified an important set of parameters that needed to be obtained in order to validate the results experimentally. One of which was the metabolic rates for lactate in the IVD. As discussed earlier, changes to the metabolic rates of lactate was shown to alter solute distribution in the IVD, and it was correlated to maximum lactate and minimum glucose (Figure 3.8). Studies reported changes in metabolic rates, especially an increase in lactate production to create harsh IVD microenvironments that led to tissue degeneration (Ito and Creemers 2013; Zhang et al. 2016).

Despite the model's limitations, the results showed general trends that were consistent across all patients which demonstrated consistent model performance. The specific trends of each patient were unique suggesting successful integration of patient data. Comparison of the specific trends for each solute across all patients showed distinct patterns that highlighted the importance of the individual morphology and physiological conditions of each disc, even among discs of the same Pfirrmann grade. Pending further development, and inclusion of more patient specific factors, this model may allow clinicians to account for the impact of increasing cell activity or density in a nutrient-starved environment. By iteratively increasing cell concentrations until a certain threshold has been reached the maximum capacity of a specific disc for new cells cell be determined. If levels were already low enough to indicate cell death, these patients could be

excluded as candidates for cell injection-based therapies and advised to seek traditional treatments. The patients identified as poor candidates for cell therapies may be able to seek other novel therapies as they become available.

5.6 Conclusion

This work described a method for incorporating patient data into a nutrient transport model of the intervertebral disc (IVD). Results showed a decrease in glucose and oxygen concentrations accompanied with an increase in extreme lactate levels in the disc as it degenerates. Disc size, AF and CEP diffusivities, metabolic rates, and cell density had significant impacts on solute distributions in the IVD. The model also demonstrated distinct diffusion behavior between patients, even between discs of the same Pfirrmann grade. The importance of the distinct disc morphologies and physiological environments of each patient to the diffusion gradients in the disc was readily apparent. Patient-specific models could allow clinicians to further personalize treatments to the patient, e.g., choosing the appropriate dose of cells to be injected into the IVD. This functionality indicated that patient-specific models could prove valuable in a clinical setting when predicting patient outcomes or treatment options.

In the following chapter, I present concluding remarks outlining the significance and application of the work presented in this dissertation. I also propose future study directions to improve the cryopreservation protocol and the finite element model.

5.7 Acknowledgements

5.8 References

Al-Raoush, Riyadh I., and Iman T. Madhoun. 2017. 'TORT3D: A MATLAB code to compute geometric tortuosity from 3D images of unconsolidated porous media', *Powder Technology*, 320: 99-107.

Albert, M. 1942. 'Calcification of the Intervertebral Disks', *Br Med J*, 1: 666-8.

Andersson, G. B. 1999. 'Epidemiological features of chronic low-back pain', *Lancet*, 354: 581-5.

Antoniou, J., C. N. Demers, G. Beaudoin, T. Goswami, F. Mwale, M. Aebi, and M. Alini. 2004. 'Apparent diffusion coefficient of intervertebral discs related to matrix composition and integrity', *Magn Reson Imaging*, 22: 963-72.

Antoniou, J., L. M. Epure, A. J. Michalek, M. P. Grant, J. C. Iatridis, and F. Mwale. 2013. 'Analysis of quantitative magnetic resonance imaging and biomechanical parameters on human discs with different grades of degeneration', *J Magn Reson Imaging*, 38: 1402-14.

Balaban, R. S., H. L. Kantor, and J. A. Ferretti. 1983. 'In vivo flux between phosphocreatine and adenosine triphosphate determined by two-dimensional phosphorous NMR', *J Biol Chem*, 258: 12787-9.

Bartels, E. M., J. C. Fairbank, C. P. Winlove, and J. P. Urban. 1998. 'Oxygen and lactate concentrations measured in vivo in the intervertebral discs of patients with scoliosis and back pain', *Spine (Phila Pa 1976)*, 23: 1-7; discussion 8.

Belavý, Daniel L., Gabriele Armbrecht, Carolyn A. Richardson, Dieter Felsenberg, and Julie A. Hides. 2011. 'Muscle Atrophy and Changes in Spinal Morphology: Is the Lumbar Spine Vulnerable After Prolonged Bed-Rest?', *Spine*, 36: 137-45.

Belykh, E., A. A. Kalinin, A. A. Patel, E. J. Miller, M. A. Bohl, I. A. Stepanov, L. A. Bardonova, T. Kerimbaev, A. O. Asantsev, M. B. Giers, M. C. Preul, and V. A. Byvaltsev. 2017. 'Apparent diffusion coefficient maps in the assessment of surgical patients with lumbar spine degeneration', *PLoS One*, 12: e0183697.

Benneker, Lorin M., Paul F. Heini, Mauro Alini, Suzanne E. Anderson, and Keita Ito. 2005. '2004 Young Investigator Award Winner: Vertebral Endplate Marrow Contact Channel Occlusions and Intervertebral Disc Degeneration', *Spine*, 30: 167-73.

Bertram, H., M. Kroeber, H. Wang, F. Unglaub, T. Guehring, C. Carstens, and W. Richter. 2005. 'Matrix-assisted cell transfer for intervertebral disc cell therapy', *Biochem Biophys Res Commun*, 331: 1185-92.

Bibby, S. R., J. C. Fairbank, M. R. Urban, and J. P. Urban. 2002. 'Cell viability in scoliotic discs in relation to disc deformity and nutrient levels', *Spine (Phila Pa 1976)*, 27: 2220-8; discussion 27-8.

Bibby, S. R., D. A. Jones, R. M. Ripley, and J. P. Urban. 2005. 'Metabolism of the intervertebral disc: effects of low levels of oxygen, glucose, and pH on rates of energy metabolism of bovine nucleus pulposus cells', *Spine (Phila Pa 1976)*, 30: 487-96.

Bibby, S. R., and J. P. Urban. 2004. 'Effect of nutrient deprivation on the viability of intervertebral disc cells', *Eur Spine J*, 13: 695-701.

Brinjikji, W., F. E. Diehn, J. G. Jarvik, C. M. Carr, D. F. Kallmes, M. H. Murad, and P. H. Luetmer. 2015. 'MRI Findings of Disc Degeneration are More Prevalent in Adults with Low Back Pain than in Asymptomatic Controls: A Systematic Review and Meta-Analysis', *AJNR Am J Neuroradiol*, 36: 2394-9.

Bush, G. B. 1934. 'The Clinical Importance of the Intervertebral Discs, with Special Reference to Nuclear Prolapses', *Bristol Med Chir J (1883)*, 51: 173-82.

Byvaltsev, V. A., S. I. Kolesnikov, L. A. Bardonova, E. G. Belykh, L. I. Korytov, M. B. Giers, and M. C. Preul. 2018. 'Assessment of Lactate Production and Proteoglycans Synthesis by the Intact and Degenerated Intervertebral Disc Cells under the Influence of Activated Macrophages: an In Vitro Study', *Bulletin of Experimental Biology and Medicine*, 166: 170-73.

Byvaltsev, V. A., S. I. Kolesnikov, E. G. Belykh, I. A. Stepanov, A. A. Kalinin, L. A. Bardonova, N. P. Sudakov, I. V. Klimenkov, S. B. Nikiforov, A. V. Semenov, D. V. Perfil'ev, I. V. Bespyatykh, S. L. Antipina, M. Giers, and M. Prul. 2017. 'Complex Analysis of Diffusion Transport and Microstructure of an Intervertebral Disk', *Bulletin of Experimental Biology and Medicine*, 164: 223-28.

Centeno, C., J. Markle, E. Dodson, I. Stemper, C. J. Williams, M. Hyzy, T. Ichim, and M. Freeman. 2017. 'Treatment of lumbar degenerative disc disease-associated radicular pain with culture-expanded autologous mesenchymal stem cells: a pilot study on safety and efficacy', *J Transl Med*, 15: 197.

Coric, D., K. Pettine, A. Sumich, and M. O. Boltes. 2013. 'Prospective study of disc repair with allogeneic chondrocytes presented at the 2012 Joint Spine Section Meeting', *J Neurosurg Spine*, 18: 85-95.

Dao, Tien Tuan, Philippe Pouletaut, Ludovic Robert, Pascal Aufaure, Fabrice Charleux, and Marie-Christine Ho Ba Tho. 2013. 'Quantitative analysis of annulus fibrosus and nucleus pulposus derived from T2 mapping, diffusion-weighted and diffusion tensor MR imaging', *Computer Methods in Biomechanics and Biomedical Engineering: Imaging & Visualization*, 1: 138-46.

Diamant, B., J. Karlsson, and A. Nachemson. 1968. 'Correlation between lactate levels and pH in discs of patients with lumbar rhizopathies', *Experientia*, 24: 1195-6.

Du, Fei, Xiao-Hong Zhu, Hongyan Qiao, Xiaoliang Zhang, and Wei Chen. 2007. 'Efficient in vivo 31P magnetization transfer approach for noninvasively determining multiple kinetic parameters and metabolic fluxes of ATP metabolism in the human brain', *Magnetic Resonance in Medicine*, 57: 103-14.

Elwinger, Fredrik, Payam Pourmand, and István Furó. 2017. 'Diffusive Transport in Pores. Tortuosity and Molecular Interaction with the Pore Wall', *The Journal of Physical Chemistry C*, 121: 13757-64.

Ferguson, S. J., K. Ito, and L. P. Nolte. 2004. 'Fluid flow and convective transport of solutes within the intervertebral disc', *J Biomech*, 37: 213-21.

Giers, Morgan B., Liudmila Bardonova, Kyle Eyster, Vadim Byvaltsev, and Mark C. Preul. 2018. 'APOPTOSIS, NUTRITION, AND METABOLISM OF TRANSPLANTED INTERVERTEBRAL DISC CELLS', *Coluna/Columna*, 17: 317-22.

Gillispie, Gregory, Sang Jin Lee, and James J. Yoo. 2019. 'Bone and Cartilage Tissue Engineering.' in Rui L. Reis (ed.), *Encyclopedia of Tissue Engineering and Regenerative Medicine* (Academic Press: Oxford).

Grunhagen, T., A. Shirazi-Adl, J. C. Fairbank, and J. P. Urban. 2011. 'Intervertebral disk nutrition: a review of factors influencing concentrations of nutrients and metabolites', *Orthop Clin North Am*, 42: 465-77, vii.

Grunhagen, Thijs, Geoffrey Wilde, Dahbia Mokhbi Soukane, Saeed A. Shirazi-Adl, and Jill P.G. Urban. 2006. 'Nutrient Supply and Intervertebral Disc Metabolism', *JBJS*, 88: 30-35.

Gullbrand, S. E., J. Peterson, J. Ahlborn, R. Mastropolo, A. Fricker, T. T. Roberts, M. Abousayed, J. P. Lawrence, J. C. Glennon, and E. H. Ledet. 2015. 'ISSLS Prize Winner: Dynamic Loading-Induced Convective Transport Enhances Intervertebral Disc Nutrition', *Spine (Phila Pa 1976)*, 40: 1158-64.

Gullbrand, S. E., J. Peterson, R. Mastropolo, T. T. Roberts, J. P. Lawrence, J. C. Glennon, D. J. DiRisio, and E. H. Ledet. 2015. 'Low rate loading-induced convection enhances net transport into the intervertebral disc in vivo', *Spine J*, 15: 1028-33.

Hohaus, C., T. M. Ganey, Y. Minkus, and H. J. Meisel. 2008. 'Cell transplantation in lumbar spine disc degeneration disease', *Eur Spine J*, 17 Suppl 4: 492-503.

Hoy, D., L. March, P. Brooks, F. Blyth, A. Woolf, C. Bain, G. Williams, E. Smith, T. Vos, J. Barendregt, C. Murray, R. Burstein, and R. Buchbinder. 2014. 'The global burden of low back pain: estimates from the Global Burden of Disease 2010 study', *Ann Rheum Dis*, 73: 968-74.

Huang, Y. C., J. P. Urban, and K. D. Luk. 2014. 'Intervertebral disc regeneration: do nutrients lead the way?', *Nat Rev Rheumatol*, 10: 561-6.

Iatridis, J. C., J. J. MacLean, M. O'Brien, and I. A. Stokes. 2007. 'Measurements of proteoglycan and water content distribution in human lumbar intervertebral discs', *Spine (Phila Pa 1976)*, 32: 1493-7.

Ishihara, H., and J. P. Urban. 1999. 'Effects of low oxygen concentrations and metabolic inhibitors on proteoglycan and protein synthesis rates in the intervertebral disc', *J Orthop Res*, 17: 829-35.

Ito, Keita, and Laura Creemers. 2013. 'Mechanisms of Intervertebral Disk Degeneration/Injury and Pain: A Review', *Global Spine Journal*, 3: 145-51.

Iwashina, T., J. Mochida, D. Sakai, Y. Yamamoto, T. Miyazaki, K. Ando, and T. Hotta. 2006. 'Feasibility of using a human nucleus pulposus cell line as a cell source in cell transplantation therapy for intervertebral disc degeneration', *Spine (Phila Pa 1976)*, 31: 1177-86.

Jackson, A. R., C. Y. Huang, and W. Y. Gu. 2011. 'Effect of endplate calcification and mechanical deformation on the distribution of glucose in intervertebral disc: a 3D finite element study', *Comput Methods Biomech Biomed Engin*, 14: 195-204.

Jackson, A. R., T. Y. Yuan, C. Y. Huang, and W. Y. Gu. 2009. 'A conductivity approach to measuring fixed charge density in intervertebral disc tissue', *Ann Biomed Eng*, 37: 2566-73.

Jackson, Alicia R., Tai-Yi Yuan, Chun-Yuh Huang, Mark D. Brown, and Wei Yong Gu. 2012. 'Nutrient Transport in Human Annulus Fibrosus is Affected by Compressive Strain and Anisotropy', *Annals of Biomedical Engineering*, 40: 2551-58.

Jackson, Alicia R., Tai-Yi Yuan, Chun-Yuh C. Huang, Francesco Travascio, and Wei Yong Gu. 2008. 'Effect of Compression and Anisotropy on the Diffusion of Glucose in Annulus Fibrosus', *Spine*, 33.

Junger, S., B. Gantenbein-Ritter, P. Lezuo, M. Alini, S. J. Ferguson, and K. Ito. 2009. 'Effect of limited nutrition on in situ intervertebral disc cells under simulated-physiological loading', *Spine (Phila Pa 1976)*, 34: 1264-71.

Kihara, T., J. Ito, and J. Miyake. 2013. 'Measurement of biomolecular diffusion in extracellular matrix condensed by fibroblasts using fluorescence correlation spectroscopy', *PLoS One*, 8: e82382.

King, T. 1959. 'Another look at the problem of lumbo-sacral pain and sciatica', *Med J Aust*, 46: 8-12.

Kraemer, J., D. Kolditz, and R. Gowin. 1985. 'Water and electrolyte content of human intervertebral discs under variable load', *Spine (Phila Pa 1976)*, 10: 69-71.

Kuo, Y. W., Y. C. Hsu, I. T. Chuang, P. H. Chao, and J. L. Wang. 2014. 'Spinal traction promotes molecular transportation in a simulated degenerative intervertebral disc model', *Spine (Phila Pa 1976)*, 39: E550-6.

Le Bihan, D., E. Breton, D. Lallemand, P. Grenier, E. Cabanis, and M. Laval-Jeantet. 1986. 'MR imaging of intravoxel incoherent motions: application to diffusion and perfusion in neurologic disorders', *Radiology*, 161: 401-7.

Li, Long-Yang, Xiao-Lin Wu, Richard J. Roman, Fan Fan, Chen-Sheng Qiu, and Bo-Hua Chen. 2018. 'Diffusion-weighted 7.0T Magnetic Resonance Imaging in Assessment of Intervertebral Disc Degeneration in Rats', *Chinese medical journal*, 131: 63-68.

Liebscher, Thomas, Mathias Haefeli, Karin Wuertz, Andreas G. Nerlich, and Norbert Boos. 2011. 'Age-Related Variation in Cell Density of Human Lumbar Intervertebral Disc', *Spine*, 36: 153-59.

Lyons, G., S. M. Eisenstein, and M. B. Sweet. 1981. 'Biochemical changes in intervertebral disc degeneration', *Biochim Biophys Acta*, 673: 443-53.

Magnier, C., O. Boiron, S. Wendling-Mansuy, P. Chabrand, and V. Deplano. 2009. 'Nutrient distribution and metabolism in the intervertebral disc in the unloaded state: a parametric study', *J Biomech*, 42: 100-8.

Malandrino, A., D. Lacroix, C. Hellmich, K. Ito, S. J. Ferguson, and J. Noailly. 2014. 'The role of endplate poromechanical properties on the nutrient availability in the intervertebral disc', *Osteoarthritis and Cartilage*, 22: 1053-60.

Malandrino, A., J. Noailly, and D. Lacroix. 2011. 'The effect of sustained compression on oxygen metabolic transport in the intervertebral disc decreases with degenerative changes', *PLoS Comput Biol*, 7: e1002112.

Malandrino, Andrea, José M. Pozo, Isaac Castro-Mateos, Alejandro F. Frangi, Marc M. van Rijsbergen, Keita Ito, Hans-Joachim Wilke, Tien Tuan Dao, Marie-Christine Ho Ba Tho, and Jérôme Noailly. 2015. 'On the Relative Relevance of Subject-Specific Geometries and Degeneration-Specific Mechanical Properties for the Study of Cell Death in Human Intervertebral Disk Models', *Frontiers in Bioengineering and Biotechnology*, 3.

Malcolmson, P. H. 1935. 'Radiologic Study of the Development of the Spine and Pathologic Changes of the Intervertebral Disc', *Radiology*, 25: 98-104.

Malko, John A., William C. Hutton, and William A. Fajman. 2002. 'An In Vivo MRI Study of the Changes in Volume (and Fluid Content) of the Lumbar Intervertebral Disc After Overnight Bed Rest and During an 8-Hour Walking Protocol', *Clinical Spine Surgery*, 15: 157-63.

Maroudas, A., R. A. Stockwell, A. Nachemson, and J. Urban. 1975. 'Factors involved in the nutrition of the human lumbar intervertebral disc: cellularity and diffusion of glucose in vitro', *J Anat*, 120: 113-30.

McMurtrey, R. J. 2016. 'Analytic Models of Oxygen and Nutrient Diffusion, Metabolism Dynamics, and Architecture Optimization in Three-Dimensional Tissue Constructs with Applications and Insights in Cerebral Organoids', *Tissue Eng Part C Methods*, 22: 221-49.

Meisel, H. J., T. Ganey, W. C. Hutton, J. Libera, Y. Minkus, and O. Alasevic. 2006a. 'Clinical experience in cell-based therapeutics: intervention and outcome', *Eur Spine J*, 15 Suppl 3: S397-405.

Meisel, Hans Joerg, Timothy Ganey, William C. Hutton, Jeanette Libera, Yvonne Minkus, and Olivera Alasevic. 2006b. 'Clinical experience in cell-based therapeutics: intervention and outcome', *European spine journal : official publication of the European Spine Society, the European Spinal Deformity Society, and the European Section of the Cervical Spine Research Society*, 15 Suppl 3: S397-S405.

Mokhbi Soukane, D., A. Shirazi-Adl, and J. P. Urban. 2009. 'Investigation of solute concentrations in a 3D model of intervertebral disc', *Eur Spine J*, 18: 254-62.

Mokhbi Soukane, D.;, A.; Shirazi-Adl, and J. P. G.; Urban. 2007. 'Computation of coupled diffusion of oxygen, glucose and lactic acid in an intervertebral disc', *Journal of Biomechanics*, 40: 2645-54.

Mwale, F., J. C. Iatridis, and J. Antoniou. 2008. 'Quantitative MRI as a diagnostic tool of intervertebral disc matrix composition and integrity', *Eur Spine J*, 17 Suppl 4: 432-40.

Mwale, Fackson, Caroline N. Demers, Arthur J. Michalek, Gilles Beaudoin, Tapas Goswami, Lorne Beckman, James C. Iatridis, and John Antoniou. 2008. 'Evaluation of quantitative magnetic resonance imaging, biochemical and mechanical properties of trypsin-treated intervertebral discs under physiological compression loading', *Journal of magnetic resonance imaging : JMRI*, 27: 563-73.

Nachemson, A., T. Lewin, A. Maroudas, and M. A. Freeman. 1970. 'In vitro diffusion of dye through the end-plates and the annulus fibrosus of human lumbar inter-vertebral discs', *Acta Orthop Scand*, 41: 589-607.

Nachemson, Alf. 1969. 'Intradiscal Measurements of pH in Patients with Lumbar Rhizopathies', *Acta Orthopaedica Scandinavica*, 40: 23-42.

Naresh-Babu, J., G. Neelima, S. Reshma Begum, and V. Siva-Leela. 2016. 'Diffusion characteristics of human annulus fibrosus-a study documenting the dependence of annulus fibrosus on end plate for diffusion', *Spine J*, 16: 1007-14.

Natarajan, R. N., J. R. Williams, and G. B. Andersson. 2006. 'Modeling changes in intervertebral disc mechanics with degeneration', *J Bone Joint Surg Am*, 88 Suppl 2: 36-40.

Naylor, A., F. Happey, and T. Macrae. 1955. 'Changes in the human intervertebral disc with age: a biophysical study', *J Am Geriatr Soc*, 3: 964-73.

Nomura, T., J. Mochida, M. Okuma, K. Nishimura, and K. Sakabe. 2001. 'Nucleus pulposus allograft retards intervertebral disc degeneration', *Clin Orthop Relat Res*: 94-101.

Noriega, D. C., F. Ardura, R. Hernandez-Ramajo, M. A. Martin-Ferrero, I. Sanchez-Lite, B. Toribio, M. Alberca, V. Garcia, J. M. Moraleda, A. Sanchez, and J. Garcia-Sancho. 2017. 'Intervertebral Disc Repair by Allogeneic Mesenchymal Bone Marrow Cells: A Randomized Controlled Trial', *Transplantation*, 101: 1945-51.

Ohtori, S., G. Inoue, M. Miyagi, and K. Takahashi. 2015. 'Pathomechanisms of discogenic low back pain in humans and animal models', *Spine J*, 15: 1347-55.

Okuma, M., J. Mochida, K. Nishimura, K. Sakabe, and K. Seiki. 2000. 'Reinsertion of stimulated nucleus pulposus cells retards intervertebral disc degeneration: an in vitro and in vivo experimental study', *J Orthop Res*, 18: 988-97.

Orozco, L., R. Soler, C. Morera, M. Alberca, A. Sanchez, and J. Garcia-Sancho. 2011. 'Intervertebral disc repair by autologous mesenchymal bone marrow cells: a pilot study', *Transplantation*, 92: 822-8.

Pardo-Alonso, Samuel, Jerome Vicente, Eusebio Solórzano, Miguel Ángel Rodriguez-Perez, and Dirk Lehmhus. 2014. 'Geometrical Tortuosity 3D Calculations in Infiltrated Aluminium Cellular Materials', *Procedia Materials Science*, 4: 145-50.

Pfirrmann, Christian W. A., Alexander Metzdorf, Marco Zanetti, Juerg Hodler, and Norbert Boos. 2001. 'Magnetic Resonance Classification of Lumbar Intervertebral Disc Degeneration', *Spine*, 26: 1873-78.

Renkin, E. M. 1954. 'Filtration, diffusion, and molecular sieving through porous cellulose membranes', *J Gen Physiol*, 38: 225-43.

Richardson, S. M., G. Kalamegam, P. N. Pushparaj, C. Matta, A. Memic, A. Khademhosseini, R. Mobasheri, F. L. Poletti, J. A. Hoyland, and A. Mobasheri. 2016. 'Mesenchymal stem cells in regenerative medicine: Focus on articular cartilage and intervertebral disc regeneration', *Methods*, 99: 69-80.

Sakai, D., and G. B. Andersson. 2015. 'Stem cell therapy for intervertebral disc regeneration: obstacles and solutions', *Nat Rev Rheumatol*, 11: 243-56.

Sakai, D., and J. Schol. 2017. 'Cell therapy for intervertebral disc repair: Clinical perspective', *J Orthop Translat*, 9: 8-18.

Sakai, Daisuke, and Sibylle Grad. 2015. 'Advancing the cellular and molecular therapy for intervertebral disc disease', *Advanced Drug Delivery Reviews*, 84: 159-71.

Sampson, S. L., M. Sylvia, and A. J. Fields. 2019. 'Effects of dynamic loading on solute transport through the human cartilage endplate', *J Biomech*, 83: 273-79.

Sato, M., T. Asazuma, M. Ishihara, M. Ishihara, T. Kikuchi, M. Kikuchi, and K. Fujikawa. 2003. 'An experimental study of the regeneration of the intervertebral disc with an allograft of cultured annulus fibrosus cells using a tissue-engineering method', *Spine (Phila Pa 1976)*, 28: 548-53.

Schol, Jordy, and Daisuke Sakai. 2019. 'Cell therapy for intervertebral disc herniation and degenerative disc disease: clinical trials', *International Orthopaedics*, 43: 1011-25.

Sélard, E., A. Shirazi-Adl, and J. P. Urban. 2003. 'Finite element study of nutrient diffusion in the human intervertebral disc', *Spine (Phila Pa 1976)*, 28: 1945-53; discussion 53.

Shirazi-Adl, A., M. Taheri, and J. P. Urban. 2010. 'Analysis of cell viability in intervertebral disc: Effect of endplate permeability on cell population', *J Biomech*, 43: 1330-6.

Shoubridge, E.A., R.W. Briggs, and G.K. Radda. 1982. '31P NMR saturation transfer measurements of the steady state rates of creatine kinase and ATP synthetase in the rat brain', *FEBS Letters*, 140: 288-92.

Shutkin, N. M. 1952. 'Syndrome of the degenerated intervertebral disc', *Am J Surg*, 84: 162-71.

Silverman, F. N. 1954. 'Calcification of the intervertebral disks in childhood', *Radiology*, 62: 801-16.

Smith, L. J., L. Silverman, D. Sakai, C. L. Le Maitre, R. L. Mauck, N. R. Malhotra, J. C. Lotz, and C. T. Buckley. 2018. 'Advancing cell therapies for intervertebral disc regeneration from the lab to the clinic: Recommendations of the ORS spine section', *JOR Spine*, 1: e1036.

Soukane, D. M., A. Shirazi-Adl, and J. P. Urban. 2005. 'Analysis of nonlinear coupled diffusion of oxygen and lactic acid in intervertebral discs', *J Biomech Eng*, 127: 1121-6.

Soukane, D. M.;, A.; Shirazi-Adl, and J. P.; Urban. 2007. 'Computation of coupled diffusion of oxygen, glucose and lactic acid in an intervertebral disc', *J Biomech*, 40: 2645-54.

Tomaszewski, K. A., J. A. Walocha, E. Mizia, T. Gładysz, R. Głowacki, and R. Tomaszewska. 2015. 'Age- and degeneration-related variations in cell density and glycosaminoglycan content in the human cervical intervertebral disc and its endplates', *Pol J Pathol*, 66: 296-309.

Tong, Wei, Zhouyu Lu, Ling Qin, Robert L. Mauck, Harvey E. Smith, Lachlan J. Smith, Neil R. Malhotra, Martin F. Heyworth, Franklin Caldera, Motomi Enomoto-Iwamoto, and Yejia Zhang. 2017. 'Cell therapy for the degenerating intervertebral disc', *Translational Research*, 181: 49-58.

Tourell, M. C., M. Kirkwood, M. J. Pearcy, K. I. Momot, and J. P. Little. 2017. 'Load-induced changes in the diffusion tensor of ovine anulus fibrosus: A pilot MRI study', *J Magn Reson Imaging*, 45: 1723-35.

Tschugg, A., F. Michnacs, M. Strowitzki, H. J. Meisel, and C. Thome. 2016. 'A prospective multicenter phase I/II clinical trial to evaluate safety and efficacy of NOVOCART Disc plus autologous disc chondrocyte transplantation in the treatment of nucleotomized and degenerative lumbar disc to avoid secondary disease: study protocol for a randomized controlled trial', *Trials*, 17: 108.

Tschugg, Anja, Michael Diepers, Steinert Simone, Felix Michnacs, Sebastian Quirbach, Martin Strowitzki, Hans Jörg Meisel, and Claudius Thomé. 2017. 'A prospective randomized multicenter phase I/II clinical trial to evaluate safety and efficacy of NOVOCART disk plus autologous disk chondrocyte transplantation in the treatment of nucleotomized and degenerative lumbar disks to avoid secondary disease: safety results of Phase I—a short report', *Neurosurgical Review*, 40: 155-62.

Urban, J. P. G., and A. Maroudas. 1979. 'The measurement of fixed charged density in the intervertebral disc', *Biochimica et Biophysica Acta (BBA) - General Subjects*, 586: 166-78.

Urban, J. P., S. Holm, and A. Maroudas. 1978. 'Diffusion of small solutes into the intervertebral disc: as in vivo study', *Biorheology*, 15: 203-21.

Urban, J. P., S. Holm, A. Maroudas, and A. Nachemson. 1977. 'Nutrition of the intervertebral disk. An in vivo study of solute transport', *Clinical orthopaedics and related research*: 101-14.

Urban, J. P., and J. F. McMullin. 1988. 'Swelling pressure of the lumbar intervertebral discs: influence of age, spinal level, composition, and degeneration', *Spine*, 13: 179-87.

Urban, J. P., and S. Roberts. 2003. 'Degeneration of the intervertebral disc', *Arthritis Res Ther*, 5: 120-30.

Urban, J. P., and C. P. Winlove. 2007. 'Pathophysiology of the intervertebral disc and the challenges for MRI', *J Magn Reson Imaging*, 25: 419-32.

Wang, A. M., P. Cao, A. Yee, D. Chan, and E. X. Wu. 2015. 'Detection of extracellular matrix degradation in intervertebral disc degeneration by diffusion magnetic resonance spectroscopy', *Magn Reson Med*, 73: 1703-12.

Wang, Jihong, Joseph Weygand, Ken-Pin Hwang, Abdallah S. R. Mohamed, Yao Ding, Clifton D. Fuller, Stephen Y. Lai, Steven J. Frank, and Jinyuan Zhou. 2016. 'Magnetic Resonance Imaging of Glucose Uptake and Metabolism in Patients with Head and Neck Cancer', *Scientific Reports*, 6: 30618.

Watanabe, K., J. Mochida, T. Nomura, M. Okuma, K. Sakabe, and K. Seiki. 2003. 'Effect of reinsertion of activated nucleus pulposus on disc degeneration: an experimental study on various types of collagen in degenerative discs', *Connect Tissue Res*, 44: 104-8.

Welty, James R., Gregory L Rorrer, and David G Foster. 2015. 'Fundamentals of Momentum, Heat, and Mass Transfer.' in, *Fundamentals of Momentum, Heat, and Mass Transfer* (Wiley: Hoboken, NJ).

Wong, J., S. L. Sampson, H. Bell-Briones, A. Ouyang, A. A. Lazar, J. C. Lotz, and A. J. Fields. 2019. 'Nutrient supply and nucleus pulposus cell function: effects of the transport properties of the cartilage endplate and potential implications for intradiscal biologic therapy', *Osteoarthritis Cartilage*, 27: 956-64.

Wu, Y., S. E. Cisewski, N. Wegner, S. Zhao, V. D. Pellegrini, Jr., E. H. Slate, and H. Yao. 2016. 'Region and strain-dependent diffusivities of glucose and lactate in healthy human cartilage endplate', *J Biomech*, 49: 2756-62.

Wu, Y., S. Cisewski, B. L. Sachs, and H. Yao. 2013. 'Effect of cartilage endplate on cell based disc regeneration: a finite element analysis', *Mol Cell Biomech*, 10: 159-82.

Yin, S., H. Du, W. Zhao, S. Ma, M. Zhang, M. Guan, and M. Liu. 2019. 'Inhibition of both endplate nutritional pathways results in intervertebral disc degeneration in a goat model', *J Orthop Surg Res*, 14: 138.

Yoshikawa, T., Y. Ueda, K. Miyazaki, M. Koizumi, and Y. Takakura. 2010. 'Disc regeneration therapy using marrow mesenchymal cell transplantation: a report of two case studies', *Spine (Phila Pa 1976)*, 35: E475-80.

Yuan, T. Y., A. R. Jackson, C. Y. Huang, and W. Y. Gu. 2009. 'Strain-Dependent Oxygen Diffusivity in Bovine Annulus Fibrosus', *Journal of Biomechanical Engineering*, 131.

Zeng, F., Y. Zha, L. Li, D. Xing, W. Gong, L. Hu, and Y. Fan. 2019. 'A comparative study of diffusion kurtosis imaging and T2* mapping in quantitative detection of lumbar intervertebral disk degeneration', *Eur Spine J*, 28: 2169-78.

Zhang, Shu-Jun, Wei Yang, Cheng Wang, Wen-Si He, Hai-Yang Deng, Yi-Guo Yan, Jian Zhang, Yong-Xiao Xiang, and Wen-Jun Wang. 2016. 'Autophagy: A double-edged sword in intervertebral disk degeneration', *Clinica Chimica Acta*, 457: 27-35.

Zhou, Zhengwei, Christopher Nguyen, Yuhua Chen, Jaime L. Shaw, Zixin Deng, Yibin Xie, James Dawkins, Eduardo Marbán, and Debiao Li. 2017. 'Optimized CEST cardiovascular magnetic resonance for assessment of metabolic activity in the heart', *Journal of Cardiovascular Magnetic Resonance*, 19: 95.

Zhu, Q., X. Gao, H. B. Levene, M. D. Brown, and W. Gu. 2016. 'Influences of Nutrition Supply and Pathways on the Degenerative Patterns in Human Intervertebral Disc', *Spine (Phila Pa 1976)*, 41: 568-76.

Zhu, Q., A. R. Jackson, and W. Y. Gu. 2012. 'Cell viability in intervertebral disc under various nutritional and dynamic loading conditions: 3d finite element analysis', *J Biomech*, 45: 2769-77.

Chapter 6: Future Directions and Conclusions

6.1 Introduction

Recent research has shown the likelihood of stem cell therapy in alleviating back pain by reversing degeneration of the IVD (Tam et al. 2014; Murrell et al. 2009; Coric et al. 2013; Richardson et al. 2016). However, the IVD's impoverished nutrient environment and restricted nutrient transport pose challenges to ensuring regenerative outcomes of cell-based therapies (Noriega et al. 2017; Orozco et al. 2011; Sakai and Andersson 2015). In addition, current IVD research lacks appropriate methods to perform studies on samples that resemble the *in vivo* nutrient microenvironment. Current research techniques utilize normoxic culture conditions, cyclical feeding regimens, and animal models, among other cultivating methods that fail to mimic the *in vivo* environment.

This chapter proposes two directions to further the study of nutrient transport in the IVD. First, I discuss the importance of cryopreservation in studying nutrient transport. I also suggest additional applications for cryopreservation that would facilitate IVD research. Second, I explain the need for finite element modeling to study solute transport in patients. I present some limitations presented in chapter 5 and propose applications of the model in a clinical setting. Lastly, the chapter concludes with the significant findings of this dissertation, highlighting its impact on the field.

6.2 A human intervertebral disc organ bank

Researchers encounter a few roadblocks when studying the IVD's regenerative mechanisms. First, the availability of fresh intact human IVDs is limited, and depends on established contacts with hospitals and procurement organizations to obtain viable specimens. Another obstacle is the storage of the IVDs upon arrival, with limited bioreactor space and freezing risking the number of viable cells in the tissue. Intact IVDs from animal models have been cultivated successfully for a week *ex vivo* and for over three weeks in a bioreactor (Gantenbein et al. 2015). However, most research laboratories lack the proper equipment and logistical support to cultivate intact human IVDs long-term. Therefore, cryopreservation emerges as a promising solution to eliminate these obstacles and facilitate IVD research (Lam et al. 2011). We innovated a novel method to cryopreserve the IVD using compression through this work. Our technique reduced the time

required for cryoprotectant (CPA) penetration by 95%, improving cell viability in treated groups from ~5% to over 80%, as explained in Chapter 4.

While the results provided a promising effort to create IVD organ banks, additional aspects of this work could be improved. Some aspects include creating a robust protocol that eliminates technical obstacles. For example, a better way to measure cell viability in the IVD should be formulated to avoid cell death introduced by the surgical blade when extracting the samples. In addition, a precise mechanism to measure DMSO percent in the tissue should be established to ensure its complete removal. It has been established that DMSO, even at low concentrations, changes the cell's phenotype, gene expression, and viability (Sugishita et al. 2021). It is crucial to ensure the complete removal of the DMSO from the IVDs to prevent confounding results. Next, our work only investigated the ability to maintain cell viability. While viability is important, other aspects of cellular health and function should be measured. These aspects include senescence, apoptosis, and cellular metabolism. Tissue samples from the CEP, outer AF, inner AF, and NP could be obtained using a biopsy to measure cell senescence and apoptosis in the cryopreserved IVDs. Additionally, tissue from the same regions of interest could be processed to examine the metabolites profile. It is essential to understand how cryopreservation affects these cellular functions providing researchers with an intact organ representing human *in vivo* conditions and eliminating the need to rely on *in vitro* or animal studies. These tests would need to be compared with samples from fresh human IVDs to validate that our novel method to cryopreserve the human IVD has no significant impact on cellular characteristics, including the phenotype and metabolic pathways. Finally, this method should be applied to create a human IVD organ bank to resolve logistical bottlenecks in clinical and benchtop research.

6.3 Improved predictive model of solute transport in the intervertebral disc

One of the problems facing researchers is accurately modeling and predicting the complex pathways that solutes take in the IVD. Our previous work on modeling solute transport, as discussed in Chapter 5, elucidates the effect of IVD-specific geometry on solute distribution (Shalash et al. 2021). We also highlighted the differences in solute transport between different IVDs within the same degeneration grade (Shalash et al. 2021). The proposed work in this section addresses some of these limitations and provides suggestions for future applications.

The model provides two-dimensional simulations of solute distributions that do not represent the 3-dimensional nature of the tissue. Including the third dimension would assist in inferring spatial and radial effects on solute transport which have been reported to be dominant, especially in the annulus fibrosus' (AF) anisotropic tissue. Additionally, there is a need to individualize parameters affecting solute transport in patients. These parameters include water gradient in the tissue, diffusion coefficients, vasculature density, and CEP calcification. These factors were determined to affect transport significantly.

Imaging techniques exist in which we could measure water gradient through the various tissues (AF and CEP) and provide a better estimate of solute availability. Alternatively, experiments could be designed in which an imaging tracer is applied to learn about effective diffusion through the CEPs, which would be sufficient to factor in the effects of vessel density and CEP calcification. Nonetheless, as presented in Chapter 5, addressing the model's limitations is vital to building a robust tool that can predict nutrient availability in the IVD.

Finally, it is crucial to validate the model results in human IVDs. Experiments could be conducted to cultivate human IVDs in our custom-built bioreactor for a few days under load. The IVDs can be scanned using CT and MRI modalities to extract (1) disc geometry, (2) water content, (3) and diffusion coefficients. Next, the IVD could be cultivated under various microenvironments for a week, including healthy, degenerated, and inflamed. For each IVD group, MRI scans can be obtained for lactate levels, and a PET scan could be applied to infer glucose distribution within the IVD. Alternatively, an oxygen probe could be utilized to measure local partial pressure. The results from this experiment should provide further information on the accuracy and precision of the model. Additional iterative modifications and adjustments to the model will need to be performed to ensure its robustness before pursuing a technology transfer. Nonetheless, these studies should present the model as an innovative proof-of-concept, providing guidelines to improve stem cell injections and the overall patient care.

6.4 Conclusions

The IVD is a complex cartilaginous structure that we are still discovering. One of its astonishing properties is cell survival under harsh conditions including starvation, hypoxia, and high acidity. CEP calcification, low vessel density, and deterioration of the ECM are factors

affecting the solute and acidity levels in the tissue. After all, recent efforts have been made to better elucidate changes in the nutrient distribution and innovate methods to improve it.

In this dissertation I discuss the importance of studying solute transport limitations in the IVD. First, I present a thorough review of the literature focusing on the conundrum of limited transport. I further explain how various research groups innovated methods to study transport phenomena including imaging modalities and finite element modeling.

I also present the bioreactor system which was applied in this work to innovate a method to cryopreserve the IVD. Whole organ bioreactors are emerging as a preferred cultivation method compared to current protocols. For instance, bioreactors offer controlled and adaptable microenvironments that could mimic various *in vivo* scenarios overcoming a limitation in common culture systems, including two- and three-dimensional.

Next, I transition to discussing the impact of the microenvironment in cultivation cultures on the AF and NP cells. In general, cells are sensitive to their environment, and they interact with it by communicating the various stressors, often in the form of proinflammatory cytokines. In this work, I established how steady glucose levels in the culture could affect IVD cells differently. We discovered that steady glucose levels increase metabolic rates in the AF while increase anerobic glycolysis in NP cells. This work further elucidates the importance of considering the *in vitro* microenvironment when designing studies.

Following this, I present and discuss an innovative method to cryopreserve the IVD using a custom-built bioreactor. I relied on the IVD's viscoelastic properties and swelling to overcome transport limitations of the cryoprotectant, reducing transport time from 72 hours to only five hours. This project also provides insight into future applications that could facilitate research and allotransplant clinical trials.

Finally, I discuss the development of a patient-specific finite element model that incorporates data from imaging modalities to provide a representation of glucose, oxygen, and lactate distributions in the patient's IVD. The model builds on the work of several groups and adds a layer of complexity constituted by the patient-specific data. Therefore, making finite element models clinically relevant and potentially translatable to improve patient spine care. Altogether, this dissertation presents an *ex vivo* platform to cultivate, store, and analyze human IVDs. Through this work, other researchers will have access to cutting edge tools and research, advancing current practices and innovating solutions to enhance transport phenomena in the human IVD.

BIBLIOGRAPHY

Adams, M. A., and W. C. Hutton. 1983. 'The effect of posture on the fluid content of lumbar intervertebral discs', *Spine (Phila Pa 1976)*, 8: 665-71.

———. 1985. 'The effect of posture on the lumbar spine', *J Bone Joint Surg Br*, 67: 625-9.

———. 1986. 'The effect of posture on diffusion into lumbar intervertebral discs', *Journal of anatomy*, 147: 121-34.

Adams, Michael A., and Peter J. Roughley. 2006. 'What is Intervertebral Disc Degeneration, and What Causes It?', *Spine*, 31: 2151-61.

Aerssens, Jeroen, Steven Boonen, Geert Lowet, and Jan Dequeker. 1998. 'Interspecies Differences in Bone Composition, Density, and Quality: Potential Implications for in Vivo Bone Research*', *Endocrinology*, 139: 663-70.

Agrawal, A., S. Gajghate, H. Smith, D. G. Anderson, T. J. Albert, I. M. Shapiro, and M. V. Risbud. 2008. 'Cited2 modulates hypoxia-inducible factor-dependent expression of vascular endothelial growth factor in nucleus pulposus cells of the rat intervertebral disc', *Arthritis Rheum*, 58: 3798-808.

Aijaz, A., M. Li, D. Smith, D. Khong, C. LeBlon, O. S. Fenton, R. M. Olabisi, S. Libutti, J. Tischfield, M. V. Maus, R. Deans, R. N. Barcia, D. G. Anderson, J. Ritz, R. Preti, and B. Parekkadan. 2018. 'Biomanufacturing for clinically advanced cell therapies', *Nat Biomed Eng*, 2: 362-76.

Al-Raoush, Riyadh I., and Iman T. Madhoun. 2017. 'TORT3D: A MATLAB code to compute geometric tortuosity from 3D images of unconsolidated porous media', *Powder Technology*, 320: 99-107.

Albert, M. 1942. 'Calcification of the Intervertebral Disks', *Br Med J*, 1: 666-8.

Alini, Mauro, Stephen M. Eisenstein, Keita Ito, Christopher Little, A. Annette Kettler, Koichi Masuda, James Melrose, Jim Ralphs, Ian Stokes, and Hans Joachim Wilke. 2008. 'Are animal models useful for studying human disc disorders/degeneration?', *European Spine Journal*, 17: 2-19.

Andersson, G. B. 1999. 'Epidemiological features of chronic low-back pain', *Lancet*, 354: 581-5.

Antoniou, J., C. N. Demers, G. Beaudoin, T. Goswami, F. Mwale, M. Aebi, and M. Alini. 2004a. 'Apparent diffusion coefficient of intervertebral discs related to matrix composition and integrity', *Magn Reson Imaging*, 22: 963-72.

Antoniou, J., L. M. Epure, A. J. Michalek, M. P. Grant, J. C. Iatridis, and F. Mwale. 2013. 'Analysis of quantitative magnetic resonance imaging and biomechanical parameters on human discs with different grades of degeneration', *J Magn Reson Imaging*, 38: 1402-14.

Antoniou, J., T. Steffen, F. Nelson, N. Winterbottom, A. P. Hollander, R. A. Poole, M. Aebi, and M. Alini. 1996. 'The human lumbar intervertebral disc: evidence for changes in the biosynthesis and denaturation of the extracellular matrix with growth, maturation, ageing, and degeneration', *J Clin Invest*, 98: 996-1003.

Antoniou, John, Caroline N. Demers, Gilles Beaudoin, Tapas Goswami, Fackson Mwale, Max Aebi, and Mauro Alini. 2004b. 'Apparent diffusion coefficient of intervertebral discs related to matrix composition and integrity', *Magnetic Resonance Imaging*, 22: 963-72.

Arpinar, Volkan Emre, Scott D. Rand, Andrew P. Klein, Dennis J. Maiman, and L. Tugan Muftuler. 2015. 'Changes in perfusion and diffusion in the endplate regions of degenerating intervertebral discs: a DCE-MRI study', *European Spine Journal*, 24: 2458-67.

Arun, Ranganathan, Brian J. C. Freeman, Brigitte E. Scammell, Donal S. McNally, Eleanor Cox, and Penny Gowland. 2009. '2009 ISSLS Prize Winner: What Influence Does Sustained Mechanical Load Have on Diffusion in the Human Intervertebral Disc?: An In Vivo Study Using Serial Postcontrast Magnetic Resonance Imaging', *Spine*, 34: 2324-37.

Ashinsky, B. G., E. D. Bonnevie, S. A. Mandalapu, S. Pickup, C. Wang, L. Han, R. L. Mauck, H. E. Smith, and S. E. Gullbrand. 2020. 'Intervertebral Disc Degeneration Is Associated With Aberrant Endplate Remodeling and Reduced Small Molecule Transport', *J Bone Miner Res*, 35: 1572-81.

Awan, Maooz, Iryna Buriak, Roland Fleck, Barry Fuller, Anatoliy Goltsev, Julie Kerby, Mark Lowdell, Pavel Mericka, Alexander Petrenko, Yuri Petrenko, Olena Rogulska, Alexandra Stolzing, and Glyn N Stacey. 2020. 'Dimethyl sulfoxide: a central player since the dawn of cryobiology, is efficacy balanced by toxicity?', *Regenerative Medicine*, 15: 1463-91.

Baber, Z., and M. A. Erdek. 2016a. 'Failed back surgery syndrome: current perspectives', *J Pain Res*, 9: 979-87.

Baber, Zafeer, and Michael A. Erdek. 2016b. 'Failed back surgery syndrome: current perspectives', *Journal of pain research*, 9: 979-87.

Bakhach, Joseph. 2009. 'The cryopreservation of composite tissues', *Organogenesis*, 5: 119-26.

Balaban, R. S., H. L. Kantor, and J. A. Ferretti. 1983. 'In vivo flux between phosphocreatine and adenosine triphosphate determined by two-dimensional phosphorous NMR', *J Biol Chem*, 258: 12787-9.

Bartels, E. M., J. C. Fairbank, C. P. Winlove, and J. P. Urban. 1998. 'Oxygen and lactate concentrations measured in vivo in the intervertebral discs of patients with scoliosis and back pain', *Spine (Phila Pa 1976)*, 23: 1-7; discussion 8.

Beattie, Paul F., Paul S. Morgan, and Denise Peters. 2008. 'Diffusion-Weighted Magnetic Resonance Imaging of Normal and Degenerative Lumbar Intervertebral Discs: A New Method to Potentially Quantify the Physiologic Effect of Physical Therapy Intervention', *Journal of Orthopaedic & Sports Physical Therapy*, 38: 42-49.

Beckstein, Jesse C., Sounok Sen, Thomas P. Schaer, Edward J. Vresilovic, and Dawn M. Elliott. 2008. 'Comparison of Animal Discs Used in Disc Research to Human Lumbar Disc: Axial Compression Mechanics and Glycosaminoglycan Content', *Spine*, 33.

Belavý, Daniel L., Gabriele Armbrecht, Carolyn A. Richardson, Dieter Felsenberg, and Julie A. Hides. 2011. 'Muscle Atrophy and Changes in Spinal Morphology: Is the Lumbar Spine Vulnerable After Prolonged Bed-Rest?', *Spine*, 36: 137-45.

Belykh, E., A. A. Kalinin, A. A. Patel, E. J. Miller, M. A. Bohl, I. A. Stepanov, L. A. Bardonova, T. Kerimbaev, A. O. Asantsev, M. B. Giers, M. C. Preul, and V. A. Byvaltsev. 2017. 'Apparent diffusion coefficient maps in the assessment of surgical patients with lumbar spine degeneration', *PLoS One*, 12: e0183697.

Benneker, Lorin M., Paul F. Heini, Mauro Alini, Suzanne E. Anderson, and Keita Ito. 2005. '2004 Young Investigator Award Winner: Vertebral Endplate Marrow Contact Channel Occlusions and Intervertebral Disc Degeneration', *Spine*, 30: 167-73.

Bernemann, I., N. Manuchehrabadi, R. Spindler, J. Choi, W. F. Wolkers, J. C. Bischof, and B. Glasmacher. 2010. 'Diffusion of dimethyl sulfoxide in tissue engineered collagen scaffolds visualized by computer tomography', *Cryo Letters*, 31: 493-503.

Bertram, H., M. Kroeber, H. Wang, F. Unglaub, T. Guehring, C. Carstens, and W. Richter. 2005. 'Matrix-assisted cell transfer for intervertebral disc cell therapy', *Biochem Biophys Res Commun*, 331: 1185-92.

Bezci, Semih E., and Grace D. O'Connell. 2018. 'Osmotic Pressure Alters Time-dependent Recovery Behavior of the Intervertebral Disc', *Spine*, 43: E334-E40.

Bezci, Semih E., Benjamin Werbner, Minhao Zhou, Katerina G. Malollari, Gabriel Dorlhiac, Carlo Carraro, Aaron Streets, and Grace D. O'Connell. 2019. 'Radial variation in biochemical composition of the bovine caudal intervertebral disc', *JOR SPINE*, 2: e1065.

BHATTACHARYA, SHAMBO, SANDIPAN ROY, MASUD RANA, SREERUP BANERJEE, SANTANU KUMAR KARMAKAR, and JAYANTA KUMAR BISWAS. 2019. 'BIOMECHANICAL PERFORMANCE OF A MODIFIED DESIGN OF DYNAMIC CERVICAL IMPLANT COMPARED TO CONVENTIONAL BALL AND SOCKET DESIGN OF AN ARTIFICIAL INTERVERTEBRAL DISC IMPLANT: A FINITE ELEMENT STUDY', *Journal of Mechanics in Medicine and Biology*, 19: 1950017.

Bibby, S. R., J. C. Fairbank, M. R. Urban, and J. P. Urban. 2002. 'Cell viability in scoliotic discs in relation to disc deformity and nutrient levels', *Spine (Phila Pa 1976)*, 27: 2220-8; discussion 27-8.

Bibby, S. R., D. A. Jones, R. M. Ripley, and J. P. Urban. 2005. 'Metabolism of the intervertebral disc: effects of low levels of oxygen, glucose, and pH on rates of energy metabolism of bovine nucleus pulposus cells', *Spine (Phila Pa 1976)*, 30: 487-96.

Bibby, S. R., and J. P. Urban. 2004. 'Effect of nutrient deprivation on the viability of intervertebral disc cells', *Eur Spine J*, 13: 695-701.

Bibby, Susan R. S., Deborah A. Jones, Robert B. Lee, Jing Yu, and Jill P. G. Urban. 2001. 'The pathophysiology of the intervertebral disc', *Joint Bone Spine*, 68: 537-42.

Biswas, Jayanta Kumar, Anindya Malas, Sourav Majumdar, and Masud Rana. 2022. 'A comparative finite element analysis of artificial intervertebral disc replacement and pedicle screw fixation of the lumbar spine', *Computer Methods in Biomechanics and Biomedical Engineering*: 1-9.

Biswas, Jayanta Kumar, Masud Rana, Anindya Malas, Sandipan Roy, Subhomoy Chatterjee, and Sandeep Choudhury. 2022. 'Effect of single and multilevel artificial inter-vertebral disc

replacement in lumbar spine: A finite element study', *The International Journal of Artificial Organs*, 45: 193-99.

Boos, N., S. Weissbach, H. Rohrbach, C. Weiler, K. F. Spratt, and A. G. Nerlich. 2002. 'Classification of age-related changes in lumbar intervertebral discs: 2002 Volvo Award in basic science', *Spine (Phila Pa 1976)*, 27: 2631-44.

Boubriak, O. A., J. P. G. Urban, S. Akhtar, K. M. Meek, and A. J. Bron. 2000. 'The Effect of Hydration and Matrix Composition on Solute Diffusion in Rabbit Sclera', *Experimental Eye Research*, 71: 503-14.

Boubriak, Olga. A., Natasha Watson, Sarit. S. Sivan, Naomi Stubbens, and Jill P. G. Urban. 2013. 'Factors regulating viable cell density in the intervertebral disc: blood supply in relation to disc height', *Journal of anatomy*, 222: 341-48.

Bradley, J. A., E. M. Bolton, and R. A. Pedersen. 2002. 'Stem cell medicine encounters the immune system', *Nat Rev Immunol*, 2: 859-71.

Brinjikji, W., F. E. Diehn, J. G. Jarvik, C. M. Carr, D. F. Kallmes, M. H. Murad, and P. H. Luetmer. 2015. 'MRI Findings of Disc Degeneration are More Prevalent in Adults with Low Back Pain than in Asymptomatic Controls: A Systematic Review and Meta-Analysis', *AJNR Am J Neuroradiol*, 36: 2394-9.

Brodin, H. 1955. 'Paths of nutrition in articular cartilage and intervertebral discs', *Acta Orthop Scand*, 24: 177-83.

Brodke, D. S., and S. M. Ritter. 2005. 'Nonsurgical management of low back pain and lumbar disk degeneration', *Instr Course Lect*, 54: 279-86.

Bruehlmann, S. B., J. B. Rattner, J. R. Matyas, and N. A. Duncan. 2002. 'Regional variations in the cellular matrix of the annulus fibrosus of the intervertebral disc', *Journal of anatomy*, 201: 159-71.

Bush, G. B. 1934. 'The Clinical Importance of the Intervertebral Discs, with Special Reference to Nuclear Prolapses', *Bristol Med Chir J (1883)*, 51: 173-82.

Byvaltsev, V. A., S. I. Kolesnikov, L. A. Bardonova, E. G. Belykh, L. I. Korytov, M. B. Giers, and M. C. Preul. 2018. 'Assessment of Lactate Production and Proteoglycans Synthesis by the Intact and Degenerated Intervertebral Disc Cells under the Influence of Activated Macrophages: an In Vitro Study', *Bulletin of Experimental Biology and Medicine*, 166: 170-73.

Byvaltsev, V. A., S. I. Kolesnikov, E. G. Belykh, I. A. Stepanov, A. A. Kalinin, L. A. Bardonova, N. P. Sudakov, I. V. Klimenkov, S. B. Nikiforov, A. V. Semenov, D. V. Perfil'ev, I. V. Bespyatykh, S. L. Antipina, M. Giers, and M. Prul. 2017. 'Complex Analysis of Diffusion Transport and Microstructure of an Intervertebral Disk', *Bulletin of Experimental Biology and Medicine*, 164: 223-28.

Cassidy, J. J., M. S. Silverstein, A. Hiltner, and E. Baer. 1990. 'A water transport model for the creep response of the intervertebral disc', *Journal of Materials Science: Materials in Medicine*, 1: 81-89.

Centeno, C., J. Markle, E. Dodson, I. Stemper, C. J. Williams, M. Hyzy, T. Ichim, and M. Freeman. 2017. 'Treatment of lumbar degenerative disc disease-associated radicular pain with culture-expanded autologous mesenchymal stem cells: a pilot study on safety and efficacy', *J Transl Med*, 15: 197.

Chan, S. C., S. Lam, V. Y. Leung, D. Chan, K. D. Luk, and K. M. Cheung. 2010. 'Minimizing cryopreservation-induced loss of disc cell activity for storage of whole intervertebral discs', *Eur Cell Mater*, 19: 273-83.

Chan, S. C., J. Walser, S. J. Ferguson, and B. Gantenbein. 2015. 'Duration-dependent influence of dynamic torsion on the intervertebral disc: an intact disc organ culture study', *Eur Spine J*, 24: 2402-10.

Chan, Samantha C. W., Benjamin Gantenbein-Ritter, Victor Y. L. Leung, Danny Chan, Kenneth M. C. Cheung, and Keita Ito. 2010. 'Cryopreserved intervertebral disc with injected bone marrow–derived stromal cells: a feasibility study using organ culture', *The Spine Journal*, 10: 486-96.

Chan, Samantha C. W., Jochen Walser, Patrick Käppeli, Mohammad Javad Shamsollahi, Stephen J. Ferguson, and Benjamin Gantenbein-Ritter. 2013. 'Region Specific Response of Intervertebral Disc Cells to Complex Dynamic Loading: An Organ Culture Study Using a Dynamic Torsion-Compression Bioreactor', *PLOS ONE*, 8: e72489.

Chang, Tie, and Gang Zhao. 2021. 'Ice Inhibition for Cryopreservation: Materials, Strategies, and Challenges', *Advanced Science*, 8: 2002425.

Chen, Deheng, Dongdong Xia, Zongyou Pan, Daoliang Xu, Yifei Zhou, Yaosen Wu, Ningyu Cai, Qian Tang, Chenggui Wang, Meijun Yan, Jing Jie Zhang, Kailiang Zhou, Quan Wang, Yongzeng Feng, Xiangyang Wang, Huazi Xu, Xiaolei Zhang, and Naifeng Tian.

2016. 'Metformin protects against apoptosis and senescence in nucleus pulposus cells and ameliorates disc degeneration in vivo', *Cell Death & Disease*, 7: e2441-e41.

Chen, Sheng, Lei Qin, Xiaohao Wu, Xuekun Fu, Sixiong Lin, Di Chen, Guozhi Xiao, Zengwu Shao, and Huiling Cao. 2020. 'Moderate Fluid Shear Stress Regulates Heme Oxygenase-1 Expression to Promote Autophagy and ECM Homeostasis in the Nucleus Pulposus Cells', *Frontiers in Cell and Developmental Biology*, 8.

Cheng, Xiaofei, Bin Ni, Feng Zhang, Ying Hu, and Jie Zhao. 2016. 'High Glucose-Induced Oxidative Stress Mediates Apoptosis and Extracellular Matrix Metabolic Imbalances Possibly via p38 MAPK Activation in Rat Nucleus Pulposus Cells', *Journal of Diabetes Research*, 2016: 3765173.

Cherif, Hosni, Daniel G. Bisson, Matthew Mannarino, Oded Rabau, Jean A. Ouellet, and Lisbet Haglund. 2020. 'Senotherapeutic drugs for human intervertebral disc degeneration and low back pain', *eLife*, 9: e54693.

Cheung, Kenneth M. C., Jaro Karppinen, Danny Chan, Daniel W. H. Ho, You-Qiang Song, Pak Sham, Kathryn S. E. Cheah, John C. Y. Leong, and Keith D. K. Luk. 2009. 'Prevalence and Pattern of Lumbar Magnetic Resonance Imaging Changes in a Population Study of One Thousand Forty-Three Individuals', *Spine*, 34: 934-40.

Chiu, Elaine J., David C. Newitt, Mark R. Segal, Serena S. Hu, Jeffrey C. Lotz, and Sharmila Majumdar. 2001. 'Magnetic Resonance Imaging Measurement of Relaxation and Water Diffusion in the Human Lumbar Intervertebral Disc Under Compression In Vitro', *Spine*, 26.

Chujo, Takehide, Howard S. An, Koji Akeda, Kei Miyamoto, Carol Muehleman, Mohamed Attawia, Gunnar Andersson, and Koichi Masuda. 2006. 'Effects of Growth Differentiation Factor-5 on the Intervertebral Disc−In Vitro Bovine Study and In Vivo Rabbit Disc Degeneration Model Study', *Spine*, 31.

Cisewski, S. E., Y. Wu, B. J. Damon, B. L. Sachs, M. J. Kern, and H. Yao. 2018. 'Comparison of Oxygen Consumption Rates of Nondegenerate and Degenerate Human Intervertebral Disc Cells', *Spine (Phila Pa 1976)*, 43: E60-E67.

Coric, D., K. Pettine, A. Sumich, and M. O. Boltes. 2013. 'Prospective study of disc repair with allogeneic chondrocytes presented at the 2012 Joint Spine Section Meeting', *J Neurosurg Spine*, 18: 85-95.

Cortes, Daniel H., Nathan T. Jacobs, John F. DeLucca, and Dawn M. Elliott. 2014. 'Elastic, permeability and swelling properties of human intervertebral disc tissues: A benchmark for tissue engineering', *Journal of Biomechanics*, 47: 2088-94.

Coulson-Thomas, Vivien Jane, and Tarsis Ferreira Gesteira. 2014. 'Dimethylmethylene Blue Assay (DMMB)', *Bio-protocol*, 4: e1236.

Crevensten, G., A. J. Walsh, D. Ananthakrishnan, P. Page, G. M. Wahba, J. C. Lotz, and S. Berven. 2004. 'Intervertebral disc cell therapy for regeneration: mesenchymal stem cell implantation in rat intervertebral discs', *Ann Biomed Eng*, 32: 430-4.

Daly, Chris, Peter Ghosh, Graham Jenkin, David Oehme, and Tony Goldschlager. 2016. 'A Review of Animal Models of Intervertebral Disc Degeneration: Pathophysiology, Regeneration, and Translation to the Clinic', *BioMed Research International*, 2016: 5952165.

Dao, Tien Tuan, Philippe Pouletaut, Ludovic Robert, Pascal Aufaure, Fabrice Charleux, and Marie-Christine Ho Ba Tho. 2013. 'Quantitative analysis of annulus fibrosus and nucleus pulposus derived from T2 mapping, diffusion-weighted and diffusion tensor MR imaging', *Computer Methods in Biomechanics and Biomedical Engineering: Imaging & Visualization*, 1: 138-46.

Das, D. B., A. Welling, J. P. Urban, and O. A. Boubriak. 2009. 'Solute transport in intervertebral disc: experiments and finite element modeling', *Ann N Y Acad Sci*, 1161: 44-61.

DeLucca, J. F., D. H. Cortes, N. T. Jacobs, E. J. Vresilovic, R. L. Duncan, and D. M. Elliott. 2016. 'Human cartilage endplate permeability varies with degeneration and intervertebral disc site', *J Biomech*, 49: 550-7.

Diamant, B., J. Karlsson, and A. Nachemson. 1968. 'Correlation between lactate levels and pH in discs of patients with lumbar rhizopathies', *Experientia*, 24: 1195-6.

Dimozi, A., E. Mavrogonatou, A. Sklirou, and D. Kletsas. 2015. 'Oxidative stress inhibits the proliferation, induces premature senescence and promotes a catabolic phenotype in human nucleus pulposus intervertebral disc cells', *Eur Cell Mater*, 30: 89-102; discussion 03.

Dolor, Aaron, Sara L. Sampson, Ann A. Lazar, Jeffrey C. Lotz, Francis C. Szoka, and Aaron J. Fields. 2019. 'Matrix modification for enhancing the transport properties of the human cartilage endplate to improve disc nutrition', *PLOS ONE*, 14: e0215218.

Du, Fei, Xiao-Hong Zhu, Hongyan Qiao, Xiaoliang Zhang, and Wei Chen. 2007. 'Efficient in vivo 31P magnetization transfer approach for noninvasively determining multiple kinetic parameters and metabolic fluxes of ATP metabolism in the human brain', *Magnetic Resonance in Medicine*, 57: 103-14.

Ejeskär, Arvid, and Sten Holm. 1979. 'Oxygen Tension Measurements in the Intervertebral Disc', *Upsala Journal of Medical Sciences*, 84: 83-93.

Elwinger, Fredrik, Payam Pourmand, and István Furó. 2017. 'Diffusive Transport in Pores. Tortuosity and Molecular Interaction with the Pore Wall', *The Journal of Physical Chemistry C*, 121: 13757-64.

Eyre, David R. 1979. 'Biochemistry of the Intervertebral Disc.' in David A. Hall and D. S. Jackson (eds.), *International Review of Connective Tissue Research* (Elsevier).

Feng, Chencheng, Huan Liu, Minghui Yang, Yang Zhang, Bo Huang, and Yue Zhou. 2016. 'Disc cell senescence in intervertebral disc degeneration: Causes and molecular pathways', *Cell Cycle*, 15: 1674-84.

Feng, Chencheng, Minghui Yang, Minghong Lan, Chang Liu, Yang Zhang, Bo Huang, Huan Liu, and Yue Zhou. 2017. 'ROS: Crucial Intermediators in the Pathogenesis of Intervertebral Disc Degeneration', *Oxidative Medicine and Cellular Longevity*, 2017: 5601593.

Ferguson, S. J., K. Ito, and L. P. Nolte. 2004. 'Fluid flow and convective transport of solutes within the intervertebral disc', *J Biomech*, 37: 213-21.

Fields, Aaron J., Alexander Ballatori, Ellen C. Liebenberg, and Jeffrey C. Lotz. 2018. 'Contribution of the Endplates to Disc Degeneration', *Current Molecular Biology Reports*, 4: 151-60.

Galbusera, Fabio, Antje Mietsch, Hendrik Schmidt, Hans-Joachim Wilke, and Cornelia Neidlinger-Wilke. 2013. 'Effect of intervertebral disc degeneration on disc cell viability: a numerical investigation', *Computer Methods in Biomechanics and Biomedical Engineering*, 16: 328-37.

Gantenbein, Benjamin, Svenja Illien-Jünger, Samantha Cw Chan, Jochen Walser, Lisbet Haglund, Stephen J. Ferguson, James C. Iatridis, and Sibylle Grad. 2015. 'Organ Culture Bioreactors – Platforms to Study Human Intervertebral Disc Degeneration and Regenerative Therapy', *Current Stem Cell Research & Therapy*, 10: 339-52.

Gao, D. Y., E. Ashworth, P. F. Watson, F. W. Kleinhans, P. Mazur, and J. K. Critser. 1993. 'Hyperosmotic Tolerance of Human Spermatozoa: Separate Effects of Glycerol, Sodium Chloride, and Sucrose on Spermolysis1', *Biology of Reproduction*, 49: 112-23.

Giers, M. B., B. T. Munter, K. J. Eyster, G. D. Ide, Agus Newcomb, J. N. Lehrman, E. Belykh, V. A. Byvaltsev, B. P. Kelly, M. C. Preul, and N. Theodore. 2017a. 'Biomechanical and Endplate Effects on Nutrient Transport in the Intervertebral Disc', *World Neurosurg*, 99: 395-402.

Giers, Morgan B., Liudmila Bardonova, Kyle Eyster, Vadim Byvaltsev, and Mark C. Preul. 2018. 'APOPTOSIS, NUTRITION, AND METABOLISM OF TRANSPLANTED INTERVERTEBRAL DISC CELLS', *Coluna/Columna*, 17: 317-22.

Giers, Morgan B., Alex C. McLaren, Jonathan D. Plasencia, David Frakes, Ryan McLemore, and Michael R. Caplan. 2013. 'Spatiotemporal Quantification of Local Drug Delivery Using MRI', *Computational and Mathematical Methods in Medicine*, 2013: 149608.

Giers, Morgan B., Bryce T. Munter, Kyle J. Eyster, George D. Ide, Anna G. U. S. Newcomb, Jennifer N. Lehrman, Evgenii Belykh, Vadim A. Byvaltsev, Brian P. Kelly, Mark C. Preul, and Nicholas Theodore. 2017b. 'Biomechanical and Endplate Effects on Nutrient Transport in the Intervertebral Disc', *World Neurosurg*, 99: 395-402.

Gilbert, H. T., N. Hodson, P. Baird, S. M. Richardson, and J. A. Hoyland. 2016. 'Acidic pH promotes intervertebral disc degeneration: Acid-sensing ion channel -3 as a potential therapeutic target', *Sci Rep*, 6: 37360.

Gillispie, Gregory, Sang Jin Lee, and James J. Yoo. 2019. 'Bone and Cartilage Tissue Engineering.' in Rui L. Reis (ed.), *Encyclopedia of Tissue Engineering and Regenerative Medicine* (Academic Press: Oxford).

Grant, Michael, Laura Epure, Omar Salem, Motaz Alaqeel, John Antoniou, and Fackson Mwale. 2016. 'Development of a Whole Bovine Long-term Organ Culture System that Retains Vertebral Bone for Intervertebral Disc Repair and Biomechanical Studies using PrimeGrowth Media', *Global Spine Journal*, 6: s-0036-1582897-s-0036-97.

Gruber, H. E., K. Leslie, J. Ingram, G. Hoelscher, H. J. Norton, and E. N. Hanley, Jr. 2004. 'Colony formation and matrix production by human anulus cells: modulation in three-dimensional culture', *Spine (Phila Pa 1976)*, 29: E267-74.

Gruber, Helen E., and Edward N. Jr. Hanley. 1998. 'Analysis of Aging and Degeneration of the Human Intervertebral Disc: Comparison of Surgical Specimens With Normal Controls', *Spine*, 23: 751-57.

Gruber, Helen E., Audrey A. Stasky, and Edward N. Hanley. 1997. 'Characterization and phenotypic stability of human disc cells in Vitro', *Matrix Biology*, 16: 285-88.

Grunhagen, T., A. Shirazi-Adl, J. C. Fairbank, and J. P. Urban. 2011. 'Intervertebral disk nutrition: a review of factors influencing concentrations of nutrients and metabolites', *Orthop Clin North Am*, 42: 465-77, vii.

Grunhagen, Thijs, Geoffrey Wilde, Dahbia Mokhbi Soukane, Saeed A. Shirazi-Adl, and Jill P.G. Urban. 2006. 'Nutrient Supply and Intervertebral Disc Metabolism', *JBJS*, 88: 30-35.

Gu, W. Y., X. G. Mao, R. J. Foster, M. Weidenbaum, V. C. Mow, and B. A. Rawlins. 1999. 'The Anisotropic Hydraulic Permeability of Human Lumbar Anulus Fibrosus: Influence of Age, Degeneration, Direction, and Water Content', *Spine*, 24: 2449.

Gu, W. Y., H. Yao, A. L. Vega, and D. Flagler. 2004. 'Diffusivity of ions in agarose gels and intervertebral disc: effect of porosity', *Ann Biomed Eng*, 32: 1710-7.

Gullbrand, S. E., J. Peterson, J. Ahlborn, R. Mastropolo, A. Fricker, T. T. Roberts, M. Abousayed, J. P. Lawrence, J. C. Glennon, and E. H. Ledet. 2015. 'ISSLS Prize Winner: Dynamic Loading-Induced Convective Transport Enhances Intervertebral Disc Nutrition', *Spine (Phila Pa 1976)*, 40: 1158-64.

Gullbrand, S. E., J. Peterson, R. Mastropolo, T. T. Roberts, J. P. Lawrence, J. C. Glennon, D. J. DiRisio, and E. H. Ledet. 2015. 'Low rate loading-induced convection enhances net transport into the intervertebral disc in vivo', *Spine J*, 15: 1028-33.

Gullbrand, Sarah E., Joshua Peterson, Rosemarie Mastropolo, James P. Lawrence, Luciana Lopes, Jeffrey Lotz, and Eric H. Ledet. 2014. 'Drug-induced changes to the vertebral endplate vasculature affect transport into the intervertebral disc in vivo', *Journal of Orthopaedic Research*, 32: 1694-700.

Guo, Jiang-Bo, Yan-Jun Che, Jun-Jun Hou, Ting Liang, Wen Zhang, Yan Lu, Hui-Lin Yang, and Zong-Ping Luo. 2020. 'Stable mechanical environments created by a low-tension traction device is beneficial for the regeneration and repair of degenerated intervertebral discs', *The Spine Journal*, 20: 1503-16.

Han, Y., X. Li, M. Yan, M. Yang, S. Wang, J. Pan, L. Li, and J. Tan. 2019. 'Oxidative damage induces apoptosis and promotes calcification in disc cartilage endplate cell through ROS/MAPK/NF-kappaB pathway: Implications for disc degeneration', *Biochem Biophys Res Commun*, 516: 1026-32.

Handley, C. J., G. Speight, K. M. Leyden, and D. A. Lowther. 1980. 'Extracellular matrix metabolism by chondrocytes 7. Evidence that L-glutamine is an essential amino acid for chondrocytes and other connective tissue cells', *Biochimica et Biophysica Acta (BBA) - General Subjects*, 627: 324-31.

Harmon, M. D., D. M. Ramos, D. Nithyadevi, R. Bordett, S. Rudraiah, S. P. Nukavarapu, I. L. Moss, and S. G. Kumbar. 2020. 'Growing a backbone - functional biomaterials and structures for intervertebral disc (IVD) repair and regeneration: challenges, innovations, and future directions', *Biomater Sci*, 8: 1216-39.

Hartman, R., P. Patil, R. Tisherman, C. St Croix, L. J. Niedernhofer, P. D. Robbins, F. Ambrosio, B. Van Houten, G. Sowa, and N. Vo. 2018. 'Age-dependent changes in intervertebral disc cell mitochondria and bioenergetics', *Eur Cell Mater*, 36: 171-83.

Hartman, Robert A., Kevin M. Bell, Richard E. Debski, James D. Kang, and Gwendolyn A. Sowa. 2012. 'Novel ex-vivo mechanobiological intervertebral disc culture system', *Journal of Biomechanics*, 45: 382-85.

Hassler, O. 1969. 'The human intervertebral disc. A micro-angiographical study on its vascular supply at various ages', *Acta Orthop Scand*, 40: 765-72.

Haufe, S. M., and A. R. Mork. 2006. 'Intradiscal injection of hematopoietic stem cells in an attempt to rejuvenate the intervertebral discs', *Stem Cells Dev*, 15: 136-7.

Haughton, Victor. 2004. 'Medical Imaging of Intervertebral Disc Degeneration: Current Status of Imaging', *Spine*, 29.

———. 2006. 'Imaging Intervertebral Disc Degeneration', *JBJS*, 88: 15-20.

Hegewald, Aldemar A., Michaela Endres, Alexander Abbushi, Mario Cabraja, Christian Woiciechowsky, Kirsten Schmieder, Christian Kaps, and Claudius Thomé. 2011. 'Adequacy of herniated disc tissue as a cell source for nucleus pulposus regeneration: Laboratory investigation', *Journal of Neurosurgery: Spine SPI*, 14: 273-80.

Hirsch, Carl. 1955. 'THE REACTION OF INTERVERTEBRAL DISCS TO COMPRESSION FORCES', *JBJS*, 37.

Hohaus, C., T. M. Ganey, Y. Minkus, and H. J. Meisel. 2008. 'Cell transplantation in lumbar spine disc degeneration disease', *Eur Spine J*, 17 Suppl 4: 492-503.

Holm, S., A. Maroudas, J. P. G. Urban, G. Selstam, and A. Nachemson. 1981a. 'Nutrition of the Intervertebral Disc: Solute Transport and Metabolism', *Connective Tissue Research*, 8: 101-19.

Holm, S., A. Maroudas, J. P. Urban, G. Selstam, and A. Nachemson. 1981b. 'Nutrition of the intervertebral disc: solute transport and metabolism', *Connect Tissue Res*, 8: 101-19.

Holm, S., and A. Nachemson. 1983. 'Variations in the nutrition of the canine intervertebral disc induced by motion', *Spine*, 8: 866-74.

Holm, Sten, and Gunnar Selstam. 1982. 'Oxygen Tension Alterations in the Intervertebral Disc as a Response to Changes in the Arterial Blood', *Upsala Journal of Medical Sciences*, 87: 163-74.

HOLM, STEN, GUNNAR SELSTAM, and ALF NACHEMSON. 1982. 'Carbohydrate metabolism and concentration profiles of solutes in the canine lumbar intervertebral disc', *Acta Physiologica Scandinavica*, 115: 147-56.

Horner, Heather A., and Jill P. G. Urban. 2001. '2001 Volvo Award Winner in Basic Science Studies: Effect of Nutrient Supply on the Viability of Cells From the Nucleus Pulposus of the Intervertebral Disc', *Spine*, 26.

Hoy, D., L. March, P. Brooks, F. Blyth, A. Woolf, C. Bain, G. Williams, E. Smith, T. Vos, J. Barendregt, C. Murray, R. Burstein, and R. Buchbinder. 2014. 'The global burden of low back pain: estimates from the Global Burden of Disease 2010 study', *Annals of the rheumatic diseases*, 73: 968-74.

Hsu, Edward W., and Lori A. Setton. 1999. 'Diffusion tensor microscopy of the intervertebral disc anulus fibrosus', *Magnetic Resonance in Medicine*, 41: 992-99.

Huang, C. Y., and W. Y. Gu. 2008. 'Effects of mechanical compression on metabolism and distribution of oxygen and lactate in intervertebral disc', *J Biomech*, 41: 1184-96.

Huang, Y. C., J. P. Urban, and K. D. Luk. 2014. 'Intervertebral disc regeneration: do nutrients lead the way?', *Nat Rev Rheumatol*, 10: 561-6.

Hughes, S. P. F., A. L. Wallace, I. D. McCarthy, R. H. Fleming, and B. C. Wyatt. 1993. 'Measurement of blood flow to the vertebral bone and disc', *European Spine Journal*, 2: 96-98.

Iatridis, J. C., J. J. MacLean, M. O'Brien, and I. A. Stokes. 2007. 'Measurements of proteoglycan and water content distribution in human lumbar intervertebral discs', *Spine (Phila Pa 1976)*, 32: 1493-7.

Ishihara, H., and J. P. Urban. 1999. 'Effects of low oxygen concentrations and metabolic inhibitors on proteoglycan and protein synthesis rates in the intervertebral disc', *J Orthop Res*, 17: 829-35.

Ishihara, Kazuhiro, Hiromi Matsuzaki, and Ken Wakabayashi. 1996. 'Cryopreserved intervertebral disc allografts in dogs: Chronological changes in 3-year period after transplantation', *Journal of Orthopaedic Science*, 1: 259-67.

Ito, Keita, and Laura Creemers. 2013. 'Mechanisms of Intervertebral Disk Degeneration/Injury and Pain: A Review', *Global Spine Journal*, 3: 145-51.

Iwashina, T., J. Mochida, D. Sakai, Y. Yamamoto, T. Miyazaki, K. Ando, and T. Hotta. 2006. 'Feasibility of using a human nucleus pulposus cell line as a cell source in cell transplantation therapy for intervertebral disc degeneration', *Spine (Phila Pa 1976)*, 31: 1177-86.

Jackson, A. R., C. Y. Huang, and W. Y. Gu. 2011. 'Effect of endplate calcification and mechanical deformation on the distribution of glucose in intervertebral disc: a 3D finite element study', *Comput Methods Biomech Biomed Engin*, 14: 195-204.

Jackson, A. R., T. Y. Yuan, C. Y. Huang, and W. Y. Gu. 2009. 'A conductivity approach to measuring fixed charge density in intervertebral disc tissue', *Ann Biomed Eng*, 37: 2566-73.

Jackson, A. R., T. Y. Yuan, C. Y. Huang, F. Travascio, and W. Yong Gu. 2008a. 'Effect of compression and anisotropy on the diffusion of glucose in annulus fibrosus', *Spine (Phila Pa 1976)*, 33: 1-7.

Jackson, Alicia R., Adam Eismont, Lu Yu, Na Li, Weiyong Gu, Frank Eismont, and Mark D. Brown. 2018. 'Diffusion of antibiotics in intervertebral disc', *Journal of Biomechanics*, 76: 259-62.

Jackson, Alicia R., Chun-Yuh C. Huang, Mark D. Brown, and Wei Yong Gu. 2011. '3D Finite Element Analysis of Nutrient Distributions and Cell Viability in the Intervertebral Disc: Effects of Deformation and Degeneration', *Journal of Biomechanical Engineering*, 133.

Jackson, Alicia R., Tai-Yi Yuan, Chun-Yuh Huang, Mark D. Brown, and Wei Yong Gu. 2012. 'Nutrient Transport in Human Annulus Fibrosus is Affected by Compressive Strain and Anisotropy', *Annals of Biomedical Engineering*, 40: 2551-58.

Jackson, Alicia R., Tai-Yi Yuan, Chun-Yuh C. Huang, Francesco Travascio, and Wei Yong Gu. 2008b. 'Effect of Compression and Anisotropy on the Diffusion of Glucose in Annulus Fibrosus', *Spine*, 33.

Jang, T. H., S. C. Park, J. H. Yang, J. Y. Kim, J. H. Seok, U. S. Park, C. W. Choi, S. R. Lee, and J. Han. 2017. 'Cryopreservation and its clinical applications', *Integr Med Res*, 6: 12-18.

Jiang, Libo, Xiaolei Zhang, Xuhao Zheng, Ao Ru, Xiao Ni, Yaosen Wu, Naifeng Tian, Yixing Huang, Enxing Xue, Xiangyang Wang, and Huazi Xu. 2013. 'Apoptosis, senescence, and autophagy in rat nucleus pulposus cells: Implications for diabetic intervertebral disc degeneration', *Journal of Orthopaedic Research*, 31: 692-702.

Jomha, Nadr M., Andrew D. H. Weiss, J. Fraser Forbes, Garson K. Law, Janet A. W. Elliott, and Locksley E. McGann. 2010. 'Cryoprotectant agent toxicity in porcine articular chondrocytes', *Cryobiology*, 61: 297-302.

Jones, W., and R. E. Roberts. 1933. 'Pathological Calcification and Ossification in Relation to Leriche and Policard's Theory', *Proc R Soc Med*, 26: 853-9.

Jouven, Xavier, Rozenn N. Lemaître, Thomas D. Rea, Nona Sotoodehnia, Jean-Philippe Empana, and David S. Siscovick. 2005. 'Diabetes, glucose level, and risk of sudden cardiac death', *European Heart Journal*, 26: 2142-47.

Junger, S., B. Gantenbein-Ritter, P. Lezuo, M. Alini, S. J. Ferguson, and K. Ito. 2009. 'Effect of limited nutrition on in situ intervertebral disc cells under simulated-physiological loading', *Spine (Phila Pa 1976)*, 34: 1264-71.

Katsuura, A., and S. Hukuda. 1994. 'Experimental study of intervertebral disc allografting in the dog', *Spine (Phila Pa 1976)*, 19: 2426-32.

KATZ, MICHAEL M., ALAN R. HARGENS, and STEVEN R. GARFIN. 1986. 'Intervertebral Disc Nutrition: Diffusion Versus Convection', *Clinical Orthopaedics and Related Research®*, 210: 243-45.

Kealey, Susan M., Todd Aho, David Delong, Daniel P. Barboriak, James M. Provenzale, and James D. Eastwood. 2005. 'Assessment of Apparent Diffusion Coefficient in Normal and Degenerated Intervertebral Lumbar Disks: Initial Experience', *Radiology*, 235: 569-74.

Keshari, K. R., J. C. Lotz, J. Kurhanewicz, and S. Majumdar. 2005. 'Correlation of HR-MAS spectroscopy derived metabolite concentrations with collagen and proteoglycan levels and Thompson grade in the degenerative disc', *Spine (Phila Pa 1976)*, 30: 2683-8.

Keshari, K. R., J. C. Lotz, T. M. Link, S. Hu, S. Majumdar, and J. Kurhanewicz. 2008. 'Lactic acid and proteoglycans as metabolic markers for discogenic back pain', *Spine (Phila Pa 1976)*, 33: 312-7.

Keshari, K. R., A. S. Zektzer, M. G. Swanson, S. Majumdar, J. C. Lotz, and J. Kurhanewicz. 2005. 'Characterization of intervertebral disc degeneration by high-resolution magic angle spinning (HR-MAS) spectroscopy', *Magn Reson Med*, 53: 519-27.

Kihara, T., J. Ito, and J. Miyake. 2013. 'Measurement of biomolecular diffusion in extracellular matrix condensed by fibroblasts using fluorescence correlation spectroscopy', *PLOS ONE*, 8: e82382.

King, T. 1959. 'Another look at the problem of lumbo-sacral pain and sciatica', *Med J Aust*, 46: 8-12.

Knight, Eleanor, and Stefan Przyborski. 2015. 'Advances in 3D cell culture technologies enabling tissue-like structures to be created in vitro', *Journal of anatomy*, 227: 746-56.

KRAEMER, J, D KOLDITZ, and R GOWIN. 1985a. 'Water and Electrolyte Content of Human Intervertebral Discs Under Variable Load', *Spine*, 10: 69-71.

Kraemer, J., D. Kolditz, and R. Gowin. 1985b. 'Water and electrolyte content of human intervertebral discs under variable load', *Spine (Phila Pa 1976)*, 10: 69-71.

Kuo, Y. W., Y. C. Hsu, I. T. Chuang, P. H. Chao, and J. L. Wang. 2014. 'Spinal traction promotes molecular transportation in a simulated degenerative intervertebral disc model', *Spine (Phila Pa 1976)*, 39: E550-6.

Kwon, Young Jik, and Ching-An Peng. 2002. 'Calcium-Alginate Gel Bead Cross-Linked with Gelatin as Microcarrier for Anchorage-Dependent Cell Culture', *BioTechniques*, 33: 212-18.

Lam, S. K., S. C. Chan, V. Y. Leung, W. W. Lu, K. M. Cheung, and K. D. Luk. 2011. 'The role of cryopreservation in the biomechanical properties of the intervertebral disc', *Eur Cell Mater*, 22: 393-402.

Lawson, A., H. Ahmad, and A. Sambanis. 2011. 'Cytotoxicity effects of cryoprotectants as single-component and cocktail vitrification solutions', *Cryobiology*, 62: 115-22.

Le Bihan, D., E. Breton, D. Lallemand, P. Grenier, E. Cabanis, and M. Laval-Jeantet. 1986. 'MR imaging of intravoxel incoherent motions: application to diffusion and perfusion in neurologic disorders', *Radiology*, 161: 401-7.

Le Maitre, Christine L., Chitra L. Dahia, Morgan Giers, Svenja Illien-Junger, Claudia Cicione, Dino Samartzis, Gianluca Vadala, Aaron Fields, and Jeffrey Lotz. 2021. 'Development of a standardized histopathology scoring system for human intervertebral disc degeneration: an Orthopaedic Research Society Spine Section Initiative', *JOR SPINE*, 4: e1167.

Le Maitre, Christine Lyn, Anthony J. Freemont, and Judith Alison Hoyland. 2005. 'The role of interleukin-1 in the pathogenesis of human Intervertebral disc degeneration', *Arthritis Research & Therapy*, 7: R732.

Le Maitre, Christine Lyn, Anthony John Freemont, and Judith Alison Hoyland. 2007. 'Accelerated cellular senescence in degenerate intervertebral discs: a possible role in the pathogenesis of intervertebral disc degeneration', *Arthritis Research & Therapy*, 9: R45.

Li, Long-Yang, Xiao-Lin Wu, Richard J. Roman, Fan Fan, Chen-Sheng Qiu, and Bo-Hua Chen. 2018. 'Diffusion-weighted 7.0T Magnetic Resonance Imaging in Assessment of Intervertebral Disc Degeneration in Rats', *Chinese medical journal*, 131: 63-68.

Liebscher, T., M. Haefeli, K. Wuertz, A. G. Nerlich, and N. Boos. 2011a. 'Age-related variation in cell density of human lumbar intervertebral disc', *Spine (Phila Pa 1976)*, 36: 153-9.

Liebscher, Thomas, Mathias Haefeli, Karin Wuertz, Andreas G. Nerlich, and Norbert Boos. 2011b. 'Age-Related Variation in Cell Density of Human Lumbar Intervertebral Disc', *Spine*, 36: 153-59.

Link, T. M., J. Neumann, and X. Li. 2017. 'Prestructural cartilage assessment using MRI', *J Magn Reson Imaging*, 45: 949-65.

Lisbet Haglund, Janet Moir, Lorne Beckman , Kyle R. Mulligan , Bernice Jim , Jean A. Ouellet , Peter Roughley , and and Thomas Steffen 2011. 'Development of a Bioreactor for Axially Loaded Intervertebral Disc Organ Culture', *Tissue Engineering Part C: Methods*, 17: 1011-19.

Liu, M. H., C. Sun, Y. Yao, X. Fan, H. Liu, Y. H. Cui, X. W. Bian, B. Huang, and Y. Zhou. 2016. 'Matrix stiffness promotes cartilage endplate chondrocyte calcification in disc degeneration via miR-20a targeting ANKH expression', *Sci Rep*, 6: 25401.

Liu, Y., Y. Li, L. P. Nan, F. Wang, S. F. Zhou, J. C. Wang, X. M. Feng, and L. Zhang. 2020. 'The effect of high glucose on the biological characteristics of nucleus pulposus-derived mesenchymal stem cells', *Cell Biochem Funct*, 38: 130-40.

Ludescher, Burkhard, Julia Effelsberg, Petros Martirosian, Günter Steidle, Bernd Markert, Claus Claussen, and Fritz Schick. 2008. 'T2- and diffusion-maps reveal diurnal changes of intervertebral disc composition: An in vivo MRI study at 1.5 Tesla', *Journal of Magnetic Resonance Imaging*, 28: 252-57.

Lyons, G., S. M. Eisenstein, and M. B. Sweet. 1981a. 'Biochemical changes in intervertebral disc degeneration', *Biochim Biophys Acta*, 673: 443-53.

Lyons, Gillian, S. M. Eisenstein, and M. B. E. Sweet. 1981b. 'Biochemical changes in intervertebral disc degeneration', *Biochimica et Biophysica Acta (BBA) - General Subjects*, 673: 443-53.

Madhu, Vedavathi, Paige K Boneski, Elizabeth Silagi, Yunping Qiu, Irwin Kurland, Anyonya R Guntur, Irving M Shapiro, and Makarand V Risbud. 2020. 'Hypoxic Regulation of Mitochondrial Metabolism and Mitophagy in Nucleus Pulposus Cells Is Dependent on HIF-1α–BNIP3 Axis', *Journal of Bone and Mineral Research*, 35: 1504-24.

Magnier, C., O. Boiron, S. Wendling-Mansuy, P. Chabrand, and V. Deplano. 2009a. 'Nutrient distribution and metabolism in the intervertebral disc in the unloaded state: a parametric study', *J Biomech*, 42: 100-8.

Magnier, Carole, Olivier Boiron, Sylvie Wendling-Mansuy, Patrick Chabrand, and Valérie Deplano. 2009b. 'Nutrient distribution and metabolism in the intervertebral disc in the unloaded state: A parametric study', *Journal of Biomechanics*, 42: 100-08.

Mahmoudifar, Nastaran, and Pauline M. Doran. 2010. 'Chondrogenic differentiation of human adipose-derived stem cells in polyglycolic acid mesh scaffolds under dynamic culture conditions', *Biomaterials*, 31: 3858-67.

Malandrino, A., D. Lacroix, C. Hellmich, K. Ito, S. J. Ferguson, and J. Noailly. 2014a. 'The role of endplate poromechanical properties on the nutrient availability in the intervertebral disc', *Osteoarthritis Cartilage*, 22: 1053-60.

———. 2014b. 'The role of endplate poromechanical properties on the nutrient availability in the intervertebral disc', *Osteoarthritis and Cartilage*, 22: 1053-60.

Malandrino, A., J. Noailly, and D. Lacroix. 2011a. 'The effect of sustained compression on oxygen metabolic transport in the intervertebral disc decreases with degenerative changes', *PLoS Comput Biol*, 7: e1002112.

Malandrino, Andrea, Jérôme Noailly, and Damien Lacroix. 2011b. 'The Effect of Sustained Compression on Oxygen Metabolic Transport in the Intervertebral Disc Decreases with Degenerative Changes', *PLOS Computational Biology*, 7: e1002112.

———. 2014. 'Numerical exploration of the combined effect of nutrient supply, tissue condition and deformation in the intervertebral disc', *Journal of Biomechanics*, 47: 1520-25.

Malandrino, Andrea, José M. Pozo, Isaac Castro-Mateos, Alejandro F. Frangi, Marc M. van Rijsbergen, Keita Ito, Hans-Joachim Wilke, Tien Tuan Dao, Marie-Christine Ho Ba Tho, and Jérôme Noailly. 2015. 'On the Relative Relevance of Subject-Specific Geometries and Degeneration-Specific Mechanical Properties for the Study of Cell Death in Human Intervertebral Disk Models', *Frontiers in Bioengineering and Biotechnology*, 3.

Malcolmson, P. H. 1935. 'Radiologic Study of the Development of the Spine and Pathologic Changes of the Intervertebral Disc', *Radiology*, 25: 98-104.

Malko, John A., William C. Hutton, and William A. Fajman. 1999. 'An In Vivo Magnetic Resonance Imaging Study of Changes in the Volume (and Fluid Content) of the Lumbar Intervertebral Discs During a Simulated Diurnal Load Cycle', *Spine*, 24: 1015-22.

———. 2002. 'An In Vivo MRI Study of the Changes in Volume (and Fluid Content) of the Lumbar Intervertebral Disc After Overnight Bed Rest and During an 8-Hour Walking Protocol', *Clinical Spine Surgery*, 15: 157-63.

Maroudas, A., R. A. Stockwell, A. Nachemson, and J. Urban. 1975. 'Factors involved in the nutrition of the human lumbar intervertebral disc: cellularity and diffusion of glucose in vitro', *Journal of anatomy*, 120: 113-30.

Martin, I., D. Wendt, and M. Heberer. 2004. 'The role of bioreactors in tissue engineering', *Trends Biotechnol*, 22: 80-6.

Martins, Delio Eulalio, Valquiria Pereira de Medeiros, Marcelo Wajchenberg, Edgar Julian Paredes-Gamero, Marcelo Lima, Rejane Daniele Reginato, Helena Bonciani Nader, Eduardo Barros Puertas, and Flavio Faloppa. 2018. 'Changes in human intervertebral disc biochemical composition and bony end plates between middle and old age', *PLOS ONE*, 13: e0203932.

McGann, L. E., H. Y. Yang, and M. Walterson. 1988. 'Manifestations of cell damage after freezing and thawing', *Cryobiology*, 25: 178-85.

McMillan, D. W., G. Garbutt, and M. A. Adams. 1996. 'Effect of sustained loading on the water content of intervertebral discs: implications for disc metabolism', *Annals of the rheumatic diseases*, 55: 880-87.

McMurtrey, R. J. 2016. 'Analytic Models of Oxygen and Nutrient Diffusion, Metabolism Dynamics, and Architecture Optimization in Three-Dimensional Tissue Constructs with Applications and Insights in Cerebral Organoids', *Tissue Eng Part C Methods*, 22: 221-49.

Meisel, H. J., T. Ganey, W. C. Hutton, J. Libera, Y. Minkus, and O. Alasevic. 2006a. 'Clinical experience in cell-based therapeutics: intervention and outcome', *Eur Spine J*, 15 Suppl 3: S397-405.

Meisel, H. J., V. Siodla, T. Ganey, Y. Minkus, W. C. Hutton, and O. J. Alasevic. 2007. 'Clinical experience in cell-based therapeutics: disc chondrocyte transplantation A treatment for degenerated or damaged intervertebral disc', *Biomol Eng*, 24: 5-21.

Meisel, Hans Joerg, Timothy Ganey, William C. Hutton, Jeanette Libera, Yvonne Minkus, and Olivera Alasevic. 2006b. 'Clinical experience in cell-based therapeutics: intervention and outcome', *European spine journal : official publication of the European Spine Society, the European Spinal Deformity Society, and the European Section of the Cervical Spine Research Society*, 15 Suppl 3: S397-S405.

Miyamoto, Kei, Koichi Masuda, Jesse G. Kim, Nozomu Inoue, Koji Akeda, Gunnar B. J. Andersson, and Howard S. An. 2006. 'Intradiscal injections of osteogenic protein-1 restore the viscoelastic properties of degenerated intervertebral discs', *The Spine Journal*, 6: 692-703.

Mizuno, S., F. Allemann, and J. Glowacki. 2001. 'Effects of medium perfusion on matrix production by bovine chondrocytes in three-dimensional collagen sponges', *J Biomed Mater Res*, 56: 368-75.

Mokhbi Soukane, D., A. Shirazi-Adl, and J. P. Urban. 2009. 'Investigation of solute concentrations in a 3D model of intervertebral disc', *Eur Spine J*, 18: 254-62.

Mokhbi Soukane, D.;, A.; Shirazi-Adl, and J. P. G.; Urban. 2007. 'Computation of coupled diffusion of oxygen, glucose and lactic acid in an intervertebral disc', *Journal of Biomechanics*, 40: 2645-54.

Motaghinasab, S., A. Shirazi-Adl, M. Parnianpour, and J. P. G. Urban. 2014. 'Disc size markedly influences concentration profiles of intravenously administered solutes in the intervertebral disc: a computational study on glucosamine as a model solute', *European Spine Journal*, 23: 715-23.

Muftuler, L. Tugan, Joshua P. Jarman, Hon J. Yu, Vance O. Gardner, Dennis J. Maiman, and Volkan Emre Arpinar. 2015. 'Association between intervertebral disc degeneration and endplate perfusion studied by DCE-MRI', *European Spine Journal*, 24: 679-85.

Murrell, W., E. Sanford, L. Anderberg, B. Cavanagh, and A. Mackay-Sim. 2009. 'Olfactory stem cells can be induced to express chondrogenic phenotype in a rat intervertebral disc injury model', *Spine J*, 9: 585-94.

Mwale, F., J. C. Iatridis, and J. Antoniou. 2008. 'Quantitative MRI as a diagnostic tool of intervertebral disc matrix composition and integrity', *Eur Spine J*, 17 Suppl 4: 432-40.

Mwale, Fackson, Ioana Ciobanu, Demetri Giannitsios, Peter Roughley, Thomas Steffen, and John Antoniou. 2011. 'Effect of Oxygen Levels on Proteoglycan Synthesis by Intervertebral Disc Cells', *Spine*, 36: E131-E38.

Mwale, Fackson, Caroline N. Demers, Arthur J. Michalek, Gilles Beaudoin, Tapas Goswami, Lorne Beckman, James C. Iatridis, and John Antoniou. 2008. 'Evaluation of quantitative magnetic resonance imaging, biochemical and mechanical properties of trypsin-treated intervertebral discs under physiological compression loading', *Journal of magnetic resonance imaging : JMRI*, 27: 563-73.

Nachemson, A., T. Lewin, A. Maroudas, and M. A. Freeman. 1970. 'In vitro diffusion of dye through the end-plates and the annulus fibrosus of human lumbar inter-vertebral discs', *Acta Orthop Scand*, 41: 589-607.

Nachemson, Alf. 1969. 'Intradiscal Measurements of pH in Patients with Lumbar Rhizopathies', *Acta Orthopaedica Scandinavica*, 40: 23-42.

Naqvi, S. M., and C. T. Buckley. 2015. 'Extracellular matrix production by nucleus pulposus and bone marrow stem cells in response to altered oxygen and glucose microenvironments', *Journal of anatomy*, 227: 757-66.

Naresh-Babu, J., G. Neelima, S. Reshma Begum, and V. Siva-Leela. 2016. 'Diffusion characteristics of human annulus fibrosus-a study documenting the dependence of annulus fibrosus on end plate for diffusion', *Spine J*, 16: 1007-14.

Natarajan, R. N., J. R. Williams, and G. B. Andersson. 2006. 'Modeling changes in intervertebral disc mechanics with degeneration', *The Journal of bone and joint surgery. American volume*, 88 Suppl 2: 36-40.

Naylor, A. 1951. 'Brachial neuritis, with particular reference to lesions of the cervical intervertebral discs', *Ann R Coll Surg Engl*, 9: 158-88.

———. 1962. 'The biophysical and biochemical aspects of intervertebral disc herniation and degeneration', *Ann R Coll Surg Engl*, 31: 91-114.

Naylor, A., F. Happey, and T. Macrae. 1955. 'Changes in the human intervertebral disc with age: a biophysical study', *J Am Geriatr Soc*, 3: 964-73.

Neidlinger-Wilke, Cornelia, Antje Mietsch, Christina Rinkler, Hans-Joachim Wilke, Anita Ignatius, and Jill Urban. 2012. 'Interactions of environmental conditions and mechanical loads have influence on matrix turnover by nucleus pulposus cells', *Journal of Orthopaedic Research*, 30: 112-21.

Nguyen-minh, C, V M Haughton, R A Papke, H An, and S C Censky. 1998. 'Measuring diffusion of solutes into intervertebral disks with MR imaging and paramagnetic contrast medium', *American Journal of Neuroradiology*, 19: 1781-84.

Nguyen-minh, C, L Riley, K C Ho, R Xu, H An, and V M Haughton. 1997. 'Effect of degeneration of the intervertebral disk on the process of diffusion', *American Journal of Neuroradiology*, 18: 435-42.

Nguyen, An M., Wade Johannessen, Jonathon H. Yoder, Andrew J. Wheaton, Edward J. Vresilovic, Arijitt Borthakur, and Dawn M. Elliott. 2008. 'Noninvasive quantification of human nucleus pulposus pressure with use of T1rho-weighted magnetic resonance imaging', *The Journal of bone and joint surgery. American volume*, 90: 796-802.

Niinimäki, Jaakko, Arto Korkiakoski, Outi Ojala, Jaro Karppinen, Jyrki Ruohonen, Marianne Haapea, Raija Korpelainen, Antero Natri, and Osmo Tervonen. 2009. 'Association between visual degeneration of intervertebral discs and the apparent diffusion coefficient', *Magnetic Resonance Imaging*, 27: 641-47.

Nomura, T., J. Mochida, M. Okuma, K. Nishimura, and K. Sakabe. 2001. 'Nucleus pulposus allograft retards intervertebral disc degeneration', *Clinical orthopaedics and related research*: 94-101.

Noriega, D. C., F. Ardura, R. Hernandez-Ramajo, M. A. Martin-Ferrero, I. Sanchez-Lite, B. Toribio, M. Alberca, V. Garcia, J. M. Moraleda, A. Sanchez, and J. Garcia-Sancho. 2017. 'Intervertebral Disc Repair by Allogeneic Mesenchymal Bone Marrow Cells: A Randomized Controlled Trial', *Transplantation*, 101: 1945-51.

O'Connell, G. D., E. J. Vresilovic, and D. M. Elliott. 2007. 'Comparison of animals used in disc research to human lumbar disc geometry', *Spine (Phila Pa 1976)*, 32: 328-33.

O'Hara, B. P., J. P. Urban, and A. Maroudas. 1990. 'Influence of cyclic loading on the nutrition of articular cartilage', *Annals of the rheumatic diseases*, 49: 536-39.

O'Connell, Grace D., Edward J. Vresilovic, and Dawn M. Elliott. 2007. 'Comparison of Animals Used in Disc Research to Human Lumbar Disc Geometry', *Spine*, 32.

Oegema, Theodore R. 1993. 'Biochemistry of the Intervertebral Disc', *Clinics in Sports Medicine*, 12: 419-38.

Ogata, K., and L. A. Whiteside. 1981. '1980 Volvo award winner in basic science. Nutritional pathways of the intervertebral disc. An experimental study using hydrogen washout technique', *Spine*, 6: 211-16.

Ogrodnik, Mikolaj. 2021. 'Cellular aging beyond cellular senescence: Markers of senescence prior to cell cycle arrest in vitro and in vivo', *Aging Cell*, 20: e13338.

Ohtori, S., G. Inoue, M. Miyagi, and K. Takahashi. 2015. 'Pathomechanisms of discogenic low back pain in humans and animal models', *Spine J*, 15: 1347-55.

Okuma, M., J. Mochida, K. Nishimura, K. Sakabe, and K. Seiki. 2000. 'Reinsertion of stimulated nucleus pulposus cells retards intervertebral disc degeneration: an in vitro and in vivo experimental study', *J Orthop Res*, 18: 988-97.

Orozco, L., R. Soler, C. Morera, M. Alberca, A. Sanchez, and J. Garcia-Sancho. 2011. 'Intervertebral disc repair by autologous mesenchymal bone marrow cells: a pilot study', *Transplantation*, 92: 822-8.

Pacholczyk-Sienicka, Barbara, Maciej Radek, Andrzej Radek, and Stefan Jankowski. 2015. 'Characterization of metabolites determined by means of 1H HR MAS NMR in

intervertebral disc degeneration', *Magnetic Resonance Materials in Physics, Biology and Medicine*, 28: 173-83.

Pardo-Alonso, Samuel, Jerome Vicente, Eusebio Solórzano, Miguel Ángel Rodriguez-Perez, and Dirk Lehmhus. 2014. 'Geometrical Tortuosity 3D Calculations in Infiltrated Aluminium Cellular Materials', *Procedia Materials Science*, 4: 145-50.

Park, Jong-Soo, Jong-Beom Park, In-Joo Park, and Eun-Young Park. 2014. 'Accelerated premature stress-induced senescence of young annulus fibrosus cells of rats by high glucose-induced oxidative stress', *International Orthopaedics*, 38: 1311-20.

Park, S., and G. Stephanopoulos. 1993. 'Packed bed bioreactor with porous ceramic beads for animal cell culture', *Biotechnol Bioeng*, 41: 25-34.

Pathak, Ranoo, and Suddhasatwa Basu. 2013. 'Mathematical modeling and experimental verification of direct glucose anion exchange membrane fuel cell', *Electrochimica Acta*, 113: 42-53.

Pattappa, G., Z. Li, M. Peroglio, N. Wismer, M. Alini, and S. Grad. 2012. 'Diversity of intervertebral disc cells: phenotype and function', *Journal of anatomy*, 221: 480-96.

Payne, E. E., and J. D. Spillane. 1957. 'The cervical spine; an anatomico-pathological study of 70 specimens (using a special technique) with particular reference to the problem of cervical spondylosis', *Brain*, 80: 571-96.

Pfannkuche, Judith-Johanna, Wei Guo, Shangbin Cui, Junxuan Ma, Gernot Lang, Marianna Peroglio, R. Geoff Richards, Mauro Alini, Sibylle Grad, and Zhen Li. 2020. 'Intervertebral disc organ culture for the investigation of disc pathology and regeneration – benefits, limitations, and future directions of bioreactors', *Connective Tissue Research*, 61: 304-21.

Pfirrmann, Christian W. A., Alexander Metzdorf, Marco Zanetti, Juerg Hodler, and Norbert Boos. 2001. 'Magnetic Resonance Classification of Lumbar Intervertebral Disc Degeneration', *Spine*, 26: 1873-78.

Preradovic, Adrijana, Guenther Kleinpeter, Hans Feichtinger, Ernest Balaun, and Walter Krugluger. 2005. 'Quantitation of collagen I, collagen II and aggrecan mRNA and expression of the corresponding proteins in human nucleus pulposus cells in monolayer cultures', *Cell and Tissue Research*, 321: 459-64.

Pulickal, Tina, Johannes Boos, Markus Konieczny, Lino Morris Sawicki, Anja Müller-Lutz, Bernd Bittersohl, Joachim Gerß, Markus Eichner, Hans-Jörg Wittsack, Gerald Antoch, and Christoph Schleich. 2019. 'MRI identifies biochemical alterations of intervertebral discs in patients with low back pain and radiculopathy', *European Radiology*, 29: 6443-46.

Rajaee, Sean S., Hyun W. Bae, Linda E. A. Kanim, and Rick B. Delamarter. 2012. 'Spinal fusion in the United States: analysis of trends from 1998 to 2008', *Spine*, 37: 67-76.

Rajasekaran, S., J. N. Babu, R. Arun, B. R. Armstrong, A. P. Shetty, and S. Murugan. 2004. 'ISSLS prize winner: A study of diffusion in human lumbar discs: a serial magnetic resonance imaging study documenting the influence of the endplate on diffusion in normal and degenerate discs', *Spine (Phila Pa 1976)*, 29: 2654-67.

Rajasekaran, S., K. Venkatadass, J. Naresh Babu, K. Ganesh, and A. P. Shetty. 2008. 'Pharmacological enhancement of disc diffusion and differentiation of healthy, ageing and degenerated discs', *European Spine Journal*, 17: 626-43.

Rajasekaran, S., S. Vidyadhara, M. Subbiah, V. Kamath, R. Karunanithi, A. P. Shetty, K. Venkateswaran, M. Babu, and J. Meenakshi. 2010. 'ISSLS prize winner: a study of effects of in vivo mechanical forces on human lumbar discs with scoliotic disc as a biological model: results from serial postcontrast diffusion studies, histopathology and biochemical analysis of twenty-one human lumbar scoliotic discs', *Spine (Phila Pa 1976)*, 35: 1930-43.

Reisener, Marie-Jacqueline, Matthias Pumberger, Jennifer Shue, Federico P. Girardi, and Alexander P. Hughes. 2020a. 'Trends in lumbar spinal fusion-a literature review', *Journal of spine surgery (Hong Kong)*, 6: 752-61.

Reisener, Marie-Jacqueline;, Matthias; Pumberger, Jennifer; Shue, Federico P.; Girardi, and Alexander P.; Hughes. 2020b. 'Trends in lumbar spinal fusion—a literature review', *Journal of Spine Surgery*, 6: 752-61.

Renkin, E. M. 1954. 'Filtration, diffusion, and molecular sieving through porous cellulose membranes', *J Gen Physiol*, 38: 225-43.

Richardson, S. M., G. Kalamegam, P. N. Pushparaj, C. Matta, A. Memic, A. Khademhosseini, R. Mobasheri, F. L. Poletti, J. A. Hoyland, and A. Mobasheri. 2016. 'Mesenchymal stem

cells in regenerative medicine: Focus on articular cartilage and intervertebral disc regeneration', *Methods*, 99: 69-80.

Risbud, M. V., A. Guttapalli, D. G. Stokes, D. Hawkins, K. G. Danielson, T. P. Schaer, T. J. Albert, and I. M. Shapiro. 2006. 'Nucleus pulposus cells express HIF-1 alpha under normoxic culture conditions: a metabolic adaptation to the intervertebral disc microenvironment', *J Cell Biochem*, 98: 152-9.

Risbud, Makarand V., Zachary R. Schoepflin, Fackson Mwale, Rita A. Kandel, Sibylle Grad, James C. Iatridis, Daisuke Sakai, and Judith A. Hoyland. 2015. 'Defining the phenotype of young healthy nucleus pulposus cells: Recommendations of the Spine Research Interest Group at the 2014 annual ORS meeting', *Journal of Orthopaedic Research*, 33: 283-93.

Roberts, S., J. Menage, and J. P. Urban. 1989. 'Biochemical and structural properties of the cartilage end-plate and its relation to the intervertebral disc', *Spine*, 14: 166-74.

Sakai, D., and G. B. Andersson. 2015. 'Stem cell therapy for intervertebral disc regeneration: obstacles and solutions', *Nat Rev Rheumatol*, 11: 243-56.

Sakai, D., and S. Grad. 2015a. 'Advancing the cellular and molecular therapy for intervertebral disc disease', *Adv Drug Deliv Rev*, 84: 159-71.

Sakai, D., and J. Schol. 2017. 'Cell therapy for intervertebral disc repair: Clinical perspective', *J Orthop Translat*, 9: 8-18.

Sakai, Daisuke, and Sibylle Grad. 2015b. 'Advancing the cellular and molecular therapy for intervertebral disc disease', *Advanced Drug Delivery Reviews*, 84: 159-71.

Sampson, S. L., M. Sylvia, and A. J. Fields. 2019. 'Effects of dynamic loading on solute transport through the human cartilage endplate', *J Biomech*, 83: 273-79.

Sato, Katsuhiko, Shinichi Kikuchi, and Takumi Yonezawa. 1999. 'In Vivo Intradiscal Pressure Measurement in Healthy Individuals and in Patients With Ongoing Back Problems', *Spine*, 24: 2468.

Sato, M., T. Asazuma, M. Ishihara, M. Ishihara, T. Kikuchi, M. Kikuchi, and K. Fujikawa. 2003. 'An experimental study of the regeneration of the intervertebral disc with an allograft of cultured annulus fibrosus cells using a tissue-engineering method', *Spine (Phila Pa 1976)*, 28: 548-53.

Sato, Masato, Takashi Asazuma, Masayuki Ishihara, Toshiyuki Kikuchi, Kazunori Masuoka, Shoichi Ichimura, Makoto Kikuchi, Akira Kurita, and Kyosuke Fujikawa. 2003. 'An atelocollagen honeycomb-shaped scaffold with a membrane seal (ACHMS-scaffold) for the culture of annulus fibrosus cells from an intervertebral disc', *Journal of Biomedical Materials Research Part A*, 64A: 248-56.

Schneider, Caroline A., Wayne S. Rasband, and Kevin W. Eliceiri. 2012. 'NIH Image to ImageJ: 25 years of image analysis', *Nature Methods*, 9: 671-75.

Schol, Jordy, and Daisuke Sakai. 2019. 'Cell therapy for intervertebral disc herniation and degenerative disc disease: clinical trials', *International Orthopaedics*, 43: 1011-25.

Schubert, Ann-Kathrin, Jeske J. Smink, Matthias Pumberger, Michael Putzier, Michael Sittinger, and Jochen Ringe. 2018. 'Standardisation of basal medium for reproducible culture of human annulus fibrosus and nucleus pulposus cells', *Journal of Orthopaedic Surgery and Research*, 13: 209.

Sélard, E., A. Shirazi-Adl, and J. P. Urban. 2003. 'Finite element study of nutrient diffusion in the human intervertebral disc', *Spine (Phila Pa 1976)*, 28: 1945-53; discussion 53.

Shalash, Ward, Sonia R. Ahrens, Liudmila A. Bardonova, Vadim A. Byvaltsev, and Morgan B. Giers. 2021a. 'Patient-specific apparent diffusion maps used to model nutrient availability in degenerated intervertebral discs', *JOR SPINE*, 4: e1179.

———. 2021b. 'Patient-specific apparent diffusion maps used to model nutrient availability in degenerated intervertebral discs', *JOR spine*, 4: e1179-e79.

Shan, Lizhen, Di Yang, Danjie Zhu, Fabo Feng, and Xiaolin Li. 2019. 'High glucose promotes annulus fibrosus cell apoptosis through activating the JNK and p38 MAPK pathways', *Bioscience Reports*, 39.

Shirazi-Adl, A., M. Taheri, and J. P. Urban. 2010. 'Analysis of cell viability in intervertebral disc: Effect of endplate permeability on cell population', *J Biomech*, 43: 1330-6.

Shoubridge, E.A., R.W. Briggs, and G.K. Radda. 1982. '31P NMR saturation transfer measurements of the steady state rates of creatine kinase and ATP synthetase in the rat brain', *FEBS Letters*, 140: 288-92.

Showalter, Brent L., Jesse C. Beckstein, John T. Martin, Elizabeth E. Beattie, Alejandro A. Espinoza Orías, Thomas P. Schaer, Edward J. Vresilovic, and Dawn M. Elliott. 2012.

'Comparison of animal discs used in disc research to human lumbar disc: torsion mechanics and collagen content', *Spine*, 37: E900-E07.

Shutkin, N. M. 1952. 'Syndrome of the degenerated intervertebral disc', *Am J Surg*, 84: 162-71.

Silagi, Elizabeth S., Emanuel J. Novais, Sara Bisetto, Aristeidis G. Telonis, Joseph Snuggs, Christine L. Le Maitre, Yunping Qiu, Irwin J. Kurland, Irving M. Shapiro, Nancy J. Philp, and Makarand V. Risbud. 2020. 'Lactate Efflux From Intervertebral Disc Cells Is Required for Maintenance of Spine Health', *Journal of Bone and Mineral Research*, 35: 550-70.

Silagi, Elizabeth S., Ernestina Schipani, Irving M. Shapiro, and Makarand V. Risbud. 2021. 'The role of HIF proteins in maintaining the metabolic health of the intervertebral disc', *Nature Reviews Rheumatology*, 17: 426-39.

Silverman, F. N. 1954. 'Calcification of the intervertebral disks in childhood', *Radiology*, 62: 801-16.

Smith, L. J., L. Silverman, D. Sakai, C. L. Le Maitre, R. L. Mauck, N. R. Malhotra, J. C. Lotz, and C. T. Buckley. 2018. 'Advancing cell therapies for intervertebral disc regeneration from the lab to the clinic: Recommendations of the ORS spine section', *JOR SPINE*, 1: e1036.

SMITH, R N. 2016. 'Discussion on Comparison of Disorders of the Intervertebral Disc in Man and Animals', *Proceedings of the Royal Society of Medicine*, 51: 569-76.

Soukane, D. M., A. Shirazi-Adl, and J. P. Urban. 2005. 'Analysis of nonlinear coupled diffusion of oxygen and lactic acid in intervertebral discs', *J Biomech Eng*, 127: 1121-6.

Soukane, D. M.;, A.; Shirazi-Adl, and J. P.; Urban. 2007. 'Computation of coupled diffusion of oxygen, glucose and lactic acid in an intervertebral disc', *J Biomech*, 40: 2645-54.

Speight, G., C. J. Handley, and D. A. Lowther. 1978. 'Extracellular matrix metabolism by chondrocytes 4. Role of glutamine in glycosaminoglycan synthesis in vitro by chondrocytes', *Biochimica et Biophysica Acta (BBA) - General Subjects*, 540: 238-45.

Stein, Dan, Yaniv Assaf, Gali Dar, Haim Cohen, Viviane Slon, Einat Kedar, Bahaa Medlej, Janan Abbas, Ori Hay, Daniel Barazany, and Israel Hershkovitz. 2021. '3D virtual reconstruction and quantitative assessment of the human intervertebral disc's annulus fibrosus: a DTI tractography study', *Scientific Reports*, 11: 6815.

Sugishita, Yodo, Lingbo Meng, Yuki Suzuki-Takahashi, Sandy Nishimura, Sayako Furuyama, Atsushi Uekawa, Akiko Tozawa-Ono, Junko Migitaka-Igarashi, Tomoe Koizumi, Hibiki Seino, Yasunori Natsuki, Manabu Kubota, Junki Koike, Keisuke Edashige, and Nao Suzuki. 2021. 'Quantification of residual cryoprotectants and cytotoxicity in thawed bovine ovarian tissues after slow freezing or vitrification', *Human Reproduction*, 37: 522-33.

Sylven, B. 1951. 'On the biology of nucleus pulposus', *Acta Orthop Scand*, 20: 275-9.

Tam, V., I. Rogers, D. Chan, V. Y. Leung, and K. M. Cheung. 2014. 'A comparison of intravenous and intradiscal delivery of multipotential stem cells on the healing of injured intervertebral disk', *J Orthop Res*, 32: 819-25.

Teraguchi, M., N. Yoshimura, H. Hashizume, S. Muraki, H. Yamada, A. Minamide, H. Oka, Y. Ishimoto, K. Nagata, R. Kagotani, N. Takiguchi, T. Akune, H. Kawaguchi, K. Nakamura, and M. Yoshida. 2014. 'Prevalence and distribution of intervertebral disc degeneration over the entire spine in a population-based cohort: the Wakayama Spine Study', *Osteoarthritis Cartilage*, 22: 104-10.

Thomas Rde, W., J. J. Batten, S. Want, I. D. McCarthy, M. Brown, and S. P. Hughes. 1995. 'A new in-vitro model to investigate antibiotic penetration of the intervertebral disc', *J Bone Joint Surg Br*, 77: 967-70.

Tomaszewski, K. A., J. A. Walocha, E. Mizia, T. Gładysz, R. Głowacki, and R. Tomaszewska. 2015. 'Age- and degeneration-related variations in cell density and glycosaminoglycan content in the human cervical intervertebral disc and its endplates', *Pol J Pathol*, 66: 296-309.

Toner, M., E. G. Cravalho, J. Stachecki, T. Fitzgerald, R. G. Tompkins, M. L. Yarmush, and D. R. Armant. 1993. 'Nonequilibrium freezing of one-cell mouse embryos. Membrane integrity and developmental potential', *Biophys J*, 64: 1908-21.

Tong, Wei, Zhouyu Lu, Ling Qin, Robert L. Mauck, Harvey E. Smith, Lachlan J. Smith, Neil R. Malhotra, Martin F. Heyworth, Franklin Caldera, Motomi Enomoto-Iwamoto, and Yejia Zhang. 2017. 'Cell therapy for the degenerating intervertebral disc', *Translational Research*, 181: 49-58.

Törner, Marianne, and Sten Holm. 1985. 'Studies of the Lumbar Vertebral End-plate Region in the Pig', *Upsala Journal of Medical Sciences*, 90: 243-58.

Torzilli P.A., Askari E., Jenkins J.T. 1990. *Water Content and Solute Diffusion Properties in Articular Cartilage* (Springer: New York, NY).

Tourell, M. C., M. Kirkwood, M. J. Pearcy, K. I. Momot, and J. P. Little. 2017. 'Load-induced changes in the diffusion tensor of ovine anulus fibrosus: A pilot MRI study', *J Magn Reson Imaging*, 45: 1723-35.

Travascio, Francesco, and Wei Yong Gu. 2007. 'Anisotropic Diffusive Transport in Annulus Fibrosus: Experimental Determination of the Diffusion Tensor by FRAP Technique', *Annals of Biomedical Engineering*, 35: 1739-48.

Travascio, Francesco, Sabrina Valladares-Prieto, and Alicia R. Jackson. 2020. 'Effects of solute size and tissue composition on molecular and macromolecular diffusivity in human knee cartilage', *Osteoarthritis and Cartilage Open*, 2: 100087.

Tschugg, A., F. Michnacs, M. Strowitzki, H. J. Meisel, and C. Thome. 2016. 'A prospective multicenter phase I/II clinical trial to evaluate safety and efficacy of NOVOCART Disc plus autologous disc chondrocyte transplantation in the treatment of nucleotomized and degenerative lumbar disc to avoid secondary disease: study protocol for a randomized controlled trial', *Trials*, 17: 108.

Tschugg, Anja, Michael Diepers, Steinert Simone, Felix Michnacs, Sebastian Quirbach, Martin Strowitzki, Hans Jörg Meisel, and Claudius Thomé. 2017. 'A prospective randomized multicenter phase I/II clinical trial to evaluate safety and efficacy of NOVOCART disk plus autologous disk chondrocyte transplantation in the treatment of nucleotomized and degenerative lumbar disks to avoid secondary disease: safety results of Phase I—a short report', *Neurosurgical Review*, 40: 155-62.

Turgut, M., A. Uysal, S. Uslu, N. Tavus, and M. E. Yurtseven. 2003. 'The effects of calcium channel antagonist nimodipine on end-plate vascularity of the degenerated intervertebral disc in rats', *J Clin Neurosci*, 10: 219-23.

Turner, V. 1959. 'The rationale of the non-operative management of lesions of the lumbar intervertebral disc', *Q Bull Northwest Univ Med Sch*, 33: 279-81.

URBAN, J. P. G., S. HOLM, A. MAROUDAS, and A. NACHEMSON. 1982. 'Nutrition of the Intervertebral Disc: Effect of Fluid Flow on Solute Transport', *Clinical Orthopaedics and Related Research®*, 170: 296-302.

Urban, J. P. G., and A. Maroudas. 1979. 'The measurement of fixed charged density in the intervertebral disc', *Biochimica et Biophysica Acta (BBA) - General Subjects*, 586: 166-78.

Urban, J. P., S. Holm, and A. Maroudas. 1978. 'Diffusion of small solutes into the intervertebral disc: as in vivo study', *Biorheology*, 15: 203-21.

Urban, J. P., S. Holm, A. Maroudas, and A. Nachemson. 1977. 'Nutrition of the intervertebral disk. An in vivo study of solute transport', *Clinical orthopaedics and related research*: 101-14.

Urban, J. P., and J. F. McMullin. 1988. 'Swelling pressure of the lumbar intervertebral discs: influence of age, spinal level, composition, and degeneration', *Spine*, 13: 179-87.

Urban, J. P., and S. Roberts. 2003a. 'Degeneration of the intervertebral disc', *Arthritis Res Ther*, 5: 120-30.

Urban, J. P., S. Smith, and J. C. Fairbank. 2004. 'Nutrition of the intervertebral disc', *Spine (Phila Pa 1976)*, 29: 2700-9.

Urban, J. P., and C. P. Winlove. 2007. 'Pathophysiology of the intervertebral disc and the challenges for MRI', *J Magn Reson Imaging*, 25: 419-32.

Urban, Jill P. G., and Sally Roberts. 2003b. 'Degeneration of the intervertebral disc', *Arthritis Res Ther*, 5: 120.

Van Der Werf, Marije, Patrick Lezuo, Otto Maissen, Corrinus C. Van Donkelaar, and Keita Ito. 2007. 'Inhibition of vertebral endplate perfusion results in decreased intervertebral disc intranuclear diffusive transport', *Journal of anatomy*, 211: 769-74.

Vergroesen, P. P. A., I. Kingma, K. S. Emanuel, R. J. W. Hoogendoorn, T. J. Welting, B. J. van Royen, J. H. van Dieën, and T. H. Smit. 2015. 'Mechanics and biology in intervertebral disc degeneration: a vicious circle', *Osteoarthritis Cartilage*, 23: 1057-70.

Vo, N. V., R. A. Hartman, P. R. Patil, M. V. Risbud, D. Kletsas, J. C. Iatridis, J. A. Hoyland, C. L. Le Maitre, G. A. Sowa, and J. D. Kang. 2016. 'Molecular mechanisms of biological aging in intervertebral discs', *J Orthop Res*, 34: 1289-306.

Wang, A. M., P. Cao, A. Yee, D. Chan, and E. X. Wu. 2015. 'Detection of extracellular matrix degradation in intervertebral disc degeneration by diffusion magnetic resonance spectroscopy', *Magn Reson Med*, 73: 1703-12.

Wang, Dong, Robert Hartman, Chao Han, Chao-Ming Zhou, Brandon Couch, Matias Malkamaki, Vera Roginskaya, Bennett Van Houten, Steven J. Mullett, Stacy G. Wendell, Michael J. Jurczak, James Kang, Joon Lee, Gwendolyn Sowa, and Nam Vo. 2021. 'Lactate oxidative phosphorylation by annulus fibrosus cells: evidence for lactate-dependent metabolic symbiosis in intervertebral discs', *Arthritis Research & Therapy*, 23: 145-45.

Wang, Jihong, Joseph Weygand, Ken-Pin Hwang, Abdallah S. R. Mohamed, Yao Ding, Clifton D. Fuller, Stephen Y. Lai, Steven J. Frank, and Jinyuan Zhou. 2016. 'Magnetic Resonance Imaging of Glucose Uptake and Metabolism in Patients with Head and Neck Cancer', *Scientific Reports*, 6: 30618.

Wang, Ping, Li Yang, and Adam H. Hsieh. 2011. 'Nucleus Pulposus Cell Response to Confined and Unconfined Compression Implicates Mechanoregulation by Fluid Shear Stress', *Annals of Biomedical Engineering*, 39: 1101-11.

Wang, Yu-Fu, Howard B. Levene, Weiyong Gu, and C. Y. Charles Huang. 2017. 'Enhancement of Energy Production of the Intervertebral Disc by the Implantation of Polyurethane Mass Transfer Devices', *Annals of Biomedical Engineering*, 45: 2098-108.

Wang, Yue, Tapio Videman, and Michele C. Battié. 2012. 'ISSLS Prize Winner: Lumbar Vertebral Endplate Lesions: Associations With Disc Degeneration and Back Pain History', *Spine*, 37: 1490-96.

Watanabe, K., J. Mochida, T. Nomura, M. Okuma, K. Sakabe, and K. Seiki. 2003. 'Effect of reinsertion of activated nucleus pulposus on disc degeneration: an experimental study on various types of collagen in degenerative discs', *Connect Tissue Res*, 44: 104-8.

Weidenbaum, M., R. J. Foster, B. A. Best, F. Saed-Nejad, E. Nickoloff, J. Newhouse, A. Ratcliffe, and V. C. Mow. 1992. 'Correlating magnetic resonance imaging with the biochemical content of the normal human intervertebral disc', *Journal of Orthopaedic Research*, 10: 552-61.

Welty, James R., Gregory L Rorrer, and David G Foster. 2015. 'Fundamentals of Momentum, Heat, and Mass Transfer.' in, *Fundamentals of Momentum, Heat, and Mass Transfer* (Wiley: Hoboken, NJ).

Willems, Nicole, Anna R. Tellegen, Niklas Bergknut, Laura B. Creemers, Jeannette Wolfswinkel, Christian Freudigmann, Karin Benz, Guy C. M. Grinwis, Marianna A.

Tryfonidou, and Björn P. Meij. 2016. 'Inflammatory profiles in canine intervertebral disc degeneration', *BMC Veterinary Research*, 12: 10.

Wiseman, M. A., H. L. Birch, M. Akmal, and A. E. Goodship. 2005. 'Segmental variation in the in vitro cell metabolism of nucleus pulposus cells isolated from a series of bovine caudal intervertebral discs', *Spine (Phila Pa 1976)*, 30: 505-11.

Wong, J., S. L. Sampson, H. Bell-Briones, A. Ouyang, A. A. Lazar, J. C. Lotz, and A. J. Fields. 2019. 'Nutrient supply and nucleus pulposus cell function: effects of the transport properties of the cartilage endplate and potential implications for intradiscal biologic therapy', *Osteoarthritis Cartilage*, 27: 956-64.

Wu, Nan, Hao Liu, Jun Chen, Luo Zhao, Wei Zuo, Yue Ming, Sen Liu, Jiaqi Liu, Xinlin Su, Baoxiang Gao, Zhiquan Tang, Guixing Qiu, Guolin Ma, and Zhihong Wu. 2013. 'Comparison of Apparent Diffusion Coefficient and T2 Relaxation Time Variation Patterns in Assessment of Age and Disc Level Related Intervertebral Disc Changes', *PLOS ONE*, 8: e69052.

Wu, Y., S. E. Cisewski, N. Wegner, S. Zhao, V. D. Pellegrini, Jr., E. H. Slate, and H. Yao. 2016. 'Region and strain-dependent diffusivities of glucose and lactate in healthy human cartilage endplate', *J Biomech*, 49: 2756-62.

Wu, Y., S. Cisewski, B. L. Sachs, and H. Yao. 2013. 'Effect of cartilage endplate on cell based disc regeneration: a finite element analysis', *Mol Cell Biomech*, 10: 159-82.

Xiao, Li, Mengmeng Ding, Osama Saadoon, Eric Vess, Andrew Fernandez, Ping Zhao, Li Jin, and Xudong Li. 2017. 'A novel culture platform for fast proliferation of human annulus fibrosus cells', *Cell and Tissue Research*, 367: 339-50.

Xin;, Hongkui, Chao Zhang;, Zhiyuan Shi; Deli Wang, Chaofeng Wang; Tao Gu, Jianhong Wu;, Yan Zhang;, Qing He;, and Dike Ruan;. 2013. 'Tissue-Engineered Allograft Intervertebral Disc Transplantation for the Treatment of Degenerative Disc Disease: Experimental Study in a Beagle Model', *Tissue Engineering Part A*, 19: 143-51.

Xiong, Xuanqi, Zhengwei Zhou, Matteo Figini, Junjie Shangguan, Zhuoli Zhang, and Wei Chen. 2018. 'Multi-parameter evaluation of lumbar intervertebral disc degeneration using quantitative magnetic resonance imaging techniques', *American journal of translational research*, 10: 444-54.

Xu, X., J. P. G. Urban, U. K. Tirlapur, and Z. Cui. 2010. 'Osmolarity effects on bovine articular chondrocytes during three-dimensional culture in alginate beads', *Osteoarthritis Cartilage*, 18: 433-39.

Yang, B., and G. D. O'Connell. 2019a. 'GAG content, fiber stiffness, and fiber angle affect swelling-based residual stress in the intact annulus fibrosus', *Biomech Model Mechanobiol*, 18: 617-30.

Yang, Bo, and Grace D. O'Connell. 2019b. 'Intervertebral disc swelling maintains strain homeostasis throughout the annulus fibrosus: A finite element analysis of healthy and degenerated discs', *Acta Biomaterialia*, 100: 61-74.

Yang, Bo, and Grace D. O'Connell. 2017. 'Effect of collagen fibre orientation on intervertebral disc torsion mechanics', *Biomechanics and Modeling in Mechanobiology*, 16: 2005-15.

Yang, Mengying, Dingding Xiang, Yuru Chen, Yangyang Cui, Song Wang, and Weiqiang Liu. 2022. 'An Artificial PVA-BC Composite That Mimics the Biomechanical Properties and Structure of a Natural Intervertebral Disc', *Materials*, 15: 1481.

Yao, Hai, and Wei Yong Gu. 2007. 'Three-dimensional inhomogeneous triphasic finite-element analysis of physical signals and solute transport in human intervertebral disc under axial compression', *Journal of Biomechanics*, 40: 2071-77.

Ye, Dongping, Weiguo Liang, Libing Dai, and Yicun Yao. 2018. 'Moderate Fluid Shear Stress Could Regulate the Cytoskeleton of Nucleus Pulposus and Surrounding Inflammatory Mediators by Activating the FAK-MEK5-ERK5-cFos-AP1 Signaling Pathway', *Disease Markers*, 2018: 9405738.

Yin, S., H. Du, W. Zhao, S. Ma, M. Zhang, M. Guan, and M. Liu. 2019a. 'Inhibition of both endplate nutritional pathways results in intervertebral disc degeneration in a goat model', *J Orthop Surg Res*, 14: 138.

Yin, Si, Heng Du, Weigong Zhao, Shaohui Ma, Ming Zhang, Min Guan, and Miao Liu. 2019b. 'Inhibition of both endplate nutritional pathways results in intervertebral disc degeneration in a goat model', *Journal of Orthopaedic Surgery and Research*, 14: 138.

Yoshikawa, T., Y. Ueda, K. Miyazaki, M. Koizumi, and Y. Takakura. 2010. 'Disc regeneration therapy using marrow mesenchymal cell transplantation: a report of two case studies', *Spine (Phila Pa 1976)*, 35: E475-80.

Yuan, T. Y., A. R. Jackson, C. Y. Huang, and W. Y. Gu. 2009a. 'Strain-dependent oxygen diffusivity in bovine annulus fibrosus', *J Biomech Eng*, 131: 074503.

———. 2009b. 'Strain-Dependent Oxygen Diffusivity in Bovine Annulus Fibrosus', *Journal of Biomechanical Engineering*, 131.

Yurube, Takashi, Masaaki Ito, Yuji Kakiuchi, Ryosuke Kuroda, and Kenichiro Kakutani. 2020. 'Autophagy and mTOR signaling during intervertebral disc aging and degeneration', *JOR SPINE*, 3: e1082.

Zeng, F., Y. Zha, L. Li, D. Xing, W. Gong, L. Hu, and Y. Fan. 2019. 'A comparative study of diffusion kurtosis imaging and T2* mapping in quantitative detection of lumbar intervertebral disk degeneration', *Eur Spine J*, 28: 2169-78.

Zhang, Shu-Jun, Wei Yang, Cheng Wang, Wen-Si He, Hai-Yang Deng, Yi-Guo Yan, Jian Zhang, Yong-Xiao Xiang, and Wen-Jun Wang. 2016. 'Autophagy: A double-edged sword in intervertebral disk degeneration', *Clinica Chimica Acta*, 457: 27-35.

Zhang, Wei, Xiaohui Ma, Yan Wang, Jian Zhao, Xujing Zhang, Yu Gao, and Shiling Li. 2014. 'Assessment of apparent diffusion coefficient in lumbar intervertebral disc degeneration', *European Spine Journal*, 23: 1830-36.

Zhang, Yuang, Biao Yang, Jingkai Wang, Feng Cheng, Kesi Shi, Liwei Ying, Chenggui Wang, Kaishun Xia, Xianpeng Huang, Zhe Gong, Chao Yu, Fangcai Li, Chengzhen Liang, and Qixin Chen. 2020. 'Cell Senescence: A Nonnegligible Cell State under Survival Stress in Pathology of Intervertebral Disc Degeneration', *Oxidative Medicine and Cellular Longevity*, 2020: 9503562.

Zheng, C. H., and M. E. Levenston. 2015. 'Fact versus artifact: avoiding erroneous estimates of sulfated glycosaminoglycan content using the dimethylmethylene blue colorimetric assay for tissue-engineered constructs', *Eur Cell Mater*, 29: 224-36; discussion 36.

Zhou, Zhengwei, Christopher Nguyen, Yuhua Chen, Jaime L. Shaw, Zixin Deng, Yibin Xie, James Dawkins, Eduardo Marbán, and Debiao Li. 2017. 'Optimized CEST cardiovascular magnetic resonance for assessment of metabolic activity in the heart', *Journal of Cardiovascular Magnetic Resonance*, 19: 95.

Zhu, Q., X. Gao, H. B. Levene, M. D. Brown, and W. Gu. 2016. 'Influences of Nutrition Supply and Pathways on the Degenerative Patterns in Human Intervertebral Disc', *Spine (Phila Pa 1976)*, 41: 568-76.

Zhu, Q., A. R. Jackson, and W. Y. Gu. 2012. 'Cell viability in intervertebral disc under various nutritional and dynamic loading conditions: 3d finite element analysis', *J Biomech*, 45: 2769-77.

Appendices

Appendix 1

Table A1.1. Summary of finite element model studies.

Modeled parameters	Results	Limitations	Reference
• **Creep response** • **Water flow** • **Viscoelastic model**	• Flow rate determined by transport properties • Permeability decreases with applied stress	• Model was verified using canine IVDs	(Cassidy et al. 1990)
• **Transport of glucose, oxygen, and lactate** • **Non-linear reactions**	• Concentration profiles of glucose and oxygen show decreasing levels towards the center of the IVD • Limited diffusivity reduced transport • Increased IVD height reduced transport • Transport through the CEP affects solute levels in the NP	• Axisymmetric anatomy • Uniform boundary conditions • Uniform values for diffusion coefficients, cell densities, and reaction rates throughout the disc • Insufficient information on metabolic rates in the CEP	(Sélard, Shirazi-Adl, and Urban 2003)
• **Effects of mechanical loading on solute transport**	• Fluid flow does not enhance transport of small molecules • Fluid exchange during swelling is more substantial than during loading	• Uncoupled fluid flow and transport • Constant swelling pressure • Axisymmetric geometries	(Ferguson, Ito, and Nolte 2004)
• **3D geometry** • **Triphasic, inhomogeneous properties** • **Axial compression**	• NP had uniform distributions of mechanical stress, and fluid pressure • Changes to material properties affect fluid pressure, solute transport, and electrical potential	• No transport through the CEP • Constructed geometry • No metabolic rates • Uniform material properties through the tissue	(Yao and Gu 2007)

Table A1.1. Summary of finite element model studies. (Continued)

Modeled parameters	Results	Limitations	Reference
• **Triphasic theory** • **Mechanical compression** • **Metabolic rates** • **Transport profiles**	• Dynamic loading increases energy conversion	• Axisymmetric geometry • Parameters obtained from different animal tissue • Metabolism is independent of mechanical loading	(Huang and Gu 2008)
• **Realistic 3D anatomy** • **Non-linear coupled metabolic reactions** • **CEP calcification** • **Sclerosis** • **Induction of growth factor**	• Realistic anatomy affects solute gradients • IVD degeneration, CEP calcification, and reduced cell density affect solute transport	• Uniform boundary conditions • Uniform values for diffusion coefficients and cell density throughout the IVD's tissues • No changes in flow content, vessel density, and mechanical loading	(Mokhbi Soukane, Shirazi-Adl, and Urban 2009)
• **Nonlinear coupled nutrition transport equations** • **CEP permeability**	• CEP permeability affects transport • Glucose is critical for cell viability • Cell death started at 0.5mM glucose and pH 6.8	• Axisymmetric geometry • Uniform IVD properties	(Shirazi-Adl, Taheri, and Urban 2010)
• **Biomechanical loading** • **Cell density** • **Oxygen levels**	• Large IVD volume changes affect solute transport • Cell density changes with changes in transport properties • Vertebral blood supply affects transport	• Limited information on boundary conditions • Ignored glucose changes • Cell viability omitted	(Malandrino, Noailly, and Lacroix 2011)
• **3D anatomical geometry** • **CEP calcification** • **Non-linear coupled metabolic rates** • **Static loading conditions**	• CEP calcification reduced glucose levels • Changes in mechanical deformations alters glucose distributions	• Cell and transport properties extracted from animal models • Limited loading configurations	(Jackson et al. 2012)

Table A1.1. Summary of finite element model studies. (Continued)

Modeled parameters	Results	Limitations	Reference
• **IVD degeneration** • **Axial compression** • **3D geometry**	• Nutrient levels at boundaries affect cell viability • Dynamic compression improved cell viability	• Only glucose was considered for cell viability • Assuming isotropic properties of the AF	(Zhu, Jackson, and Gu 2012)
• **Endplate calcification** • **Water loss** • **Reduction in IVD height** • **Cyclic loading** • **Cell density** • **Transport of glucose, oxygen, and lactate**	• Changes to transport properties in a degenerated IVD lower cell viability • Shortening of the IVD's height enhanced solute transport	• Simple IVD anatomy • Vascularization of degenerated CEPs was not modeled • Diffusion coefficients were calculated using an empirical formula • Mechanical properties did not represent degenerated IVDs • Cell proliferation was not considered • Tissue structure did not change with degeneration	(Galbusera et al. 2013)
• **IVD degeneration level** • **Vasculature density** • **Mechanical loading** • **Cell viability** • **Poromechanical properties**	• Low metabolic transport at the CEP reduced cell viability • Mechanical deformations had a negligible effect on preservation of cell viability in degenerated IVDs	• No cell proliferation or clustering • No changes in ECM due to degeneration	(Malandrino, Noailly, and Lacroix 2014)
• **Transport of administered glucosamine** • **Human VS animal IVDs** • **Varying IVD size**	• IVD size determines concentration profiles for larger solutes • CEP permeability affects transport • Animal models may not be ideal to study transport in human IVDs	• Axisymmetric geometry • Uniform transport properties • Uniform tissue properties • Mechanical deformation was ignored	(Motaghinasab et al. 2014)

Table A1.1. Summary of finite element model studies. (Continued)

Modeled parameters	Results	Limitations	Reference
• **Patient-specific diffusion data in NP** • **Nonlinear coupled reaction rates**	• Concentration profiles vary between patients • Metabolic rates, IVD size, CEP and AF diffusivities affected solute profiles	• Uniform IVD properties including water content, cell density, boundary conditions • Solute profile predictors (excluding IVD geometry and diffusivity in the NP) were not patient-specific • 2D model	(Shalash et al. 2021)

Table A1.2. T_{2w}, ADC maps, and solute distribution maps for IVDs in groups grade 2, 3, 4, and 5 are presented. pH maps are not included in this table to avoid redundancy with lactate data since pH is linearly correlated to pH. All discs are presented with the posterior aspect on the left and the anterior aspect on the right.

				Grade 2 (n=10)		
Patient	Disc level	T_{2w}	ADC	Glucose gradient (mM) 5.0 2.5 0.5	Lactate gradient (mM) 6.0 3.0 0.0	Oxygen gradient (mM) 6.0 4.5 3.5
1	L3L4					
2	L5S1					
3	L3L4					
4	L3L4					
5	L4L5					
6	L3L4					

Table A1.2. T_{2w}, ADC maps, and solute distribution maps for IVDs in groups grade 2, 3, 4, and 5 are presented. pH maps are not included in this table to avoid redundancy with lactate data since pH is linearly correlated to pH. All discs are presented with the posterior aspect on the left and the anterior aspect on the right. (Continued)

Patient	Disc level	T_{2w}	ADC	Glucose gradient (mM)	Lactate gradient (mM)	Oxygen gradient (mM)
7	L3L4					
8	L5S1					
9	L3L4					
Grade 3 (n=10)						
Patient	Disc level	T_{2w}	ADC	Glucose gradient (mM) 5.0 / 2.5 / 0.5	Lactate gradient (mM) 6.0 / 3.0 / 0.0	Oxygen gradient (mM) 6.0 / 4.5 / 3.5
11	L3L4					
11	L4L5					
1	L4L5					

Table A1.2. T_{2w}, ADC maps, and solute distribution maps for IVDs in groups grade 2, 3, 4, and 5 are presented. pH maps are not included in this table to avoid redundancy with lactate data since pH is linearly correlated to pH. All discs are presented with the posterior aspect on the left and the anterior aspect on the right. (Continued)
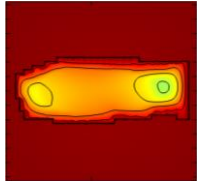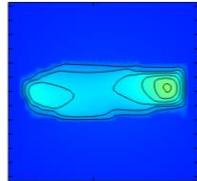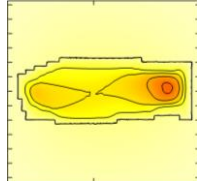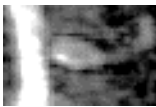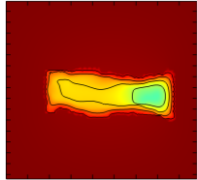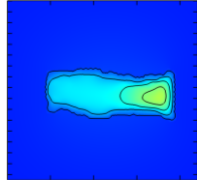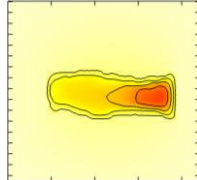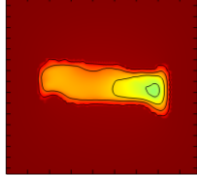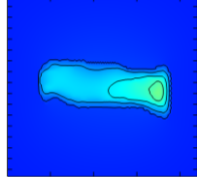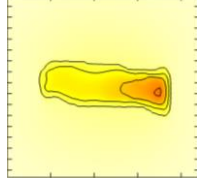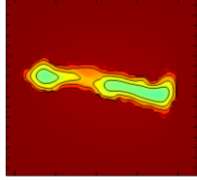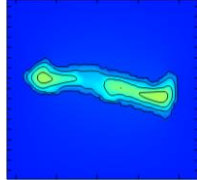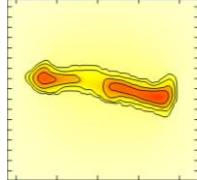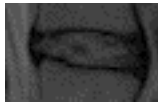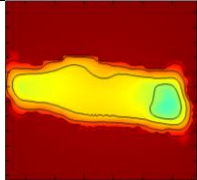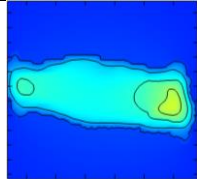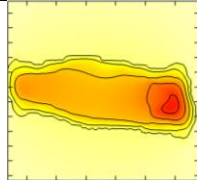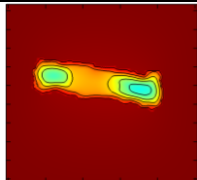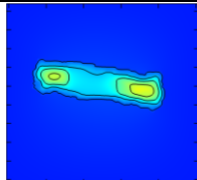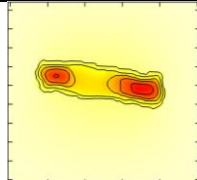
2	L3L4					
12	L3L4					
12	L4L5					
13	L5S1					
3	L4L5					
4	L4L5					

Table A1.2. T_{2w}, ADC maps, and solute distribution maps for IVDs in groups grade 2, 3, 4, and 5 are presented. pH maps are not included in this table to avoid redundancy with lactate data since pH is linearly correlated to pH. All discs are presented with the posterior aspect on the left and the anterior aspect on the right. (Continued)
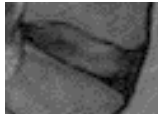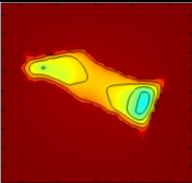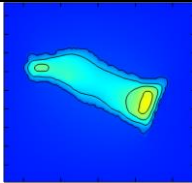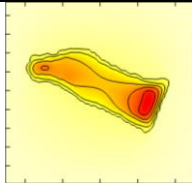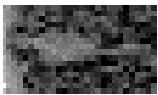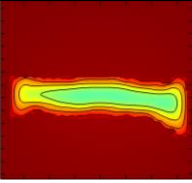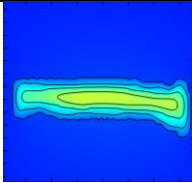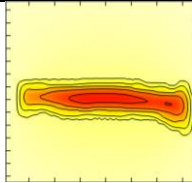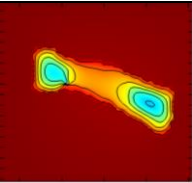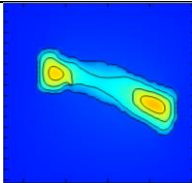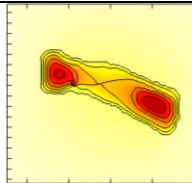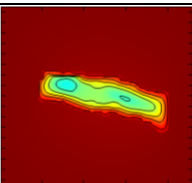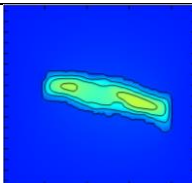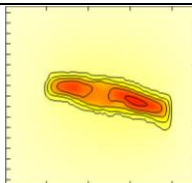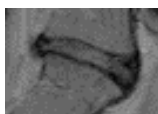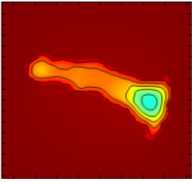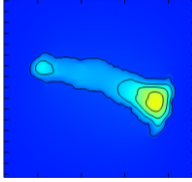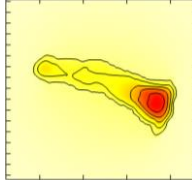
14	L4L5					

Grade 4 (n=10)

Patient	Disc level	T_{2w}	ADC	Glucose gradient (mM) 5.0 2.5 0.5	Lactate gradient (mM) 6.0 3.0 0.0	Oxygen gradient (mM) 6.0 4.5 3.5
15	L3L4					
1	L5S1					
2	L4L5					
12	L5S1					

Table A1.2. T_{2w}, ADC maps, and solute distribution maps for IVDs in groups grade 2, 3, 4, and 5 are presented. pH maps are not included in this table to avoid redundancy with lactate data since pH is linearly correlated to pH. All discs are presented with the posterior aspect on the left and the anterior aspect on the right. (Continued)
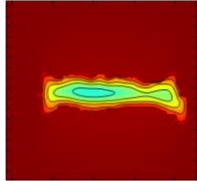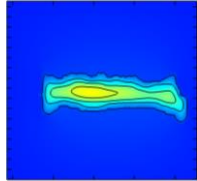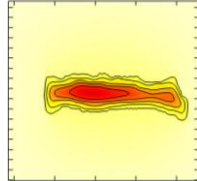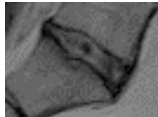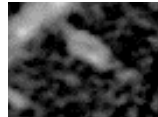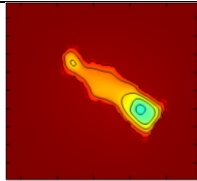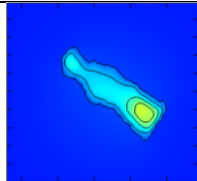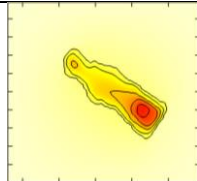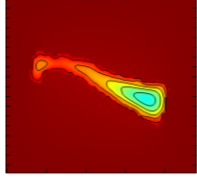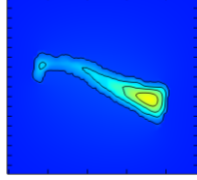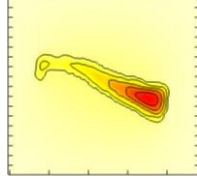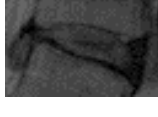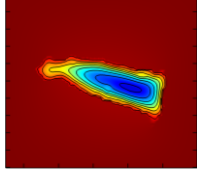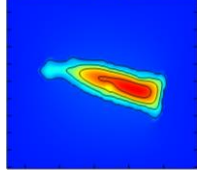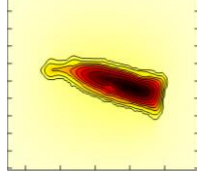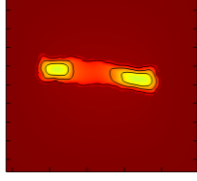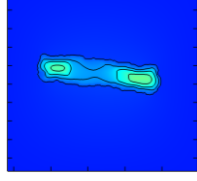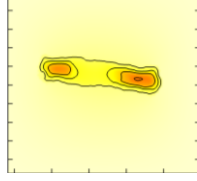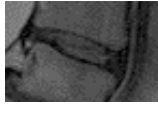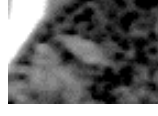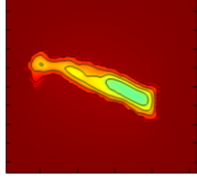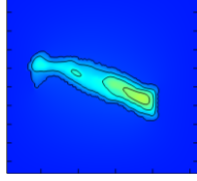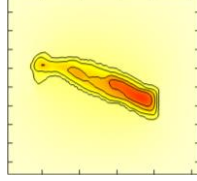
13	L4L5					
16	L5S1					
17	L5S1					
18	L4L5					
4	L5S1					
10	L4L5					

Table A1.2. T_{2w}, ADC maps, and solute distribution maps for IVDs in groups grade 2, 3, 4, and 5 are presented. pH maps are not included in this table to avoid redundancy with lactate data since pH is linearly correlated to pH. All discs are presented with the posterior aspect on the left and the anterior aspect on the right. (Continued)
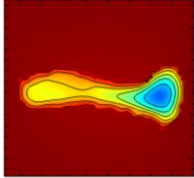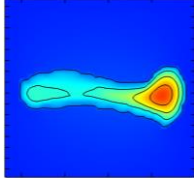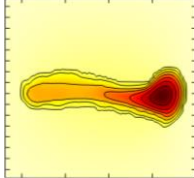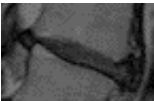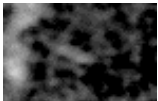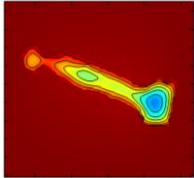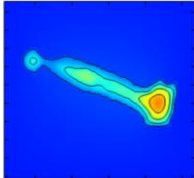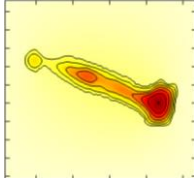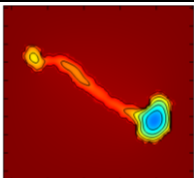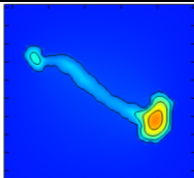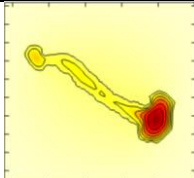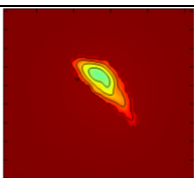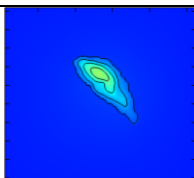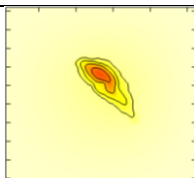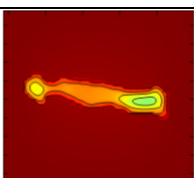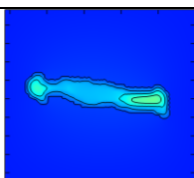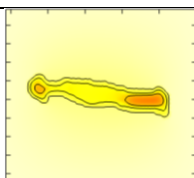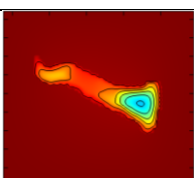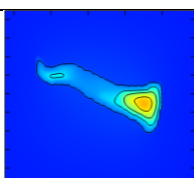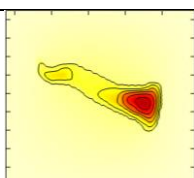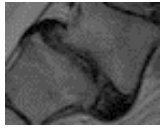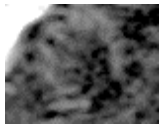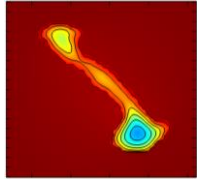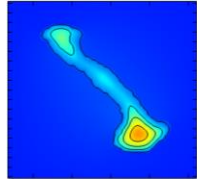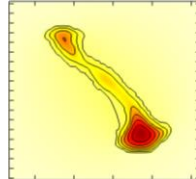
Grade 5 (n=7)						
Patient	Disc level	T_{2w}	ADC	Glucose gradient (mM)	Lactate gradient (mM)	Oxygen gradient (mM)
11	L3L4					
19	L5S1					
19	L4L5					
20	L5S1					
21	L4L5					
21	L5S1					

Table A1.2. T$_{2w}$, ADC maps, and solute distribution maps for IVDs in groups grade 2, 3, 4, and 5 are presented. pH maps are not included in this table to avoid redundancy with lactate data since pH is linearly correlated to pH. All discs are presented with the posterior aspect on the left and the anterior aspect on the right. (Continued)

| 10 | L5S1 | | | | | |